Distribution, Geochemistry and Geochronology of Sellafield Waste in Contaminated Solway Firth Floodplain Deposits

Robert Lindsay Allan
Department of Chemistry, University of Glasgow
and
Scottish Universities Research and Reactor Centre

presented as a thesis for the degree of
Doctor of Philosophy
in the University of Glasgow
November 1993

ProQuest LLC.
789 East Eisenhower Parkway
P.O. Box 1346
Ann Arbor, MI 48106 – 1346

CONTENTS LIST

Page

ACKNOWLEDGEMENTS 1

ABSTRACT 2

CHAPTER 1 ANTHROPOGENIC RADIONUCLIDES WITHIN THE IRISH SEA BASIN 4

1.1 INTRODUCTION 4

1.1.1 The Sellafield Nuclear Fuel Reprocessing Plant 4
1.1.2 Discharge Data for Sellafield Liquid Radioactive Waste 8

1.2 ADDITIONAL SOURCES OF ANTHROPOGENIC RADIONUCLIDES TO THE STUDY AREA 16

1.2.1 Local Sources of Pollutant Radionuclides to the Irish Sea other than Sellafield 17
1.2.2 Global Sources of Pollutant Radionuclides 18

1.3 SEDIMENTS OF THE IRISH SEA 22

1.3.1 The Coastline of the Solway Firth 29
1.3.2 Intertidal Sediments 31

1.4. RADIONUCLIDES IN THE IRISH SEA 41

1.4.1 Radiological Significance of the Sellafield Discharges 41
1.4.2 General Aspects of the Geochemistry of Radiocaesium, Plutonium and Americium in the Irish Sea 43
1.4.3 Sellafield Radionuclides in the Offshore Sediments of the Irish Sea 48
1.4.4 Radionuclide Supply To The Intertidal And Floodplain Environments 52

1.4.4.1 . . . Lateral Variation in Surface Sediment Concentrations 52
1.4.4.2 . . Temporal Trends in Surface Sediment Concentrations 57
1.4.4.3 . . Vertical Distributions of Radionuclides in Intertidal Sediments 58
1.4.4.4 . . On-shore Transfer of Radionuclides 62

1.4.5 Geochemical Behaviour of Caesium, Plutonium and Americium in the Floodplain Environment 64

Page

SUMMARY OF CHAPTER 1 67

AIMS OF RESEARCH 68

CHAPTER 2 EXPERIMENTAL 69

2.1 SAMPLE COLLECTION 69

2.1.1 Southwick Water 70
2.1.2 Transects Across Floodplain Deposits 76
2.1.3 Southwick Water T2 86
2.1.4 Southwick Water T3 88

2.2 HIGH RESOLUTION GAMMA SPECTROMETRY ANALYSIS OF SEDIMENT SAMPLES 88

2.3 ALPHA DETECTORS 99

2.4 RADIOCHEMICAL ANALYSIS 100

2.4.1 Plutonium Analysis 100
2.4.2 ^{210}Pb Analysis 105

2.5 DETERMINATION OF CAESIUM CONCENTRATIONS IN AQUEOUS MEDIA USING A NaI(Tl) DETECTOR 106

2.6 SEQUENTIAL EXTRACTION OF SEDIMENT SAMPLES 108

2.7 FLOW DESORPTION EXPERIMENT 111

2.7.1 Batch Desorption Experiment 113

2.8 LOSS ON IGNITION 117

2.9 PARTICLE SIZE ANALYSIS OF SEDIMENT SAMPLES 117

2.10 MINERALOGY OF SEDIMENTS 119

2.11 NEUTRON ACTIVATION ANALYSIS 119

CHAPTER 3 RESULTS 124

CHAPTER 4 DISCUSSION 166

4.1 RADIONUCLIDE VERTICAL PROFILES AND TRANSPORT MECHANISM TO FLOODPLAIN DEPOSITS AT SOUTHWICK WATER 166

Page

4.1.1 Vertical Profiles 166
4.1.2 Transportation Mechanism 171

4.1.2.1 Comparison of the Isotope Activity Ratio Profiles 177
4.1.2.2 Non-Isotopic Activity Ratio Profiles 184

4.1.3 Modelling The Processes Affecting Radionuclide Supply 191

4.2 LATERAL DISTRIBUTION OF RADIONUCLIDES ACROSS MERSE DEPOSITS 205

4.2.1 Creetown 206
4.2.2 Wigtown 218
4.2.3 Southwick 224
4.2.4 Orchardton 235
4.2.5 Kippford 243
4.2.6 Carse Bay 248
4.2.7 Overview of Radionuclide Distribution in Merse Transects 255

4.3 VERTICAL DISTRIBUTION OF RADIONUCLIDES IN MERSE ENVIRONMENTS 265

4.4 CONCEPTUAL MODEL OF THE MERSE 286

4.4.1 Radionuclide Inventories for the Coast of South West Scotland 289

4.5 GEOCHEMICAL ASSOCIATIONS OF SELLAFIELD DERIVED RADIONUCLIDES IN MERSE LOCATIONS 295

4.5.1 ^{137}Cs Leaching Studies 297
4.5.2 $^{239+240}Pu$ Leaching Studies 301

4.6 FLOW DESORPTION EXPERIMENTS 305

4.6.1 Freshwater 309
4.6.2 Field Drain Water 309
4.6.3 Seawater 311
4.6.4 Batch Experiment 314
4.6.5 Conclusions 314

4.7 NEUTRON ACTIVATION ANALYSIS OF SEDIMENT SAMPLES 317

CONCLUSIONS 322

REFERENCES 325

LIST OF TABLES

Table **Page**

Chapter 1

1.1 Annual Discharges from BNFL Sellafield Reprocessing Plant 1952-1990 11

1.2 Integrated Discharges (Decay Corrected Cumulative Environmental Inventory) of ^{137}Cs, $^{239+240}Pu$ and ^{241}Am (including ingrowth from ^{241}Pu) from BNFL Sellafield 12

1.3 Isotope activity ratios for liquid effluent discharged from BNFL Sellafield 15

1.4 Decay characteristics of selected radionuclides 16

1.5 Global and localised sources of anthropogenic radionuclide emissions 17

1.6 Comparison of Annual Discharges of Liquid Radioactive Effluent Sellafield, Chapelcross and Springfields (BNFL, 1990) 19

1.7 Annual Discharges of ^{134}Cs and ^{137}Cs from Cap de la Hague to the Marine Environment 1966-1982 (Calmet and Guegueniat, 1985) 22

1.8 Ionic Potentials for selected radionuclides of interest in this study. (Ben Shaban, (1989) based on data from Greenwood and Earnshaw, 1984) 45

1.9 Concentrations and percentages of $^{239+240}Pu$ associated with particle size fractions and mass balance in 50 g sediment sample from Allonby, Cumbria. (Eakins *et al.*, 1990) 55

1.10 The geochemical associations of $^{239+240}Pu$ in soils from South West Scotland (McDonald *et al.*,1992) 66

1.11 Geochemical associations of ^{137}Cs in Caithness soils (Cook *et al.*, 1984a) 66

Chapter 2

2.1 The Energies and Relative Intensities of the ^{152}Eu Calibration Source 91

2.2 Quality Assurance Results from Periodic Analyses of IAEA Standard Irish Sea Sediment 306 and IAEA Soil 6. The Certified Value is Displayed in Bold with the Range of Values in Brackets Below 92

Page

2.3 Analytical Data for 9 Repeat Analyses of Sediment from SC1 35-40 by γ spectroscopy, June 1991 94

2.4 Analytical Data for 10 Repeat Analyses of Bulk Sediment from SC1 (0-35 cm), January 1992 95

2.5 Analytical Data for 10 Repeat Analyses of Bulk Sediment SC1 (30-35 cm), August 1992 96

2.6 Analytical Data for Analyses of 10 Sub-Samples from SC1 (30-35 cm), 21/12/91 - 10/1/92 97

2.7 Analytical Data for Analyses of 10 Sub-Samples of Sediment from SC1 (30-35 cm), August 1992 98

2.8 Alpha Energies Used for the Determination of Pu Isotopes in Environmental Materials 100

2.9 α Particle Energies and Half Lives of ^{208}Po and ^{210}Po 106

2.10 Soil Fractionation Sizes According to the Soil Survey of England and Wales (ADAS, 1981) 118

2.11 Radionuclides analyzed by NAA 123

Chapter 3

3.1 Analytical Results for Southwick Core No. 1 (errors 1σ) 125

3.2 Analytical Results for Southwick Core No. 2 (errors 1σ) 126

3.3 Analytical Results Showing ^{137}Cs and ^{241}Am Concentrations for Southwick Core No. 3 127

3.4 Radionuclide Concentrations and Inventories for the 0-15 cm Depth Intervals from Creetown Transect T1, Collected 28/8/90 . . . 128

3.5 Radionuclide Concentrations and Inventories for the 15-30 cm Depth Intervals from Creetown Transect T1, Collected 28/8/90 . . . 129

3.6 Radionuclide Concentrations and Inventories for the 0-15 cm Depth Intervals from Wigtown Transect T1, Collected 27/8/90 . . . 130

3.7 Radionuclide Concentrations and Inventories for the 15-30 cm Depth Intervals from Wigtown Transect T1, Collected 27/8/90 131

3.8 Radionuclide Concentrations and Inventories for the 0-15 cm Depth Intervals from Southwick Transect T1, Collected 25/7/91 . . . 132

Page

3.9 Radionuclide Concentrations and Inventories for the 15-30 cm Depth Intervals from Southwick Transect T1, Collected 25/7/91 .. 133

3.10 Radionuclide Concentrations and Inventories for the 0-15 cm Depth Interval from Orchardton Transect T1, Collected 29/8/90 ... 134

3.11 Radionuclide Concentrations and Inventories for the 15-30 cm Depth Intervals from Orchardton Transect T1, Collected 29/8/90 .. 135

3.12 Radionuclide Concentrations and Inventories for the 0-15 cm Depth Intervals from Kippford Transect T1, Collected 28/8/90 136

3.13 Radionuclide Concentrations and Inventories for the 15-30 cm Depth Intervals from Kippford Transect T1, Collected 28/8/90 137

3.14 Radionuclide Concentrations and Inventories for the 0-15 cm Depth Intervals from Carse Bay Transect T1, Collected 15/8/91 ... 138

3.15 Radionuclide Concentrations and Inventories for the 15-30 cm Depth Intervals from Carse Bay Transect T1,Collected 15/8/91 ... 139

3.16 Analytical Results for Southwick Water Transect T2 5m Core (T2.5), Collected 24/1/92 140

3.17 Analytical Results for Southwick Water Transect T2 10m (T2.10) Core, Collected 24/1/92. 141

3.18 Analytical Results from Southwick Transect T2, 20 m Core (T2.20) Collected on 24/1/92. 142

3.19 Analytical Results from Southwick Transect T2, 30 m Core (T2.30) Collected on 24/1/92. 143

3.20 Analytical Results from Southwick Transect T3 5 m Core (S3.5), Collected 27/5/92. 144

3.21 Analytical Results from Southwick Transect T3 10 m Core (S3.10), Collected 27/5/92. 145

3.22 Analytical Results from Southwick Transect T3 15 m Core (S3.15), Collected 27/5/92 146

3.23 Percentage Content of Particle Size Fractions within Core SC1 and Irish Sea Sediment 147

3.24 Results of X-ray Diffraction Analysis for Mineralogical Content of Sediment Samples 148

Page

3.25 Analytical Results for Sequential Leaching of ^{137}Cs and $^{239+240}Pu$ from Intertidal Sediment from Southwick Water 149

3.26 Analytical Results for Sequential Leaching of ^{137}Cs from Sediment Samples Derived from Southwick Water Core SC1 150

3.27 Analytical Results for Sequential Leaching of ^{137}Cs from Sediment Samples from Southwick Core T3 10m (S3.10) 151

3.28 Analytical Results for $^{239+240}Pu$ from Sequential Extraction of Sediment Samples from SC1 152

3.29 Analytical Results for Sequential Leaching of $^{239+240}Pu$ from Sediment Samples derived from Southwick Core T3 10 m (S3.10) 153

3.30 Sequential Extraction of $^{239+240}Pu$ from Marine Sediments and Terrestrial Soils Compiled from McDonald *et al.,* (1990; 1992) . 154

3.31 Analytical Results for the Flow Desorption Experiment, Leaching ^{137}Cs from the 0-5 cm Interval SC1 (sediment conc. 406Bq kg^{-1}) with Freshwater (Mains) 155

3.32 Analytical Results for the Flow Desorption Experiment leaching ^{137}Cs from the 40-45 cm Interval SC1 (sediment conc. 1450 Bq kg^{-1}) with Freshwater (Mains) 156

3.33 Analytical Results for the Flow Desorption Experiment, Leaching ^{137}Cs from the 0-5 cm Interval SC1 (sediment conc. 406 Bq kg^{-1}) with Field Drain Water (Ground Water) 156

3.34 Analytical Results for the Flow Desorption Experiment, Leaching ^{137}Cs from the 0-5cm Interval SC1(sediment conc. 1450 Bq kg^{-1}) with Field Drain Water (Ground Water) 157

3.35 Analytical Results for the Flow Desorption Experiment Leaching ^{137}Cs from the 0-5 cm Interval SC1 (sediment conc. 406 Bq kg^{-1}) with Seawater 157

3.36 Analytical Results for the Flow Desorption Experiment Leaching ^{137}Cs from the 40-45 cm Interval SC1 (sediment conc. 1450 Bq kg^{-1}) with Seawater 158

3.37 Analytical Results for the Leaching of ^{137}Cs from the 0-5 cm Interval SC1 (sediment conc. 406 Bq kg^{-1}) with Competing Cations 158

3.38 Analytical Results from Batch Desorption Experiment (sediment conc. 421 Bq kg^{-1}) 158

3.39 Analytical Results from Neutron Activation Analysis of Sediment Samples 159

3.40 Analytical results from NAA of sediment samples 160

3.41 Analytical Results from NAA of Sediment Samples (contd) 161

3.42 Analytical Results from NAA of Sediment Samples (contd) 162

3.43 Analytical Results from NAA of Sediment Samples 163

3.44 Concentration and K_D Values from NAA of Desorption Media. 164

3.45 Analytical Results from Desorption Experiment involving Neutron Activation Analysis of Water Samples in Contact with Contaminated Sediment (SC1 0-5 cm) 165

Chapter 4

4.1 Maximum, Minimum And Mean ^{137}Cs And ^{241}Am Concentration Values In The 0-15 cm Interval For The Merse At Each Transect . . . 256

4.2 Maximum, Minimum And Mean ^{137}Cs And ^{241}Am Inventories For 0-30 cm Interval From The Merse Area Within Each Transect 260

4.3 Total ^{137}Cs And ^{241}Am Inventories (0-30 cm) Observed At Each Transect Location, With The Areas Determined From NCC(1989) 261

4.4 Linear Mass Absorption Coefficients Calculated for ^{137}Cs and ^{241}Am in Si at Different Depths within a Sediment Profile 286

4.5 Maximum and Minimum Radionuclide Inventories (0-15 cm) Estimated for the Floodplain Deposits of the Solway Coast. 292

4.6 Maximum and Minimum Radionuclide Inventories (0-30 cm) Estimated for the Floodplain Deposits of the Solway Coast 292

4.7 Dynamic and Stable Zone Areas within the Merse Deposits of South West Scotland 294

LIST OF FIGURES

Figure		Page
1.1	Map showing the main establishments discharging liquid radioactive waste into the Irish Sea	5
1.2	Flow diagram of the Magnox fuel reprocessing procedure at BNFL Sellafield. (BNFL, 1985)	7
1.3	Schematic diagram of the SIXEP processing plant at Sellafield	9
1.4	Temporal variations in ^{137}Cs in annual discharges from Sellafield	13
1.5	Temporal variations in ^{134}Cs in annual discharges from Sellafield	13
1.6	Temporal variations in ^{241}Am in annual discharges from Sellafield	13
1.7	Temporal variations in $^{239+240}Pu$ in annual discharges from Sellafield	13
1.8	Map showing the location of Sellafield within the Irish Sea Basin and its proximity to the North Channel and St Georges Channel in the south.	24
1.9	Suggested bed transport paths in the Irish Sea according to Belderson (1964).	25
1.10	Surface sediment distribution within the Irish Sea according to Pantin (1978)	26
1.11	Map illustrating the location of major areas of saltmarsh along the northern Solway Coast (NCC, 1989)	32
1.12	Map illustrating the locationof major areas of saltmarsh along the north west coast of England (NCC, 1989)	34
1.13	Map illustrating the location of major areas of saltmarsh along the northern coast of Wales (NNCC, 1989)	35
1.14	Idealised saltmarsh showing main vegetation zones adapted from Ranwell, 1972	37
1.15	A schematic diagram of the chemical processes involving plutonium in the Irish Sea, adapted from Edgington (1981)	47
1.16	Temporal trends in $^{239+240}Pu$ concentrations in surface sediments at various locations along the coastline of the Irish Sea (MAFF, 1977-1989)	60

Page

Chapter 2

2.1 Location map of sampling sites along the coast of south west Scotland 71

2.2 Southwick 72

2.3 Farnel corer used to collect samples 75

2.4 Wigtown 77

2.5 Creetown 80

2.6 Ordcharton 81

2.7 Kippford 82

2.8 Carse Bay 85

2.9 Efficiency Calibration Curve for Detector 1.4 Geometry 8 90

2.10 Electrolysis cell used for plating planchettes during analysis for plutonium isotopes 103

2.11 Apparatus used in the Flow Desorption Experiment 114

2.12 Filtration equipment used in the Flow Desorption Experiment 115

2.13 Experimental apparatus used to extract caesium from leaching solutions in the Flow Desorption Experiment 116

Chapter 4

4.1 Concentration profiles of radionuclides for sediment core SC1 collected from Southwick merse 8/12/89 167

4.2 Concentration profiles of radionuclides for sediment cores SC2 collected from Southwick merse 21/3/90 168

4.3 Temporal variations in Annual Discharges from Sellafield 172

4.4 Plot of natural log of unsupported ^{210}Pb concentration versus depth in core SC1 173

4.5 Sediment chronology for core SC1 produced by the 2.4cm y^{-1} sedimentation rate. Assuming an error of 15% 175

4.6 Sediment $^{238}Pu/^{239+240}Pu$ activity ratios for SC1 decay corrected to time of deposition plotted with the corresponding annual discharge activity ratios 179

4.7 $^{238}Pu/^{239+240}Pu$ activity ratios (decay corrected to time of deposition) for sediment sections 1) SC1 and 2) NCS862 along with corresponding data for 3) Maryport Harbour cores (Kershaw *et al.*, 1990) surface sediment from 4) Newbigging (Hetherington, 1975; Hunt, 1985) and 5) the Sellafield discharge (BNFL, 1977-1989) 180

4.8 $^{134}Cs/^{137}Cs$ activity ratio for Core SC1 decay corrected to time of deposition, plotted against the corresponding activity ratios for the Sellafield annual discharges 182

4.9 $^{134}Cs/^{137}Cs$ activity ratios for Core SC1 decay corrected to time of deposition, with corresponding activity ratios in the annual discharge and an amended ratio for SC1 which brings the maximum sediment ratio value into agreement with the corresponding ratio value in the Sellafield discharge 183

4.10 $^{134}Cs/^{137}Cs$ activity ratios for core SC1 decay corrected to time of deposition and normalised to the integrated discharge ratio from Sellafield 185

4.11 $^{241}Am/^{239+240}Pu$ activity ratio for core SC1 normalised to (1) Annual Discharge, (2) Annual Discharge plus in-situ ingrowth and (3) Integrated Discharge plus ingrowth 186

4.12a $^{241}Am/^{239+240}Pu$ activity ratio for core NCS862 normalised to (1) Annual Discharge, (2) Annual Discharge plus in-situ ingrowth and (3) Integrated Discharge plus ingrowth 189

4.12b $^{241}Am/^{239+240}Pu$ activity ratio for the Maryport Core normalised to (1) Annual Discharge, (2) Annual Discharge plus ingrowth and (3) Integrated Discharge plus ingrowth 189

4.13 $^{137}Cs/^{241}Am$ activity ratio core SC1 normalised to (1) Annual Discharge, (2) Annual Discharge plus ingrowth and (3) Integrated Discharge plus ingrowth 190

4.14 Natural log of sediment $^{239+240}Pu$ concentration SC1, decay corrected to time of deposition, divided by the integrated $^{239+240}Pu$ discharge from Sellafield 193

Page

4.15 Natural log of sediment ^{241}Am concentration SC1, decay corrected to time of deposition, divided by integrated of ^{241}Am plus ingrowth from ^{241}Pu from Sellafield 195

4.16 Natural log of sediment ^{137}Cs concentration SC1, decay corrected to time of deposition, divided by Integrated ^{137}Cs discharges from Sellafield 196

4.17 Model curves for temporal variations in relative $^{239+240}Pu$ concentrations in Irish Sea sediments 199

4.18 Model curves for temporal variations in relative concentrations of ^{241}Am in Irish Sea sediment 200

4.19 Model curves for temporal variations in relative concentrations of ^{137}Cs in Irish Sea sediment 201

4.20 Model prediction for ^{137}Cs using re-calculated sedimentation rate 2.95 cm y^{-1}, data normalised to 1977 ratio between sediment and model curve 202

4.21 Model prediction for ^{241}Am using the re-calculated sedimentation rate 2.95 cm y^{-1}, peak in model curve (1976) normalised to peak in sediment concentration (1974) 203

4.22 Model prediction for $^{239+240}Pu$ using re-calculated sedimentation rate of 2.95 cm y^{-1}, peak in model curve (1978) normalised to peak in sediment curve (1978) 204

4.23 Radionuclide concentrations for the 0-15 cm samples from Creetown transect T1 collected 28/8/90 207

4.24 Radionuclide and Isotope activity ratios for 0-15 cm samples from Creetown transect T1 208

4.25 Radionuclide concentrations for 15-30 cm samples from Creetown transect T1, collected 28/8/90 209

4.26 Radionuclide and Isotope activity ratios for 15-30 cm samples from Creetown transect T1 212

4.27 The lateral distribution pattern of ^{137}Cs within the 0-15 cm, 15-30 cm and the combined total in the 0-30 cm depth interval for the Creetown transect T1 214

4.28a The ^{137}Cs inventories in the 0-15 cm, 15-30 cm and 0-30 cm depth intervals for the Creetown transect T1 216

Page

4.28b The ^{241}Am inventories in the 0-15 cm, 15-30 cm and 0-30 cm depth intervals for the Creetown transect T1. 216

4.28c The $^{329+240}Pu$ inventories in the 0-15 cm, 15-30 cm and 0-30 cm depth intervals for the Creetown transect T1 217

4.29 ^{137}Cs, ^{134}Cs and ^{241}Am concentrations from the 0-15 cm samples from Wigtown transect T1 collected 27/8/90 219

4.30 $^{134}Cs/^{137}Cs$ and $^{137}Cs/^{241}Am$ activity ratios of 0-15 cm samples from Wigtown transect T1 220

4.31 Radionuclide concentrations and activity ratios for 15-30 cm samples from Wigtown transect T1 221

4.32a The ^{137}Cs inventories for the 0-15 cm, 15-30 cm and 0-30 cm depth intervals from Wigtown transect T1 225

4.32b The ^{241}Am inventories for the 0-15 cm, 15-30 cm and 0-30 cm depth intervals from Wigtown transect T1 225

4.33 Radionuclide concentrations for 0-15 cm samples from Southwick transect T1, collected 25/7/91 226

4.34 Radionuclide and Isotope activity ratios for 0-15 cm samples from Southwick transect T1 227

4.35 Radionuclide concentrations for 15-30 cm samples from Southwick transect T1, collected 25/7/91 228

4.36 Radionuclide and Isotope activity ratios for 15-30 cm samples from Southwick transect T1 232

4.37a The ^{137}Cs inventories for the 0-15 cm, 15-30 cm and 0-30 cm depth intervals from Southwick transect T1 233

4.37b The ^{241}Am inventories for the 0-15 cm, 15-30 cm and 0-30 cm depth intervals from Southwick transect T1 233

4.37c The $^{239+240}Pu$ inventories in the 0-15cm, 15-30 cm and 0-30 cm depth intervals for Southwick transect T1 234

4.38 Radionuclide concentrations for 0-15 cm samples from Orchardton transect T1 collected 29/8/90 237

4.39 Radionuclide and Isotope activity ratios of 0-15 cm samples from Orchardton transect T1 238

Page

4.40 Radionuclide concentrations for 15-30 cm samples from Orchardton transect T1 239

4.41 Radionuclide and Isotope activity ratios for 15-30 cm samples from Orchardton transect T1 241

4.42a The ^{137}Cs inventories for the 0-15 cm, 15-30 cm and 0-30 cm depth intervals for Orchardton transect T1 242

4.42b The ^{241}Am inventories from the 0-15 cm, 15-30 cm and 0-30 cm depth intervals for Orchardton transect T1 242

4.43 Radionuclide concentrations for 0-15 cm samples from Kippford transect T1, collected 28/8/90 244

4.44 Radionuclide and Isotope activity ratios of 0-15 cm samples from Kippford transect T1 245

4.45 Radionuclide concentrations and isotope activity ratios for 15-30 cm samples from Kippford transect T1 246

4.46a The ^{137}Cs inventories in the 0-15 cm, 15-30 cm and 0-30 cm depth intervals for Kippford transect T1 247

4.46b The ^{241}Am inventories in the 0-15 cm, 15-30 cm and 0-30 cm depth intervals for Kippford transect T1 247

4.47 Radionuclide concentrations of 0-15 cm samples from Carse Bay transect T1 collected 15/8/91 249

4.48 Radionuclide and Isotope activity ratios of 0-15 cm samples from Carse Bay transect T1 250

4.49 Radionuclide concentrations in 15-30 cm samples from Carse Bay transect T1 251

4.50 Radionuclide and Isotope activity ratios for 15-30 cm samples from Carse Bay transect T1 253

4.51a The ^{137}Cs inventories for the 0-15 cm, 15-30 cm and 0-30 cm depth intervals from Carse Bay transect T1 254

4.51b The ^{241}Am inventories for the 0-15 cm, 15-30 cm and 0-30 cm depth intervals from Carse Bay transect T1 254

4.52 The maximum, minimum and mean ^{137}Cs concentrations within the 0-15 cm depth intervals of the transects collected along the coast of the Solway Firth 257

Page

4.53 The maximum, minimum and mean ^{241}Am concentrations in the 0-15 cm depth intervals from the transects collected along the coast of the Solway Firth 258

4.54 The maximum, minimum and mean ^{137}Cs inventories within the transects collected along the coast of the Solway Firth 262

4.55 The maximum, minimum and mean ^{241}Am inventories for the merse transects collected along the coast of the Solway Firth 263

4.56 Concentrations of radionuclides in Southwick T2 5m 266

4.57 Concentrations of radionuclides in Southwick T2 10m 266

4.58 Radionuclide concentrations in Southwick T2 20m 270

4.59 Radionuclide concentrations in Southwick T2 30m 270

4.60 Concentrations of radionuclides in Southwick T3 5m 273

4.61 Comparison of the ^{137}Cs concentration profiles for transect T2 (core) and transect T3 (section) at a location of 5m inland from the MHWM at Southwick Water 275

4.62 Model prediction for ^{137}Cs in Southwick section T3 5m (T3.5) using the sedimentation rate of 1.88 cm y^{-1}, data normalised to ratio between sediment (1979) and the model (1978) 276

4.63 Concentrations of radionuclides in Southwick T3 10m 278

4.64 Comparison of the concentration profiles produced by transect T2 (core) and transect T3 (section) at a location of 10 m inland from the MHWM at Southwick Water 279

4.65 Model prediction for ^{137}Cs in Southwick section T3 10 m (T3.10) using the sedimentation rate of 1.46 cm y^{-1}, data normalised to ratio between sediment (1980) and the model (1978) 281

4.66 Concentrations of radionuclides in Southwick T3 15m 284

4.67 Depth of occurrence of ^{137}Cs sub-surface maxima from Southwick transect T3 285

4.68 Schematic model of the component zones within the merse 288

4.69 Box model of supply routes of sediment to the merse deposits 288

Page

4.70 Major plutonium associations in section SC1 300

4.71 Variation in LOI content within sediment cores SC1 and S3.10 collected from Southwick merse 302

4.72 K_D values (log scale) derived from the leaching of a) 0-5 cm and b) 40-45 cm sediment samples with Freshwater 307

4.73 K_D values (log scale) derived from the leaching of a) 0-5 cm and b) 40-45 cm sediment samples with ground water (field drain) . 308

4.74 K_D values (log scale) derived from the leaching a) 0-5 cm and b) 40-45 cm sediment samples with saltwater 310

4.75 Range of K_D values (log scale) obtained from m leaching 0-5 cm depth interval with various aqueous media 312

4.76 Range of K_D values (log scale) obtained from leaching 40-45 cm depth interval with various aqueous media 312

4.77 Concentration profiles of ^{133}Cs, Fe, Br and Sm from sediment samples form SCI 319

4.78 Concentration profiles of ^{133}Cs, Fe, Br and Sm from sediment samples from S3.10 320

LIST OF PLATES

Plate		Page
1.1	Rotational slipping	39
1.2	Slumping and undercutting	39
1.3	Slumping and undercutting	40
1.4	Slumping and undercutting	40
2.1	Photograph shows collection of section SC1 from the MHWM of the merse at Southwick Water	73
2.2	Photograph shows the collection of section SC2 from the bank of the Southwick Water	74
2.3	Illustrating the elevation of the MHWM and flat topography of Wigtown merse	78
2.4	Illustrates the slumping of the banks along the saltmarsh Creeks at Wigtown merse	78
2.5	Illustrates the vertical cliff face of the merse at Creetown	83
2.6	Illustrates the merse at Kippford	83
2.7	Illustrates the topography and vegetation cover present at Southwick Water. The two figures represent the location of transect T1	84
2.8	Vertical face of soil pit from which samples for transect T3 were collected	87
2.9	Collection of samples from Transect T3 Southwick merse	87

DECLARATION

Except where specific reference is made to other sources, the work presented in this thesis is the original work of the author. It has not been submitted, in part or in whole, for any other degree.

Certain of the results have been published elsewhere.

Robert L Allan

ACKNOWLEDGEMENTS

This work says more about what I am not rather than what I am, that it has got to this stage owes much to the efforts and persistence of my supervisors. I would like to formally thank Dr G T Cook, Dr I D Pulford and most especially Dr A B MacKenzie for their invaluable help and encouragement. Without their supervision this thesis would not have been completed. They had faith that my arts based background would not be a hindrance to successfully completing this research. I hope I have come some way in justifying that faith.

I owe much gratitude to the personnel at SURRC, both staff and students for their help and encouragement. However, I would especially like to thank Dr P McDonald, my 4th supervisor, and Mrs (Dr) Tracy Shimmield for her patience when teaching me basic computing skills. I would like to thank Mrs M Kerr and Ms I Woodburn for their help and advice when formatting this text.

I would like to thank English Natural Heritage for permission to reproduce their maps. My thanks also to Dr A Hall, Mr D Turner and Mr M McLeod from the Department of Geology and Applied Geology at the University of Glasgow for their analysis of sediment mineralogy.

I would like to thank NERC for providing the funding which enable me to undertake this research. I must thank Mr B W Gibson for producing the diagrams and for his support throughout this research.

Finally, I would like to thank my family for their support and especially my mother for putting up with my chaotic filing system.

I would like to dedicate this work to my late father who died before it was completed.

William Wilson Allan

1927-1992

a friend who is sadly missed

ABSTRACT

This thesis describes a study of the distribution and geochemical behaviour of ^{137}Cs, ^{241}Am and $^{239+240}Pu$ within the floodplain deposits of south west Scotland. These sediments have been contaminated with low level effluent discharged from BNFL's reprocessing plant at Sellafield on the Cumbrian coast.

The study establishes that the dominant supply mechanism of anthropogenic radionuclides to the floodplain is via on-shore transfer of contaminated particulate material which has been mathematically modelled.

A series of lateral transects across the floodplain has confirmed previous observations of highest concentrations furthest inland, illustrating the relationship between particle size and radionuclide concentration. The inventories observed for ^{137}Cs were of the order of $\sim 10^6$ to 10^7 Bq m^{-2} and were somewhat higher than previously published data.

The vertical distribution of radionuclides was investigated at Southwick merse and indicated a declining depth of occurrence of maximum radionuclide concentrations with distance inland. The observations from a series of transects, using a variety of sample collection methods permitted the construction of a schematic model of the merse. This model identified three distinct zones within the floodplain and enabled estimation of the total inventory for the coastline of south west Scotland. By these estimates less than 1% of the total environmental inventory of ^{137}Cs discharged from Sellafield has been returned on-shore.

Speciation studies on the availability of ^{137}Cs and $^{239+240}Pu$ indicate that ^{137}Cs is strongly retained within the residual phase of the sediment and that $^{239+240}Pu$ exhibits slightly enhanced availability, being associated with the organics and secondary Fe/Mn mineral phases. Evidence suggests that despite the increased environmental availability of $^{239+240}Pu$, both these radionuclides and ^{137}Cs are not

generally in a form which is available for plant uptake.

Flow desorption studies have indicated that ^{137}Cs is tightly bound to the sediment particles producing a K_D of $\sim 10^5$ lkg^{-1}.

CHAPTER 1

ANTHROPOGENIC RADIONUCLIDES WITHIN THE IRISH SEA BASIN

1.1 INTRODUCTION

The basic rationale for this research was to provide an improved understanding of the spatial distribution and geochemical behaviour of pollutant radionuclides discharged into the marine environment from the British Nuclear Fuels plc (BNFL) nuclear fuel reprocessing facility at Sellafield (Fig 1.1). The Sellafield plant is the largest facility of its kind in the United Kingdom and, as such, is the dominant source of anthropogenic radionuclides within the confines of the Irish Sea basin. It is of fundamental importance to increase our awareness of the environmental consequences of pollutant discharges particularly when assessing the possible exposure risks to mankind. The present research was centred upon the floodplain sediments of the Solway Firth which have been contaminated with Sellafield-derived radionuclides.

1.1.1 The Sellafield Nuclear Fuel Reprocessing Plant

Operations at Sellafield, formerly called Windscale, have been an integral part of Britain's nuclear energy programme since 1952. The plant's main function at present is as a facility for the recovery of unburnt, fissile ^{235}U and ^{239}Pu from irradiated nuclear fuel. Sellafield has been primarily concerned with reprocessing irradiated fuel from Magnox reactors, however, the plant is also capable of reprocessing Oxide fuels used in Advanced Gas Cooled Reactors (AGRs) and Light Water Reactors (LWRs).

Since reprocessing of irradiated fuel started at Sellafield in 1952, more than 2.5×10^4 tonnes of Magnox fuel and about 100 tonnes of Oxide fuel have been reprocessed. Reprocessing involves separation of the fissile species (^{235}U,^{239}Pu) from waste, fission and activation, products and the cladding material of the spent fuel. These waste materials are highly radioactive and the operation consequently

Fig 1.1 Map showing the main establishments discharging liquid radioactive waste into the Irish Sea.

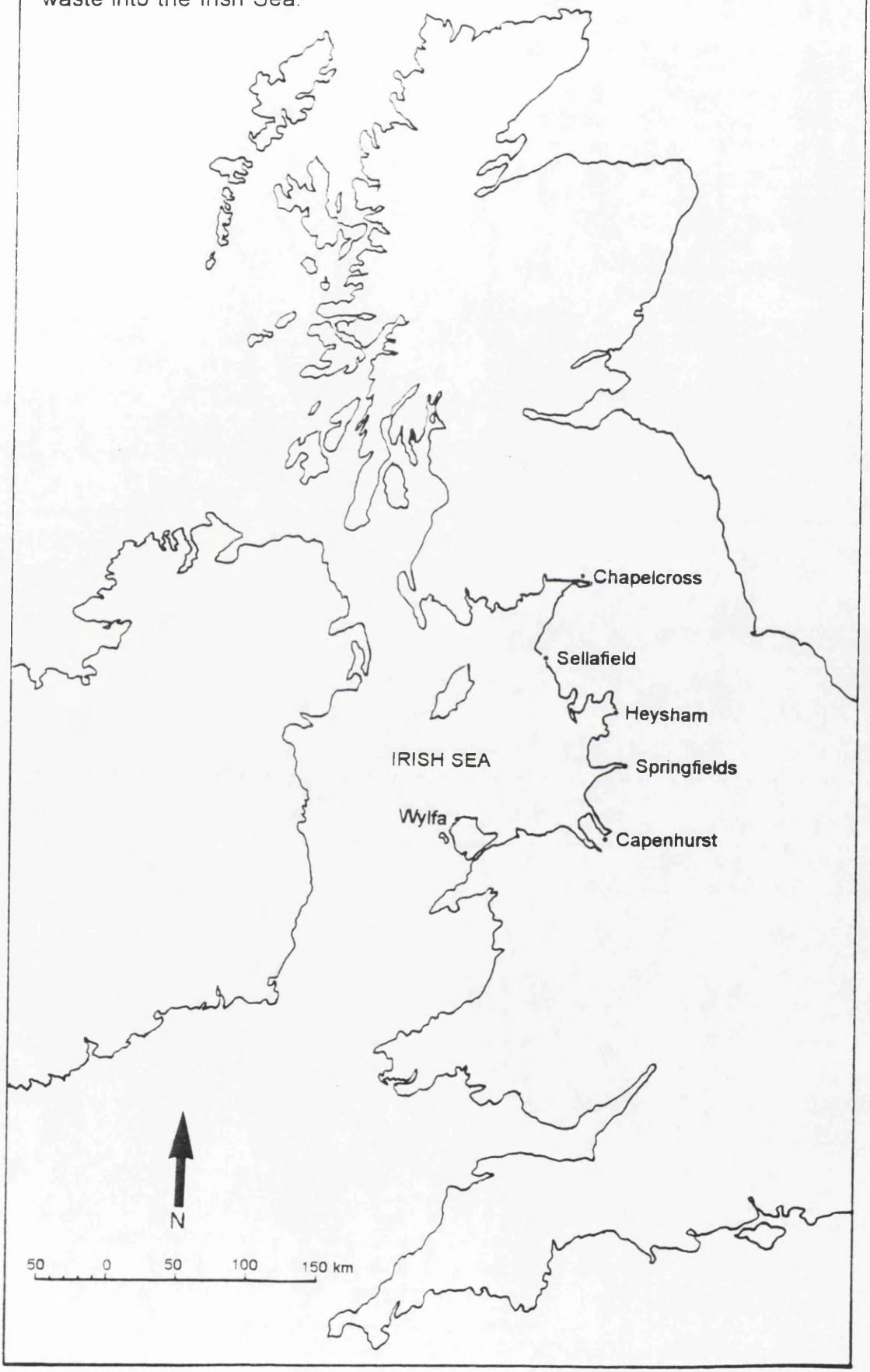

generates considerable quantities of radioactive waste in both solid and liquid form. For example, the Magnox fuel which underwent reprocessing in 1985 had a typical composition of 99.2% by weight residual uranium, 0.5% fission products and 0.3% plutonium (BNFL, 1985). The scheme for reprocessing Magnox fuel is outlined in Fig. 1.2. Fuel elements delivered to Sellafield from reactors have previously been stored underwater in ponds at the reactor sites to permit short-lived radionuclides to decay (BNFL, 1985). After a suitable storage period, the Magnox cladding is removed and the uranium rods are dissolved in nitric acid. The uranium and plutonium are separated, first from the fission products and then from each other by solvent extraction in mixer-settler tanks. The reprocessing of the 100 tonnes of Oxide fuel at Sellafield utilised the existing Magnox facilities, however, the requirements to reprocess irradiated fuel from the UK's AGRs and overseas facilities have resulted in the design and construction of the Thermal Oxide Fuel Reprocessing Plant (THORP) which was due to come into operation in 1993 pending the outcome of a Public Enquiry. The THORP plant will carry out all operations from receipt, storage and shearing of fuel, through chemical separation of uranium, plutonium and waste, to the production of uranium and plutonium in chemical forms suitable for fabrication into more nuclear fuel.

The solid and liquid radioactive waste produced during reprocessing operations is classified within high, intermediate or low level categories. High and intermediate level wastes are considered to be too highly radioactive for discharge into the environment and undergo specialised treatment to permit interim storage on-site until a suitable location is found for permanent disposal in an underground repository. To date, only low level wastes have been discharged into the environment from Sellafield. Low level wastes which are classified by BNFL as not exceeding a specific activity of 4 G Bq t^{-1} of α activity or 12 G Bq t^{-1} of β/γ activity (BNFL, 1986) are discharged as liquids to the sea, as gases to the atmosphere or disposed of as solids at BNFL's land storage site at Drigg (Fig. 1.8).

Fig 1.2 Flow diagram of the MAGNOX fuel reprocessing procedure at BNFL Sellafield (BNFL, 1985).

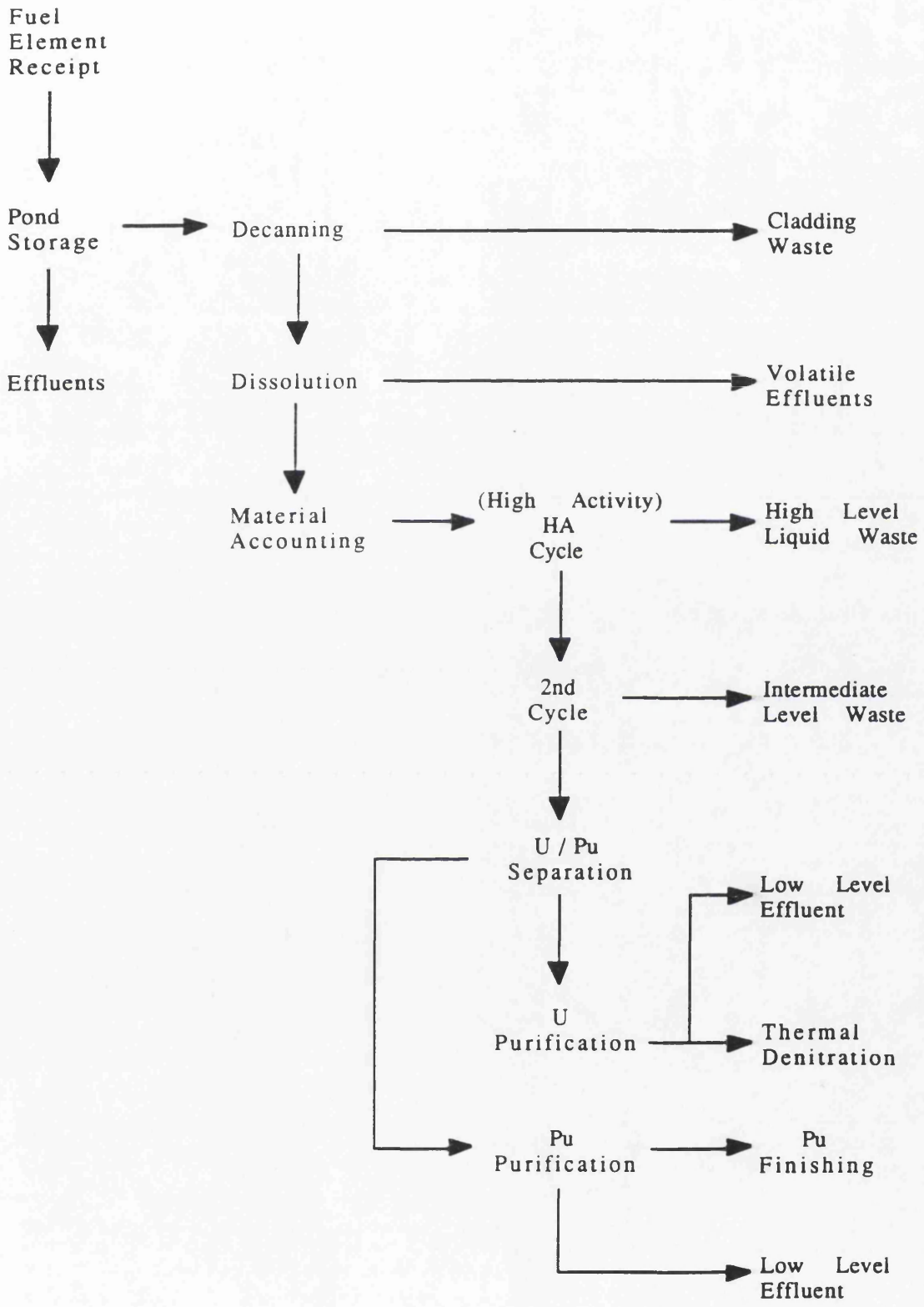

Liquid effluents which are discharged into the Irish Sea come from several sources, the principal being the storage pond water from the Magnox decanning plant which becomes contaminated with radionuclides from fuel elements stored there. The water is replaced continuously, with the contaminated fraction being directed to the Site Ion Exchange Plant (SIXEP) (Fig. 1.3) where, prior to discharge to the environment, it is passed through an array of sand filters and clinoptilite ion exchangers. This process removes the bulk of the fission and activation products, particularly radiocaesium and radiostrontium, from the effluent, incorporating these radionuclides in the crystal lattice structure of the alumino silicate material. Low level liquid waste from other parts of the site is diverted to the Salt Evaporator Plant, the residue being discharged into the sea after monitoring.

1.1.2 Discharge Data for Sellafield Liquid Radioactive Waste

In England, discharges of radioactive wastes must, by law, be within specific authorizations issued jointly by the Ministry of Agriculture, Fisheries and Food (MAFF) and the Department of the Environment (DOE). In the rest of the UK the appropriate Government departments issue the necessary documentation. These authorizations impose limitations on the methods of disposal and the quantities and the content of the waste permitted to be discharged. The authorizations also stipulate that records must be kept of the discharges. The relevant data for Sellafield, in a summarised form, are published in BNFL annual reports on Radioactive Discharges and Monitoring of the Environment (BNFL, 1971-90). These reports, together with those of BNFL's predecessor, the former production group of the United Kingdom Atomic Energy Authority (UKAEA) (UKAEA 1952-1970) constitute a comprehensive data set of Sellafield discharges. For example, the BNFL 1989 annual report (BNFL, 1989) lists 31 different radionuclides which are monitored on a daily basis. In addition, specifically identified under Schedule 3 of the Certificate of Authorization (30/6/86), are 15 longer-lived radionuclides which are discharged subject to both annual and quarterly limits. There are additional limitations imposed on the "total α" and "total β" activities which can be discharged (over any two day period). The Sellafield liquid effluent thus contains a complex mixture of radionuclides but the present research is concerned only with radiocaesium, plutonium and americium which are three of the most radiologically significant

Fig 1.3 Schematic diagram of the SIXEP processing plant at Sellafield.

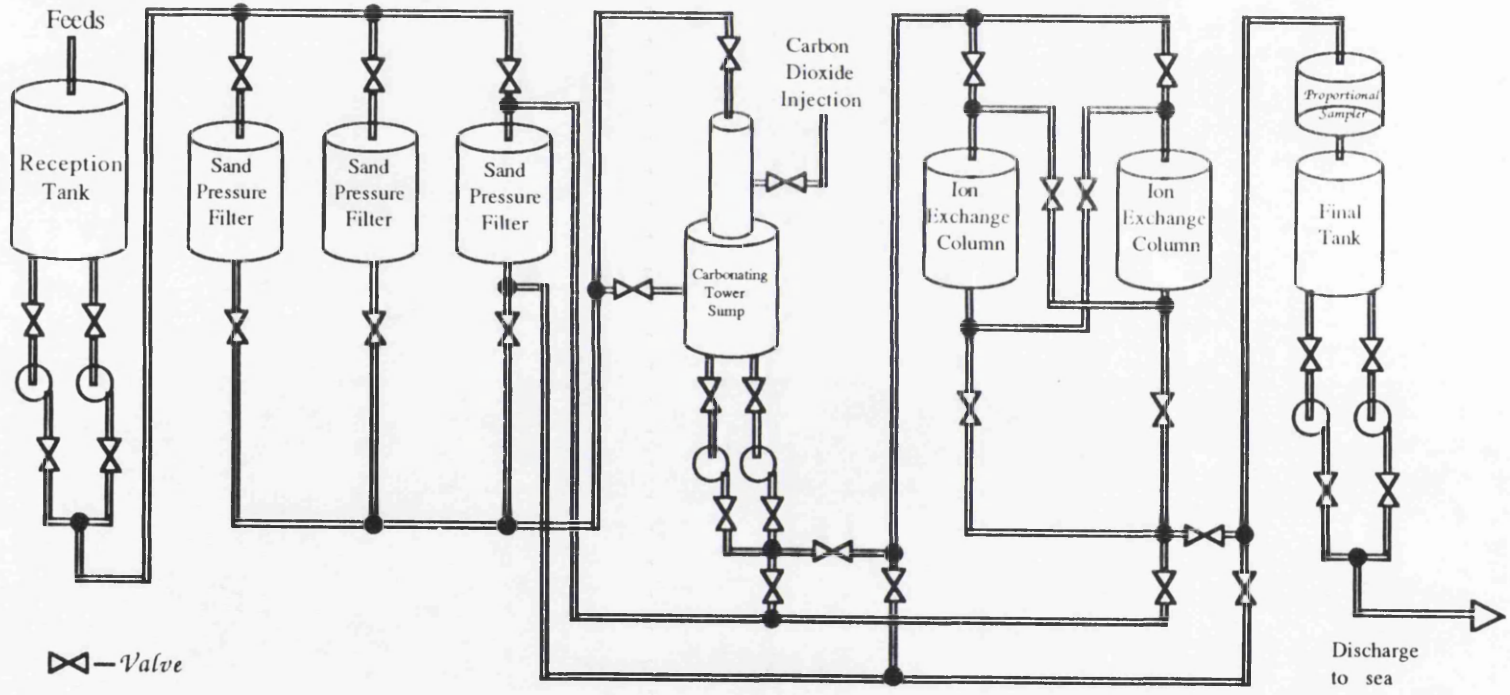

components of the waste.

The chemical nature of the low level liquid effluent which is discharged from Sellafield has not been extensively reported. Pentreath *et al.*, (1986) observed that the effluent from the fuel storage ponds and sea tanks is acidic and undergoes neutralisation by the addition of ammonia before discharge into the environment. They further indicated that the effluent consists of two phases, a particulate and an aqueous component, with the transuranics being primarily associated with the particulate portion which forms a brown floc within the neutralised liquid. A summarised version of the Sellafield discharge data for the radionuclides of interest in this study is presented as annual discharges in Table 1.1 and as integrated discharges in Table 1.2. It is apparent from Figs. 1.4 to 1.7, which show plots of temporal trends in the Sellafield discharges, that the quantities of ^{137}Cs, ^{134}Cs, $^{239+240}Pu$ and ^{241}Am released annually have varied considerably, with maximum discharges during the early to mid 1970's. The SIXEP plant, introduced in 1985, (outlined above) greatly reduced the quantities of ^{137}Cs discharged and the new Enhanced Actinide Removal Plant (EARP) will also reduce the marine discharges of plutonium and americium, once on stream in 1993 (BNFL, 1991). Future marine discharges will, however, increase during the 1990s due to the reprocessing of Oxide fuel from the UK and overseas reactors which has been stockpiled, awaiting completion and commissioning of THORP by 1993.

Appropriate nuclide and isotope activity ratios can be used to differentiate between Sellafield-derived waste and other anthropogenic sources. The use of these ratios has to be tempered by the knowledge that radionuclide activity ratios from any anthropogenic source are subject to alteration during environmental processes due to differences in chemical behaviour between radionuclides of different elements and physical mixing in the environment. Isotopic activity ratios (of high Z value nuclides) are unaffected by chemical fractionation, although, mixing with previous discharges or radionuclides from another source may mean that there is not a simple relationship between isotope activity ratios observed in the environment and those in the discharges. Despite the comprehensive data set for Sellafield discharges as detailed in the annual reports, there are certain prominent omissions. Particular radionuclides, especially the isotopes of plutonium, were not specifically identified in early reports.

Table 1.1 Annual Discharges from BNFL Sellafield Reprocessing Plant 1952-1990

YEAR	^{137}Cs (TBq)	$^{239+240}Pu$ (TBq)	^{241}Am (TBq)
1952	46	0.56	0.00
1953	46	0.52	0.00
1954	46	0.63	0.00
1955	21	0.70	0.00
1956	164	1.85	0.00
1957	138	1.70	0.00
1958	229	1.96	0.00
1959	73	2.18	0.00
1960	34	2.81	0.00
1961	40	4.70	0.00
1962	41	6.77	0.00
1963	14	8.36	0.00
1964	104	5.70	4.55
1965	110	7.18	8.10
1966	181	13.88	7.55
1967	150	18.09	17.09
1968	372	30.38	21.13
1969	444	30.16	14.43
1970	1154	35.08	18.94
1971	1325	55.54	37.67
1972	1289	57.13	80.18
1973	768	65.53	109.19
1974	4061	46.14	118.25
1975	5231	44.14	36.26
1976	4289	46.77	11.95
1977	4458	36.26	3.66
1978	4088	45.62	7.95
1979	2562	37.43	7.83
1980	2966	20.36	8.22
1981	2357	15.34	8.77
1982	2000	16.07	6.43
1983	1200	8.72	2.21
1984	434	8.23	2.25
1985	325	2.65	1.58
1986	18	2.04	1.24
1987	12	0.98	0.64
1988	12	1.00	0.75
1989	21	0.73	0.81
1990	5	0.24	0.19

Table 1.2 Integrated Discharges (Decay Corrected Cumulative Environmental Inventory) of ^{137}Cs, $^{239+240}Pu$ and ^{241}Am (including ingrowth from ^{241}Pu) from BNFL Sellafield

YEAR	^{137}Cs (TBq)	$^{239+240}Pu$ (TBq)	^{241}Am (TBq)
1952	46	0.56	0.00
1953	91	1.07	0.01
1954	135	1.70	0.01
1955	153	2.40	0.02
1956	313	4.25	0.03
1957	444	5.96	0.05
1958	663	7.92	0.08
1959	721	10.10	0.11
1960	738	12.91	0.14
1961	762	17.61	0.19
1962	785	24.38	0.29
1963	781	32.74	0.45
1964	867	38.44	5.25
1965	957	45.62	13.70
1966	1,116	59.49	21.76
1967	1,240	77.58	39.71
1968	1,584	107.96	62.33
1969	1,991	138.11	79.25
1970	3,087	173.18	101.91
1971	4,326	228.71	145.28
1972	5,501	285.83	233.51
1973	6,135	351.35	354.27
1974	10,022	397.48	486.37
1975	14,967	441.61	538.86
1976	18,870	488.37	568.15
1977	22,849	524.61	590.11
1978	26,375	570.22	617.65
1979	28,306	607.63	646.84
1980	30,589	627.97	676.97
1981	32,221	643.29	707.62
1982	33,463	659.34	735.59
1983	33,883	668.04	758.88
1984	33,538	676.25	781.67
1985	33,092	678.88	803.01
1986	32,354	680.9	823.06
1987	31,627	681.86	841.53
1988	30,917	682.84	859.18
1989	30,231	683.55	876.01
1990	29,546	683.77	

Figures illustrate the temporal variations in annual discharges from Sellafield

Fig 1.4

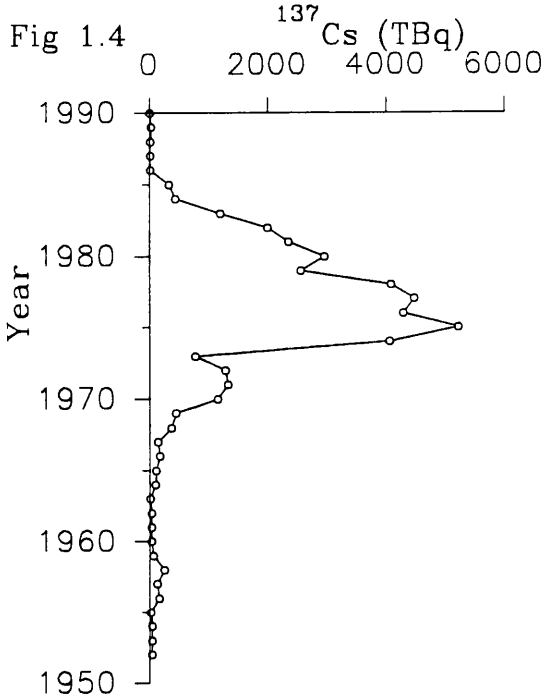

Fig 1.5

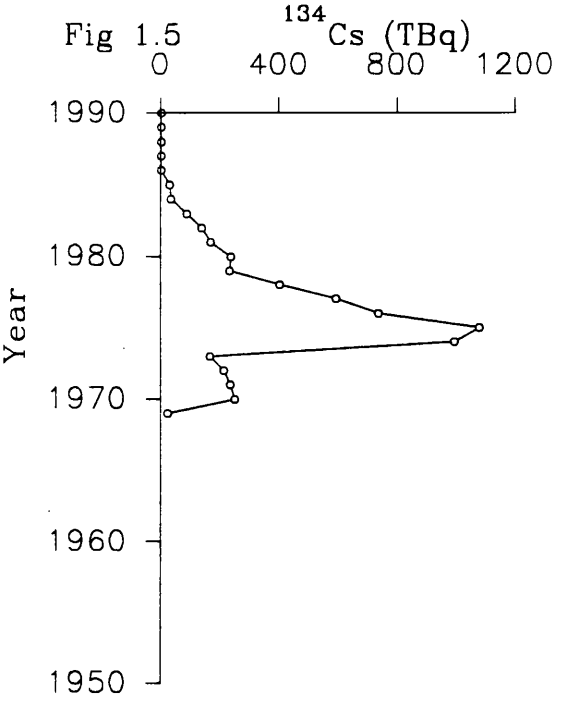

Fig 1.6

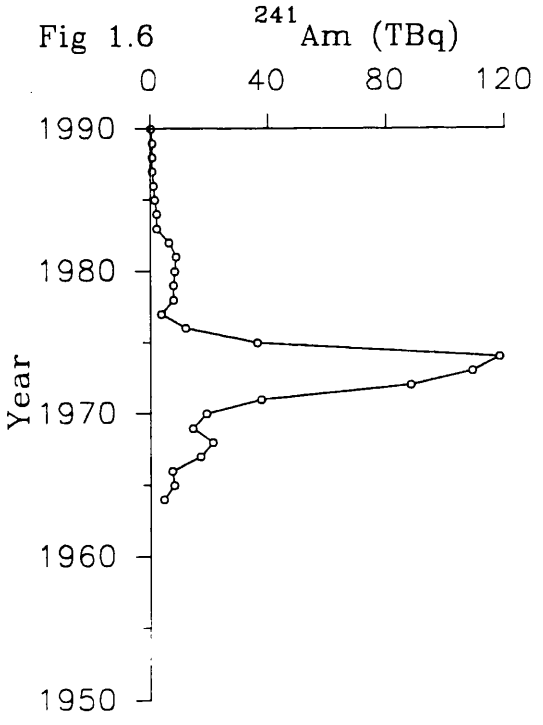

Fig 1.7

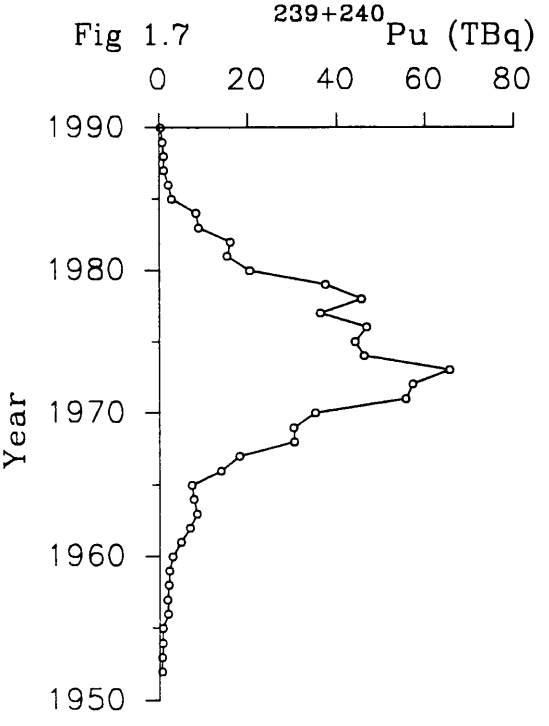

Prior to 1978, ^{238}Pu discharges were not reported separately, but were combined with $^{239+240}Pu$ and classified as Pu α. One approach to estimating ^{238}Pu discharges from Sellafield, adopted by Hetherington (1975), has been to analyse surface samples of intertidal sediment and thereby estimate annual discharges for plutonium isotopes. This approach has been extended by Kershaw *et al.*, (1990) using undisturbed sediment cores from Maryport Harbour, Cumbria. The authors compared the resultant depth profile with the Sellafield discharges to estimate ^{238}Pu discharge data back to 1959. Clearly, such an approach requires a direct relationship between the radionuclide concentration and isotope activity ratios in the sediment with those of the corresponding year's discharge. As discussed in detail later, however, this may be invalidated by any environmental process which is capable of distorting this relationship.

The caesium isotope data for the Sellafield discharges are more comprehensive. Discharges of the fission product ^{137}Cs have been recorded since 1952, while information for ^{134}Cs, an activation product, goes back to 1959 (Cambray, 1982; BNFL, 1971-1990). Table 1.3 illustrates the plutonium and caesium activity ratios for the Sellafield discharge.

The data for ^{241}Am presented in BNFL Annual Reports have to be used in conjunction with considerations of ingrowth of ^{241}Am from the decay of ^{241}Pu which is also present in the effluent.

$$^{241}Pu \xrightarrow[14.35y]{\beta^-} {}^{241}Am \xrightarrow[433y]{\alpha} {}^{237}Np$$

$$A_{Am} = \frac{\lambda Pu}{\lambda Am - \lambda Pu} (A_{Pu})o \left[e^{-\lambda Pu\, t} - e^{-\lambda Am\, t} \right]$$

Table 1.3 Isotope Activity Ratios for Liquid Effluent Discharged from BNFL Sellafield

YEAR	$^{238}Pu/^{239+240}Pu$	$^{134}Cs/^{137}Cs$
1969	NA	0.0518
1970	NA	0.2175
1971	NA	0.1781
1972	NA	0.1668
1973	NA	0.2161
1974	NA	0.2453
1975	NA	0.2067
1976	NA	0.1721
1977	NA	0.1326
1978	0.2705	0.0988
1979	0.3193	0.0917
1980	0.3379	0.0806
1981	0.3233	0.0713
1982	0.2925	0.0690
1983	0.3280	0.0742
1984	0.3159	0.0806
1985	0.2906	0.0923
1986	0.3039	0.0726
1987	0.3673	0.1017
1988	0.3800	0.0714
1989	0.3425	0.0604
1990	NA	0.0489

NA = Not Available

Despite the decline in Sellafield discharges during the 1980s and 1990s, the longevity (Table 1.4) and environmental behaviour of specific α and β emitting nuclides means that their inventories within the Irish Sea will be of significant environmental interest for many years to come.

If radioactive decay and ingrowth are taken into account it can be calculated that the Sellafield discharge had generated total environmental inventories by 1990 of about 3×10^4 T Bq of ^{137}Cs, 6.8×10^2 T Bq of $^{239+240}Pu$ and 8.9×10^2 T Bq of ^{241}Am (BNFL, 1977-89; NRPB, 1984).

Table 1.4 Decay Characteristics of Selected Radionuclides

Nuclide	Half Life (Year)	Decay Mode
^{137}Cs	30.18	$\beta\gamma$
^{134}Cs	2.06	$\beta\gamma$
^{238}Pu	87.71	α
^{239}Pu	24130	α
^{240}Pu	6570	α
^{241}Pu	14.35	β
^{241}Am	433	$\alpha\gamma$

(Lederer and Shirley, 1978)

1.2 ADDITIONAL SOURCES OF ANTHROPOGENIC RADIONUCLIDES TO THE STUDY AREA

Sellafield is not the only source of anthropogenic radionuclide pollution affecting the Irish Sea. Levels have been augmented by global fallout and other local sources. Atmospheric weapons testing, accidental releases and controlled emissions from nuclear facilities all contribute to the radionuclide inventory within the Irish Sea. Table 1.5 lists the various incidents and facilities which have contributed to the

radionuclide pollution of the Irish Sea.

Table 1.5 Global and localised sources of anthropogenic radionuclide emissions

Global	
Atmospheric Weapons Testing	1945-1963
SNAP-9A Satellite Burn-up	1964
Chernobyl Nuclear Accident	1986
Local	
Chapelcross Nuclear Power Station	
Heysham Nuclear Power Station	
Wylfa Nuclear Power Station	
Springfields Fuel Element Manufacturing Plant	
Capenhurst Uranium Enrichment Facility	

1.2.1 Local Sources of Pollutant Radionuclides to the Irish Sea other than Sellafield

Various local sources, other than Sellafield contribute anthropogenic radionuclides to the Irish Sea. A comparison of annual discharges from the principal contributors, however, illustrates that Sellafield is by far the dominant source (Table 1.6). The nuclear power station at Chapelcross on the Solway coast, near Annan (Figure 1.1), periodically discharges fuel storage pond water into the Solway Firth, but the activities discharged are several orders of magnitude lower than the corresponding Sellafield effluents.

The Springfields works near Preston, Lancashire, manufactures fuel for nuclear power stations. The plant's waste byproducts, which are discharged into the Ribble Estuary, are lower for total α activity by one order of magnitude than the Sellafield discharges and about the same for total β emitters. However, the β emitting radionuclides are the short-lived daughter products of uranium, namely ^{234}Th and ^{234}Pa. The radiological significance of the Springfields discharge is therefore low

compared to the impact that the Sellafield discharges have on the Irish Sea.

The other facilities which are authorised to discharge low level radioactive effluent into the Irish Sea, the uranium fuel enrichment plant at Capenhurst and the nuclear power stations at Heysham and Wylfa (Fig. 1.1) discharge negligible quantities compared with the magnitude of the Sellafield discharges.

1.2.2 Global Sources of Pollutant Radionuclides

It is estimated that, during the course of nuclear weapons tests from 1945-1963, approximately 1.33 x 10^4 T Bq of $^{239+240}$Pu and 1.26 x 10^6 T Bq of ^{137}Cs were introduced into the atmosphere. Little ^{241}Am was released directly to the atmosphere from nuclear weapons during the test period, however, substantial quantities of ^{241}Pu were released, the decay of which has subsequently led to *in-situ* growth of ^{241}Am in environments contaminated by weapons testing fallout. (Joseph *et al.*, 1971. Perkin and Thomas, 1980). In 1963 a treaty banning atmospheric testing of nuclear weapons came into effect and there has consequently been a massive reduction in deposition of fallout radionuclides from this source since then. In 1964, however, the accidental burn-up in the upper atmosphere of a United States' satellite powered by a SNAP-9A nuclear power system containing 1 kg of ^{238}Pu, resulted in widespread deposition of ^{238}Pu, especially in the Southern Hemisphere and led to a three fold increase in the global environmental content of this nuclide. (Hardy *et al.*, 1973). As a consequence of these incidents a background level of anthropogenic radionuclides has been deposited over the earth's surface.

Table 1.6 Comparison of Annual Discharges of Liquid Radioactive Effluent Sellafield, Chapelcross and Springfields (BNFL, 1990)

Nuclide	Annual Discharges TBq				
	1986	1987	1988	1989	1990
Sellafield					
Total α	4.4	2.2	2.1	2.7	2.16
Total β	118.0	89.2	81.3	101.0	70.9
^{134}Cs	1.3	1.2	0.95	1.73	1.15
^{137}Cs	17.9	11.8	13.3	28.6	23.5
Chapelcross					
Total α	0.0008	0.004	0.003	0.003	0.0005
Total β	0.09	0.5	0.17	0.22	0.11
^{134}Cs	0.001	0.005	0.0011	0.0015	0.0016
^{137}Cs	0.05	0.25	0.066	0.033	0.018
Springfields					
Total α	0.6	0.5	0.4	0.4	0.2
Total β	115	77	110	114	92
^{134}Cs	NA	NA	NA	NA	NA
^{137}Cs	NA	NA	NA	NA	NA

NA = Not Available

For UK latitudes, it has been estimated that the average inventory of fallout $^{239+240}Pu$ is 55 Bq m^{-2} in the top 30 cm of soils, while the corresponding ^{137}Cs inventory is 3,700 Bq m^{-2}, both estimates being standardised to a rainfall of 1000 mm y^{-1} (Cawse and Horrill, 1986).

In south west Scotland Baxter *et al.*, (1989) reported higher $^{239+240}Pu$ inventories than the national average, however, the results were not normalised to rainfall. The $^{239+240}Pu$ values observed to a depth of 30 cm ranged from 66-319 Bq m^{-2} producing a mean inventory of 106 Bq m^{-2}. However, the ^{137}Cs inventories with appropriate decay correction, attributed to fallout pre-Chernobyl, range from 2000-7000 Bq m^{-2} which are similar to the national average. The enhanced radionuclide inventories within south west Scotland reflect the meterological conditions which prevail in this area. The maritime climate with frequent and intense precipitation combines with prevailing south westerly winds to produce conditions conducive for deposition of airborne material.

It is possible to identify clearly the particular source of plutonium contamination using the $^{238}Pu/^{239+240}Pu$ activity ratio. Hardy *et al.*, (1973) reported an average $^{238}Pu/^{239+240}Pu$ activity ratio for weapons testing fallout of 0.03 in environmental materials between latitudes 50° and 60°N for 1970-71. This compares with a $^{238}Pu/^{239+240}Pu$ activity ratio of about 0.3 for the Sellafield liquid effluent discharges between 1978-82 (BNFL, 1979-1983). McDonald *et al.*, (1992) reported ^{238}Pu, $^{239+240}Pu$ activity ratios, for the top 30 cm of soils in south west Scotland in the range 0.017-0.073. The majority of sites were consistent with fallout levels (0.03) but one outlier exhibited an enhanced ratio suggesting an input of Sellafield waste.

The accident at the Chernobyl nuclear power plant in the Ukraine on 26th April 1986 is estimated to have released some 2×10^{18} T Bq of fission and activation products into the atmosphere (Clark and Smith, 1988). A significant proportion of this material was transported north westwards by the prevailing winds, travelling over Scandinavia and north west Europe. Deposition of radionuclides including ^{134}Cs and ^{137}Cs occurred primarily during precipitation, with enhanced accumulation in areas which experienced frequent and intense rainfall within days of the accident. Clark and Smith (1988) estimate that the United

Kingdom received 300 T Bq of ^{137}Cs, or 3% of the total Chernobyl release. Variations in the rainfall pattern and the trajectory of the Chernobyl plume resulted in a heterogeneous deposition of radionuclides in the UK. South west Scotland and Cumbria received high levels of deposition, with McDonald *et al.*,(1992) reporting Chernobyl ^{137}Cs inventories of up to 38,700 Bq m^{-2}. Again, the isotope activity ratios can clearly identify the source of the pollutant radionuclides. The Chernobyl contamination had a characteristic $^{134}Cs/^{137}Cs$ activity ratio of about 0.6 (Clark and Smith, 1988) compared with a 0.07 ratio for Sellafield waste discharges in 1986. McDonald *et al.*, (1992) have examined the impact of Chernobyl radiocaesium on the radionuclide inventory of south west Scotland. They report that the majority of their study sites received an almost two fold increase in ^{137}Cs levels due to Chernobyl fallout. The values observed for ^{137}Cs inventories ranged from 3,750 to 38,700 Bq m^{-2}, with a mean 13,000 Bq m^{-2} in the top 30 cm of the soil. The $^{134}Cs/^{137}Cs$ activity ratios ranged from 0.12-0.4 clearly identifying the main source as Chernobyl fallout.

The Irish Sea, with a surface area of approximately 900 km^2, was also subject to variations in Chernobyl fallout deposition. Concentrations of ^{137}Cs in seawater sampled in early May 1986 were enhanced at particular locations (MAFF, 1986). Dispersion of the fallout radiocaesium within the Irish Sea appears to have been rapid, with a substantial decline in concentrations recorded over a period of days. At Southerness, ^{137}Cs concentrations in seawater samples collected between 4th May and 1st July declined from 5.4 Bq l^{-1} to 1.2 Bq l^{-1} (MAFF, 1986). The $^{134}Cs/^{137}Cs$ activity ratios ranged from 0.08 to 0.54. These trends reflect the dispersion of Chernobyl fallout from this location and activity ratio values tending towards the Sellafield liquid discharge value prevalent in the area at that time.

The French nuclear fuel reprocessing facility at Cap de la Hague in Normandy discharges low level liquid effluent into the English Channel. As Table 1.7 illustrates, the activities discharged into the marine environment between 1966 and 1982 for ^{134}Cs and ^{137}Cs are an order of magnitude lower than the corresponding Sellafield discharges (Calmet and Guegueniat, 1985). These discharges have a negligible impact on the radionuclide inventories within the Irish Sea due to the prevailing tides and currents transporting the pollutants north east along the French

coastline through the English Channel and into the North Sea (Salomon *et al.*, 1991).

Table 1.7 Annual Discharges of ^{134}Cs and ^{137}Cs from Cap de la Hague to the Marine Environment 1966-1982 (Calmet and Guegueniat, 1985)

Year	^{134}Cs (T Bq)	^{137}Cs (T Bq)
1966	0.281	7.289
1967	1.628	16.391
1968	3.034	28.416
1969	1.295	20.165
1970	13.838	89.133
1971	48.026	242.000
1972	6.142	32.930
1973	8.399	69.264
1974	9.028	55.981
1975	4.255	34.447
1976	6.549	34.743
1977	9.546	50.764
1978	7.844	39.035
1979	3.574	22.533
1980	3.925	26.758
1981	5.957	38.591
1982	8.412	50.535

1.3 SEDIMENTS OF THE IRISH SEA

The textural composition of the sediments of the Irish Sea is diverse, ranging from fine silts and clays to coarse grained sands and gravels and this has a fundamental impact on the fate of pollutants, including radionuclides, which are discharged into this environment. Clays and silts have a large surface area per unit weight and provide suitable surface characteristics for adsorption processes, resulting in a greater affinity for the uptake of trace elements by these fine sediments than by

coarse-grained material such as sand (Hamilton and Clarke, 1984). Therefore the spatial distribution and transportation of the different types of sediment have a direct bearing on the aqueous phase/solid phase partitioning and dispersion of anthropogenic radionuclides discharged into the Irish Sea. The following section provides a brief description of the nature and distribution of sediments in the Irish Sea and of the processes affecting them.

The Irish Sea comprises an area of nearly 900 km^2 in an elongate basin which is almost enclosed by the coastlines of north Wales, north west England, south west Scotland and the east coast of Ireland. In the north, the Irish Sea is connected to the Atlantic Ocean through the narrow North Channel between Scotland and Northern Ireland and in the south via the St George's Channel between south Wales and Ireland (Fig 1.8). The Irish Sea can be divided into two distinct zones according to depth. The segment lying east of the Isle of Man is relatively shallow with a water depth ranging between 20-40 m, while west of the Isle of Man, a deep trench runs north to south, with bathymetry ranging from 100-180 m.

Smith *et al.*, (1980) briefly reviewed the geological structure of the Irish Sea stating that the area consists of a number of sedimentary basins, formed by subsidence due to faulting, which contain Carboniferous and Permo Triassic rocks, overlain by sediments deposited since the Pleistocene period (1.6×10^6 years B.P. to 10^4 B.P.). During the glacial retreat from 12,000 B.P., a series of proglacial lakes was formed, resulting in the deposition of highly stratified lacustrine sediments. The discharge rivers from these lakes produced fluvioglacial deposits of well-sorted, rounded material. These processes produced the sedimentary deposits which have been reworked by tides and currents, during the intervening millennia, to form the present day sediment distribution pattern.

Early research on Holocene sedimentation (10^4 years B.P. to present) was carried out by Belderson (1964), Belderson and Stride (1969) and Cronin (1969,1970). Cronin (1969) stated that the sediments throughout the whole of the Irish Sea are subject to wave and current action and, when combined with the shallow nature of the basin, these processes play a prominent part in sediment redistribution. Strong currents, especially around the St. George's Channel and the North Channel,

Fig 1.8 Map showing the location of Sellafield within the Irish Sea Basin and its proximity to the North Channel and St. Georges Channel in the south.

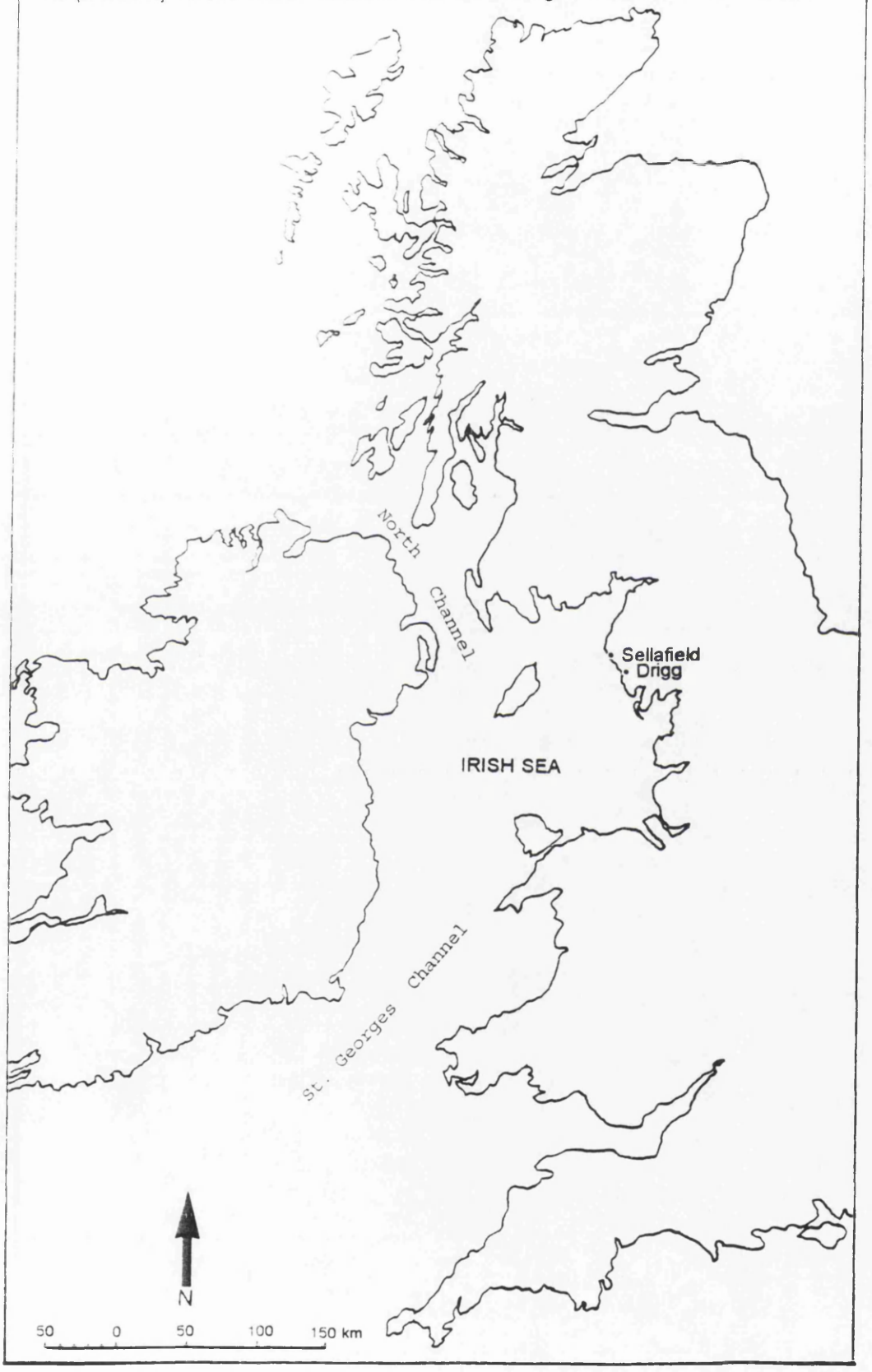

Fig 1.9 Suggested bed transport paths in the Irish Sea according to Belderson (1964)

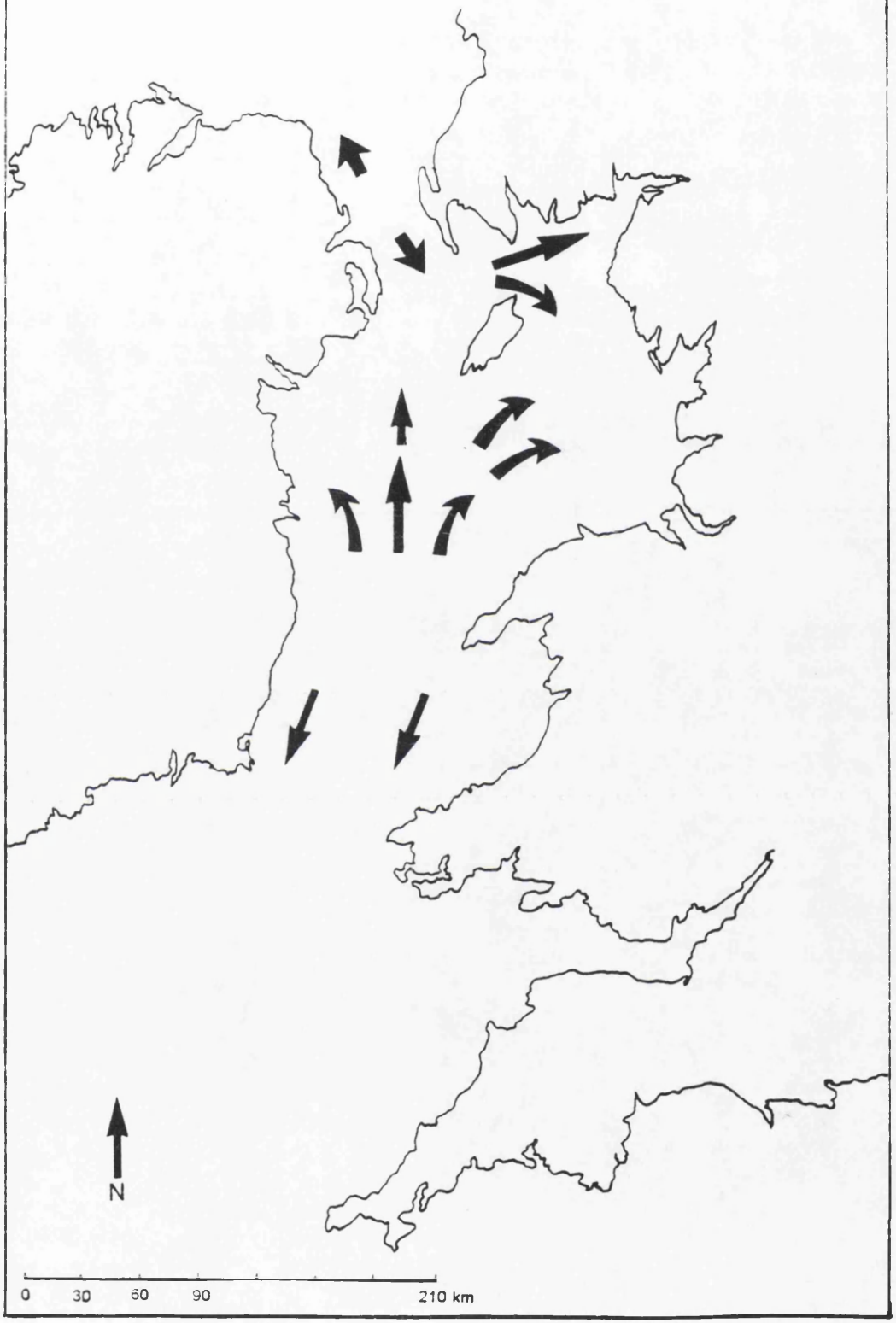

Fig 1.10 Surface sediment distribution within the Irish Sea according to Pantin (1978)

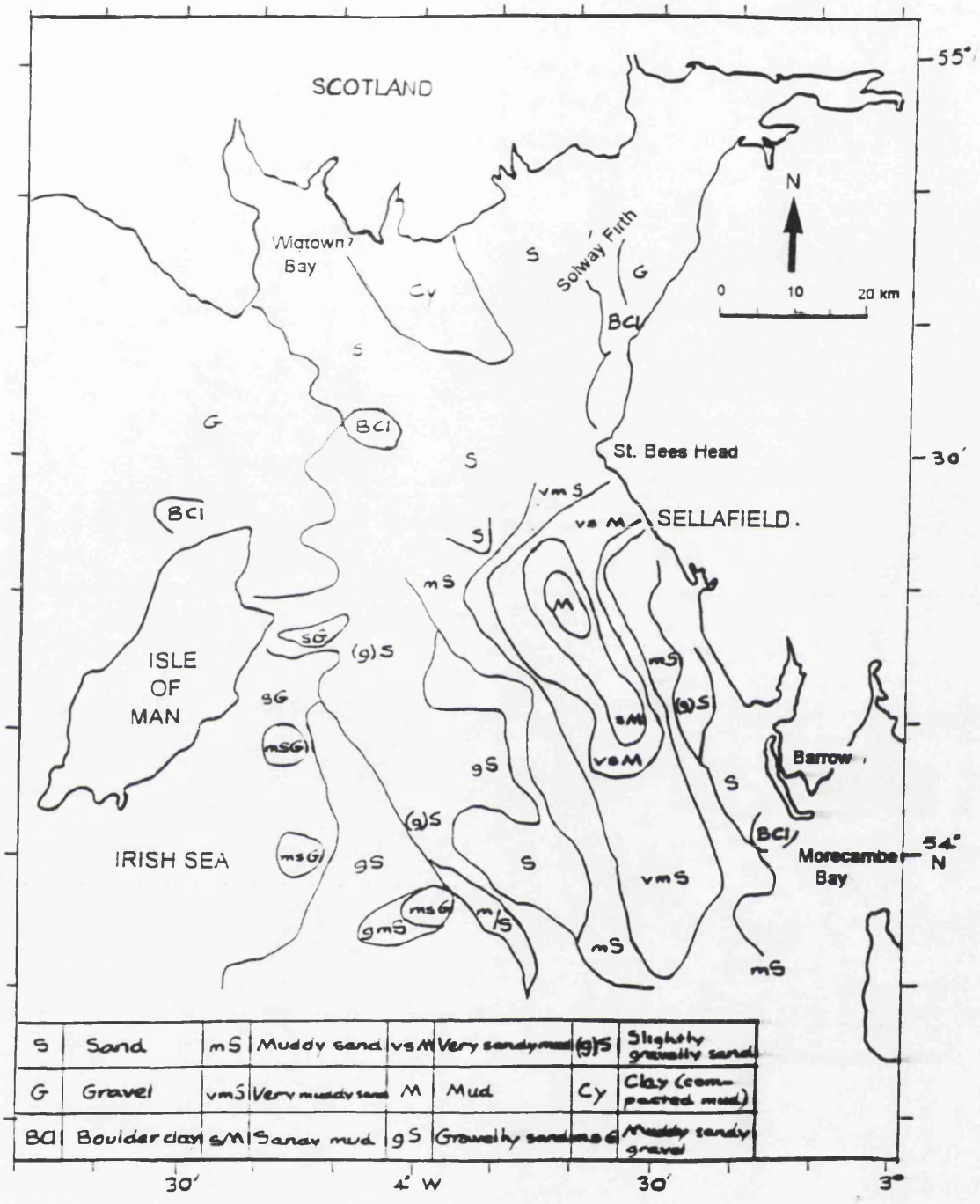

have transported finer material away from these areas. This material is sorted by physical processes, winnowing the fine particles or flocs of clay and transporting them to areas of lower energy. Belderson and Stride (1969) postulated that residual, coarse-grained sand waves around the North Channel and St. George's Channel may represent directional markers for tidal movements (Fig 1.9). These processes have resulted in the present sediment distribution, illustrated in Fig 1.10. Two areas of fine sediment deposits have been identified: firstly an area of mud, consisting of silt and clay, (the clay fraction being predominantly illitic), off the Cumbrian coast and secondly an area of mud lying west and southwest of the Isle of Man (Kirby *et al.,* 1983). The present day location of the mud patch off the Cumbrian coast corresponds to the position of lacustrine sediments deposited in proglacial lakes at least 10^4 years B.P., and Williams *et al.*, (1981) indicated, from interpretation of seismic records, that this area contains up to 40m depth of Holocene sediments. The mud patch off the Cumbrian coast tails off into muddy sands and then into coarser material towards the coast of south west Scotland. Cronin (1969) inferred that the reworking of glacial debris on the floor of the Irish Sea can account for the origin of these superficial sediments.

The area of fine sediment off the Cumbrian coast is of major importance as a sink for radionuclides discharged from Sellafield and characterisation of the accumulation, mixing and other processes affecting the sediment is of fundamental importance in evaluating the environmental fate of these radionuclides. There remains, however, much uncertainty attached to understanding the behaviour of the mud patch.

Pantin (1977) reviewed the work of the Institute of Geological Science (I.G.S.) on northern Irish Sea sediments and concluded that the sedimentary succession can be explained in terms of deglaciation, eustatic sea level changes and isostatic recovery. This supports the previous argument advocating deglaciation followed by inundation by the sea, with subsequent reworking of the glacial sediments by tides and currents. Pantin's review also stated that both advective and diffusive processes appear to play a part in the transportation and deposition of the mud fraction off the Cumbrian coast. Kirby *et al.*, (1983) questioned whether these processes are occurring at present and argued that there is no clear evidence for

fine sediment transport and deposition. Dyer (1986) countered this argument by pointing out that alternative sources of sedimentary material, such as influent rivers or coastal and seabed erosion, could not provide a sufficient mass of sediment to have supplied the area with fine silt since the last glaciation. Aston and Stanners (1982) supported this argument through the observation that the embayments of the Cumbrian coast are accretionary and therefore could not be regarded as a potential source of sedimentary material. More recently Sills and Edge (1989) studied a number of sediment cores from the mud patch off the Cumbrian coast and, on the basis of measurements of core densities, shear strength and moisture content, postulated that there has been very limited recent deposition of sediment within this area.

Kershaw (1986) applied ^{14}C dating techniques to sediment cores from the mud patch. Analysis of bulk sediment from three cores indicated that there had been extensive reworking by bioturbation, down to a depth of 140 cm, illustrated by an almost constant age of 12,500 ± 1,000 ys B.P. over this depth range. An average sedimentation rate of about 0.002 cm y^{-1} (with a maximum of 0.08 cm y^{-1}) was obtained from these cores. Kershaw *et al.*,(1988) also applied ^{14}C dating to shells of the gastropod *Turitella communis (Risso)* which were found in marine cores extracted from the mud patch. The results from three cores are ambiguous: two cores exhibited an increase in the age of the shells with depth, which is to be expected for a depositional site, however, results from a third core indicated a decline in shell age with depth. This places doubt upon the validity of ^{14}C chronology derived from the shells and is difficult to reconcile with the observations by Kershaw (1986) of intense mixing of these sediments by bioturbation. More recent work by Begg (1992) on the contribution of Sellafield derived ^{14}C to the inorganic and organic sedimentary carbon pools in the Irish Sea, has shown that the organic component is enriched in Sellafield ^{14}C. This suggests that the *Turitella* shells collected by Kershaw may also have been enriched through contamination with ^{14}C effluent from Sellafield.

Sills and Edge (1989) analyzed a suite of Reineck (0-45 cm) and Kasten (0-200 cm) cores from the north east Irish Sea and results indicated that all the cores extracted from the area of fine silt had evidence of bioturbation (worm burrows) to variable

depths, and showed distinct trends of increasing strength of clay and silt deposits with depth. They interpreted this observation as indicating that the process of bioturbation mixes the sediments, however the extrusion of faecal pellets, which can be smeared around the walls of the burrow, acts as a cement which binds the particulate material together. This process increases the strength of the sediments and therefore their resistance to erosion in the bioturbative zone (0-45 cm). Sills and Edge (1989) postulated that the trend of increasing strength with depth could also be attributable to previous over-consolidation by sediments which have been removed through erosion or could be due to present day creep in the seabed sediments. The authors drew the conclusion, that it was unlikely that the areas examined had recently experienced much deposition of sediment, with the exception of the top 10 mm. They also suggested that this surface layer of sediment could be mobile within the area as a result of transient local erosion and sedimentation processes.

1.3.1 The Coastline of the Solway Firth

The coastline of Dumfries and Galloway in south west Scotland is extremely varied, ranging from rocky promontories and cliff faces to the sheltered low energy environments of the influent river valleys and coastal embayments.

The rivers of the region rise in the hinterland of Dumfries and Galloway and flow southward towards the Irish Sea. They flow into the sea through river valleys cut during the glacial retreat, with floodplains bounded in general by high ground to the east and west. In the lower reaches the mature meandering rivers flow through extensive areas of floodplain deposits. These floodplain deposits are protected by the rocky promontories of the coastline and by off-shore sand/mud banks which dissipate incoming tidal energy. Larger, more coarse-grained particles are deposited in more exposed locations in the estuaries and river valleys with the finer-grained material (silts and clays) being transported further upstream during the flow tides. The low energy environments of the river valleys and coastal embayments represent areas of sedimentary accumulation and this combined with their land use functions, makes them highly relevant locations for assessing the potential exposure risks to mankind from Sellafield derived-radionuclides. The mature

saltmarsh ecosystem provides a rich sward of grass cover which farmers have traditionally used to graze cattle and sheep during the summer months. The coastline of south west Scotland is illustrated in Fig 1.11.

The saltmarsh development at Wigtown fringes the extensive sand flats of Wigtown and Baldoon sands on the west coast of Wigtown Bay. Inland to the west lies the town of Wigtown, situated on a hill rising above this coastal transition zone. The saltmarsh deposits are formed on raised beach material and are deeply dissected by tidally-influenced drainage channels. To the south of Wigtown the merse has been reclaimed behind protective breakwaters and an airfield is located there at present. Despite the presence of this facility the traditional land use of the saltmarsh in this area remains the grazing of sheep and cattle during the summer months.

On the east coast of Wigtown Bay lies Creetown, where more limited saltmarsh development has occurred. Creetown nestles below the high hilly ground of Cambret Moor (300-400 m), on a section of raised beach along which the A75 runs. The limited saltmarsh development along the banks of the River Cree and the Moneypool Burn is used as summer pasture for livestock, for access to salmon fisheries and as moorings for small boats. The total area of saltmarsh at Wigtown and Creetown has been estimated by the Nature Conservancy Council (NCC, 1989) as being approximately 553 ha.

Along the coast to the east, the rocky indented coastline produces a series of sandy bays with limited raised beach and saltmarsh development in the upper reaches. The rocky outcrops comprise well-bedded greywackes, grits, flags and shales (Steers, 1973). The calciferous sandstone series forms a strip along the shore producing a craggy and very broken coastline containing Auchencairn Bay, Orchardton Bay and Rough Firth which are cut back into the western parts of the Criffel granite (Countryside Commission for Scotland, 1978). These bays are sand filled and within the upper reaches raised beach and saltmarsh development has occurred (area Auchencairn/Orchardton 78 ha). Rough Firth, where Kippford is located, is a sunken ria or drowned river valley where extensive saltmarsh deposits, approximately 57 ha, have been created along the meandering Water of Urr.

The rocky coastline continues eastward passed Sandyhills Bay and along the coast to Caulkerbush. The cliff, on which the A710 runs, rises up to a height of 40 m in places and dominates the low-lying sand and saltmarsh deposits to the south and east. This cliff is formed by the outcropping of the granite pluton of Criffel and marks a distinct change in coastal landscape. The meandering Southwick Water flows below and parallel to the cliff gently flowing in its senile stage across the raised beach and saltmarsh development (56 ha) of Mersehead Plantation, beyond which stretches the wide tidal flats of Mersehead Sands. Mersehead Plantation and Preston Merse have been partially reclaimed for agricultural and forestry land use. Beyond Southerness the raised beach and reclaimed saltmarsh are used for recreational and tourist developments; golf course and caravan parks.

Carsethorn is located north of Southerness in Carse Bay, where extensive intertidal sand and mudflat deposits are fringed by saltmarshes. The location of Carse Bay has a very open appearance, the relief is low to the east across the mouth of the River Nith, where the tidal channel migrates towards Caerlaverock across the exposed sand flats. To the west of Carse Bay a low ridge runs parallel to the Nith, while inland the scenery is dominated by the granite cone of Criffel rising to over 569 m. The coastal strip is used for agricultural purposes, predominantly livestock grazing but with some limited arable cultivation.

1.3.2 Intertidal Sediments

The offshore sediments which were deposited during the last glaciation have been subjected to physical transportation processes which have resulted in the redistribution of sedimentary material to the intertidal zones along the coastlines of south west Scotland, north west England and north Wales (Steers,1973). These intertidal sediments can be subdivided into true intertidal sediments and floodplain deposits.

Fig 1.11 Map illustrating the location of major areas of saltmarsh along the northern Solway coast (NCC, 1989).

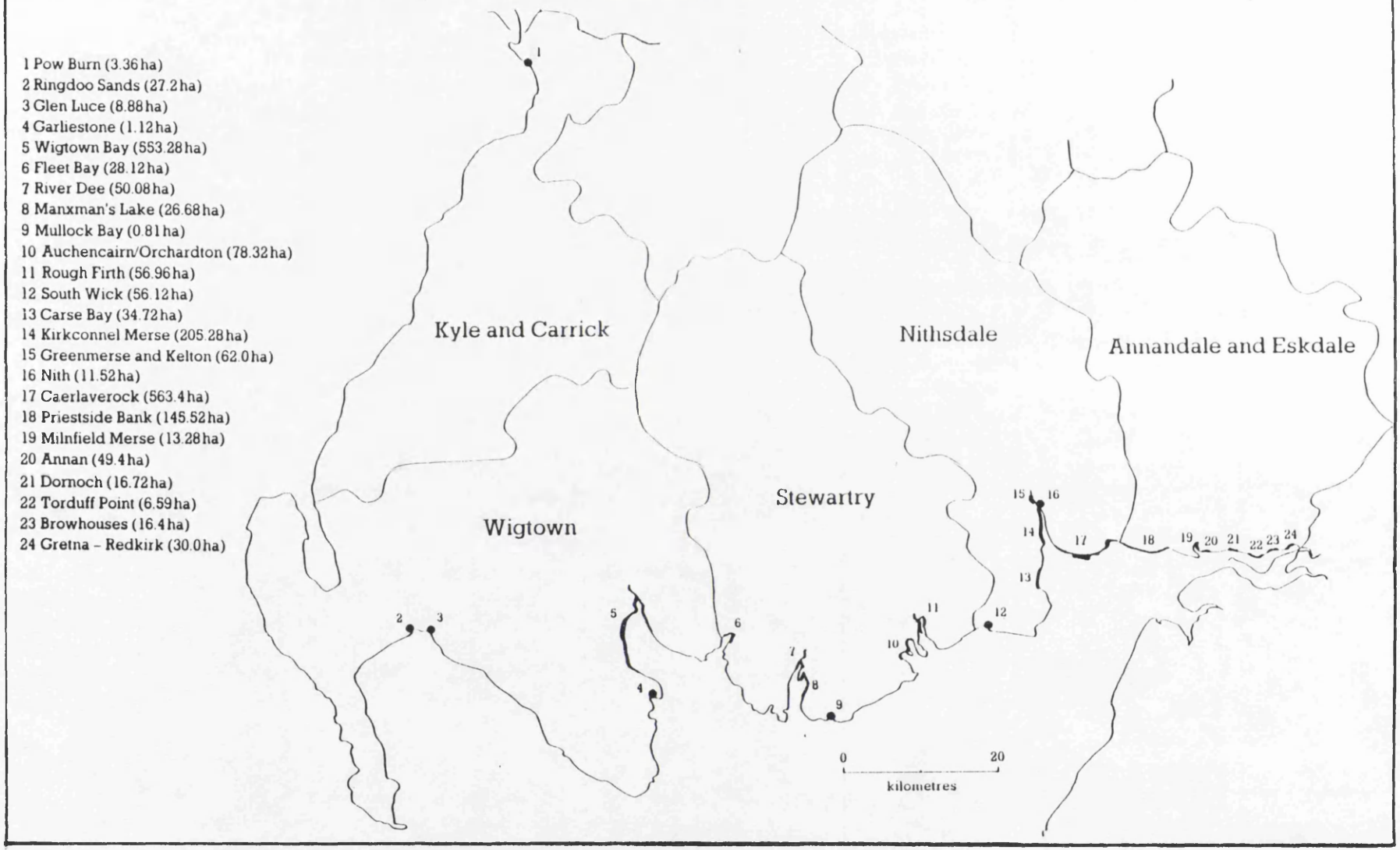

a) True Intertidal Sediments

True intertidal sediments, which are subject to twice daily inundation by the sea, form transition zones between the marine and terrestrial environments. The beach materials are well-sorted as a result of the repeated winnowing by wave action. In the high energy environments, found along exposed stretches of the coastline, coarse-grained sandy material predominates. On less exposed stretches of coastline, within sheltered bays and behind protective offshore sand bars, the energy of the incoming waves is dissipated, resulting in the deposition of fine-grained silts, e.g. Kippford and Orchardton Bay. The degree of pollutant contamination reflects these subdivisions between the high and low energy environments. The coarse-grained sands have a smaller surface area than the fine silts and have correspondingly lower concentrations of radionuclides associated with them. There is a natural progression at these sheltered locations for the intertidal sediments to accumulate in height above the mean high water mark (MHWM), eventually establishing floodplain deposits of fine-grained materials.

b) Floodplain Deposits

Large expanses of saltmarsh deposits, known locally as 'merse', have been created along the Solway coast from Wigtown in the west to Rockcliffe Marsh in the east (Figs 1.11 and 1.12). The combination of tidal inflow, prevailing south westerly wind and topography produces a small tidal bore (amplitude 0.5 m) within the inner reaches of the Solway Firth. This has meant that east of Caerlaverock, on the northern Solway coast, there has been less extensive development of floodplain deposits. This is in contrast with the southern shore of the estuary where extensive saltmarsh development has occurred at Rockcliffe Marsh, Burgh Marsh and Moricambe Bay as Fig 1.12 illustrates.

These saltmarshes are dominated by halophytic vegetation, in particular, the grasses *Puccinellia* and *Festuca*, (NCC, 1989). These sedimentary developments are also mirrored in other parts of the Irish Sea basin; saltmarshes have developed

Fig 1.12 Map illustrating the location of major areas of saltmarsh along the north west coast of England (NCC, 1989).

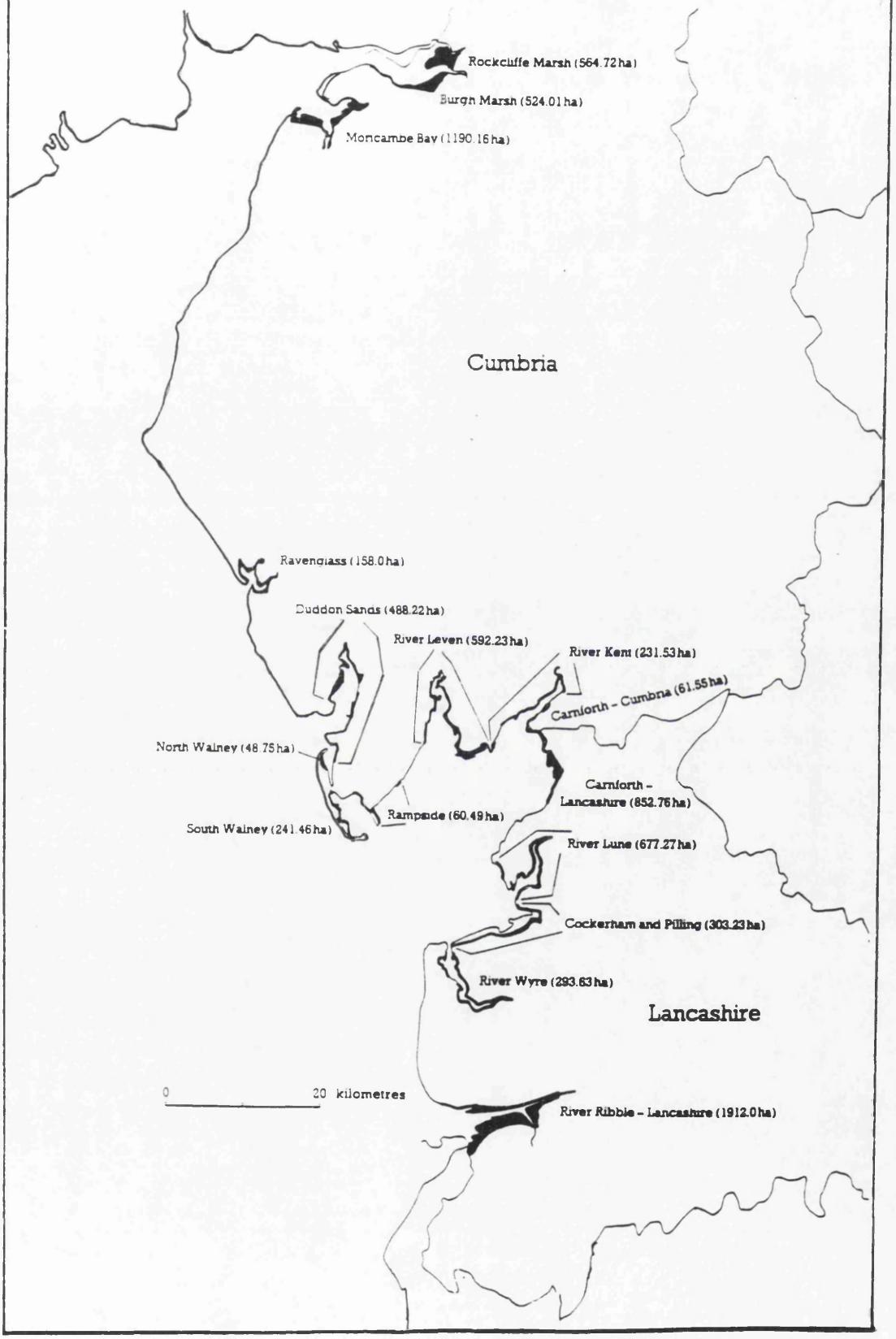

Fig 1.13 Map illustrating the location of major areas of saltmarsh along the northern coast of Wales (NCC, 1989).

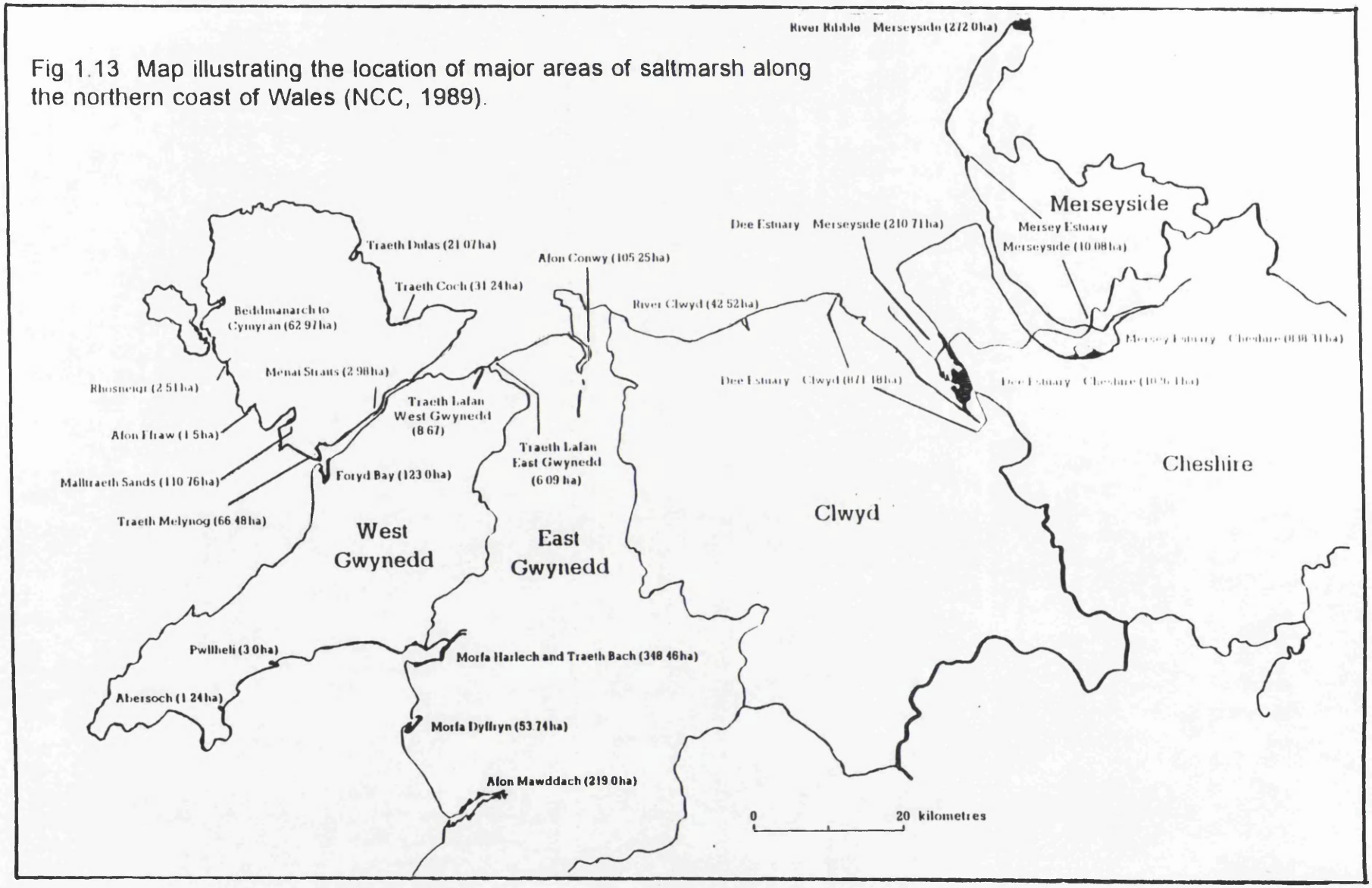

in the lower energy environments found in the estuaries of Cumbria, Lancashire and parts of north Wales and are illustrated in Fig 1.12 and Fig 1.13. Extensive areas of saltmarshes are to be found at Ravenglass, Duddon Sands, South End in the lee of Walney Island, the fringes of Morecambe Bay and in the estuaries of the rivers Crake, Lune and Ribble.

The geomorphology of the saltmarshes of the Solway Firth has been studied by Marshall (1962) who stated that the inner Solway Firth is infilling due to accumulation of marine-derived material which consists predominantly of fine sands. Allen (1989) indicated that the Solway Firth exhibits terrace-like features which are characteristic of saltmarshes on the west coast of Britain. These stepped terraces are separated by slopes of varying severity going from near vertical cliff faces (up to 1m in height) to gentle grassy slopes. Such terraces run parallel to the coast, producing a series of seral stages with corresponding ecological specialization. These seral stages are development stages in ecological progression towards a steady state or climax ecosystem (Tivy and O'Hare, 1981). Foliar trapping of particulate material by tidally exposed vegetation leads to rapid build-up of the sediments (Hamilton, 1984). As these deposits grow, tidal inundations become less frequent through time as a consequence of the increase in height and the salinity gradients of the upper marsh alter, with lower salinities permitting a wider variety of plants to survive and more complex plant communities to develop as illustrated in Fig 1.14 (Ranwell, 1972). Thus, the saltmarshes contain a series of tide-stressed environments where ecological colonization and diversity are controlled by salinity and frequency of tidal inundation. The rich diversity of vegetation, especially the rich grass sward, results in these floodplain areas being extensively used for agricultural purposes with livestock grazing dominating the land use.

There is considerable lateral variation of sediment particle size in the floodplain areas, as illustrated by the work of Hamilton and Clarke (1984) who investigated the particle size distribution of sediments in the saltmarsh deposits of the Esk Estuary. They observed that there was a gradation of particle size from the finest material, being predominantly associated with areas covered in saltmarsh vegetation, followed by areas of fine silts and muds sparsely covered with

Fig 1.14 Idealised Saltmarsh Showing Main Vegetation Zones, Adapted From Ranwell (1972)

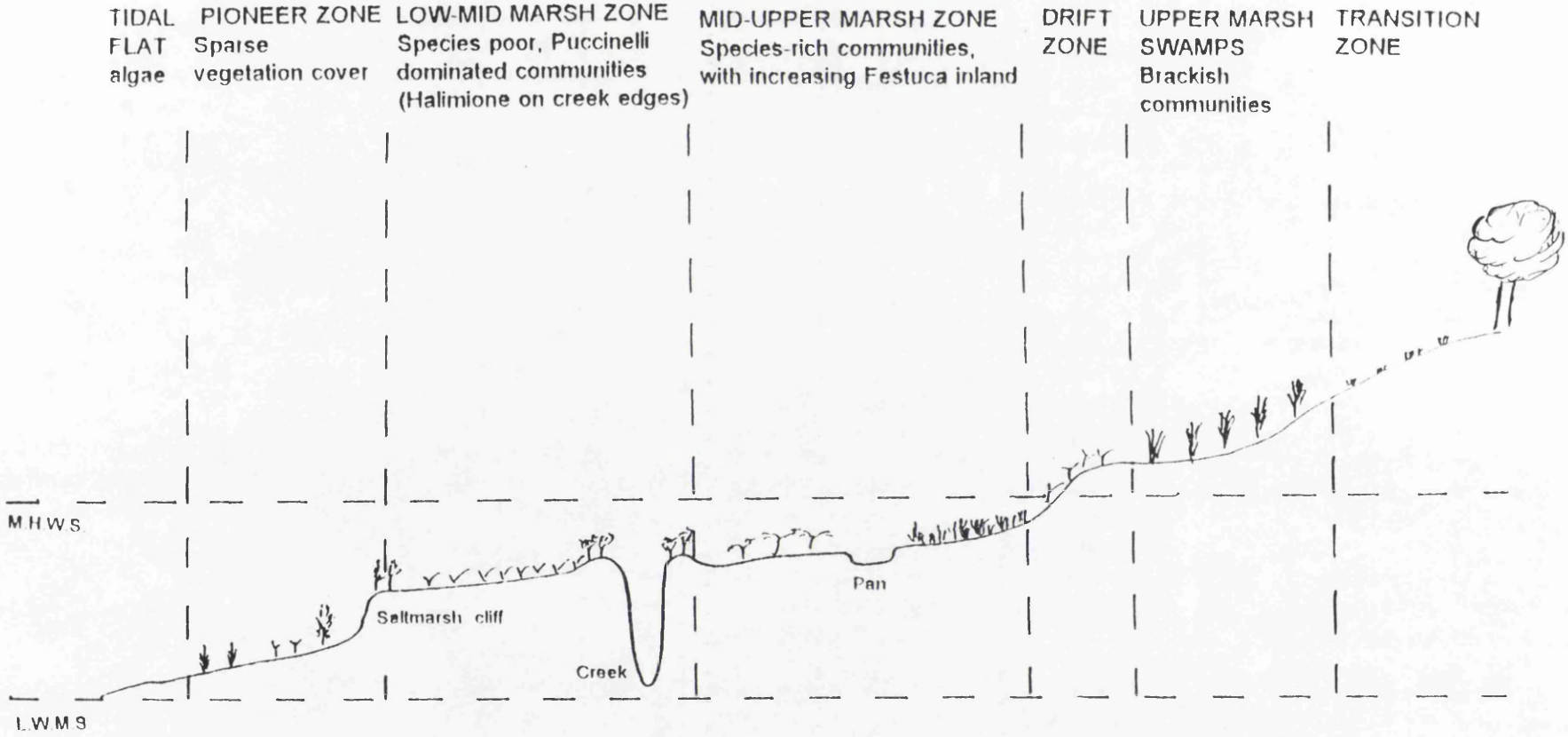

vegetation and finally coarse material, associated with the sand deposits in the higher energy environments of the estuary.

The floodplain sediments of the Solway Firth and other parts of the Irish Sea contain numerous deep-cut, meandering rivers and estuaries, and the tidal cycle within
these systems drives the depositional processes in this part of the floodplain. After the ebb tide turns, there is a short period when the incoming flow tide creates a degree of turbidity within saltmarsh drainage creeks, causing previously deposited material to be resuspended and transported further upriver. This results in the remobilization of fine-grained material from the river beds and lower reaches for deposition around the mean HWM on the river banks or beyond onto the vegetation covered floodplain (Kelly *et al.*, 1991).

Allen (1989) observed that the sandy sediments of the Solway Firth floodplain contain rather low and comparatively weak cliffs, up to 1m in height, which are susceptible at high tide to grain by grain wave attack below the thick, root-strengthened portion of the marsh profile. As plates (1-4) indicate, this erosion can be produced by; (a) rotational slipping (plate 1) where saturated sediment in surface layers exerts increasing stress on drier sediment below, resulting in movement of material along a curved shear plane (the sandy nature of the deposits combined with the comparatively low cliff height makes this process largely insignificant in the Solway), or (b) toppling and collapse of blocks of sediment due to undercutting of the cliff face by water movement (plates 2-4). These erosional processes combine with high spring tides to result in the removal of consolidated material which is then transported and deposited further eastwards due to the prevailing south-west winds and longshore drift. These areas of merse which have been contaminated with pollutant radionuclides from Sellafield represent an important interface between members of the public and possible contact with Sellafield derived radionuclides. Radiation exposure is possible through direct external exposure to β/γ radiation, inhalation of contaminated material or consumption of contaminated arable and livestock products.

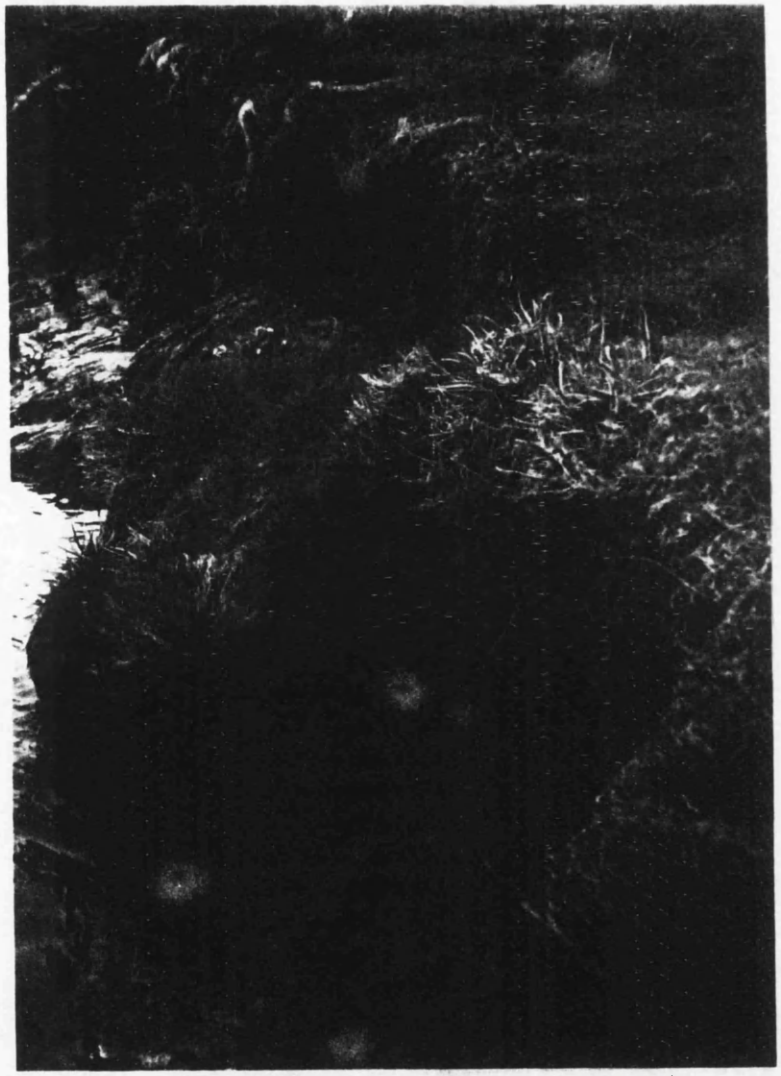

Plate 1.2 Photograph illustrates slumping and undercutting of the bank (ebb tide).

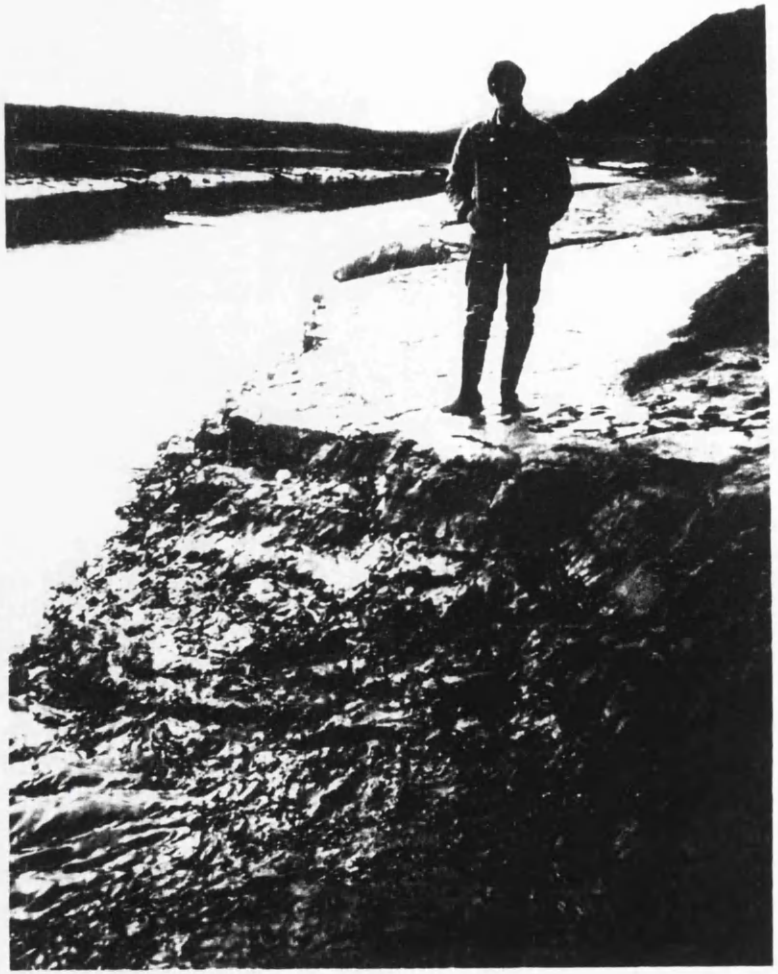

Plate 1.1 Photograph illustrates rotational slipping of the river bank at Southwick merse.

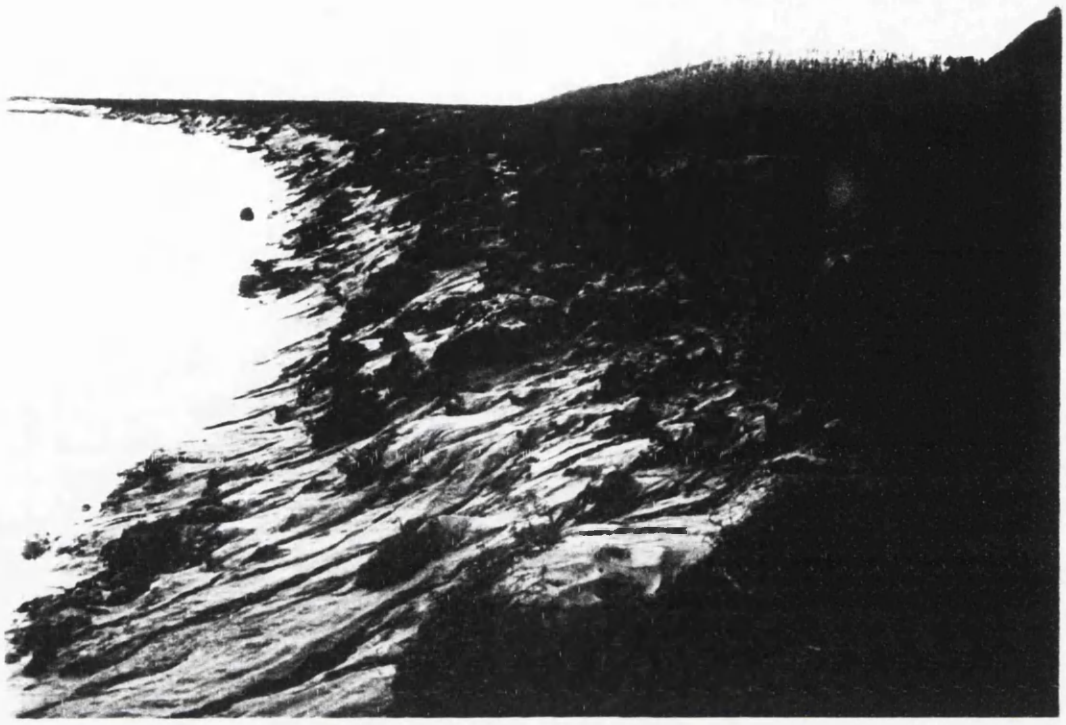

Plate 1.3 Slumping and undercutting of the bank at Southwick (flow tide)

Plate 1.4 Erosion of the stepped edge of the merse at Wigtown.

1.4. RADIONUCLIDES IN THE IRISH SEA

Liquid radioactive effluent discharges from Sellafield (Section 1.1.2.) have resulted in widespread radionuclide contamination of the sediments of the Irish Sea. Concern over the radiological significance of this contamination has stimulated considerable research on the spatial distributions, environmental concentrations, geochemistry and redistribution processes affecting the pollutant radionuclides.

1.4.1 Radiological Significance of the Sellafield Discharges

There are a number of pathways by which radionuclides discharged into the marine environment can return to man. A key method for assessing the dose to the public is the use of the critical pathway concept. This approach encompasses the identification of a group of people who, through their dietary preferences, occupation or recreational pursuits, are the most exposed members of the public to radionuclides from particular nuclear facilities. As such, the critical group represents the upper limit of public exposure to radiation. A number of critical groups may be identified depending on the form of waste, its radionuclide content and the transportation mechanism to man. The radiation dose to each critical group is quantified using measurements of environmental radioactivity together with published data on the metabolic behaviour of radionuclides. The present work focuses on providing additional information on the transportation and geochemical behaviour of radionuclides discharged from Sellafield into the marine environment of the Irish Sea basin. An improved understanding of the environmental consequences of pollutant radionuclide discharges is an essential component for improving and updating the critical pathway assessments.

Every nuclear facility within the UK has its own specific critical pathway by which the dose to the public is calculated. The two main pathways leading to human exposure to radiation from Sellafield waste radionuclides are the consumption of contaminated fish and shellfish and external exposure to β and γ emitting nuclides in marine materials. An equally important facet of radiological protection is the estimation of the radiation dose to the whole population. This introduces the concept of collective dose; that is the summation of all individual radiation doses

received by a population over a defined period of time.

It is important to identify and quantify the processes governing the environmental dispersion of the radionuclides if the radiological impact of the discharges, in particular dose assessments for the critical groups in the population, are to be adequately evaluated. Such evaluation of contemporary discharges is achieved by monitoring, however, it is desirable to develop a model capable of quantitatively predicting doses that will arise from the environmental persistence of past and future discharges. Of major importance in this context are processes which result in the transport of waste radionuclides to the intertidal areas, where contact with the human population is likely. The radionuclides of interest within the present study, ^{238}Pu, $^{239+240}Pu$, ^{137}Cs and ^{241}Am, make a significant contribution to critical group internal and external exposure resulting from the release of radionuclides from Sellafield (MAFF, 1972-1990). The α emitting radionuclides, ^{238}Pu, $^{239+240}Pu$ and ^{241}Am, constitute only an internal exposure risk since α particles are highly ionizing and produce intense damage along short tracks of tissue. Conversely in an environmental context, total shielding is provided by a few centimetres of air or several μm of solid material so α emitting nuclides pose little external hazard. The β/γ emitting nuclides are of less importance with regard to internal exposure risks because their radiation gives a lower specific ionization, but the greater ranges of β and γ radiation mean that such nuclides represent a significant external exposure hazard.

The levels of radionuclide contamination have been interpreted by the relevant organisations (MAFF, NRPB) in terms of radiation exposure they cause to the critical group.

The dose limit for individual members of the public, recommended in ICRP-60, (International Commission for Radiological Protection) is an effective dose of 1 mSv in a year. However in special circumstances, a higher value of effective dose could be allowed in a single year provided that the average over 5 years does not exceed 1 mSv per year.

The authorizations to discharge low-level radioactive effluent into the environment

require BNFL to use 'best practicable means' (BPM) to control discharges. This reflects the objective of keeping radiation exposures 'as low as reasonably achievable' (ALARA) to comply with ICRP principles.

The critical group for internal exposure to Sellafield radionuclides consists of fish consumers living in the Sellafield coastal area, which extends 15 km north and south of Sellafield from St Bees Head to Selker. The critical group internal exposure fell by an order of magnitude from a maximum of 2.3 mSv in 1981 to 0.19 mSv in 1989 (MAFF, 1982 and 1990). Bait diggers are representative of those who receive the highest external exposures in intertidal areas because of the occupancy times involved in this activity. The external dose has declined from a maximum of 0.55 mSv in 1980 to 0.079 mSv in 1989 (MAFF, 1981 and 1990).

These reductions in critical group exposure are small in comparison with the two orders of magnitude decrease in the Sellafield discharge over the same period. This implies that during the period of declining Sellafield discharges, radionuclides present in the environment from previous discharges continued to make a significant contribution to the critical group exposure.

1.4.2 General Aspects of the Geochemistry of Radiocaesium, Plutonium and Americium in the Irish Sea

The geochemical behaviour of the various radionuclides, which have been discharged into the Irish Sea from Sellafield, control their spatial distribution patterns and behaviour in the environment. Solid phase aqueous phase partitioning is of particular concern in this context. The degree of solubility of a radionuclide in a given environment is dependent on a number of geochemical variables such as Eh/pH conditions, its ionic potential, the availability and concentration of complexing ions, temperature and pressure.

The dominant factor controlling the solubility of a radionuclide is its ionic potential, (defined as the ratio of ionic charge to ionic radius (Å)), which controls the degree of hydration, hydrolysis, complex formation and particle reactivity of an ion. Ionic potential is a measurement of the intensity of charge on the surface of the ion and

this determines its interaction with other charged species. For example, the magnitude of the repulsive force between the positive charge on the cation surface and the protons of the dipolar water molecules attracted to it or the magnitude of the forces of attraction between the cation and the negative charges on the oxygen atoms produces distinctive chemical behaviour in the aqueous phase. Depending on the magnitude of the ionic potential these effects of repulsion and attraction can result in any of: hydration (low ionic potential), precipitation of an insoluble hydroxide i.e. hydrolysis (intermediate ionic potential) or the formation of a soluble oxyion (high ionic potential). Ionic potential also controls particle reactivity. Pu^{4+} and Am^{3+} which have intermediate ionic potentials are highly particle reactive, whereas Cs^{+} with a low ionic potential is less particle reactive except in the presence of illitic clays which provide suitable sites for sorption of this ion. Table 1.8 illustrates the ionic potentials for the radionuclides of interest in this study.

A good indication of the behaviour of a radionuclide with respect to aqueous phase solubility in the environment is given by the distribution coefficient (K_D), defined in this work as

$$K_D = \frac{Concentration\ (solid\ phase)}{Concentration\ (aqueous\ phase)} \qquad (1.2)$$

K_D values are defined by observation of the partitioning of the radionuclides between the solid and aqueous phases in the environment which is determined by the thermodynamics of sorption. However, K_D values cannot be rigorously defined in many natural systems due to problems of replicating complex environmental conditions within a laboratory, so the term is used in a semi-quantitative way. K_D values for radionuclides in the Irish Sea have been reported in a number of publications; Aston and Duursma, (1973); Nelson and Lovett, (1978); Stanners and Aston, (1981); IAEA, (1985). The K_D value for ^{137}Cs ranges between 10^2 and 10^3 reflecting its conservative behaviour, $^{239+240}Pu$ has differing values depending on the oxidation state, Pu^{5+} has a K_D value of 10^4, in contrast the reduced Pu^{4+} has a value of 10^5 reflecting its predominantly particulate association and ^{241}Am has a K_D of 10^6 illustrating a high particle reactivity.

Caesium is a group 1A element and consequently exists only in the 1 + oxidation

state. As Table 1.8 illustrates, Cs has a low ionic potential (0.6) which results in a high degree of hydration. Radiocaesium is readily dissolved and the ions become

Table 1.8 Ionic Potentials for selected radionuclides of interest in this study. (Ben-Shaban, (1989) based on data from Greenwood and Earnshaw, 1984).

Actinide	Radius (Å)	Ionic Potential	Solubility
Cs^{+}	1.67	0.60	soluble
Pu^{3+}	1.00	3.00	insoluble
Am^{3+}	0.98	3.06	insoluble
Pu^{4+}	0.86	4.65	insoluble
Pu^{5+}	0.74	6.76	intermediate
Pu^{6+}	0.71	8.45	soluble

isotopically diluted with stable ^{133}Cs which shows conservative behaviour in seawater. That is the concentration of the ion varies in direct proportion to salinity, assuming that there are no alterations to the concentration except through the processes of mixing and dilution. Most of the radiocaesium released from Sellafield remains in solution, exhibiting conservative behaviour, and is transported out of the Irish Sea, however, a small proportion is retained in the clay-rich sediments lying off the Cumbrian coast (Miller *et al.,* 1982; Jones *et al.*, 1988). Jefferies *et al.*, (1973) identified a slow-moving 'plume' of radiocaesium rich water which travels northwards out of the Irish Sea and around the west coast of Scotland in a clockwise direction. Baxter *et al.*, (1979) reported that approximately 30% of the Sellafield radiocaesium output passes through the Clyde Sea Area during its northwards passage, with only about 0.3% being retained by the sediments. The plume travels northwards around the Scottish coast and down into the North Sea, the average timescale for this process being about 2 years (Jefferies *et al.*, 1973). Once in the North Sea, the plume follows an anti-clockwise circulation pattern before exiting along the Norwegian coast after approximately 6 years (Prandle and Beechy, 1991).

It has been estimated recently that the sediments of the Irish Sea retain about 10% of the discharged ^{137}Cs (Smith *et al.*, 1980; Miller *et al.* 1982; Jones *et al.*, 1984). Hetherington and Jefferies (1974) and Stanners and Aston (1981, 1982) have shown that the uptake of ^{137}Cs by bottom sediment is mainly a surface adsorption process and that ^{137}Cs is concentrated in the fine sediments.

The chemistry of plutonium is more complex and it can exist in four oxidation states (3+, 4+, 5+, 6+) in aqueous solutions, resulting in variations in geochemical behaviour (Katz and Seaborg, 1986). As Table 1.8 illustrates the various oxidation states of plutonium have different ionic potentials which results in contrasting degrees of solubility. The reduced forms of plutonium, Pu^{3+} and Pu^{4+}, have ionic potentials of 3 and 4.65 respectively and are highly insoluble in aqueous solutions. In contrast the oxidized forms exhibit greater solubility. Pu^{5+} with an ionic potential of 6.76 has intermediate solubility while Pu^{6+} with an ionic potential of 8.45 is termed soluble (Ben-Shaban, 1989; Greenwood and Earnshaw, 1984). The high charge densities of the reduced plutonium nuclides result in a high degree of hydrolysis and particle association. Hetherington (1975) described the behaviour of plutonium in the Irish Sea, noting that 95% of the plutonium which is introduced is rapidly lost from the aqueous phase to the sediments, either as a hydrous compound of plutonium or in association with suspended material in the seawater. The residual fraction which remains in solution appears to behave conservatively. Nelson and Lovett (1978) examined the oxidation state of plutonium in seawater samples collected along the Cumbrian coast, and observed that, in the area of study, generally $>75\%$ of the plutonium which remained in the aqueous phase and $<10\%$ of the plutonium on particulate matter was in the oxidized, more soluble (5+,6+) form. Nelson and Lovett (1981) extended their work on the oxidation states of plutonium to the interstitial waters of the Irish Sea sediments and found that the dissolved plutonium in the interstitial water was primarily in a reduced form (3+, 4+) while that in the overlying water was predominantly in an oxidized form (5+, 6+). The plutonium adsorbed to the solid phase was almost entirely in the reduced form (Nelson and Lovett, 1981).

Edgington (1981) illustrated that the concentrations of trace metals in ocean waters are controlled by an equilibrium distribution between the dissolved and solid phases.

The marine chemistry of plutonium is outlined in Fig 1.15 and is controlled largely by changes in the oxidation state between the overlying water and the sediments. The redox equilibrium between oxidation states in the water column is affected by the formation of complexes with ligands including; OH^-, HCO_3^-, CO_3^{2-}, SO_4^{2-}, Cl, organic molecules and the reaction of these complexes with iron/manganese surface layers of the sediment.

Fig 1.15 A schematic diagram of the chemical processes involving plutonium in the Irish Sea, adapted from Edgington (1981).

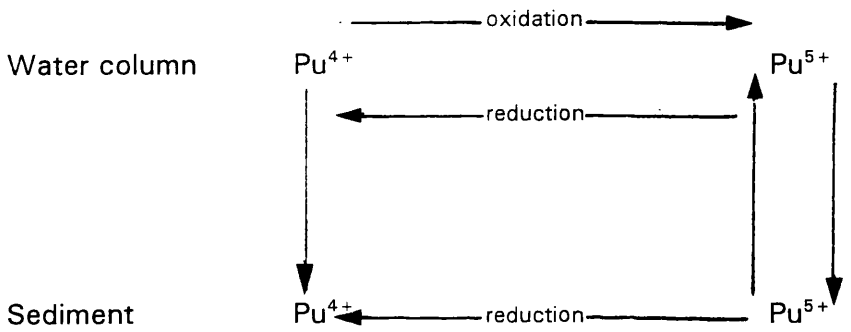

Pentreath *et al.*, (1984) found that in the Sellafield liquid effluent, the majority of the plutonium discharged from the sea tanks was in the reduced form (4+). Over 98% was associated with the particulate phase (> 0.22μm) in the neutralized effluent and less than 2% with the aqueous phase. The oxidized plutonium (6+) predominated in the effluent from the cooling ponds. However, in view of the small contribution that the pond effluents make to the total plutonium discharge, only about 1% of the total appeared to be in an oxidized form (Pentreath, 1984). It has been estimated that some 95% of the discharged plutonium becomes associated with the sediments of the Irish Sea, the majority being concentrated in the area of fine silt and clay off the Cumbrian coast (Hetherington, 1976).

Pentreath (1984) postulated that during the period 1973 to 1979, between 1% and 4% of the $^{239+240}Pu$ discharged from Sellafield was transported out of the Irish Sea in solution. This estimate was calculated by taking the concentration of the total (filtrate plus particulate >0.22μm) $^{239+240}Pu$ in the waters of the North Channel, assuming a flow rate of 5 km^3 per day and comparing the estimated rate of loss

with the annual discharges.

In summary, plutonium is discharged from Sellafield primarily in the reduced form and is rapidly incorporated into the offshore sediments. The small proportion of the plutonium which is in the more soluble oxidized state is transported by the water movements out of the Irish Sea in solution.

Americium has several possible oxidation states, however the trivalent state is the stable aqueous oxidation state (Katz and Seaborg, 1986). Americium has an intermediate ionic potential (Table 1.8) and is consequently susceptible to hydrolysis in aqueous solution and is highly particle reactive. Pentreath *et al.*, (1986) found that Am^{3+} discharged from the Sellafield sea tanks and pond water was clearly associated with particulate material ($>0.22\mu m$). Pentreath *et al.*, (1984) have observed, from sediment and seawater studies, that ^{241}Am is almost totally associated with the sediments in the area of fine silt and clay off the Cumbrian coast. The K_D for ^{241}Am in the Irish Sea is 10^6 reflecting its high degree of particle association (Pentreath *et al.*, 1984; IAEA, 1985).

1.4.3 Sellafield Radionuclides in the Offshore Sediments of the Irish Sea

During the period of high annual discharges of radionuclides from Sellafield in the 1970's (Section 1.2) the area of fine silt and clay off the Cumbrian coast constituted an important sink for discharged radionuclides (Hetherington *et al.*, 1976; Pentreath, 1984). However, since the rapid decline in the quantities of radionuclides discharged from Sellafield this sediment now represents a potentially important source of pollutant radionuclides (Pentreath, 1986). During the 1970's the concentrations of radionuclides within these sediments were not extensively reported. MAFF did collect samples from this area from the 1960's onwards, but limitations of the sampling strategy, place large margins of error on any conclusions drawn from the data (McCartney *et al.*, 1993). Sediment samples were collected by MAFF on a number of cruises and between 1975 and 1983 surface sediments exhibited concentrations of up to 1×10^4 Bq kg^{-1} of ^{137}Cs (McCartney *et al.*, 1993) and the highest recorded concentration was 12,900 Bq kg^{-1} in 1982 (Jones *et al.*, 1988). However, McCartney *et al.*, (1993) showed that by 1988 the surface

concentrations of ^{137}Cs in the fine sediments had declined by one order of magnitude to 10^3 Bq kg^{-1}.

This decline in radionuclide concentrations in the offshore sediments can be attributed to two separate environmental processes; redistribution of contaminated particulate material away from the area and re-dissolution of radionuclides from the sediments.

The offshore sediments are subjected to physical reworking by tides and currents with the distribution of the nuclides in the seabed sediments being controlled by water movements (Jones *et al.,* 1988), particle size distribution (Hetherington, 1975) and geochemical behaviour (McDonald *et al.,* 1990). Jones *et al.,* (1988) drew their conclusions from comparison of a series of surveys of ^{137}Cs in the sea bed sediment using a towed gamma-ray spectrometer. The original survey in 1978 (Miller *et al.,* 1982) of the whole Irish Sea identified a northward movement of particle associated radionuclides and was followed by more detailed studies of the Solway Firth in 1980 and 1981 (Jones *et al.,* 1984) and the area of fine silt adjacent to Sellafield in 1982 (Jones *et al.,* 1988). Several research projects observed trends regarding the lateral distribution of the Sellafield waste radionuclides in Irish Sea sediments. Pentreath *et al.* (1984) observed maximum inventories of 10^6 Bq m^{-2} of $^{239+240}Pu$ and ^{241}Am in the area of fine silt off the Cumbrian coast, corresponding to concentrations of 10^3 Bq kg^{-1}. The authors observed that the inventories of these radionuclides declined to approximately 3 x 10^3 Bq m^{-2} at the entrance to the North Channel, approximately 100 km away. Miller *et al.,* (1982) had previously reported similar observations for ^{137}Cs, with concentrations decreasing from 4,000 Bq kg^{-1} close to the pipeline to 40 Bq kg^{-1} near the North Channel, a decline of two orders of magnitude over a distance of 100 km. McDonald *et al.,* (1990) observed in 1987 that ^{137}Cs, $^{239+240}Pu$ and ^{241}Am concentrations were linearly correlated with each other in offshore surface sediments collected along a transect extending from the silt deposit near Sellafield to Kirkcudbright Bay on the Scottish coast. The radionuclide concentrations reported in this study varied with the nature of the sediment but did not vary systematically with increasing distance from Sellafield.

In addition to the lateral distribution of the offshore sediments the vertical mixing of these deposits has also been investigated.

Kershaw *et al.,* (1983,1984) have established through analyses of $^{239+240}Pu/^{238}Pu$ activity ratios in the burrow linings created by the large echiuroid *Maxmulleria lankestri* (Bock) and adjacent sediment samples, that there has been mixing of the sediment down to a depth of about 0.5 m by bioturbation. This has caused the penetration of Sellafield waste radionuclides to this depth and is consistent with Kershaw's work (section 1.3) on ^{14}C dating. The *in situ* mixing of these contaminated sediments has important implications for the long-term availability of radionuclides discharged into the Irish Sea where marine processes can result in the exposure of radionuclides within previously consolidated sediment to re-dissolution and redistribution processes, leading to their eventual return on-shore.

MacKenzie *et al.,* (1987) established through the application of radionuclide activity ratios and linear correlations between radionuclide concentrations, that the dominant mechanism of supply to intertidal areas of south west Scotland, during the 1980's, had been particulate transportation. McDonald *et al.*, (1990) adopted the philosophy of MacKenzie *et al.,* (1987) in a study of the lateral distribution of surface marine sediments, along a transect running from the area of fine silt off the Sellafield coast to Kirkcudbright Bay in south west Scotland. McDonald *et al.,* (1990) showed that the dominant mechanism for radionuclide transportation to the Solway involves migration and subsequent deposition of particulate material. The radionuclide concentrations recorded along this transect reflected the particle size distribution within the sediments. Despite the considerable distance involved, the activities of ^{241}Am, ^{137}Cs and $^{239+240}Pu$ in four of the five cores studied were all of the same order of magnitude (10^2 Bq kg^{-1}), in the fifth core the activities were generally one order of magnitude lower, clearly reflecting the sandy nature of the matrix. The $^{137}Cs/^{241}Am$ and $^{137}Cs/^{239+240}Pu$ activity ratios for the five sediment cores taken over this 60 km transect were virtually constant ($^{137}Cs/^{241}Am$ range 1.11-1.52, $^{137}Cs/^{239+240}Pu$ range 1.12-1.82) indicating well-mixed sediment. All the cores had lower $^{238}Pu/^{239+240}Pu$ activity ratios (0.19-0.23) than the Sellafield discharge (0.3). This suggests that the mixing which had occurred happened before deposition, and that the combination of bioturbation within the area of fine silt

adjacent to the pipeline (Kershaw *et al.*, 1983, 1984) and the transportation process affecting the radionuclides had thoroughly homogenized the sediments, mixing older discharges with more recent material. No evidence of post-depositional mixing by bioturbation was recorded within the cores, although post-depositional mixing by water movements cannot be discounted.

The contrast between the surveys carried out in the 1980's (McDonald *et al.*, 1990) which reported relatively uniform radionuclide concentrations within similar sediment types over a wide geographic area and those of the 1970's in which concentrations decrease rapidly with increasing distance from Sellafield, implies that a large degree of lateral re-distribution of sediment has occurred over the last decade consistent with particulate transport processes.

A secondary or contributory process postulated as being responsible for the decline in radionuclide concentrations within offshore sediments has been the re-dissolution of radionuclides from contaminated sediment. McCartney *et al.*, (1993) have estimated that there has been a net loss of ^{137}Cs from the offshore sediments during the period 1983-1988. The magnitude of this re-dissolution amounted to approximately 75% of the expected ^{137}Cs activity in the top 5cm of the sediment. The authors analyzed a number of marine sediment samples collected between 1968 and 1988. Information from the $^{137}Cs/^{239+240}Pu$ activity ratios suggests that the decrease in ^{137}Cs activities within the surface sediments was due to desorption of ^{137}Cs from the sediments by ion exchange reactions with relatively clean (lower ^{137}Cs concentration) seawater. The $^{137}Cs/^{239+240}Pu$ activity ratio has been gradually declining, reflecting the conservative nature of ^{137}Cs and the reductions in the Sellafield discharges during the 1970's. This contrasts with the particle reactive behaviour of $^{239+240}Pu$ which exhibits a K_D value of 10^5 for the reduced 4^+ form which is the principal oxidation state in the Irish Sea and implies a relatively low level of re-dissolution from the Irish Sea sediments. Hunt and Kershaw (1990) estimated, on the basis of the difference between observed and predicted radionuclide concentrations in seawater samples, that 8 T Bq Pu(α) and 2.5 T Bq ^{241}Am had been remobilised from the sediments, between 1979-87 and 1976-87 respectively. The percentages remobilised, 5% and 4% respectively, are very small when compared with the quantities discharged, 147 T Bq Pu(α) and 62 T Bq ^{241}Am,

over the same period. Stanners and Aston, (1982) demonstrated in laboratory experiments a 30% loss of ^{137}Cs from contaminated sediments from Newbiggin when in contact with Irish Sea seawater over a period of 10 days.

1.4.4 Radionuclide Supply To The Intertidal And Floodplain Environments

1.4.4.1 Lateral Variation in Surface Sediment Concentrations

The intertidal sediments of the Irish Sea have been extensively studied to ascertain the spatial distribution and concentrations of pollutant radionuclides, and to assess any possible exposure risks to the human population. Physical redistribution of contaminated sediment away from the area of fine silt constitutes a potential pathway leading to human exposure to radiation if the sediments are re-deposited on-shore. This on-shore transfer of contaminated sediment to terrestrial locations has been extensively studied (Aston *et al.,* 1981; Aston and Stanners, 1982; Hunt, 1985; Jones *et al.,* 1988), however, until recently, identifying the transportation mechanism had not been satisfactorily established. There are two possible mechanisms for radionuclide transport to intertidal locations; (1) through movement of radionuclides in solution and (2) through transport of particle-associated radionuclides by sediment movement. Information gathered on the lateral distribution of the contaminated sediment, including radionuclide and isotope activity ratios, together with relevant water movement within the Irish Sea could permit identification of the transportation mechanism.

Hunt (1985) argued that observations of declining radionuclide concentrations in environmental materials near Sellafield during the 1970's reflected not only reductions in annual discharges but also the effect of lateral dispersion of ^{241}Am and $^{239+240}Pu$ contaminated sediment away from the point of discharge, resulting in dilution of the contaminated sediment as it mixed with uncontaminated material. MacKenzie *et al.,* (1987) observed that radionuclide concentrations in intertidal sediments collected along the length of the Solway coast of south west Scotland in 1986-87 exhibited $^{137}Cs/^{239+240}Pu$ and ^{241}Am concentrations which varied according to sediment type, with higher concentrations in the finer sediments, but did not decrease systematically with increasing distance from Sellafield. This

followed on from work by various authors including Hetherington (1976,1978), Aston *et al.,* (1981) and Aston and Stanners (1982) who all cited the dispersion of particle-reactive radionuclides as being attributable to transportation of marine sediments to low energy environments on the Cumbrian coast.

MacKenzie *et al.*, (1987) established that during the 1980's, the dominant mechanism for supply of Sellafield-derived radionuclides to the coast of south west Scotland was particulate transportation. Radionuclide activity ratios ($^{137}Cs/^{239+240}Pu$, $^{137}Cs/^{241}Am$, $^{241}Am/^{239+240}Pu$) and linear correlations between radionuclide concentrations in surface intertidal sediments clearly demonstrated that particulate transportation was the dominant mechanism. There was, however, a problem with this approach which primarily involved the lack of specific data regarding the concentrations of $^{239+240}Pu$ and ^{241}Am in filtered seawater samples, which had to be estimated on the basis of Hetherington's work (1975) and published K_D values for the various radionuclides. (The K_D value for ^{137}Cs of 10^2 used in this case may be too low and therefore could distort the calculation). The K_D value for ^{137}Cs reflects the generally conservative behaviour of ^{137}Cs within the Irish Sea, however the value fails to take into consideration that ^{137}Cs may be irreversibly adsorbed onto clay lattice materials (Evans *et al.,* 1983; Alberts *et al.,* 1989) especially the interlayer sites of illites, the predominant clay mineral in Irish Sea sediments (Kirby *et al.,* 1983), where K_D values could be considerably higher.

Ben-Shaban (1989) applied the MacKenzie *et al.,* (1987) argument to a series of environmental samples collected from intertidal and saltmarsh deposits along the coast of the Solway Firth. At Skyreburn Bay and Netherclifton Merse the radionuclide and isotope activity ratios confirmed that particle-associated transport was the dominant mechanism of Sellafield waste radionuclide supply.

Much work has been done on the spatial distribution of radionuclides in estuaries. An important facet of this research was investigation of the association of radionuclides with fine sediment and identifying possible transport mechanisms. As part of their environmental monitoring programme primarily concerned with the external exposure of the critical group to γ radiation MAFF (1971-1990) have undertaken a systematic investigation of the radionuclide content of intertidal

sediments in areas frequented by the public. Concentrations of up to 1.2×10^4 Bq kg^{-1} of ^{137}Cs and 2.3×10^3 Bq kg^{-1} of $^{239+240}Pu$ have been recorded in the mud at Whitehaven, while similar figures of 9.2×10^3 Bq kg^{-1} of ^{137}Cs and 3.6×10^3 Bq kg^{-1} of $^{239+240}Pu$ were reported for the mud deposits at Newbiggin. In contrast, concentrations of ^{137}Cs in the sand deposits at St. Bees Head were an order of magnitude lower (7×10^2 Bq kg^{-1}) and the concentrations of plutonium isotopes were below the detection limit. Aston and Stanners (1982a) conducted a detailed survey of ^{137}Cs in the surface sediments of the Ravenglass Estuary, which showed that considerable variations did occur in concentrations of this nuclide in surface sediments and that the proportion of silt present was an important control on the spatial distribution. Observations indicated that activities increased upriver in the Irt, while in the River Esk, higher concentrations were found in the inner to middle reaches. The same authors in 1981 described the distribution of ^{241}Am in the intertidal zones of the Cumbrian coast (Aston and Stanners, 1981b). It was found that ^{241}Am had a strong affinity for the finer sediments. Using a series of surface samples taken from a 10 m x 10 m grid it was found that the sand fraction had the lowest concentrations (< 111 Bq kg^{-1}), followed by silts (148-318 Bq kg^{-1}), with highest activities being measured in the silt and clay fraction, (266-2,220 Bq kg^{-1}). These particle size distribution groupings reflected the concentrations in the environment, where intertidal sand had the lowest activities while the river bank silt and adjacent saltmarshes were enriched in ^{241}Am. Eakins *et al.*, (1990) have undertaken measurements of α-emitting Pu and ^{241}Am in the intertidal sands of west Cumbria. With the exception of the estuarine areas, the foreshore between the Solway Firth and Morecambe Bay consists mainly of sandy beaches, interspersed with rocky outcrops and stony areas usually backed by shingle above the high water mark. The authors found a high sand content (>98%) with the 125-250 μm fraction representing the largest component of the bulk sand. If a mass balance is taken into account, (Table 1.9), it is apparent that more than 95% of the transuranic nuclide inventory was associated with the sand fraction and less than 5% with the silt (which represented < 2% of the particle size distribution). The quantity of silt within a 50 g sample is relatively small (0.25 g) which means that the activity of $^{239+240}Pu$ is only 65 Bq, in contrast, the bulk of the sample comprises 30 g in the 125-250 μm fraction which produces 1,560 Bq. Although the silt fraction exhibits the highest concentration of $^{239+240}Pu$ per unit weight, the Particle

Size Distribution (PSD) of the 50 g sediment sample masks the contribution that this fraction makes to the total concentration in the sample.

Table 1.9 Concentrations and Percentages of $^{239+240}Pu$ Associated with Particle Size Fractions and Mass Balance in 50 g Sediment Sample from Allonby, Cumbria. (Eakins *et al.*, 1990)

PARTICLE SIZE FRACTION	$^{239+240}Pu$ ($Bqkg^{-1}$)	COMPOSITION OF BULK SAMPLE (%)	MASS BALANCE IN SAMPLE (g)	$^{239+240}Pu$ (Bq) IN MASS BALANCE AND (%)
Bulk Sand	49	39.5	19.75	968 (37%)
125-250μm	52	60.0	30.00	1560 (60%)
Silt	259	0.5	0.25	65 (0.25%)

Jones *et al.*, (1984) undertook a hovercraft-borne radiometric survey of the ^{137}Cs distribution in the intertidal sediments of the Solway Firth. They reported that the lowest activities (74-148 Bq kg^{-1}) were associated with the fine sands which were commonly moulded into sand waves and mega-ripples by the action of strong currents. The mudflats (muddy sands, sandy muds) which were frequently rippled and bioturbated exhibited higher activities (370-1,110 Bq kg^{-1}). Radiocaesium activity increased shorewards in concert with diminishing tidal current strength and decreasing grain size. The authors also noted that the saltmarsh/mudflat interface was a very important sink for fine sedimentary material.

During their work on the transfer of radionuclides from Sellafield to south west Scotland, McDonald *et al.*, (1990) observed similar trends to those reported by Jones *et al.*, (1984) but, more importantly, extended the area of investigation from the intertidal areas inland some 3 km. They reported that the presence of Sellafield-derived radionuclides was confined to the immediate vicinity of the shoreline and to the banks of tidally-influenced rivers. Concentrations of Sellafield-derived ^{137}Cs

and $^{239+240}Pu$ on the banks of these rivers at five locations along the Solway Coast ranged from 9 x 10^4 to 1.1 x 10^5 Bq m^{-2} and 2 x 10^2 to 3 x 10^3 Bq m^{-2} respectively. Sea to land transfer was restricted to 500 m inland, with tidal inundation highlighted as the dominant mechanism for on-shore transfer. Along the banks of tidally-influenced rivers, enrichment of Sellafield-derived radionuclides was confined in general to within 5 m of the primary course of the rivers but this area increased towards the river mouths. Several determinant factors in controlling the spatial distribution of radionuclides in saltmarsh locations were suggested; location of site, frequency of inundation, sediment type/particle size distribution and suspended particle loading.

Hamilton and Clarke, (1984) investigated the sedimentation history of the Esk Estuary using radionuclides from the Sellafield discharges as a dating tool. Central to this study was examination of the physical processes which affect the spatial distribution of the radionuclides within the estuary. They observed that higher concentrations of the radionuclides were associated with the finer silts found in the low energy environs at the banks of saltmarsh creeks. The more coarse-grained sands were associated with the higher energy environments of the lower river reaches. Seasonal differences in deposition were also pointed out. During more settled summer months, fine particles were deposited in contrast to the deposition of coarse-grained sands during the stormy winter period. The work initiated by Hamilton and Clarke (1984) on the impact of radionuclides on saltmarsh environments has been extended by Kelly *et al.*, (1991) who investigated the relationship between sediment and plutonium budgets in the Esk Estuary. Their findings are applicable to any small macrotidal estuary in the Irish Sea basin. The Esk Estuary is characterised by a strongly asymmetric tidal cycle and a meandering river channel through a series of sedimentary deposits which varied from permanent gravel and mussel beds of the deep water channel to more mobile sand and mud banks further upstream with saltmarsh vegetation established above the mean high water mark. Kelly *et al.*, (1991) observed that the various water movements within the estuary play a significant role in erosional/depositional processes within the estuary. There is a short flood tide (3.3 hours) which brings a net input of sediment to the estuary of approximately 18 tonnes. Sedimentary material from the Irish Sea accounts for nearly 90% of the deposits in the inner estuary. These

sediments are transported upriver by the incoming saltwater body. Preceding this movement, as the tide turns, the mixing of the salt and fresh water creates an initial tidal surge as brackish water moves upstream. This surge results in the remobilization of sedimentary material from the lower reaches for deposition on the intertidal banks upstream. Kelly *et al.,* (1991) estimated that this process accounts for the supply of about 10% of the deposits in the inner estuary. During the longer ebb tide (8.75 hours) there is limited transportation of eroded material out of the estuary. As far as the transportation of particle-associated plutonium is concerned, it is deposited within the sediments of the inner estuary by the incoming tide. However, a small proportion is desorbed during the above processes, as particulate phase plutonium which is equilibrated with saline pore water comes into contact with low pH brackish water. As the authors observed, this can result in the removal of this component from one location to another within the estuary.

1.4.4.2 Temporal Trends in Surface Sediment Concentrations

Radionuclide concentrations in surface intertidal sediments have shown a gradual decline since the mid 1970's (MAFF, 1972-1990). The decline has been less than one order of magnitude compared with the two orders of magnitude decline in Sellafield annual discharges over the same period. The rate of decrease has been greatest for the more highly contaminated sites close to Sellafield. For example, the concentration of $^{239+240}Pu$ in the surface sediment at Newbiggin, on the Ravenglass Estuary, has declined from a peak of 4,500 Bq kg^{-1} in 1979 to 1,100 Bq kg^{-1} in 1989. In contrast, locations more distant from Sellafield have not experienced such a pronounced decline, with for example, $^{239+240}Pu$ concentrations at Kippford (silt) on the Solway Coast declining from a peak of 540 Bq kg^{-1} down to 210 Bq kg^{-1} in 1989. Temporal variations in surface sediment concentrations at various locations along the coast of the Irish Sea are illustrated in Fig 1.16. The pronounced decline in concentrations in the more highly contaminated sites close to Sellafield reflects the decline in discharges from the plant and the gradual dilution and dispersion of contaminated sediment from the reservoir of fine silt off the Cumbrian Coast (Hunt, 1985). The isotope activity ratios of $^{134}Cs/^{137}Cs$ and $^{238}Pu/^{239+240}Pu$ recorded at the various sample locations showed close general agreement between different sites and were systematically lower than the activity

ratios of the discharges.

In conclusion the concentrations of radionuclides in intertidal sediments have not declined in proportion to the decrease in the Sellafield discharges. The results are consistent with and lend support to the suggested mechanism of redistribution of sediment between the highly contaminated and less contaminated areas.

1.4.4.3 Vertical Distributions of Radionuclides in Intertidal Sediments

The depth distributions of radionuclides in Irish Sea intertidal sediments have been investigated in attempts to derive information on sedimentation rates and transportation processes operating within this environment.

Accumulating sediments preserve a record of temporal variations in radionuclide concentrations and activity ratios at the site of deposition, providing there is no post-depositional mixing. Numerous studies of Sellafield waste radionuclide distributions in accumulating intertidal and saltmarsh sediments of the Irish Sea have been reported in which the radionuclide concentration profiles exhibit distinct sub-surface maxima and the profiles bear a qualitative resemblance to the Sellafield discharge pattern (Aston and Stanners, 1979; Aston and Stanners, 1981a; Aston and Stanners, 1982a, b, c; Hamilton and Clarke, 1984; Ben-Shaban, 1989; Kershaw *et al.,* 1990).

Aston and Stanners (1981a) describe the transportation and deposition of $^{239+240}$Pu in the Ravenglass Estuary. Radionuclide concentration profiles in sediment cores of varying depth were compared with the ^{238}Pu/$^{239+240}$Pu activity ratio in the Sellafield annual discharges. In order to achieve a satisfactory fit between the peak concentration and maximum discharge the authors suggested that a 'lag time' between discharge from Sellafield and deposition on site should be adopted. With a lag time of 2.6 year the ^{238}Pu/$^{239+240}$Pu activity ratio produced a closer fit to the sediment profile. The lag times were found to vary for different radionuclides; eg 2-3 years for plutonium isotopes compared with 1.5 years for ^{134}Cs and ^{137}Cs: a situation which is hard to make compatible with the particulate accumulation model. Moreover, discharge data on the plutonium isotopes were not recorded

separately in the BNFL Annual Reports before 1979, so it was necessary to estimate the Sellafield $^{238}Pu/^{239+240}Pu$ activity ratios from recorded annual measurements of surface sediment concentrations in the Ravenglass Estuary (Hetherington, 1978). The mechanism of radionuclide transport suggested by Aston and Stanners (1981a) requires that after each discharge event, the radionuclides are taken up by particulate material and deposited on the seabed, subsequently being transported by bed-load to the sample site over a 2.6 year period. In order to retain the isotopic signature of the discharge it must be assumed that no mixing of the discharged radionuclides occurs during transport to the site of deposition and that no post-depositional mixing occurs.

However, Kershaw *et al.*, (1983,1984) have subsequently established that mixing by bioturbation does occur in the fine silt off the Cumbrian coast. In addition, transportation by bed-load requires movement of particles along the sea floor by several processes. In marine environments in general, the larger particles (pebbles) are transported by a rolling action, finer particles by a combination of collisions between particles on the bed and those which are saltating, (i.e. hopping along the bed) (Selby, 1985). The most probable mechanism of transport affecting the area of fine silt off the Cumbrian coast is almost certainly resuspension, as a consequence of the high velocity of water induced by wind, tidal and current action in the shallow sea. These processes result in well-sorted abraded material which implies that any material which has been subject to such transportation will have experienced some degree of physical mixing. Thus, to use a straight correlation between the Sellafield annual discharges and sediment profiles is too simplistic and does not adequately take into account the physical processes taking place within the marine environment.

MacKenzie and Scott (1982) presented ^{137}Cs and $^{239+240}Pu$ concentrations for sediment cores from four intertidal sites around the Scottish coast. At Skyreburn Bay on the Solway Coast, the profiles exhibited sub-surface maxima with the maximum concentration of ^{137}Cs (950 Bq kg^{-1}) and $^{239+240}Pu$ (77 Bq kg^{-1}) in the 9-12 cm depth interval. The authors indicated that these profiles were inconsistent with a simple accumulation model but were compatible with a mechanism involving post-depositional mixing in conjunction with accumulation. They postulated that

Fig 1.16 Temporal variations in $^{239+240}Pu$ concentrations in surface sediments at various locations along the coastline of the Irish Sea.

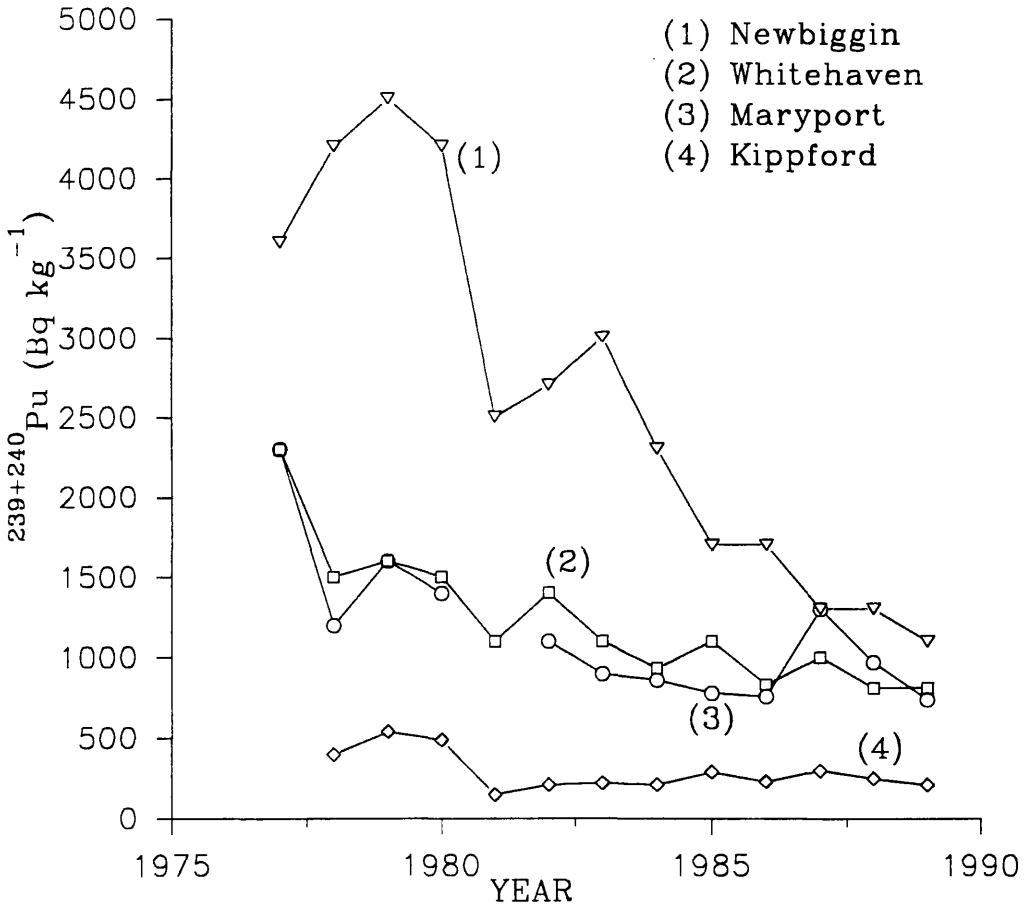

the sedimentation is probably a transient component of a complex, long-term reworking of these sediments because the bay has been stable over long periods. A major omission in this work was the assumption that all the mixing was post-depositional, the authors did not consider that pre-depositional mixing due to transportation processes, (solution and particulate) would have an impact on the core profile. The authors concluded that the mixing of discharges of different ages and isotope ratios in Irish Sea waters and surface sediments leads to uncertainty in relating observed profiles to discharge data.

Hamilton and Clarke (1984) investigated the sedimentation history of the Esk Estuary. A number of sediment cores and surface samples were collected from various sites which were deemed to be representative of the estuary. Sediment core A, collected from the intertidal zone, was sparsely covered with vegetation (*Salicornia*) and exhibited a sub-surface maximum at a depth of 18 cm (1.6×10^4 Bq kg^{-1} of ^{137}Cs). In contrast, core B located near the limit of the mean high water mark (MHWM) was covered by various species of grass and produced a sub-surface maximum at a depth of only 7 cm (1.7×10^4 Bq kg^{-1} of ^{137}Cs). It can be concluded that the deposition of the radionuclides corresponded to the particle size distribution within the sediments and that the frequency of tidal inundation in the more vegetated areas was lower, thereby reducing the depth but not the concentration of deposited material.

More recently, Kershaw *et al.*, (1990) have reported a highly detailed study of sediment cores from Maryport Harbour, Cumbria. The harbour was dredged in the 1950's and has been subject to rapid sedimentation with little post-depositional mixing since then. The radionuclide concentration profiles in the sediment cores exhibited sub-surface maxima which have been assumed by the authors to correspond to the period of maximum discharges from Sellafield in the 1970's (Table 1.1). These were used to determine the rate of sediment accumulation and as with Aston and Stanners (1982), a lag time of 2 years was assumed between discharge of radionuclides from Sellafield and their deposition in the harbour. The resultant chronology, partially supported by ^{210}Pb dating, was used in conjunction with plutonium isotopic data from the cores and published discharge data for α-emitting isotopes of plutonium, in an attempt to quantify the ^{238}Pu discharged from

Sellafield prior to 1979 when releases of this isotope were not recorded separately (Kershaw *et al.*, 1990). The application of ^{210}Pb dating techniques to the Maryport core has a potential shortcoming, since the distribution of ^{226}Ra and ^{210}Pb within the sediments of the eastern Irish Sea is not in a natural steady state system but has been perturbed by discharges from the Albright and Wilson, Marchon chemical plant at Whitehaven. This plant is involved in the manufacture of phosphates from sedimentary rocks which have a characteristically high U content (including all decay products in the ^{238}U and ^{235}U series). McCartney *et al.*, (1990) stated that the enhanced levels of ^{226}Ra in the Irish Sea are in fact the result of discharges from the Marchon plant and that releases of ^{210}Pb are responsible for some of the variability observed in the Maryport core. The releases from Marchon lead to potential difficulties in using the $^{210}Pb_{excess}$ distribution to calculate sedimentation rates independent of the Sellafield chronology. However, the technique does provide supporting evidence when used in conjunction with the Sellafield chronology.

1.4.4.4 On-shore Transfer of Radionuclides

Since 1976, personnel from A.E.R.E. Harwell have undertaken research into possible on-shore transfer of radionuclides via suspension in sea spray along the Cumbrian coast (Cambray and Eakins, 1980; Eakins *et al.*, 1981; Eakins and Lally, 1984; Eakins *et al.*, 1987). This process is based on the observation that the actinides are associated with the very finest sediment particles which could possibly be transported within water droplets or aerosols. Eakins *et al.*, (1981) recorded enhanced accumulations of $^{239+240}$Pu in soil samples taken along a transect running inland from the coast. Plutonium concentrations declined with increasing distance inland, and the authors used the ^{238}Pu/$^{239+240}$Pu activity ratio to support the argument that the excess over fallout levels was due to on-shore transfer of Sellafield-derived radionuclides. Muslin screens were used to collect airborne particulate material brought on-shore by the sea spray in an attempt to estimate the magnitude of the on-shore transfer. Eakins *et al.*, (1981) estimated that about 3.7 x 10^{10} Bq to 7.4 x 10^{10} Bq of Pu α emitting radionuclides had been transported on shore in this way.

Pierson *et al.*, (1982) suggested three possible mechanisms for the enhanced radionuclide concentrations inland from the Cumbrian coast, namely: (a) suspension of the sea surface microlayer in the form of spray, either by the wind or bubble bursting, (b) injection of seawater and sediment into the air by waves breaking in the surf zone and (c) movement of sediment to intertidal regions and subsequent resuspension by wind. Eakins and Lally (1984) investigated the mechanisms of on-shore transfer of actinides in Cumbria. Measurements of the concentration of actinides in air at various heights and distances inland from the sea indicated that there was a marked decline in concentration with distance for samples collected near the ground (2 m elevation), while at a height of 10 m the decline was less pronounced. These measurements suggested that there were two sources of actinide-bearing sea spray affecting the sample sites. The major source, the surf zone, produced enhanced concentrations closer to the beach with a decline inland. In contrast the minor source, located further out to sea, produced lower concentrations than the surf zone but sustained the concentrations for much greater distances inland. The $^{241}Am/^{239+240}Pu$ activity ratios were constant for both sources indicating a common origin of suspended sediment in seawater. Eakins and Lally (1984) concluded that foam flotation of sediment in the surf zone, with subsequent injection of particulates into the atmosphere by bursting bubbles was the major mechanism whereby sea spray is enriched with actinides. The enrichment of the sea-surface microlayer was suggested as a possible contributor to concentrations of actinides in air, however, it was felt that when the wind strength was sufficient to generate breaking waves the microlayer would probably be unstable. McHugh and Hetherington (1987) investigated the on-shore transfer of actinides using air samplers at five locations along the Solway coast of south west Scotland. The $^{239+240}Pu/^{238}Pu$ activity ratio in air samples indicated that the actinides in air along the Galloway shoreline arose mainly from resuspension of radionuclides of marine origin rather than atmospheric sources. Garland *et al.*, (1989) investigated the spatial distribution and on-shore transfer of Sellafield-derived radionuclides in the Cree Estuary in south west Scotland. McDonald *et al.*, (1990), reported similar results, with radionuclide concentrations reflecting particle size distribution and concluded that the on-shore transfer of actinides within sea spray was an order of magnitude lower in south west Scotland when compared with recorded levels in Cumbria. McDonald *et al.*, (1992) examined the on-shore

transfer of radionuclides along the river banks and inland areas of the Solway coast. The soil samples collected along the river banks exhibited isotopic and nuclide activity ratios characteristic of the Sellafield discharges. In addition the transects running from the mean high water mark, inland for 3km, indicated that on-land transfer by aerial deposition may have been occurring up to a distance of <1 km inland at transect (C). This transect, at Chapel Croft, was elevated and produced $^{238}Pu/^{239+240}Pu$ activity ratios characteristic of the Sellafield discharges (ranging from 0.17 to 0.1), weapons fallout levels (0.04) were not attained until reaching a distance of 1 km inland. The authors indicated that tidal inundation was responsible for localized enhancements in radionuclide activity ratios recorded at the 5 other low lying transects. McKay and Pattenden (1990), in their review of on-shore transfer from sea to land via the air, establish that this particular mechanism could give rise to a human exposure of less than 5% of the ICRP-60 principal limit of 1 mSv y^{-1} along the Cumbrian coast.

1.4.5 Geochemical Behaviour of Caesium, Plutonium and Americium in the Floodplain Environment

While much work has been concentrated on the spatial distribution of Sellafield-derived radionuclides, another equally important facet of research is understanding the chemical behaviour of ^{137}Cs, ^{241}Am and $^{239+240}Pu$ within the environment. It is of fundamental importance when estimating potential exposure risks to identify how the radionuclides behave once they are brought on-shore and to ascertain whether there will be any change in associations as geochemical conditions alter from the saline, well oxygenated, alkaline, marine environment of the Irish Sea to the saltmarsh environment with variable salinity, acidic/ neutral pH and variable Eh with reducing conditions in places.

Several workers have reported results of investigations into the geochemical behaviour of ^{137}Cs and $^{239+240}Pu$ within Irish Sea sedimentary materials. (Aston and Stanners, 1981c,e; Livens and Baxter, 1988; Baxter *et al.*, 1989 and McDonald *et al.*, 1992). Central to these investigations has been the adoption of some form of sequential extraction scheme utilising a series of increasingly aggressive chemical reagents to remove ions from notionally discrete components of the soil. The

sequential extraction schemes outlined by Tessier *et al.,* (1979), Maher, (1984) and Chester *et al.,* (1986) have been recently criticised by Wilkins *et al.,* (1986), Kheoboian and Bauer, (1987) and Mudge *et al.,* (1988), on the basis that the use of more aggressive leaching solutions for the initial washes may generate severe experimental artefacts and that differences in the geological and chemical composition of samples may prevent accurate comparisons between leaching schemes and sample matrixes. The results from such schemes remain operationally defined and therefore should be interpreted as providing relative rather than absolute data (McDonald *et al.,* 1992). Aston and Stanners (1981a) subjected surface sediment samples from the intertidal reaches of the Ravenglass Estuary to a single acid leach in order to determine the quantities of plutonium associated with the non-detrital Fe/Mn phases. It was observed that on average, 84% of the $^{239+240}$Pu present was associated with this phase. Livens and Baxter (1988) investigated variations in possible chemical associations of $^{239+240}$Pu within four different soil types from Cumbria. Of major importance as far as the present research is concerned are their findings for a sand sample collected 25 m above the MHWM. The sample was subjected to a leaching procedure established by McLaren and Crawford (1973), modified by lu *et al.*, (1981a, b) and further modified for radionuclide speciation studies in Caithness by Cook *et al.*, (1984a, b). The results from Livens and Baxter (1988) indicated that 71% of the $^{239+240}$Pu was associated with the residual phase, 12% with the oxide, 11% with the exchangeable, 5% with the organic and 1% with the adsorbed phase.

McDonald *et al.*, (1992) examined a series of marine sediments and soil samples from the Solway coast. The observed order of geochemical association within the marine sediments was sesquioxide > organic > residual > specific adsorption > readily available, a trend which supports Aston and Stanners (1981a) findings, of an almost total association between plutonium and the oxhydroxide phase of intertidal sediments. The results for the inland soil (Table 1.10), illustrate yet another variation in plutonium phase distribution. The order of geochemical association indicates that plutonium is predominantly associated with the organic phase with a major reduction in the sesquioxide component.

Table 1.10 The Geochemical Associations of $^{239+240}Pu$ in Soils from South West Scotland (McDonald *et al.*,1992)

	% $^{239+240}Pu$				
Sample	Readily Available	Exchangeable Specific Adsorption Sites	Insoluble Organic Chelated Complexes	Sesquioxides	Residual
Kippford Intertidal	<0.05	<0.05	32.4 ± 1.7	56.4 ± 3.3	11.2 ± 0.6
Culkeist	5.6 ± 0.1	3.6 ± 0.4	65.6 ± 5.6	16.6 ± 2.2	8.6 ± 0.9

These observations are very similar to results of a leaching scheme applied to soils in Caithness, northern Scotland by Cook *et al.*, (1984a,b). This research was primarily a study of plutonium associations but also focused on the geochemical associations of ^{137}Cs (Table 1.11), which displayed very different affiliations from that of plutonium.

Table 1.11 Geochemical Associations of ^{137}Cs in Caithness Soils (Cook *et al.*, 1984a)

SITE A (0-5cm)	^{137}Cs %
Readily Available	0.7
Exchangeable, Specific Sites	BDL
Chelated with Organics	13.7
Sesquioxides	1.2
Clay Lattice Edges	29.4
Residual	55.0

These investigations illustrate the differing geochemical behaviour exhibited by plutonium and caesium within soils and sediments. Plutonium is clearly associated with the organic and the secondary Fe/Mn mineral phases with differences in

distribution between intertidal and terrestrial locations. In contrast caesium exhibits a preference for the residual phase and the more acid soluble component (possibly clay lattice edges). The geochemical behaviour of these radionuclides has a fundamental impact on their mobility and availability for re-dissolution, with possible exposure consequences for the human population.

SUMMARY OF CHAPTER 1

The BNFL plant at Sellafield has discharged low level liquid effluent into the Irish Sea since the early 1950's. These discharges have contaminated an area of fine silt off the Cumbrian Coast, which was viewed as a sink for the radionuclides during the 1970's. The rapid decline in the Sellafield annual discharges by two orders of magnitude since the mid 1970's has led to a reassessment of the function of this area and it is now viewed as a potential source of radionuclides as a result of re-dissolution of radionuclides or movement of contaminated silt within the Irish Sea. Surface concentrations of radionuclides within this area of fine sediment have declined since the mid 1970's, indicating re-dissolution and redistribution of contaminated sediment. The tides and currents have transported the radionuclides throughout the Irish Sea basin, with a discernable northwards movement of contaminated sediment. The radionuclides are well mixed during the transportation process and are brought on-shore and deposited in low energy environments of the coastal region. Their spatial distribution is correlated with particle size, the highest concentrations of radionuclides being associated with the finest grains of silt and clay. The surface concentrations of radionuclides in the estuaries and coastal environment around Sellafield have declined by one order of magnitude since the mid 1970's, while further afield on the Solway Coast of south west Scotland the decline has been less pronounced. This implies that, with the decline in the Sellafield discharges, the offshore sediments are the main source of radionuclides and they are subject to mixing, dissolution and redistribution before being deposited on-shore.

AIMS OF RESEARCH

There are four main aims of this project;

1. The merse deposits are known to have high and increasing radionuclide inventories, however, the spatial distribution (lateral and vertical) is not well defined. One aim of this research is to investigate the spatial distribution of $^{137}Cs/^{239+240}Pu$ and ^{241}Am in intertidal and saltmarsh locations within the Solway floodplain.

2. To investigate the transportation mechanism of Sellafield-derived radionuclides to the Solway coast of south west Scotland.

3. To investigate the variations in geochemical behaviour of ^{137}Cs and $^{239+240}Pu$ under contrasting environmental conditions prevalent in saltmarsh and offshore deposits and to investigate the effects of diagenetic processes on geochemical associations and radionuclide behaviour after deposition in saltmarsh environments.

4. To investigate the desorption of ^{137}Cs from contaminated sediment using a variety of leaching media.

CHAPTER 2
EXPERIMENTAL

2.1 SAMPLE COLLECTION

The main areas of study within this project were the merse deposits of the Solway Firth floodplain. The aim of the sampling programme was to collect a comprehensive suite of merse material to enable a detailed study of concentrations, spatial distributions, inventories, activity ratios and geochemical associations of anthropogenic radionuclides in this environment.

Several sampling techniques were adopted during the course of this research and the three principal methods were:

1) Vertical profiles of river bank sediments were collected by preparing a clean vertical face at the stepped edges of the merse and extracting the sediment samples in 5cm depth intervals with a trowel, down to a maximum depth of 1 m. The typical surface area from which the sample was extracted was 10 cm x 15 cm.

2) Vertical profiles of saltmarsh sediments were collected by digging pits, inland from the river bank. Thereafter, a vertical face was prepared for extraction of the samples by the method described above.

3) Samples for transect and inventory studies (0-30 cm) were also collected using a Farnel Corer. This device was employed to extract cylindrical cores of diameter 3.8 cm, down to a depth of 30 cm.

A number of sites were studied during the course of this work, the sampling locations being indicated in Fig 2.1. A brief description of the sampling techniques used at each location is presented in the following sections.

Following collection, the samples were placed in marked polythene bags and returned to the laboratory for pretreatment prior to analysis. The 'wet' sediment samples were subjected to an initial mixing process. The samples were 'kneaded'

by hand within the polythene bags to break up any large lumps, a spoon was then used to mix the sediment before a sub sample was extracted. The sub sample from each bag was dried overnight at 60°C and sieved through a 2 mm mesh prior to γ spectroscopy. In addition, selected samples underwent: (i) further radiochemical analyses for the determination of ^{238}Pu, $^{239+240}Pu$ and ^{210}Pb (via ^{210}Po) and (ii) selective extraction to determine geochemical associations of ^{137}Cs and $^{239+240}Pu$ as described in detail below. The portions of the sample not used for γ spectroscopy were kept in plastic bags under refrigerated conditions.

2.1.1 Southwick Water

Three sample sites were selected at Southwick water, (illustrated in Fig 2.2). These were subject to contrasting geomorphological processes which permitted the investigation of the vertical distribution of radionuclides within saltmarsh sediments at sites which were subject to alternating erosion and deposition. Visual observation at the sites revealed that they had been subject to accumulation and sediment profiles from these locations therefore had the potential to provide information on temporal trends in deposition processes. However, areas of the bank adjacent to the sample sites were subject to undercutting and slumping as discussed in Section 1.3.

Sediment samples (15 x 10 x 5 cm) were obtained from the bank of the Southwick Water by cleaning and sampling the vertical cliff face as described above.

Southwick Core No.1 [(SC1), NX 914 562 (Landranger 1:50,000, Sheet 84) collected 8/12/89 and illustrated in Plate 2.1] was located 200 m downstream from the intersection of the path from the entrance to the Scottish Wildlife Trust's Southwick Coast nature reserve at Netherclifton. A visual inspection of this site suggested that it was a location subject to net sedimentation and a 70 cm core was extracted.

Fig 2.1 Location map of sampling sites along the coast of south west Scotland.

1. Wigtown
2. Creetown
3. Orchardton
4. Kippford
5. Southwick
6. Carse Bay

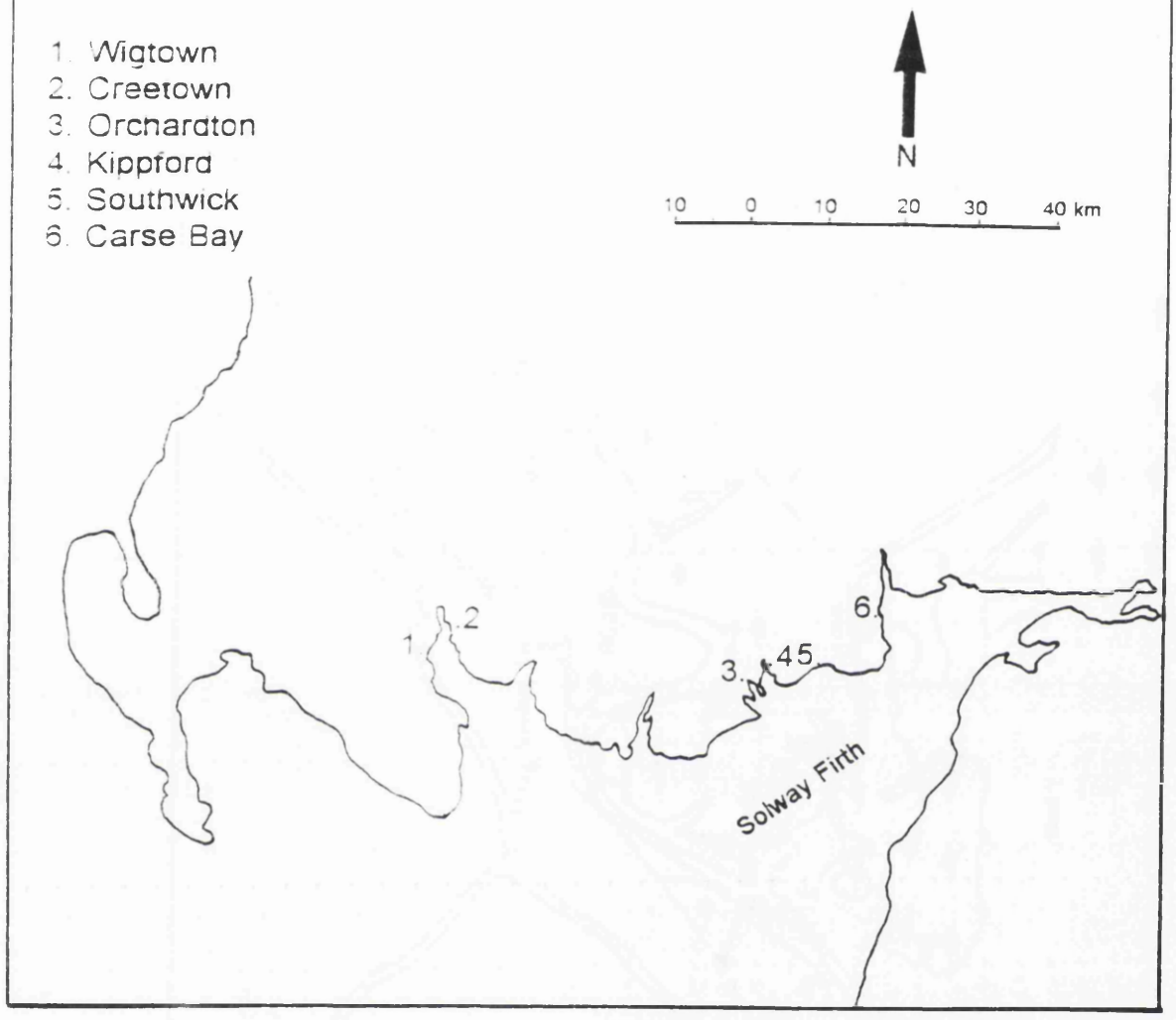

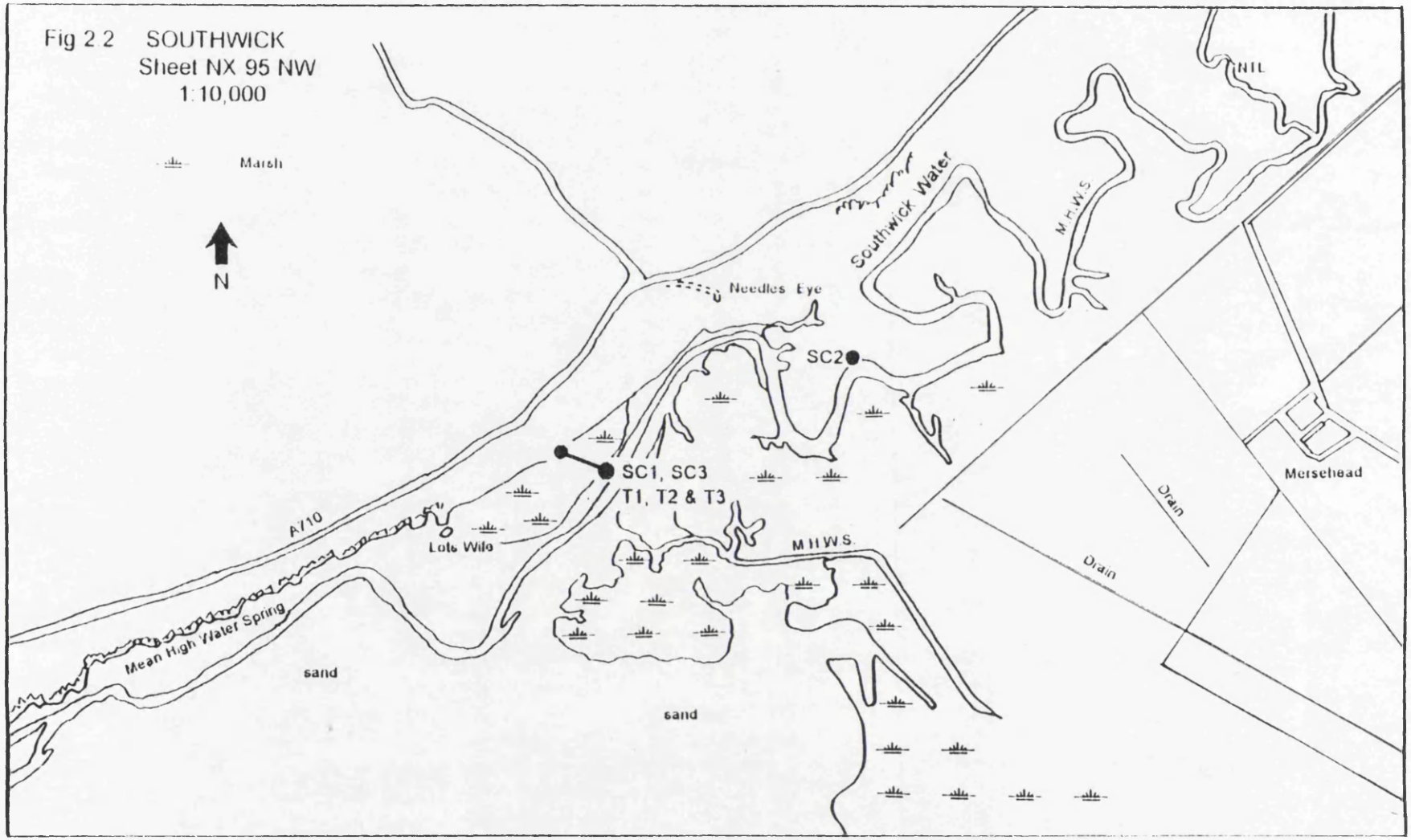
Fig 2 2 SOUTHWICK
Sheet NX 95 NW
1:10,000
Marsh
N
Needles Eye
Southwick Water
M.H.W.S.
NTL
SC2
SC1, SC3
T1, T2 & T3
Mersehead
Drain
Drain
M.H.W.S.
A710
Lots Wife
Mean High Water Spring
sand
sand

Plate 2.1 Photograph shows collection of section SC1 from the MHWM of the merse at Southwick Water.

Plate 2.2 Photograph shows the collection of section SC2 from the bank of Southwick Water.

Fig 2.3 Farnel Corer used to collect transect samples.

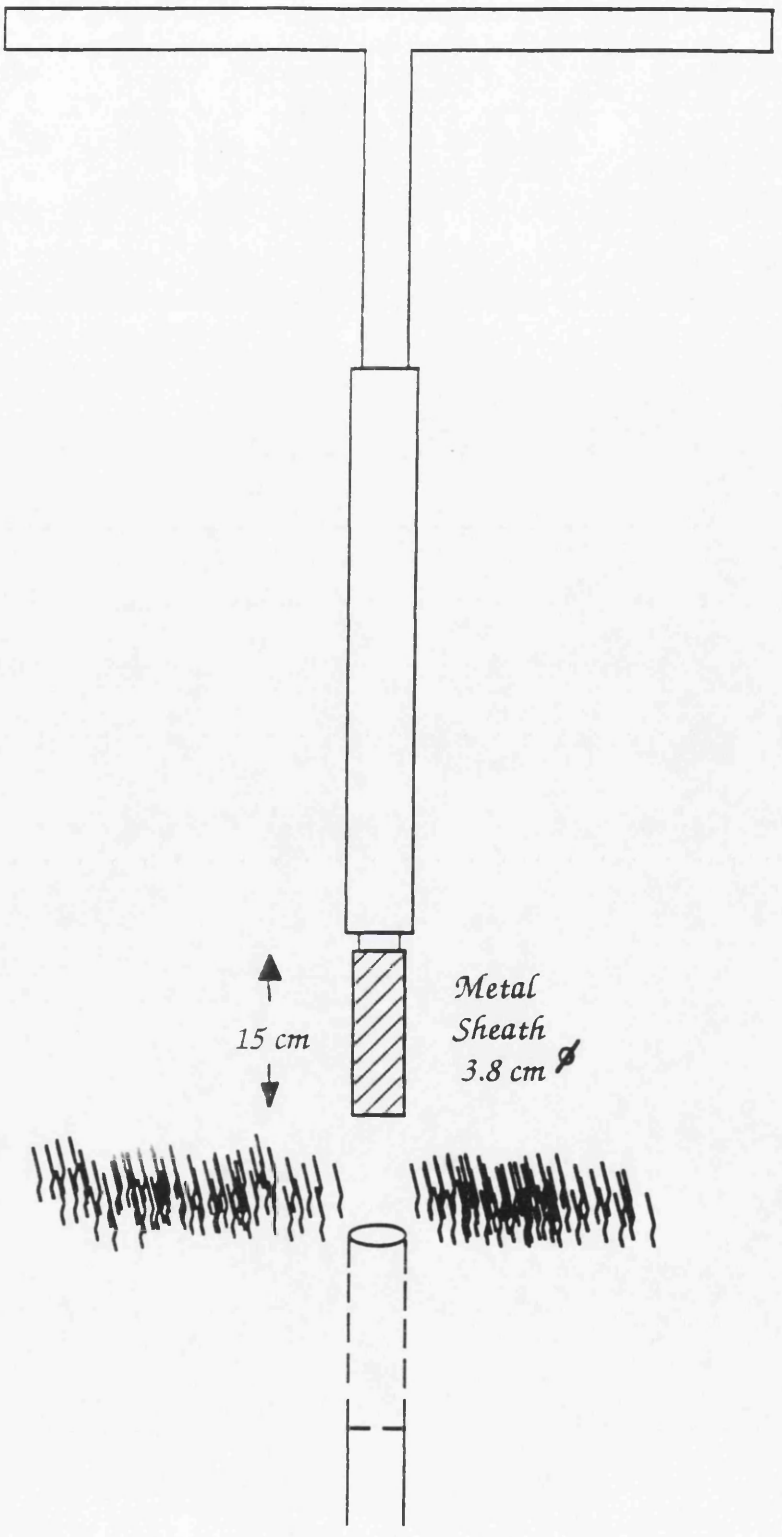

Southwick Core No.2 [(SC2), NX 918 561 collected 21/3/90 and illustrated in Plate 2.2] was obtained from the exposed vertical cliff face (height 1 m) at the second meander of the Southwick Water, some 200 m upstream from the intersection of the path and the river. A 1 m core was extracted from this site which being on the outer curve of a meander (convex bank), suggested that it was subject to erosion processes.

Southwick Core No.3 [(SC3) NX 914 562 collected 10/10/91] was located close to the site of SC1. Three depth intervals, 0 - 5cm, 40 - 45 cm and 65 - 70 cm were extracted, for use in the batch desorption experiment (described in Section 2.7.1) with the rest of the core being discarded.

2.1.2 Transects Across Floodplain Deposits

In order to establish the spatial distribution of radionuclides in the top 30 cm of the Solway merse, a series of sample transects, running inland across the merse, was collected from locations along the coastline as outlined in Fig 2.1. Samples were collected at regular intervals along horizontal transects running inland across the merse from the intertidal zone. The stepped edge of the merse, marking the mean high water mark (MHWM), was taken as the zero point of the transect. The transect was extended out from the river bank into the intertidal deposits for distances up to 100 m with the sample points in these locations being identified by negative numbers in the relevant tables in Chapter 3. A Farnel Corer, illustrated in Fig 2.3, was used to collect cores from 0-15 cm and 15-30 cm depth intervals at each location. The detachable metal sheath was driven into the ground by the handle in a hammering action down to a depth of 15 cm. The apparatus was withdrawn, the sheath removed and the sample extruded using a 3.8 cm diameter metal plunger. The sheath was cleaned and re-inserted into the hole to extract the 15-30 cm interval. This procedure was repeated at each sampling location along the transect. The samples were placed in marked plastic bags for transportation back to the laboratory. Details of the individual transects are as follows.

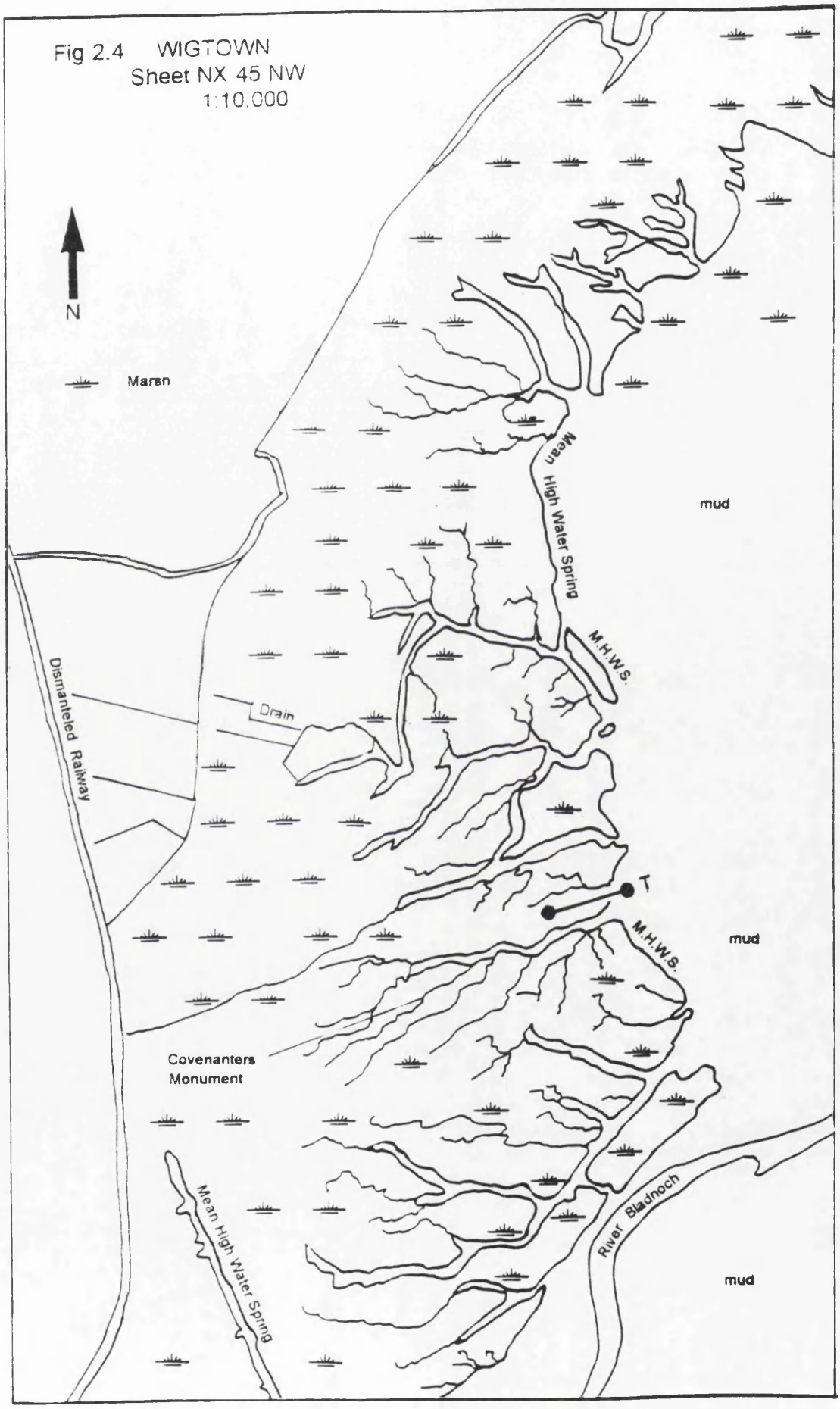
Fig 2.4 WIGTOWN
Sheet NX 45 NW
1:10,000
N
Marsh
Mean High Water Spring
mud
M.H.W.S.
Drain
Dismantled Railway
T
M.H.W.S.
mud
Covenanters Monument
Mean High Water Spring
River Bladnoch
mud

Plate 2.4 Illustrates the slumping of the banks along the saltmarsh creeks at Wigtown merse.

Plate 2.3 Illustrates the elevation of the MHWM and the flat topography of Wigtown merse.

i. Wigtown T1

This transect (collected 27/8/90) covered 120 m of intertidal and merse deposits from NX 445 561 to 443 560 (Landranger Sheet 83)and is illustrated in Fig 2.4 and Plates 2.3 and 2.4) began at site No.1, 40 m out from the stepped bank (0 m) of the saltmarsh in an area of subsided and eroded merse, subject to daily inundation by tidal processes. It continued at 20 m intervals to site No.7, 80 m inland across the consolidated merse, an area subject to periodic tidal inundation during high spring tides and storm surge events.

ii. Creetown T1

This transect (collected 28/8/90 and illustrated in Fig 2.5 and Plate 2.5) traversed over 200 m of floodplain deposits from NX 464 583 to 468 583 (Landranger Sheet 83). Samples 1-3 were collected from the intertidal deposits within the River Cree channel at distances up to 100 m out from the stepped edge of the merse (0 m). Samples 4-9 were extracted at 20 m intervals from the grass-covered, consolidated material of the merse, between the river and the A75 road.

iii. Orchardton Bay T1

This transect (illustrated in Fig 2.6 and collected 29/8/90) covering 190 m of merse from NX 820 534 to 822 537, began in the exposed river bed of the Orchardton Burn/Pottleland Lane and ran north-east across an area covered in salt tolerant vegetation and ended in the improved pasture land south-west of the access road to Almorness House. The whole area covered by the transect was subject to periodic tidal inundation during high spring tides and storm surge events, indicated by flotsam and other marine debris around the retaining wall of the pasture land.

iv. Kippford T1

This transect (collected 28/8/90 and illustrated in Fig 2.7 and Plate 2.6) ran north-east from NX 835 553 to 836 554 (Landranger Sheet 84) over a distance of 85 m.

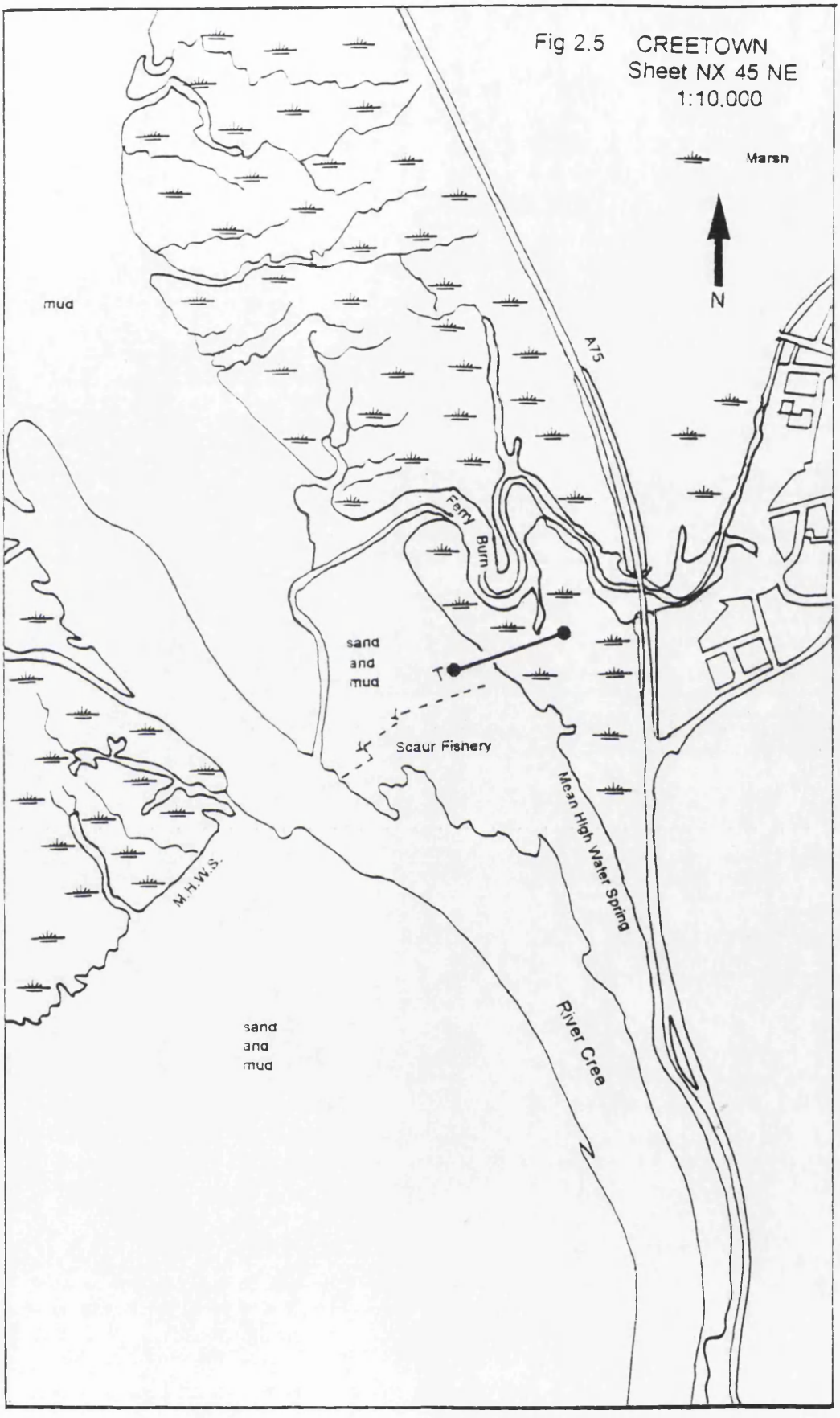
Fig 2.5 CREETOWN
Sheet NX 45 NE
1:10.000
Marsh
N
mud
A75
Fenn Burn
sand
and
mud
Scaur Fishery
Mean High Water Spring
M.H.W.S.
River Cree
sand
and
mud

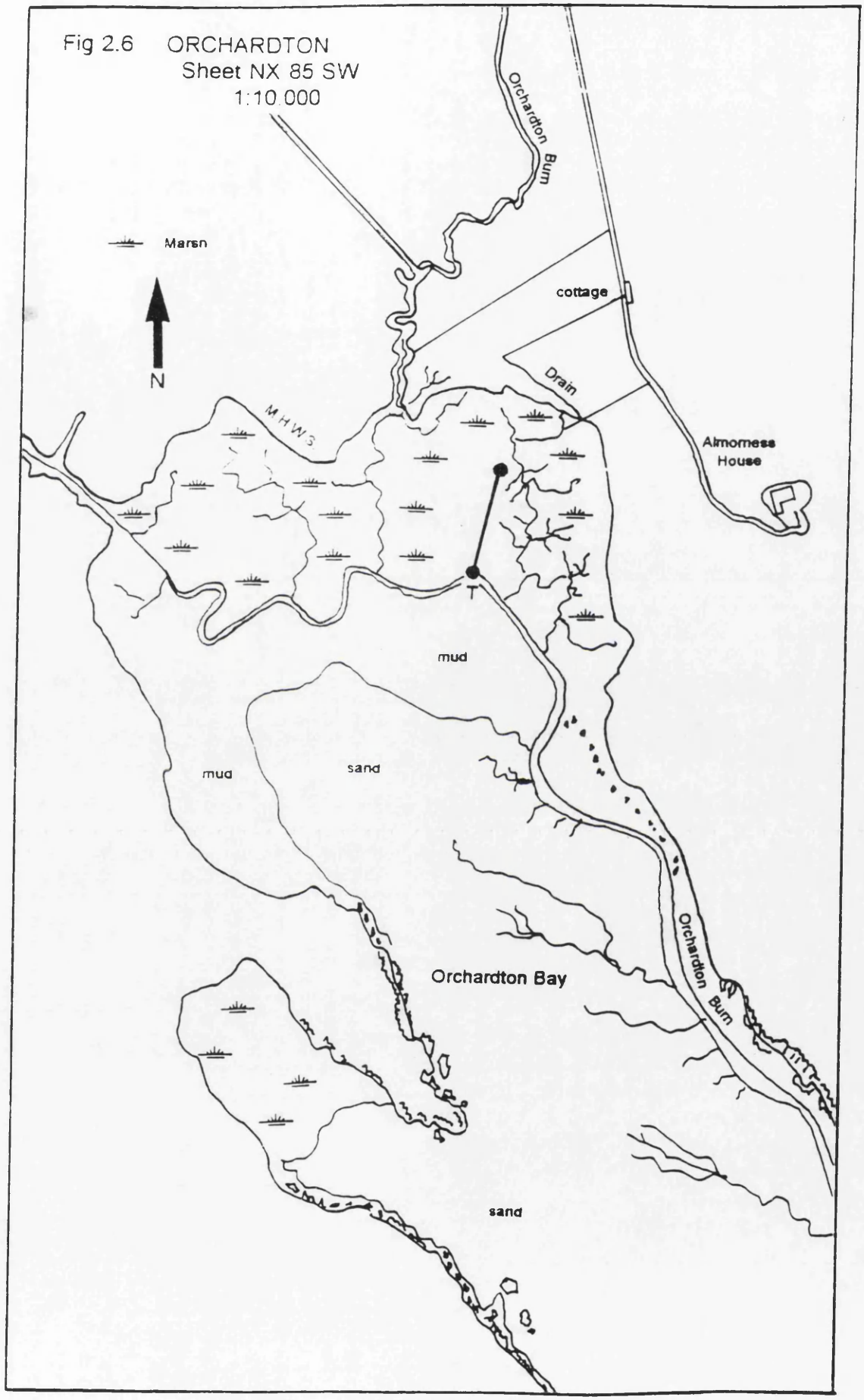
Fig 2.6 ORCHARDTON
Sheet NX 85 SW
1:10,000
Orchardton Burn
Marsh
N
cottage
Drain
MHWS
Almorness House
mud
mud
sand
Orchardton Bay
Orchardton Burn
sand

Fig 2.7 KIPPFORD
Sheet NX 85 NW/SW
1:10.000

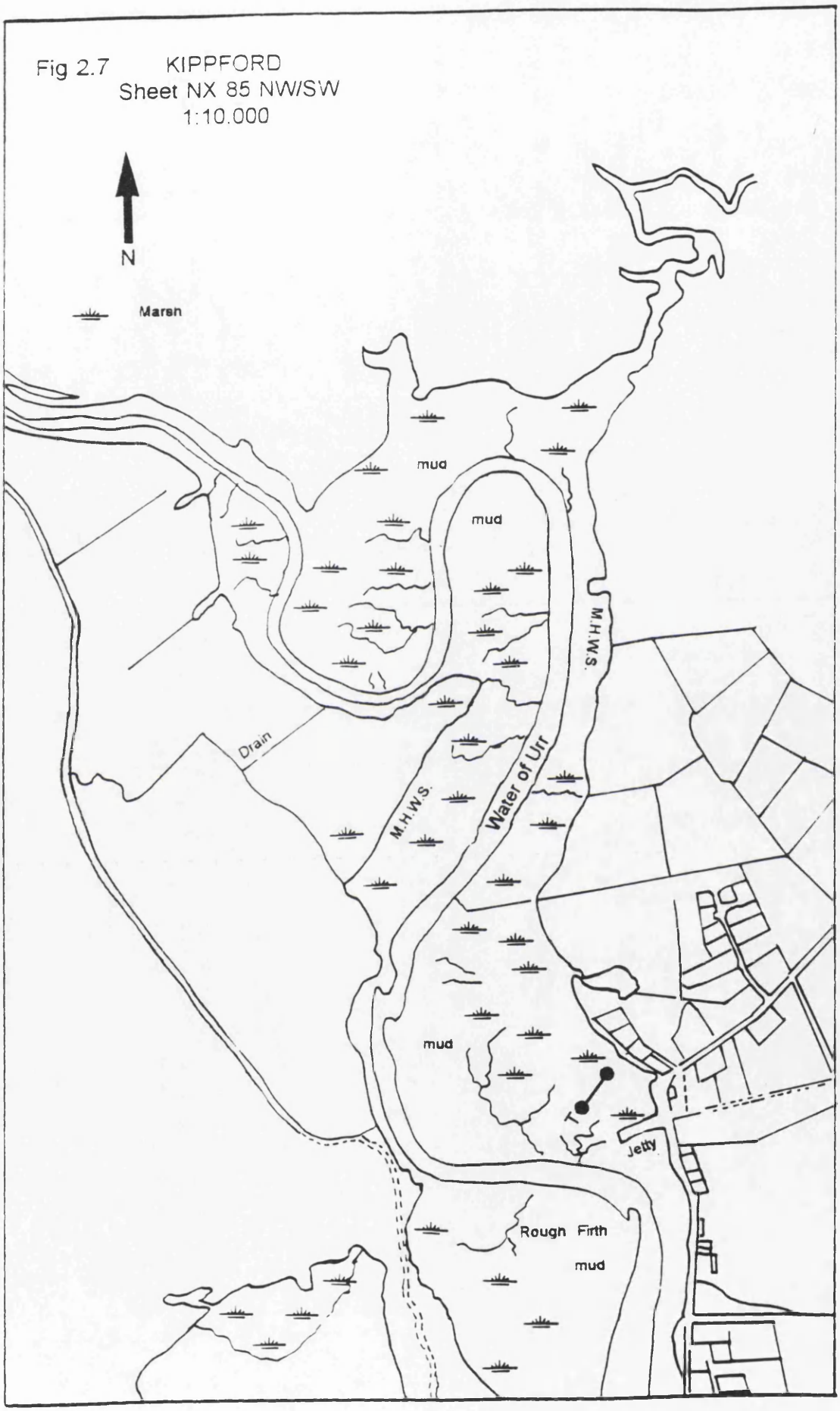

Plate 2.5 Photograph illustrates the vertical cliff face (MHWM) at Creetown merse.

Plate 2.6 Photograph illustrates the merse at Kippford.

Plate 2.7 Photograph illustrates the topography and vegetation cover present at Southwick Water. The two figures represents the approximate location of transect T1.

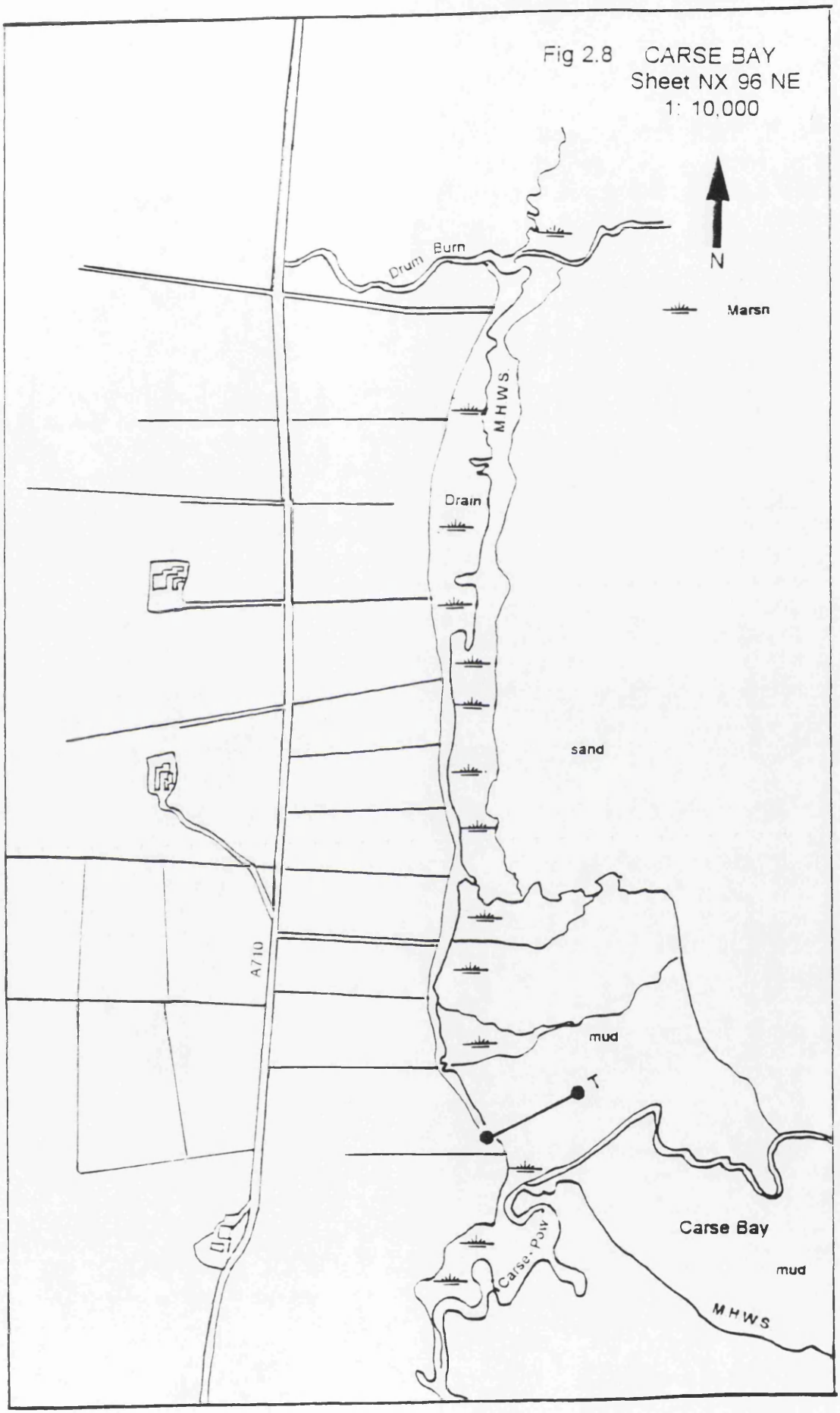
Fig 2.8 CARSE BAY
Sheet NX 96 NE
1: 10,000
N
Marsh
Drum Burn
MHWS
Drain
sand
A710
mud
T
Carse Bay
mud
Carse Pow
MHWS

The sampling area was on the north bank of the Water of Urr. Some time after sample collection, a stone jetty was constructed to the south of the sampling site. This structure, has affected the depositional pattern within the area, acting as a breakwater and protecting the saltmarsh directly behind it to the north, thus enhancing deposition of sediment at this location.

v. Southwick Water T1

This transect (collected 25/7/91 and illustrated in Fig 2.1 and Plate 2.7) started in the exposed intertidal deposits of the Southwick Water less than 1 m from the site of Southwick Core No.1 at NX 914 562 and traversed 70 m across the merse ending at NX 913 563 under the trees at the base of the cliff formed by the edge of the Criffel pluton.

vi. Carse Bay T1

This transect (collected 15/8/91 and illustrated in Fig 2.8) traversed an area of isolated clumps of grassland surrounded by large expanses of mud. The transect was located north of the influent river at Brickhouse and ran inland 200 m from NX 988 605 to 984 604.

2.1.3 Southwick Water T2

In order to determine the vertical distribution and lateral variation of radionuclides within merse deposits, a series of cores was collected from Southwick Water, close to the original transect T1. Five 1 m cores were extracted from the merse at 5 m, 10 m, 20 m, 30 m and 50 m inland from the bank of the Southwick Water. The Farnel Corer (outlined above) was used to extract the cores in 15 cm depth intervals. The samples were extruded and dissected into 5 cm intervals before being placed in marked polythene bags for transportation back to the laboratory. The metal sheaths were cleaned and re-inserted into the hole for extraction of the next 15 cm interval. This procedure was repeated down to a depth of approximately 1 m with the bottom 5 cm of the 90 - 105 cm increment being

Plate 2.9 Collection of samples from transect T3 from Southwick merse.

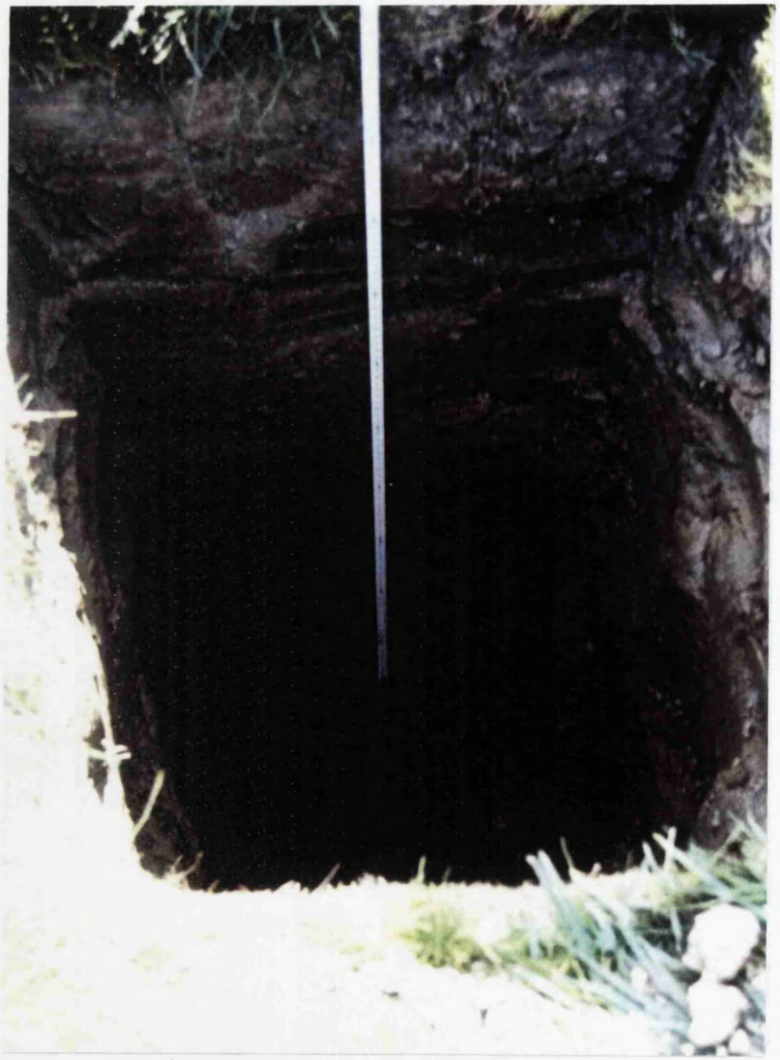

Plate 2.8 Illustrates the vertical face of the soil pit from which samples for transect T3 were collected.

discarded.

2.1.4 Southwick Water T3

As a result of anomalous results obtained in the analysis of cores from Southwick Transect T2, it was decided to re-sample the depth profiles along this transect. On the second occasion, pits were dug at 5 m, 10 m and 15 m inland from the stepped edge of the merse at the river bank close to the location of transect T2, (illustrated in Plates 2.8 and 2.9). A clean vertical face was prepared using a spade and vertical profiles down to a depth of 1 m were extracted in 5 cm intervals. These samples were extracted from a surface area of 15 x 10 cm.

2.2 HIGH RESOLUTION GAMMA SPECTROMETRY ANALYSIS OF SEDIMENT SAMPLES

The detector used for direct γ spectrometric analysis of sediment samples was a co-axial N type HPGe (high purity intrinsic germanium) detector with a thin beryllium window, manufactured by Canberra Industries Inc. The efficiency was 35% (relative to a 3" x 3" NaI(Tl) crystal) with a resolution of 1.9 keV (FWHM) at 1.33 MeV. Shielding for the detector was provided by 10 cm of Pb with a graded lining of Cd and Cu.

The sediment samples were air dried at 60^0 and homogenized to a fine powder by sieving through a 2 mm mesh and grinding using a mortar and pestle. Samples of approximately 200 g weight were accurately weighed into perspex containers of a standard size (150 ml) which were positioned directly over the thin window of the detector. Determination of ^{241}Am, ^{134}Cs and ^{137}Cs used the photopeaks at 59.9 keV, 604 keV and 662 keV respectively. Spectra were typically accumulated for 8×10^4 seconds using a Canberra Series 85 MCA (4096 channels). The spectra were transferred to an IBM-PC for subsequent analysis using Spectran AT software (Canberra Industries, 1986). Spectran-AT is a set of programmes written in IBM° Professional FORTRAN that provides capability for nuclide analysis of radioactive samples based on spectra collected by germanium detectors. The programme includes procedures for peak location, area calculation, multiplet deconvolution and

nuclide identification. A quantitative analysis report, containing nuclide identification and activity concentrations, was obtained by running the appropriate programme. Calculation of concentrations required additional information, extraneous background contributions were subtracted using the appropriate counting geometry spectrum file and all activities were decay corrected to the time of sample collection.

Energy calibration was performed by the accurate determination of the channel location of peaks from a 29.6 kBq ^{152}Eu source. This calibration source produced well defined peaks spaced over the energy range of interest, the energies and relative intensities are listed in Table 2.1.

Energy calibration was undertaken using a standard source and energy plotted against channel number produces a straight line.

Efficiency calibration was performed using the appropriate counting geometries (containers) filled with a standard blank matrix which consisted of a similar material to the samples, doped with a mixed gamma spike (National Physics Laboratory). The blank matrix consisted of a material which exhibited similar properties (Z value) to those found in the sample. The efficiency calibration for Detector 1.4 with a 150 ml perspex tub is illustrated in Fig 2.9. This perspex tub (Geometry 8) was a typical example of the containers used to retain the sediment samples during γ spectrometric analysis.

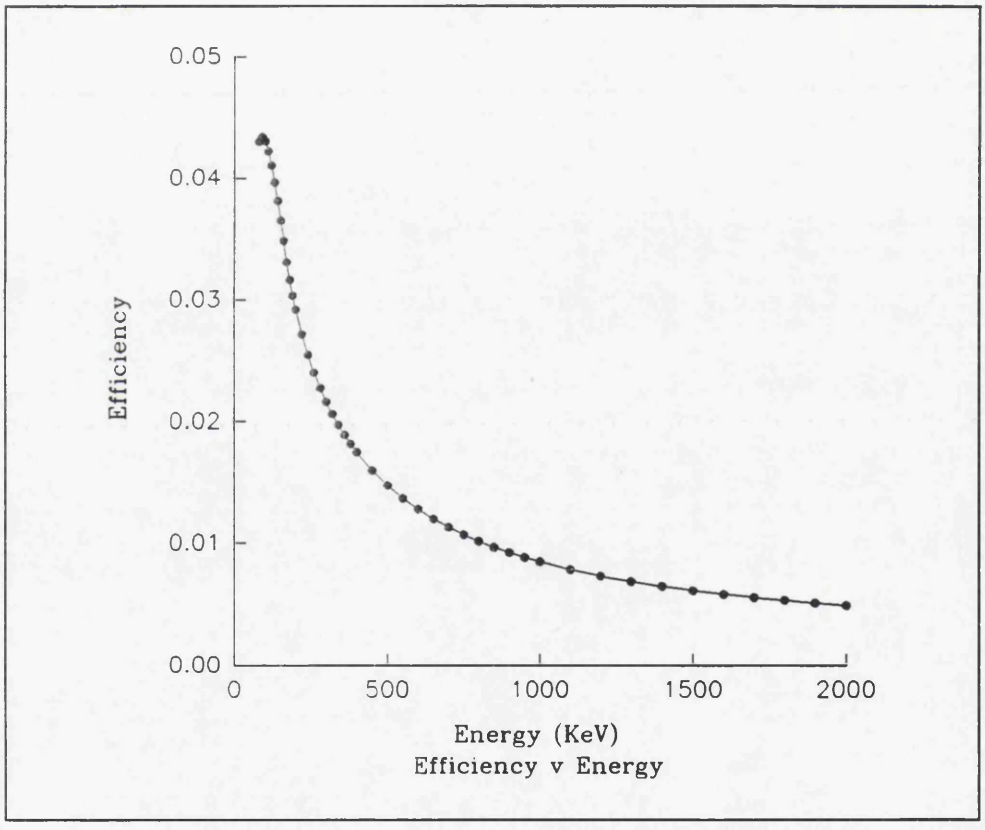

Fig 2.9 Efficiency Calibration Curve for Detector 1.4 Geometry 8.

Table 2.1 The Energies and Relative Intensities of the ^{152}Eu Calibration Source

^{152}Eu Gamma Calibration Energies	
Energy (keV)	Relative Intensity (%)
121.7824	136.2
244.692	35.8
295.939	21.1
344.27	127.5
367.789	40.5
411.115	10.7
586.294	2.2
688.678	4.0
779.08	61.9
810.459	1.52
841.586	0.78
867.388	19.9
919.401	2.09
1005.279	3.1
1085.914	8.2
1089.700	46.5
1112.116	64.9
1212.950	6.7
1408.011	100.0

The accuracy of the procedure was evaluated by periodic analysis of the IAEA Standard Irish Sea Sediment 306 and IAEA Soil 6, the results being illustrated in Table 2.2.

Table 2.2 **Quality Assurance Results from Periodic Analyses of IAEA Standard Irish Sea Sediment 306 and IAEA Soil 6. The Certified Value is Displayed in Bold with the Range of Values in Brackets Below**

IAEA Soil 6	^{137}Cs (Bq kg^{-1}) **(53.6)** (51.4 - 57.9)	^{241}Am
7/12/89	57.1 ± 1.1	NA
12/1/90	55.3 ± 2.0	NA
9/5/92	59.7 ± 2.1	NA
IAEA 306	^{137}Cs (Bq kg^{-1}) **(201)** (194 - 206)	^{241}Am (Bq kg^{-1}) **(1.8)** (1.6 - 2.1)
1/6/92	212 ± 3	3.3 ± 1.0
7/9/92	217 ± 3	4.9 ± 1.7
9/9/92	217 ± 4	3.9 ± 1.4

NA = Not Applicable

The results from these analyses indicate that the values recorded for ^{137}Cs were within the range expected for IAEA Soil 6 and within 10% of the certified value of IAEA 306. The results for the determination of ^{241}Am appear to be less impressive, however, the discrepancies between the Standards and the calibration can be explained. The certified value for ^{241}Am in IAEA 306 is close to the limit of detection for the γ spectroscopy system, the values obtained are therefore also correspondingly close to the limits of the system. At 2σ the values obtained are in much closer agreement with the certified value.

The precision of the γ spectroscopy technique was established by repeated analysis of a sample of Solway Firth intertidal sediment. Two sets of analyses were undertaken to establish 1) the precision based upon counting uncertainties only and 2) the effects of variations in sample geometry and heterogeneity. The precision

of the counting procedure was initially determined by repeated analysis of a sediment sample from Southwick Core No.1, 35-40 cm depth increment, weighing 197.8g. This sample was counted nine times without being moved. The results are listed in Table 2.3. This procedure was supplemented with the introduction of a bulk sample of Southwick Core No.1 30-35 cm depth increment which was sub-sampled. A 1 kg bulk sample of air dried sediment was mixed in a glass jar and a sub sample weighing 206.8 g was extracted and counted ten times in a standard geometry (150 ml container) for 8×10^4 seconds without removing the sample from the detector. This procedure was then repeated with a sub-sample weighing 211.2 g, the results are listed in Tables 2.4 and 2.5. Geometry and sample heterogeneity was examined by selecting a different sub-sample on each occasion (of weight approximately 200g) from the total bulk sediment. On each separate occasion the bulk sample was thoroughly mixed within the jar using an end over end actionfor 2 minutes before the sub-sample was extracted and placed in a standard geometry (150 ml container) using the same filling procedure as adopted for all sediment samples, the results are listed in Tables 2.6 and 2.7 below.

The precision based upon the counting uncertainties was established as being between 0.2% and 0.5%. The Standard Deviation of the values in Tables 2.3 to 2.5 produced a variation around the mean of 0.5%, 0.2% and 0.25% respectively. The precision determined by the variations in sample heterogeneity was established as being between 2% and 3%. The Standard Deviation in Tables 2.6 and 2.7 produced variations around the mean values of ± 34 and ± 48 or 2% and 3% respectively. Therefore the precision of the counting procedures adopted during the analysis of sediment samples by high resolution γ spectrometry was acceptable.

Table 2.3 Analytical Data for 9 Repeat Analyses of Sediment from SC1 35-40 by γ spectroscopy, June 1991

Southwick Core No.1 (35-40 cm) 197.8 g	^{137}Cs (Bq kg^{-1})
SD1000	1643 ± 7
SD1001	1670 ± 7
SD1002	1664 ± 7
SD1003	1658 ± 7
SD1004	1659 ± 7
SD1005	1665 ± 7
SD1006	1665 ± 7
SD1007	1665 ± 7
SD1008	1665 ± 7
Mean	1662 ± 8

Table 2.4 Analytical Data for 10 Repeat Analyses of Bulk Sediment from SC1 (0-35 cm), January 1992

Southwick Core No.1 (30-35 cm) 206.8 g	^{137}Cs (Bq kg^{-1})
SD194	1572 ± 6
SD195	1572 ± 6
SD196	1572 ± 6
SD197	1578 ± 6
SD198	1573 ± 6
SD199	1573 ± 6
SD200	1573 ± 6
SD201	1572 ± 6
SD202	1579 ± 6
SD203	1579 ± 6
Mean	1574 ± 3

Table 2.5 Analytical Data for 10 Repeat Analyses of Bulk Sediment SC1 (30-35 cm), August 1992

Southwick Core No.1 (30-35 cm) 211.2 g	^{137}Cs (Bq kg^{-1})
SD331	1555 ± 6
SD332	1555 ± 6
SD333	1561 ± 6
SD334	1555 ± 6
SD335	1549 ± 6
SD336	1555 ± 6
SD337	1555 ± 6
SD338	1555 ± 6
SD339	1550 ± 6
SD340	1562 ± 6
Mean	1555 ± 4

Table 2.6 Analytical Data for Analyses of 10 Sub-Samples from SC1 (30-35 cm), 21/12/91 - 10/1/92

Southwick Core No.1 (30-35 cm) Bulk	Weight (g)	^{137}Cs (Bq kg^{-1})
SD184	209.5	1567 ± 3
SD185	201.2	1495 ± 3
SD186	206.6	1584 ± 6
SD187	207.9	1568 ± 6
SD188	207.2	1556 ± 6
SD189	205.6	1604 ± 6
SD190	212.8	1602 ± 6
SD191	207.6	1571 ± 6
SD192	207.4	1621 ± 3
SD193	206.8	1572 ± 6
Mean		1579 ± 34

Table 2.7 Analytical Data for Analyses of 10 Sub-Samples of Sediment from SC1 (30-35 cm), August 1992

Southwick Core No.1 (30-35 cm) Bulk	Weight (g)	^{137}Cs (Bq kg^{-1})
SD341	211.2	1562 ± 6
SD342	201.8	1610 ± 6
SD343	204.4	1571 ± 6
SD344	203.0	1588 ± 6
SD345	204.1	1574 ± 6
SD346	194.2	1622 ± 6
SD347	207.0	1570 ± 6
SD348	208.3	1560 ± 6
SD350	209.8	1554 ± 6
Mean		1579 ± 48

NA = Not Available

2.3 ALPHA DETECTORS

Alpha spectroscopy employing silicon surface barrier (SSB) detectors was used to determine concentrations of ^{238}Pu, $^{239+240}Pu$ and ^{210}Po in the sediment samples. Each detector consists of a thin wafer of Si containing a junction of n-type and p-type material. The electrical contact on the face of the detector is extremely fragile, consisting of a layer of gold evaporated onto one side to act as a positive contact, with aluminium being deposited on the reverse to act as the negative contact. Samples underwent radiochemical separations culminating in electro-deposition onto metal planchettes in order to provide suitably thin sources for alpha spectroscopy. The α energies used for the analysis of plutonium isotopes are listed in Table 2.8. The planchettes were positioned as close to the detector as possible for counting, giving detection efficiencies of approximately 25% for 450 mm^2 and 17% for 300 mm^2 detectors. Counting was performed under vacuum to prevent attenuation of the energy of the α particles before they interact with the detector.

A standard source of ^{240}Cm, ^{241}Am and ^{239}Pu was used to produce a straight line energy calibration for each detector. Resolution varied between detectors, but generally for the commonly measured α particles (4 to 6 MeV) was of the order of 16 - 20 keV (FWHM). Observed resolutions for the analyses which reflected the effects of source thickness were typically 35 - 40 keV (McDonald per. comm.). Backgrounds were checked on a regular basis since recoil effects can result in contamination of the detector and produce increases in background levels through time. Background count rates were less than 40 counts over a 2×10^5 second counting period, with typical levels of below 10 counts being recorded.

Table 2.8 **Alpha Energies Used for the Determination of Pu Isotopes in Environmental Materials**

ISOTOPE	α Energies (MeV)
^{238}Pu	5.499
^{239}Pu	5.155
^{240}Pu	5.168
^{242}Pu	4.901

2.4 RADIOCHEMICAL ANALYSIS

2.4.1 Plutonium Analysis

Plutonium analysis of sediment samples was performed by a method based upon that of Lally and Eakins (1978) which was modified by Cook *et al.,* (1984a). This technique includes extraction with HNO_3/HF, followed by HCl, separation of plutonium using anion exchange techniques and electrodeposition of the final sample onto a stainless steel planchette for subsequent α spectrometry, with ^{242}Pu being used as a yield monitor.

Sediment samples were dried overnight at 110°C and then ashed for 8 hours at 650°C to remove organic matter. A 20 g aliquot was placed in a crystallising dish to which 70 ml of (15.6M) HNO_3 was added. The sample was then spiked with 1 ml of ^{242}Pu (0.1445 Bq ml^{-1}), delivered from a suitably calibrated pipette and 10 ml of HF was then carefully added and the sample heated gently until a crust formed. Addition of the HF dissolved silicates and silica (quartz) within the sediment sample. The sample was then boiled for 1 hour in the presence of (11.4 M) HCl. After cooling, the solid and aqueous phases were separated by filtration. The residue was washed with 100 ml of 11.4 M HCl and the filtrate and washings were evaporated to 200 ml before an equal volume of 11.4 M HCl was added and the volume made up to 500 ml by the addition of 8 M HCl. A di-iso-propyl ether (DIPE) solvent extraction was then performed to remove Fe. The residual ether was evaporated off and hydrated aluminium chloride was carefully added to remove any

remaining HF, 100 ml of 11.4 M HCl was added and the solution left to cool. The volume was made up with 11.4 M HCl and 10 ml of (15.6M) HNO_3 was added to ensure that the Pu was in the 4+ oxidation state.

The solution was then passed through a 3 cm diameter by 12 cm length BioRad AG1x8 (100 - 200 mesh) anion exchange column (chloride form) pre-conditioned with 8 M HCl. Under these conditions the Pu in the 4+ oxidation state together with U and Fe were taken up by the resin. Subsequent washes with 8 M HCl removed residual Th and washes with 2 x 150 ml of 8 M HNO_3 were used to elute Fe and U from the resin which was then returned to the chloride form by the addition of an excess of 11.4 M HCl before the Pu was eluted with HI (11.4 M Hydrochloric acid/0.2 M Hydriodic acid), the I^- being used to reduce the Pu. All washes were discarded except the HI solution containing the Pu, which was reduced in volume to 10 ml. 50 ml of 15.6 M HNO_3 were added and the volume was reduced to 2 ml after which the sample was taken up in 50 ml 8 M HCl. The solution was passed through a second AG1x8 anion exchange column, (8 cm x 1 cm diameter) which had been pre-conditioned with 8 M HCl.

The elution process described above was repeated for this column but on a smaller scale. After the HI had passed through the column, 1 ml of $NaHSO_4$ (sodium hydrogen sulphate) was added to the solution to act as a carrier for the Pu and as an electrolyte salt for electrodeposition. The solution was boiled down to dryness and the I^- removed by oxidation via dropwise addition of 15.6 M HNO_3 until all the I^- (purple discolouration) was removed and the residue was white. The sample was then dissolved in 2 ml of 1.8M H_2SO_4 and 5 ml of deionized water, 0.2 ml of EDTA complexing agent and methyl red indicator (used to indicate gross changes in pH) were added and the pH raised by the addition of ammonia solution. The sample was re-acidified (to pH 2.4) by the addition of 0.5 M H_2SO_4 and transferred to an electro-deposition cell. The electro-deposition cell illustrated in Fig 2.10, consisted of a modified polystyrene centrifuge tube, 9 cm long and 2.5 cm in diameter. The conical base was removed and the screw top trimmed by machining. The electrical contact for the cathode was formed by a brass disc attached to a metal pin by a brass screw. The steel planchette, was placed on top of the brass disc and an O-ring was used to provide a water tight seal when the polystyrene tube was

screwed into the base. The anode was formed by a length of platinum wire, coiled at the end, which was passed through another plastic end cap, forming a support to position it centrally in the tube (Kressin, 1977; McDonald, 1989). The wire was attached to a Weir 762 constant current power supply by a crocodile clip. The current was set at 0.5 Amp and the sample was electroplated for three hours. After this time, 2 ml of ammonia solution were added to raise the pH and prevent loss of Pu from the planchette. The solution was electroplated for a further 1 minute and the planchette removed from the electro-deposition cell, rinsed with deionized water, then acetone and dried using a hot air blower. This technique produced the very thin, clean, sources which are required for α spectroscopy. Prior to each plating, the assembled cell was checked for leaks. The advantages of this system were that the polystyrene tubes were disposable, thereby reducing the risks of contamination and also the system was easy to maintain. The brass discs were cleaned after use with 'Brasso' and the Pt wire (anode) was stored in 8M HCl, again reducing the possibility of cross contamination. Blanks were run on a regular basis to ensure the cleanliness of the system.

Alpha spectroscopy was performed using the silicon surface barrier detectors outlined in Section 2.3. Samples were counted for at least 2×10^5 seconds to ensure that sufficient counts from the yield tracer were recorded, to produce suitable counting errors of below 3%.

The sample activity was calculated from the simple ratio of counts in the ^{242}Pu yield tracer peak to the peaks from the ^{238}Pu or $^{239+240}$Pu.

In practice, a number of corrections were made. First, the background (if any) was subtracted from each integral and then the sample peaks were corrected where necessary for cross contamination or overlap caused by tailing of peaks. The correction for tailing was determined by estimating the area under the peak which was produced by the tailing effect of the adjacent peak. This was achieved by

Fig 2.10 Electrolysis cell used for plating planchettes during analysis for plutonium isotopes.

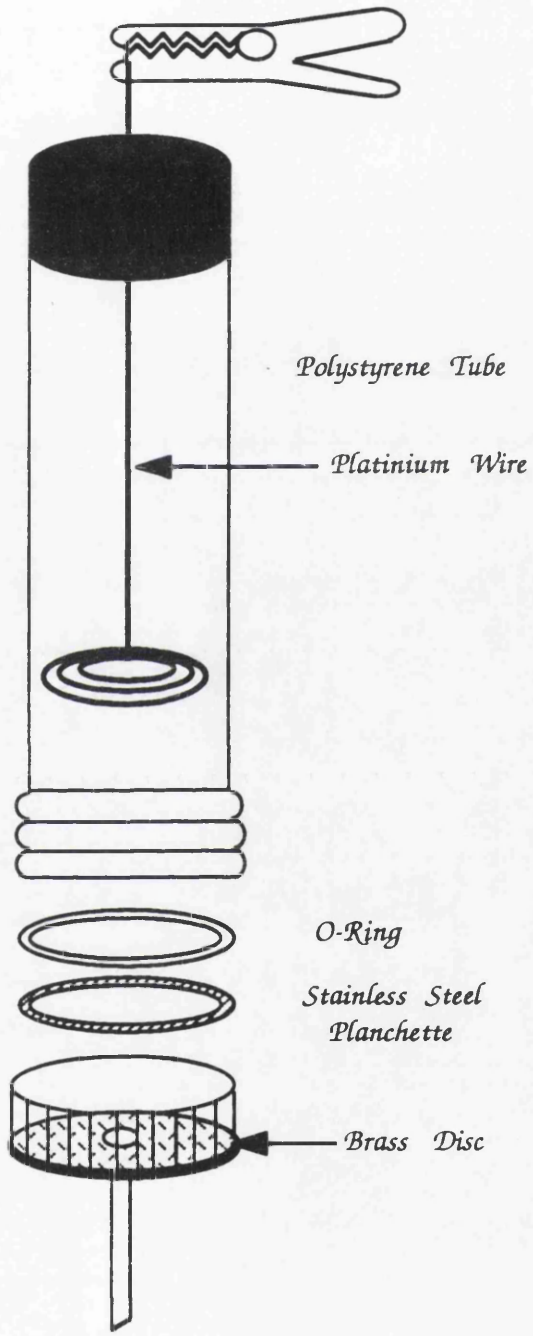

taking 10 channels either side of the region of interest (ROI) of the peak in question and calculating the number of counts per channel. The number of counts per channel was multiplied by the number of channels in the peak responsible for the tailing effect. The product was then subtracted from the affected peak to produce a corrected value for that peak. The product was also added to the peak producing the tailing in order to account for the fact that the tailing effect would distort the true value for that peak. In practice, interference from tailing was not a major problem. The data used in this research were produced from spectra exhibiting well defined peaks.

The major source of experimental error in α spectrometric analysis is the uncertainty from the counting statistics. Provided that the peak intervals are large (at least several hundred counts), the distribution of the counts can be described by the Poisson distribution, which enables modelling of the number of discrete events which occur in a defined interval. The standard deviation of the number of counts recorded in the sample with the fewest counts (800) was 3.5%, in contrast a typical spectrum would contain at least 2,000 counts in the ^{242}Pu peak producing a standard deviation of 2.2%. For a peak interval of I counts, the counting uncertainty is given by $\sqrt{I}$ so that the relative error is $\sqrt{I}/I$. The errors for the determination of plutonium concentrations are described in equation 2.1 below.

$$e = conc.\ x \sqrt{\frac{1}{I_a}} + \sqrt{\frac{1}{I_b}} \qquad (2.1)$$

e = error

I_a = Number of counts of ^{242}Pu

I_b = Number of counts of $^{239+240}Pu$

2.4.2 ^{210}Pb Analysis

The analysis of ^{210}Pb was effected indirectly by the spontaneous deposition of its grand daughter ^{210}Po (half-life = 138.4 days) onto copper foil, followed by α spectrometric determination of the deposited activity and the assumption of secular equilibrium between ^{210}Pb and ^{210}Po to derive the ^{210}Pb content of the samples. The deposition of ^{210}Po on copper is a relatively simple technique with the only significant complication being that ^{210}Bi is also deposited onto the foil, but the ^{210}Bi can be rapidly and totally removed by washing the foil with cold distilled water (MacKenzie and Scott, 1979). The scheme used for the determination of ^{210}Pb in this study is outlined below.

A 5 g sample of sediment was slightly moistened with 2 ml of deionized water and spiked with 0.1 ml of ^{208}Po (6.94 Bq ml^{-1}) yield tracer. Then, 10 ml of 11.4M HCl were added followed by 10 ml of 15.6M HNO_3 and the solution heated for 1 hour at a temperature between 60 - 70^{o}C. The samples were cooled overnight and the supernatant decanted into a beaker. The residual sediment was leached with 6M HCl and this was added to the supernatant, with the solution being evaporated to dryness at low heat to avoid vaporizing the Po.

If the sample appeared rust coloured, due to the presence of Fe, the precipitate was dissolved in 6M HCl and a DIPE extraction was performed. Thereafter the solution was again evaporated to dryness. The sample was re-dissolved in 60 - 70 ml of 0.1M HCl and transferred to a 100 ml beaker.

Copper discs (2.5 cm diameter) were attached to cellophane with 'Araldite' and inserted face up into the liquid. The beaker was heated at 95^{o}C with continuous stirring for 1 hour or until the copper darkened. Hot deionized water, from a beaker on the same hot plate was added as necessary to maintain the solution volume. On completion of this procedure, the disc was washed with cold deionized water to remove the ^{210}Bi.

Determination of the ^{208}Po and ^{210}Po deposited on the disc was by surface barrier detector using the techniques discussed in Section 2.3. The energies used to

identify the relevant peaks in the spectrum are presented in Table 2.9.

Table 2.9 α Particle Energies and Half Lives of ^{208}Po and ^{210}Po

Nuclide	α Energy (MeV)	Half Life
^{208}Po	5.116	2.898 (years)
^{210}Po	5.304	138 (days)

The equation used in the calculation of ^{210}Po assumes that ^{210}Po and ^{210}Pb are in secular equilibrium.

$$^{210}Po\ activity = \frac{counts,^{210}Po}{counts,^{208}Po} \times \frac{decay\ corrected\ spike\ activity}{weight} \times 100 \quad (2.2)$$

2.5 DETERMINATION OF CAESIUM CONCENTRATIONS IN AQUEOUS MEDIA USING A NaI(Tl) DETECTOR

Certain materials undergo the process of scintillation, in which the particles or photons of radiation transfer their energy to the material, resulting in the excitation of electrons which immediately return to the ground state, re-emitting their excitation energy as photons of light. The amount of light emitted is directly proportional to the amount of radiation energy deposited in the material.

A NaI(Tl) detector consists of a NaI crystal deliberately doped with 0.1 to 0.2% Tl, to provide suitable energy levels to facilitate the scintillation process. The high density of NaI (3.7 g cm^{-3}) and the high Z value of Iodine (53) mean that the crystals have a relatively high absorbance power for γ photons and are consequently relatively efficient γ photon detectors. However, NaI(Tl) detectors have limited resolution, the best available resolutions for ^{137}Cs at 662 keV being about 7%. This is largely as a result of the amount of energy required to generate each electron at the photocathode of the photomultiplier tube.

The detector system used for the determination of ^{137}Cs in fresh and saltwater samples was a Bicron 3"x3" well type NaI(Tl) detector with a quoted resolution of 8%. Shielding against extraneous sources of *y* photons was provided by 10 cm of Pb. A Canberra Series 80 MCA was used for spectrum accumulation and net peak areas were determined using Covells' method (Covell, 1959).

The detection efficiency of the NaI(Tl) detector was determined for the ^{137}Cs photopeak at 662 keV using a cartridge of KCFC spiked with a known activity of ^{137}Cs. This gave a value of 22.5%.

Determination of ^{137}Cs concentrations in fresh and salt water samples entailed passing the aqueous media through a cartridge of KCFC (potassium hexacynaocobalt II ferrate II) and measuring the activity in the dried cartridge on the NaI(Tl) detector. KCFC is an inorganic ion exchanger which preferentially removes caesium from aqueous media by direct displacement of potassium. The extraction of radiocaesium from aqueous media followed the method of MacKenzie *et al.,* (1979) which was based upon those of Prout *et al.,* (1965) and Boni (1966).

It had been previously observed that ^{137}Cs was predominantly concentrated in the top 1 cm of the cartridge, a 4 cm long column of resin was regarded as ideal for ensuring complete removal of caesium (McKinley, 1979). The cartridge was inverted and carefully positioned within the well of the detector crystal for analysis. Results were calculated using Covell's equation to separate the net counts due to ^{137}Cs in the sample from the continuum produced by Compton scattering. The net counts were divided by the counting efficiency of the detector 22.5% (0.225), the count time (82,800 sec) and the volume of sample passed through that particular cartridge. This produced a concentration of ^{137}Cs per unit volume (Bq l^{-1}), which was divided into the concentration of ^{137}Cs (Bq kg^{-1}) in the air dried portion of the sediment sample to obtain a K_D value in units of l kg^{-1}.

2.6 SEQUENTIAL EXTRACTION OF SEDIMENT SAMPLES

Sequential extraction of a range of sediment samples from Southwick merse (Southwick Core 1 and Southwick S3.10) and surface deposits from the intertidal sediments from the bed of Southwick Water was carried out primarily on the basis of the procedures of McLaren and Crawford (1973), modified by Iu *et al.,* (1981) and Cook *et al.,*(1984a).

This technique relies on the use of progressively more aggressive chemical reagents to remove notionally discrete components of the sediment. The technique has been applied to identifying the percentages of ^{137}Cs and $^{239+240}Pu$ retained by sedimentary materials in the following forms: (i) readily available, (ii) exchangeable and bound to specific sorption sites, (iii) associated with organic matter as chelated complexes, (iv) occluded or co-precipitated with secondary Fe/Mn minerals and (v) a residual fraction (largely irreversibly held). One additional soil component was examined, i.e. the more acid soluble. This required a modification to the procedure which is outlined below. This component was introduced as a mechanism for identifying concentrations of radionuclides held by resistant oxides and silicates not removed by the acid oxalate leach but which would be by the HF acid digestion.

Plutonium analysis of the leaching solutions was performed by the method described in Section 2.4.1.

^{137}Cs analysis of the leaching solutions was undertaken by passing the filtered leachate through a cartridge of KCFC ion exchange resin (Section 2.5). This procedure was adopted for all the chemical leaches except the more acid soluble phase (1M HNO_3) and the residual component. The more acid soluble phase was boiled to dryness, transferred into a suitable container (50 ml beaker) and the gamma spectrum recorded using a high resolution HPGe detector. The residual phase was dried at 110^0C, weighed and transferred to a container with a calibrated detection efficiency, and analysed as described for γ spectroscopy of sediments.

SEQUENTIAL EXTRACTION METHOD

1. Readily Available

This component was extracted by 0.05M $CaCl_2$. 20 g sediment samples were extracted with 240 ml of reagent for 18 hours on an end over end shaker. The slurry was then centrifuged at 3000 rpm for 20 minutes and the supernatant filtered and passed through a cartridge of KCFC resin. The supernatant was then acidified with 15.6M (conc) HNO_3, spiked with ^{242}Pu yield tracer, reduced to dryness and processed for plutonium analysis as previously described in Section 2.4.1.

2. Exchangeable Or Bound To Specific Sorption Sites

This component was extracted with 0.5M acetic acid. The soil residue from the above extraction was shaken for 18 hours with 240 ml of reagent. Centrifugation and analyses were described as above.

3. Associated With Organic Matter As Chelated Complexes

This component was extracted with 0.1M tetra sodium pyrophosphate. The soil residue from the acetic acid extraction was shaken for 18 hours with 800 ml of reagent and the slurry treated as previously described for the determination of ^{137}Cs. Following acidification, spiking with ^{242}Pu and evaporation to dryness, 50 ml of 15.6M HNO_3 were added to oxidise any remaining organic matter. The volume was reduced to approximately 2 ml and 100 ml 8M HCl were added before a DIPE extraction was undertaken to remove Fe. On completion, the standard procedure was followed for plutonium determination.

4. Occluded or Co-precipitated with Secondary Fe/Mn Minerals

This component was extracted with Tamms acid oxalate (0.1M oxalic acid/0.175M ammonium oxalate). The sediment residue from the previous extraction was shaken with 800 ml of reagent and the solution treated as for the pyrophosphate

leach for the determination of ^{137}Cs and $^{239+240}Pu$.

5. More Acid Soluble

This component was introduced as a modification to the procedure described by Cook *et al.,* (1984a). The sediment was shaken with 800 ml of 1M HNO_3, filtered and the supernatant reduced in volume, before being transferred to a 50 ml beaker (previously weighed to 4 decimal places) and evaporated to dryness. The beaker was cooled, reweighed, sealed with Nesco tape and counted on a high resolution HPGe detector. After counting, the samples were redissolved in 8M HNO_3 reduced to 2 ml and reconstituted with 50 ml 8M HCl to permit standard plutonium analysis.

6. Residual

Determination of ^{137}Cs was undertaken by drying the residual sediment at 110°C overnight and transferring the sample to a previously calibrated counting geometry, whereupon the samples were accurately weighed and the ^{137}Cs concentration determined by direct counting on a HPGe detector. Plutonium analysis of the residual phase was undertaken using the same technique as for the total sediment concentration outlined in Section 2.4.1.

Sequential extraction techniques for the determination of ^{137}Cs and $^{239+240}Pu$ were performed on two sections from the merse deposits of the floodplain and a sample of surface intertidal silt from the Southwick Water. These samples represented sediment material from locations which were subjected to contrasting environmental influences. Sediment samples from SC1, located at the stepped edge of the merse at the river bank represented the transition zone between the marine and terrestial environments. Several depth intervals were examined to give sediments of different age; 0-5 cm, 20-25 cm, 40-45 cm, 55-60 cm, and 65-70 cm. The second section subjected to sequential extraction analysis was Southwick S3.10. This section was situated 10 m inland across the merse from the site of SC1 and was subject to different environmental conditions. The site did not experience tidal incursions on a daily basis and therefore was considered a

terrestrial location at which the dominant leaching medium was fresh/brackish water within the water table. The depth intervals investigated were 0-5 cm, 15-20 cm and 25-30 cm. A sample of surface silt from the intertidal zone of Southwick Water was also subjected to analysis.

Comparison of data from within individual sections provided information on changes in geochemical association with depth and by inference time. Comparison between the sections provided information on changes in associations of ^{137}Cs and $^{239+240}Pu$ between the predominantly marine environment and a terrestial location.

2.7 FLOW DESORPTION EXPERIMENT

The objective of the flow desorption experiments was to try to ascertain the quantity of ^{137}Cs which could be desorbed from contaminated sediment using various leaching media. The sediment samples were leached with aqueous media which reflected the fluctuating environmental conditions prevalent at the stepped edge of the merse. Successive volumes of an aqueous medium; either freshwater, field drain water or seawater were passed through separate 20 g samples. The desorbed caesium was extracted onto KCFC inorganic ion exchange resin and the ^{137}Cs concentration analyzed by NaI(Tl) gamma spectroscopy as described in Section 2.5.

Sample sediments at 0-5 cm and 40-45 cm depth intervals, were collected from the merse deposits at Southwick Water, Core No.1, on 8/12/89 as previously described in Section 2.1.1. Sub-samples from the remaining refrigerated portions were used for the desorption experiments. Comparison of the concentration of ^{137}Cs in the known volume of leachate with that of the sediment sample provided an indication of the quantities of ^{137}Cs desorbed.

The desorption experiment apparatus is illustrated in Fig 2.11. A 20 g aliquot of 'wet' sediment was placed in a glass leaching column (15 cm long by 2 cm diameter) and allowed to settle out into distinct aqueous and solid phases. The tapered bottom of the column was plugged with glass wool before the sediment was added and connected to a 10 l PVC aspirator by clear PVC tubing (11 mm OD,

8 mm ID) which was held in place by a metal compression clip. A glass wool plug was inserted above the sediment sample and the column was stoppered with a rubber bung through which a U bend glass tube (3 mm OD) was passed. The column and tubing were then encased in aluminium foil in order to exclude light and prevent the growth of algae.

The leaching medium was slowly passed through the column with great care to avoid causing the sediment sample to separate. A flow rate of approximately 0.1 ml/min was controlled by the reservoir stopcock and the Hoffman screw clip below the base of the column. The leachate was collected in a 15 l plastic bucket and then transferred to the filtration apparatus (Fig 2.12) which comprised two modified glass columns with flat flanges. The bottom column had a slight indentation which housed a 45 mm, zero porosity, sintered glass disc which held the filter papers in place. The zero porosity disc was the coarsest sintered glass available and would not adversely affect the flow rate of the filtration system. This unit was inserted into a 30 l glass aspirator to collect the leachate which was drawn through the system under vacuum by a Charles Austin Mk5 pump. The leachate was filtered through a 0.22 μm (90 mm diameter) Millipore membrane filter with a Whatman No.1 pre-filter which removed any coarse particulate material.

The solution was then transferred to a 10 l perspex bulb (illustrated in Fig 2.13) with a stop cock and tapered cone attachment, to which a KCFC cartridge was connected. The cartridge comprised: (i) a length of PVC tubing which contained approximately 4-5 cm of well washed KCFC resin and cotton wool plug at the base (ii) a small glass stop cock at the bottom and a socket joint at the top for attachment to the 10 l bulb. The leachate was collected in a 30 l plastic jerry can and discarded. The KCFC cartridge was dried under vacuum and sealed with a wooden plug and cellotape at the top, while the cotton wool plug and cellotape were sufficient to seal the base. The cartridge was counted on a suitably calibrated NaI(Tl) scintillation detector.

Sediment samples were subjected to leaching by fresh water, field drain water and seawater. The fresh water was obtained from the laboratory mains system and was used without any pre-treatment. The field drain water was obtained from a

drainage pipe located near the entrance to the Scottish Wildlife Trust's Nature Reserve at Netherclifton (Southwick Water) and was assumed to be representative of the groundwater flowing through the merse. This water was filtered through a 0.22μm Millipore membrane filter with a Whatman No.1 pre-filter before use. The seawater was collected from Kinghorn in Fife, which is sufficiently distant from Sellafield to provide a relatively low concentration of ^{137}Cs (0.01 $\pm$0.0002 Bql^{-1}). However, to ensure that the seawater would not contribute any experimental artefact, it was passed through KCFC to remove any caesium present. The ^{137}Cs concentration of the water was below detection limit after completion of this process. In order to save time, financial expense and to avoid the inefficient use of resources, it was decided to recycle the seawater within the desorption experiment once it had passed through the KCFC.

2.7.1 Batch Desorption Experiment

A batch desorption experiment was developed to provide an estimate of the concentration of ^{137}Cs desorbed by freshwater in a system which had reached equilibrium compared with the flow desorption experiment where equilibrium was potentially difficult to achieve. A 1 kg sample of sediment from Southwick Core No.3 0-5 cm, was placed in a 30 l PVC jerry can and shaken with 25 l of mains water for 2 minutes. The suspension was allowed to settle for periods of up to 30 days, the supernatant syphoned into a filtration system as outlined above and subsequently passed through a KCFC cartridge and analyzed on a NaI(Tl) scintillation detector. There were limitations within the design of this experiment which will be discussed more fully in Section 4.4.4. For example, the filtration system became blocked with suspended material within the supernatant after the passage of only a few litres. Despite continual replacement of the micropore filters and increasing the standing time of the suspension the problems continued to undermine the progress of this experiment.

Fig 2.11 Apparatus used in the Flow Desorption Experiment.

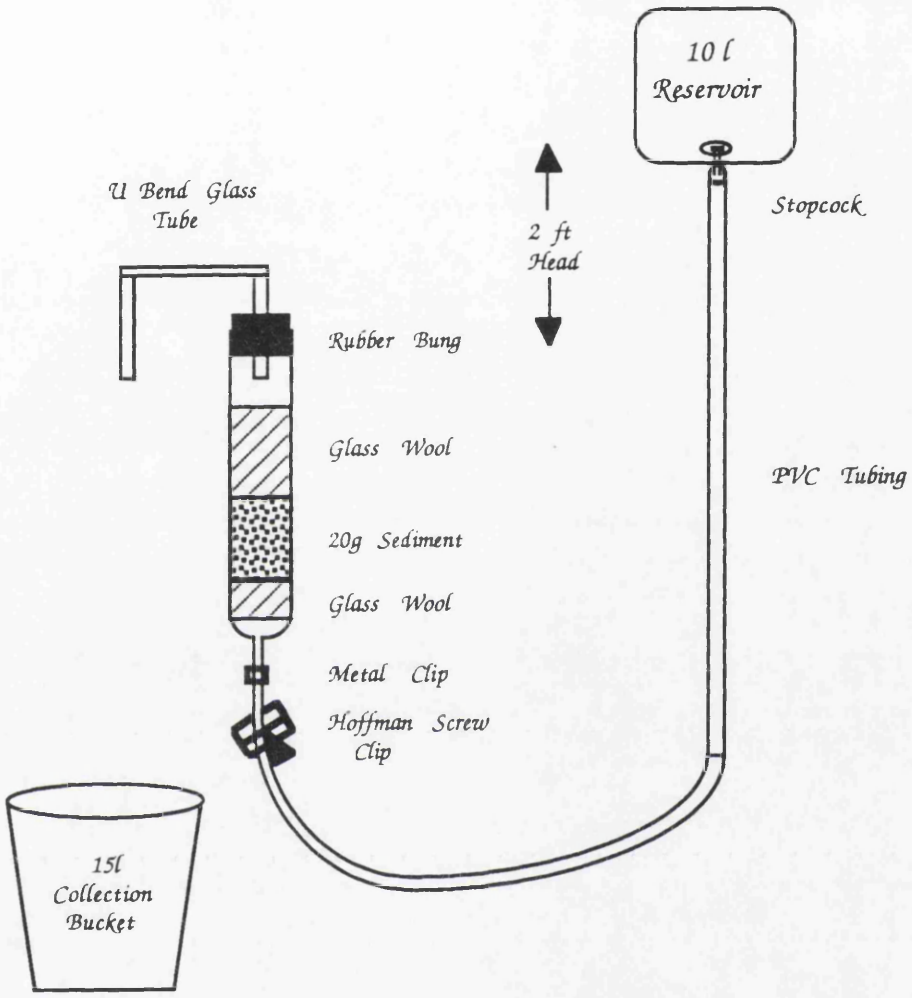

Fig 2.12 Filtration equipment used in the Flow Desorption Experiment.

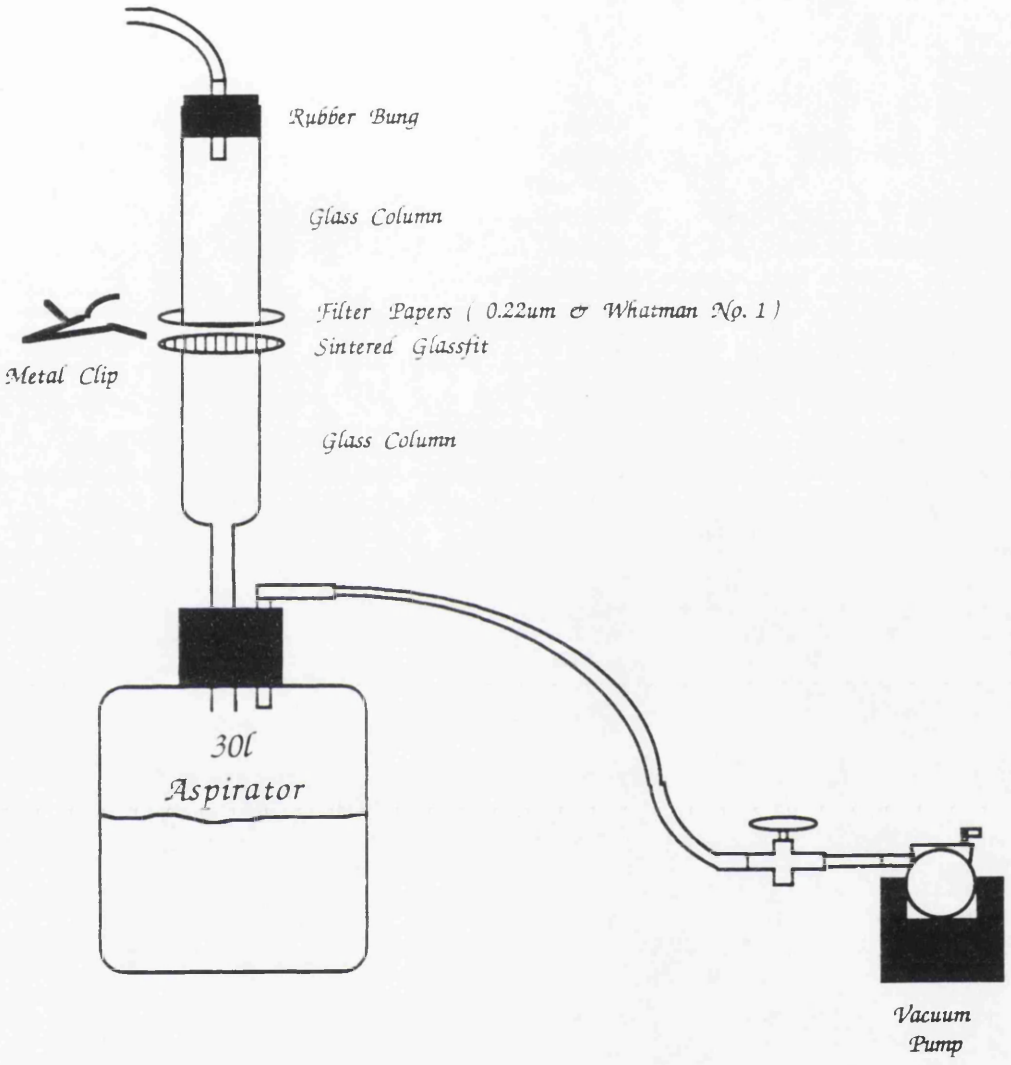

Fig 2.13 Experimental apparatus used to extract caesium from leaching solutions in the Flow Desorption Experiment.

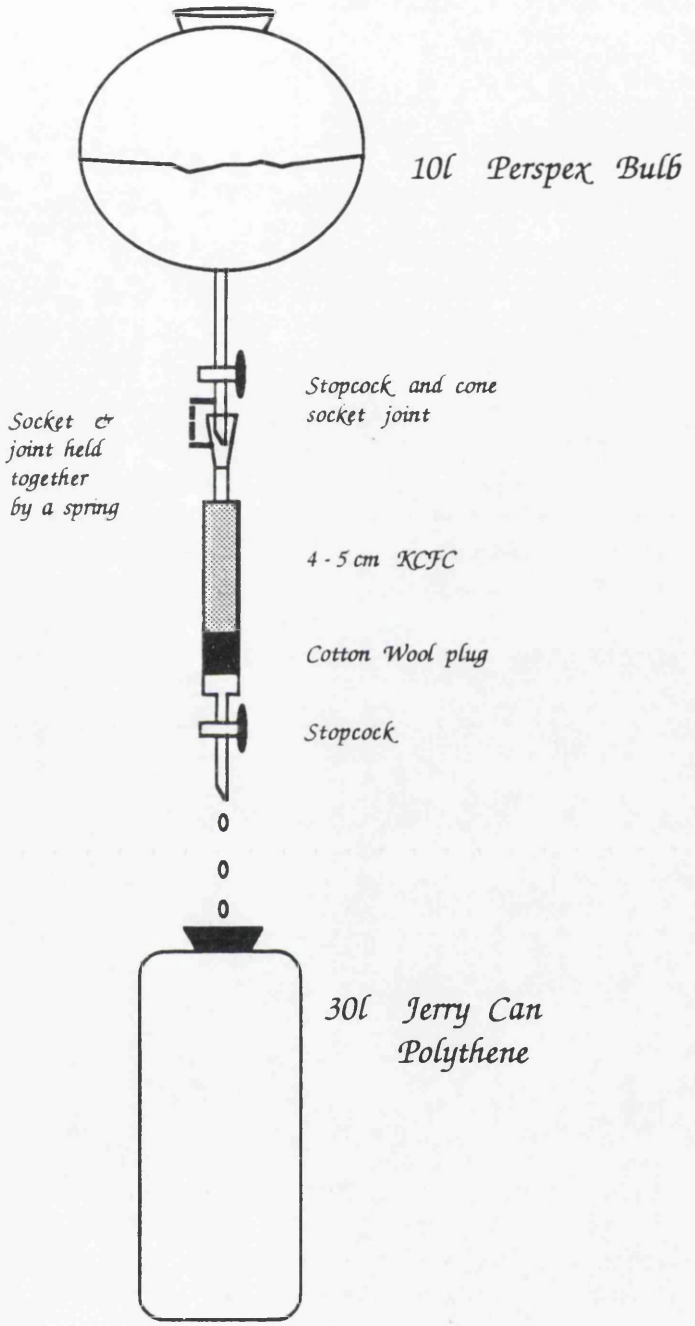

2.8 LOSS ON IGNITION

The loss of weight on ignition (LOI) was used as an indication of the organic content of the sediment samples (Hetherington, 1978). All sediment samples which were analyzed by γ spectroscopy were subjected to LOI determination.

Silica crucibles were heated in an oven at 110°C for 12 hours, cooled in a desiccator and weighed to 4 decimal places. 5 g samples of air dried sediment were accurately weighed into the crucibles and heated overnight at 110°C to drive off any moisture. The crucibles were cooled and reweighed before the samples were ashed in a furnace at 650°C for 8 hours in order to combust any organic material present. On completion, the crucibles were cooled in the desiccator and reweighed.

2.9 PARTICLE SIZE ANALYSIS OF SEDIMENT SAMPLES

The method adopted for determining the textural class of the sediment samples was developed by the Agricultural Development and Advisory Service (ADAS, 1981) and modified by Qasim (1988). The sediment samples were separated into their primary particles of sand, silt and clay by chemical dispersion and wet and dry sieving. The particles were fractionated according to the recommendations of the Soil Survey of England and Wales illustrated in Table 2.10.

Table 2.10 Soil Fractionation Sizes According to the Soil Survey of England and Wales (ADAS, 1981)

SOIL FRACTION	EQUIVALENT SETTLING DIAMETER (mm)
Coarse Sand	2-0.6
Medium Sand	0.6-0.2
Fine Sand	0.2-0.06
Coarse Silt	0.06-0.02
Medium Silt	0.02-0.006
Fine Silt	0.006-0.002
Clay	< 0.002

DISPERSION

The sediment was dispersed by a combination of oxidation of organics with 30% hydrogen peroxide and removal of carbonates with 2M HCl followed by chemical dispersion with calgon and ultrasonic vibrations.

SAND FRACTION

The sand fraction was separated by wet sieving through 180 μm and 53 μm sieves banked together on top of a 1000 cm^3 graduated cylinder. These sieves correspond to the medium sand - fine sand and the fine sand - coarse silt boundaries and allow separation of the coarse and medium sand fraction and the fine sand fraction respectively.

SILT PLUS CLAY AND CLAY FRACTION

These finer particles were separated using a pipette method based on the sedimentation rates of the particles. The relationship between the radius of the particle and its settling velocity in a medium of given viscosity is given by Stokes

Law. In practice, measurement of the concentration of particles which fell for time (t) through a certain depth of liquid at a specified temperature were recorded. The temperature in the cylinder was noted and the appropriate time for the silt & clay fraction (64 sec) at a depth of 20 cm and the clay fraction (479 min) at 10 cm were selected from the table which was prepared by the Soil Survey of England and Wales (1976). After the suspension had stood for the appropriate time, 10 ml samples were pipetted at the given depth. The samples for both fractions were dispensed into weighed and labelled porcelain dishes and evaporated to dryness on a steam bath.

2.10 MINERALOGY OF SEDIMENTS

The mineralogy of selected samples of sedimentary material was determined by the x-ray diffraction analysis service provided by the Department of Geology and Applied Geology at the University of Glasgow. (This research was carried out by Mr D. Turner and Mr M. McLeod with interpretation of results by Dr. A. Hall, all personnel employed within The Department of Geology and Applied Geology at the University of Glasgow).

2.11 NEUTRON ACTIVATION ANALYSIS

Instrumental neutron activation analysis was used to establish the concentration of stable caesium (^{133}Cs) within the samples and to quantify any contribution the isotope had on the partitioning of ^{137}Cs, in the process additional information on the geochemical composition of the samples was provided. The elements analyzed in this study are listed in Table 2.11. In this technique, sediment samples and suitable standards were exposed to a flux of thermal neutrons in a nuclear reactor. Neutron capture by the constituent atoms of the sample produces radioactive species and in suitable cases, β^-/γ decay of the radioactive products gives rise to the emission of gamma radiation which can be detected using gamma spectroscopy techniques as outlined above (section 2.2). The count rates of selected photopeaks in the gamma spectra of samples and standards are used to derive elemental concentrations in the samples. The standard used in this study was a standard clay prepared by the Royal Museum of Scotland, Edinburgh, which has been well

characterized in an inter laboratory study (Tate pers. comm.)

All irradiations were performed using the Scottish Universities Research and Reactor Centre (SURRC) UTR-300 research reactor which at full power of 300 kW, provides a neutron flux of about 3×10^{12} n cm^{-2} sec^{-1} in the core area. The sample irradiations (6 hours duration) were preformed using the central vertical stringer (CVS) of the reactor. In the irradiation process, approximately 0.13 g each of sample and standard materials were accurately weighed into clean, high purity polythene vials of 1 ml volume. These were then wrapped in aluminium foil as a secondary containment in case of vial rupture or partial melting as a consequence of heat production during irradiation. The samples were then placed in a graphite container which was lowered through an access hole into the irradiation position in the centre of the reactor core.

Small variations occur in the neutron flux experienced by individual samples during irradiation and in order to compensate for this effect, flux monitors of iron wire (weighing approximately 0.04 g and with a 99.5% purity) were attached to all of the sample and standard irradiation vials. The sample identification code was also marked on the aluminium foil rather than on the vials themselves in order to prevent any blank contribution from the marker pen ink.

Batches of 10 samples and 1 Edinburgh clay standard were packaged together in aluminium foil and irradiated. After irradiation, the radiation dose rate from each batch of samples and from individual vials was monitored using a calibrated dosemeter. After a decay period of 3 days, during which the samples were kept in an isotope store to allow the decay of excess short half-life radionuclides, the samples and standards were, with appropriate radiological precautions, safe to handle. After carefully unwrapping the aluminium foil, the vials were wiped clean of surface contamination and transferred to suitably labelled polythene bags and stored behind lead shielding prior to counting. The iron flux monitors were also recovered and transferred to labelled polythene bags and stored with the samples until required for counting.

Two series of counts were performed: The first series, carried out 3 days after

irradiation, consisted of 1 hour counts with the samples accurately and reproducibly positioned in a sample holder at a height of 10 cm above the detector in order to reduce the dead time to a level below 10% (normally below 5%). The detector used in this research was a Tennelec HPGe (ERVDS-30) which had an efficiency of 30% (relative to 3" x 3" NaI detector) and a resolution of 1.95 keV at 1.33 MeV. Analysis was performed using the EG + G software package MINIGAM II, which provided peak location, area calculation and nuclide identification. The spectra recorded in the 1 hour counts were dominated by species with half-lives in the range of tens of hours up to a few days. The lower activities of the longer-lived activation products cannot in general be detected until the shorter-lived species decay to a large extent so that the samples and standard can be re-counted in a position close to the detector. The second series of counts consisted of 16 hour counts with the samples held in a plastic mount in contact with the detector can and were performed approximately three weeks after irradiation.

The slight variations in neutron flux experienced by samples during irradiation were corrected for by assuming that the specific activity induced in the flux monitor for each sample is proportional to the neutron flux experienced by the sample. Thus, the iron wires were counted in a standard geometry and the specific activity of ^{59}Fe calculated at a defined reference time in each case. The observed gamma spectroscopy results for the various elements analyzed were, during subsequent computer based calculations, normalised to an average flux based upon the flux monitor results.

Element concentrations were calculated from the peak search programme results with the aid of the SURRC activation analysis programme NAA (Harris, 1987). This programme takes the output file from the Ortec GAMMA 2 programme directly from disc and performs a conventional activation analysis calculation based upon the equation

$$\frac{\textit{weight of } Y \textit{ , sample}}{\textit{weight of } Y \textit{ , standard}} = \frac{\textit{count rate of } X \textit{ , sample}}{\textit{count rate of } X \textit{ , standard}}$$

(2.3)

X = the induced activity of any species produced as a result of neutron capture by a stable element Y (Adam and Dams, 1970; Friedlander *et al.,* 1981)

This programme corrects all observed count rates to a defined reference time, corrects for decay during counting, and incorporates a *priori* error, which allows for uncertainties in counting geometry (with a value of 2% being used for a *priori* error in this case), weight etc., and systematic errors to allow for flux variations. The final results are expressed as concentrations in ppm (mg kg^{-1}).

Table 2.11 Radionuclides analyzed by NAA

RADIONUCLIDE	HALF LIFE	ENERGY (keV) Used in Analysis	DECAY TIME
^{24}Na	15 h	1368.7	3 weeks
^{57}Cr	27.8 d	320.08	3 weeks
^{59}Fe	45.1 d	1099	3 weeks
^{60}Co	5.26 y	1332.48	3 weeks
^{86}Rb	18.7 d	1078	3 weeks
^{124}Sb	60.3 d	1691	3 weeks
^{134}Cs	2.05 y	795.8	3 weeks
^{82}Br	35.3 h	776.5	3 days
^{140}La	40.2 h	1596.2	3 days
^{141}Ce	33 d	145.44	3 weeks
^{152}Eu	13 y	1408.1	3 weeks
^{153}Sm	4.68 h	103.23	3 days
^{160}Tb	73 d	879.3	3 weeks
^{177}Lu	6.7 d	208.36	3 weeks
^{181}Hf	42/4 d	482	3 weeks
^{182}Ta	115 d	1221.4	3 weeks
^{233}Pa	1.41 y	311.9	3 weeks

CHAPTER 3

RESULTS

The analytical data obtained in this research are presented in Tables 3.1 to 3.45.

Radionuclide specific activities are expressed in units Bq kg^{-1} throughout and the quoted uncertainties are based upon propagated 1σ statistical uncertainties.

The inventory results are expressed in units of Bq m^{-2} and the activation analysis results in units of ppm unless otherwise stated. The uncertainties quoted for the instrumental neutron activation analysis data are based upon 1σ counting statistics plus a *priori* error.

The desorption results are expressed as K_D values with units of Kg 1^{-1}.

Table 3.1 Analytical Results for Southwick Core No. 1 (errors 1σ)

Depth (cm)	^{137}Cs (Bq kg^{-1})	^{134}Cs (Bq kg^{-1})	^{241}Am (Bq kg^{-1})	$^{239+240}Pu$ (Bq kg^{-1})	^{238}Pu (Bq kg^{-1})	^{210}Pb (Bq kg^{-1})	$^{134}Cs/^{137}Cs$	$^{238}Pu/^{239+240}Pu$
0-05	406 ± 3	5.6 ± 0.6	199 ± 4.0	185 ± 5	38 ± 4	42 ± 1.0	0.014 ± 0.001	0.20 ± 0.02
5-10	651 ± 4	25.3 ± 1.0	303 ± 10.0	149 ± 13	31 ± 2	40 ± 1.0	0.039 ± 0.002	0.21 ± 0.01
10-15	595 ± 4	10.0 ± 0.7	205 ± 4.0	178 ± 5	36 ± 1	33 ± 1.0	0.017 ± 0.001	0.20 ± 0.01
15-20	796 ± 5	5.2 ± 0.5	229 ± 3.0	174 ± 8	35 ± 2	33 ± 1.0	0.006 ± 0.0006	0.20 ± 0.02
20-25	1,430 ± 8	5.7 ± 0.5	339 ± 3.0	253 ± 15	53 ± 3	40 ± 1.0	0.004 ± 0.0003	0.21 ± 0.03
25-30	1,820 ± 10	5.8 ± 0.5	452 ± 4.0	321 ± 19	64 ± 4	42 ± 1.0	0.003 ± 0.0003	0.20 ± 0.02
30-35	1,680 ± 10	4.6 ± 0.5	498 ± 6.0	386 ± 11	74 ± 2	43 ± 1.0	0.003 ± 0.0003	0.19 ± 0.02
35-40	1,880 ± 11	3.9 ± 0.4	687 ± 8.0	330 ± 21	60 ± 4	46 ± 2.0	0.002 ± 0.0002	0.18 ± 0.02
40-45	1,450 ± 8	2.6 ± 0.4	675 ± 8.0	311 ± 36	46 ± 6	29 ± 1.0	0.002 ± 0.0003	0.15 ± 0.02
45-50	1,250 ± 7	1.6 ± 0.3	498 ± 9.0	373 ± 10	42 ± 1	44 ± 2.0	0.001 ± 0.0003	0.12 ± 0.03
50-55	558 ± 4	BDL	185 ± 3.0	265 ± 52	17 ± 4	30 ± 1.0	BDL	0.06 ± 0.02
55-60	342 ± 2	BDL	76 ± 2.0	50 ± 4	3 ± 0.4	32 ± 1.0	BDL	0.06 ± 0.02
60-65	131 ± 1	BDL	11 ± 0.4	97 ± 10	5 ± 1	16 ± 2.0	BDL	0.05 ± 0.02
65-70	103 ± 1	BDL	5 ± 0.3	21 ± 1	0.4 ± 0.1	21 ± 0.4	BDL	0.02 ± 0.002

BDL = Below Detection Limits Detection Limits: ^{134}Cs = 0.6 (Bq kg^{-1})

Table 3.2 Analytical Results for Southwick Core No. 2 (errors 1σ)

Depth (cm)	^{137}Cs (Bq kg^{-1})	^{134}Cs (Bq kg^{-1})	^{241}Am (Bq kg^{-1})	$^{239+240}Pu$ (Bq kg^{-1})	^{238}Pu (Bq kg^{1})	$^{134}Cs/^{137}Cs$	$^{238}Pu/^{239+240}Pu$
0- 5	401 ± 2.0	7.9 ± 0.4	144 ± 4	123 ± 9.0	24 ± 1	0.019 ± 0.001	0.19 ± 0.01
5-10	772 ± 3.0	3.2 ± 0.3	192 ± 1	162 ± 3.0	29 ± 1	0.004 ± 0.0003	0.18 ± 0.01
10-15	1,138 ± 5.0	2.3 ± 0.3	334 ± 9	249 ± 3.0	44 ± 1	0.002 ± 0.0003	0.18 ± 0.003
15-20	582 ± 4.0	BDL	730 ± 28	106 ± 10.0	7 ± 0.3	NA	0.07 ± 0.01
20-25	138 ± 1.0	BDL	3 ± 0.3	6.6 ± 0.4	0.4 ± 0.04	NA	NA
25-30	35 ± 1.0	BDL	BDL	1.3 ± 0.3	BDL	NA	NA
30-35	18 ± 0.8	BDL	2 ± 0.6	1.0 ± 0.1	BDL	NA	NA
35-40	6 ± 0.5	BDL	BDL	0.4 ± 0.1	BDL	NA	NA
40-45	4 ± 0.7	BDL	BDL	0.3 ± 0.04	BDL	NA	NA
45-50	1 ± 0.6	BDL	BDL	0.2 ± 0.03	BDL	NA	NA
50-55	2 ± 0.4	BDL	BDL	0.3 ± 0.02	BDL	NA	NA
55-60	BDL	BDL	BDL	0.3 ± 0.03	BDL	NA	NA

BDL = Below Detection Limits, NA = Not Available. Samples analysed between 60 and 100cm were below detection limits.
Detection Limits: ^{137}Cs = 0.4 Bq kg^{-1}, ^{134}Cs = 0.6 Bq kg^{-1}, ^{241}Am = 1.1 Bq kg^{-1}, $^{239+240}Pu$ = 0.03 Bq kg^{-1}

Table 3.3 Analytical Results Showing ^{137}Cs and ^{241}Am Concentrations for Southwick Core No. 3

Depth (cm)	^{137}Cs (Bq kg $^{-1}$)	^{134}Cs (Bq kg^{-1})	^{241}Am (Bq kg^{-1})
0- 5	421 ± 5	6.6 ± 0.7	227 ± 8
40-45	71 ± 2	BDL	4 ± 1
65-70	2 ± 1	BDL	BDL

Table 3.4 Radionuclide Concentrations and Inventories for the 0-15 cm Depth Intervals from Creetown Transect T1, Collected 28/8/90

Distance (m)	LOI (%)	^{137}Cs (Bq kg^{-1})	^{134}Cs (Bq kg^{-1})	^{241}Am (Bq kg^{-1})	$^{239+240}Pu$ (Bq kg^{-1})	^{238}Pu (Bq kg^{-1})	^{137}Cs (Bq m^{-2})	^{241}Am (Bq m^{-2})	$^{239+240}Pu$ (Bq m^{-2})
-100	4.3	714 ± 9	2.4 ± 0.4	150 ± 6	107 ± 3	20 ± 0.6	186,777	39,239	27,912
- 40	5.3	72 ± 2	BDL	31 ± 3	22 ± 1	4 ± 0.3	22,256	9,459	6,831
- 20	6.5	74 ± 2	BDL	37 ± 2	27 ± 1	5 ± 0.3	17,943	8,850	6,474
0	6.7	789 ± 9	11.1 ± 0.8	265 ± 8	218 ± 8	44 ± 2.0	285,506	95,892	78,921
20	7.9	1,030 ± 12	11.3 ± 1.0	310 ± 5	268 ± 4	52 ± 1.0	361,776	108,884	94,132
40	6.6	880 ± 10	8.3 ± 1.0	221 ± 7	164 ± 2	27 ± 0.4	299,901	75,316	55,822
60	7.7	1,260 ± 15	8.6 ± 0.7	378 ± 6	261 ± 4	46 ± 1.0	385,248	115,574	79,679
80	8.5	1,210 ± 14	12.0 ± 2.1	352 ± 6	252 ± 3	46 ± 1.0	354,541	103,139	73,809
100	9.6	1,680 ± 19	14.4 ± 1.3	516 ± 9	355 ± 5	64 ± 1.0	480,064	147,448	101,499

Distance = Distance from the MHWM (negative values to seaward; positive values to landward)
LOI = Loss on Ignition
BDL = Below Detection Limit Detection Limit for ^{134}Cs = 0.6 Bq kg^{-1}

Table 3.5 Radionuclide Concentrations and Inventories for the 15-30 cm Depth Intervals from Creetown Transect T1, Collected 28/8/90

Distance (m)	LOI (%)	^{137}Cs (Bq kg^{-1})	^{134}Cs (Bq kg^{-1})	^{241}Am (Bq kg^{-1})	$^{239+240}Pu$ (Bq kg^{-1})	^{238}Pu (Bq kg^{-1})	^{137}Cs (Bq m^{-2})	^{241}Am (Bq m^{-2})	$^{239+240}Pu$ (Bq m^{-2})
-100	3.3	534 ± 7	1.1 ± 0.3	90 ± 3	60 ± 2	NA	218,940	36,859	24,641
- 40	6.1	28 ± 1	BDL	12 ± 1	100 ± 1	64 ± 1.9	10,122	4,338	36,006
- 20	6.3	74 ± 2	0.9 ± 0.3	37 ± 2	NA	54 ± 0.8	25,769	12,885	BDL
0	6.0	1,340 ± 15	2.5 ± 0.5	298 ± 5	198 ± 6	4 ± 0.1	470,779	104,696	69,580
20	6.5	1,040 ± 12	1.7 ± 0.3	417 ± 12	258 ± 4	1 ± 0.1	342,648	137,389	85,035
40	5.1	251 ± 4	BDL	47 ± 2	43 ± 1	BDL	91,893	17,134	15,669
60	5.9	482 ± 6	0.9 ± 0.2	125 ± 4	77 ± 1	BDL	158,932	41,217	25,324
80	6.2	243 ± 4	BDL	78 ± 3	78 ± 1	BDL	83,480	26,830	26,968
100	6.9	406 ± 5	1.8 ± 0.3	95 ± 4	10 ± 0.2	BDL	137,717	32,360	3,358

Distance = Distance from the MHWM (negative values to seaward; positive values to landward)
LOI = Loss on Ignition
BDL = Below Detection Limit Detection Limit for ^{134}Cs = 0.6 Bq kg^{-1}, ^{238}Pu = 0.03 Bq kg^{-1}
NA = Not Available

Table 3.6 Radionuclide Concentrations and Inventories for the 0-15 cm Depth Intervals from Wigtown Transect T1, Collected 27/8/90

Distance (m)	LOI (%)	^{137}Cs (Bg kg^{-1})	^{134}Cs (Bq kg^{-1})	^{241}Am (Bq kg^{-1})	^{137}Cs (Bq m^{-2})	^{241}Am (Bq m^{-2})
-40	6.2	582 ± 7	10.3 ± 1.1	314 ± 5	210,086	113,346
-20	4.8	441 ± 6	6.5 ± 0.5	172 ± 6	151,813	59,211
0	5.3	30 ± 1	BDL	19 ± 1	8,894	5,521
20	4.7	416 ± 5	15.5 ± 1.1	93 ± 4	163,860	36,632
40	4.9	497 ± 6	12.4 ± 0.7	84 ± 4	194,270	32,991
60	5.9	688 ± 8	18.1 ± 0.9	143 ± 5	234,407	48,721
80	6.5	729 ± 9	15.2 ± 1.1	176 ± 7	188,056	45,402

Distance = Distance from the MHWM (negative values to seaward; positive values to landward)
LOI = Loss on Ignition
BDL = Below Detection Limits Detection Limit for ^{134}Cs = 0.6 Bq kg^{-1}

Table 3.7 Radionuclide Concentrations and Inventories for the 15-30 cm Depth Intervals from Wigtown Transect T1, Collected 27/8/90

Distance (m)	LOI (%)	^{137}Cs (Bq kg^{-1})	^{134}Cs (Bq kg^{-1})	^{241}Am (Bq kg^{-1})	^{137}Cs (Bq m^{-2})	^{241}Am (Bq m^{-2})
-40	5.4	802 ± 10	5.0 ± 0.5	248 ± 8	284,320	87,919
-20	4.0	128 ± 2	BDL	31 ± 2	54,644	13,277
0	4.5	2 ± 0.5	BDL	BDL	759	BDL
20	4.4	227 ± 3	BDL	26 ± 2	85,276	9,805
40	4.5	329 ± 4	BDL	67 ± 3	83,997	17,106
60	5.0	316 ± 4	BDL	51 ± 4	97,596	15,791
80	6.0	750 ± 9	1.5 ± 0.3	177 ± 5	242,655	57,266

Distance = Distance from the MHWM (negative values to seaward; positive values to landward)
LOI = Loss on Ignition
BDL = Below Detection Limit Detection Limit for ^{134}Cs = 0.6 Bq kg^{-1}, ^{241}Am = 1.5 Bq kg^{-1}

Table 3.8 Radionuclide Concentrations and Inventories for the 0-15 cm Depth Intervals from Southwick Transect T1, Collected 25/7/91

Distance (m)	LOI (%)	^{137}Cs (Bq kg^{-1})	^{134}Cs (Bq kg^{-1})	^{241}Am (Bq kg^{1})	$^{239+240}Pu$ (Bq kg^{-1})	^{238}Pu (Bq kg^{-1})	^{137}Cs (Bq m^{-2})	^{241}Am (Bq m^{-2})	$^{239+240}Pu$ (Bq m^{-2})
-3	3.0	239 ± 4	BDL	123 ± 5	87 ± 2	18 ± 0.6	58,481	30,097	21,383
0	5.3	817 ± 1	4.7 ± 0.7	253 ± 9	203 ± 6	41 ± 1.4	126,527	39,181	31,485
10	6.7	703 ± 9	9.1 ± 1.4	341 ± 6	246 ± 3	51 ± 0.8	97,487	47,287	34,141
20	9.3	2,070 ± 23	18.5 ± 2.4	610 ± 10	469 ± 5	84 ± 1.0	267,451	78,814	60,721
30	6.6	408 ± 6	9.3 ± 1.3	106 ± 4	60 ± 1	10 ± 0.2	58,853	15,290	8,626
40	8.0	230 ± 4	4.6 ± 1.0	50 ± 3	35 ± 1	6 ± 0.1	26,195	5,717	4,031
50	12.6	359 ± 6	11.8 ± 1.3	50 ± 3	49 ± 1	7 ± 0.2	27,798	3,833	3,811
70	17.3	228 ± 4	14.7 ± 1.7	13 ± 1	10 ± 0.2	1 ± 0.1	16,545	907	718

Distance = Distance from the MHWM (negative values to seaward; positive values to landward)
LOI = Loss on Ignition
BDL = Below Detection Limit Detection Limit for ^{134}Cs = 0.6 Bq kg^{-1}

Table 3.9 Radionuclide Concentrations and Inventories for the 15-30 cm Depth Intervals from Southwick Transect T1, Collected 25/7/91

Distance (m)	LOI (%)	^{137}Cs (Bq kg^{-1})	^{134}Cs (Bq kg^{-1})	^{241}Am (Bq kg^{-1})	$^{239+240}Pu$ (Bq kg^{-1})	^{238}Pu (Bq kg^{-1})	^{137}Cs (Bq m^{2})	^{241}Am (Bq m^{-2})	$^{239+240}Pu$ (Bq m^{-2})
-3	3.2	9 ± 1	BDL	4 ± 1	BDL	BDL	1,926	849	BDL
0	5.4	1,590 ± 18	2.4 ± 0.9	575 ± 9	374 ± 10	64 ± 1.9	212,469	76,836	50,719
10	6.3	1,280 ± 15	4.4 ± 0.9	445 ± 12	371 ± 5	54 ± 0.8	217,260	75,532	50,277
20	4.2	205 ± 4	BDL	32 ± 2	29 ± 0.5	4 ± 0.1	37,553	5,953	5,239
30	3.2	42 ± 2	BDL	10 ± 1	7 ± 0.1	1 ± 0.1	5,515	1,339	955
40	3.2	26 ± 2	BDL	5 ± 1	3 ± 0.1	BDL	4,341	905	503
50	7.9	47 ± 2	BDL	7 ± 1	6 ± 0.1	BDL	5,436	856	659
70	9.0	48 ± 2	2.6 ± 0.4	BDL	2 ± 0.1	BDL	5,740	BDL	252

Distance = Distance from the MHWM (negative values to seaward; positive values to landward)
LOI = Loss on Ignition
BDL = Below Detection Limits Detection Limit for ^{134}Cs = 0.6 Bq kg^{-1}, ^{241}Am = 1.5 Bq kg^{-1}, $^{239+240}Pu$ = 0.03 Bq kg^{-1}, ^{238}Pu = 0.03 Bq kg^{-1}

Table 3.10 Radionuclide Concentrations and Inventories for the 0-15 cm Depth Interval from Orchardton Transect T1, Collected 29/8/90

Distance (m)	LOI (%)	^{137}Cs (Bq kg^{-1})	^{134}Cs (Bq kg^{-1})	^{241}Am (Bq kg^{-1})	^{137}Cs (Bq m^{-2})	^{241}Am (Bq m^{-2})
-10	3.7	183 ± 3	1.3 ± 0.4	BDL	38,025	BDL
0	3.8	4 ± 1	BDL	BDL	1,360	BDL
20	5.6	876 ± 10	6.7 ± 0.9	397 ± 28	202,100	91,591
40	5.9	1,340 ± 15	6.8 ± 0.9	503 ± 11	475,641	178,543
60	7.6	2,170 ± 24	1.7 ± 0.2	792 ± 13	528,865	193,024
80	7.7	2,210 ± 24	13.8 ± 1.5	755 ± 12	396,235	135,365
100	7.6	2,420 ± 27	10.0 ± 1.1	966 ± 20	803,954	320,917
120	NA	2,560 ± 28	17.6 ± 1.5	943 ± 15	724,956	267,044
180	10.1	994 ± 12	10.4 ± 0.9	287 ± 9	278,848	80,512

Distance = Distance from the MHWM (negative values to seaward; positive values to landward)
LOI = Loss on Ignition
BDL = Below Detection Limit Detection Limit for ^{134}Cs = 0.6 Bq kg^{-1}, ^{241}Am = 1.5 Bq kg^{-1}
NA = Not Available

Table 3.11 Radionuclide Concentrations and Inventories for the 15-30 cm Depth Intervals from Orchardton Transect T1, Collected 29/8/90

DISTANCE (m)	LOI (%)	^{137}Cs (Bq kg^{-1})	^{134}Cs (Bq kg^{-1})	^{241}Am (Bq kg^{-1})	^{137}Cs (Bq m^{-2})	^{241}Am (Bq m^{-2})
-10	3.7	148 ± 2	0.9 ± 0.2	5 ± 3	59,933	2,146
0	5.1	2 ± 0.4	BDL	BDL	538	BDL
20	6.0	1480 ± 17	2.9 ± 0.5	624 ± 3	439,416	185,267
40	6.2	1010 ± 12	1.2 ± 0.4	473 ± 8	296,833	139,012
60	7.2	841 ± 10	1.2 ± 0.4	472 ± 8	240,169	134,792
80	7.4	1460 ± 16	2.8 ± 0.6	771 ± 12	426,888	225,432
100	7.1	667 ± 8	BDL	348 ± 6	245,491	128,082
120	8.1	2250 ± 25	4.2 ± 0.7	824 ± 13	610,288	223,501
180	4.6	52 ± 2	BDL	17 ± 1	18,243	5,869

Distance = Distance from the MHWM (negative values to seaward; positive values to landward)
LOI = Loss on Ignition
BDL = Below Detection Limit Detection Limit for ^{134}Cs = 0.6 Bq kg^{-1}, ^{241}Am = 1.5 Bq kg^{-1}

Table 3.12 Radionuclide Concentrations and Inventories for the 0-15 cm Depth Intervals from Kippford Transect T1, Collected 28/8/90

DISTANCE (m)	LOI (%)	^{137}Cs (Bq kg^{-1})	^{134}Cs (Bq kg^{-1})	^{241}Am (Bq kg^{-1})	^{137}Cs (Bq m^{-2})	^{241}Am (Bq m^{-2})
-5	5.8	26 ±1	BDL	11 ±1	8,916	3,806
0	4.8	1,090 ±13	7.3 ± 0.8	400 ±9	426,547	156,472
20	5.8	1,850 ±21	9.4 ± 0.8	626 ±13	722,482	244,472
40	6.3	2,010 ±22	13.8 ± 1.4	BDL	582,544	BDL
60	7.3	2,460 ±27	17.0 ± 1.7	BDL	622,184	BDL
80	8.4	1,750 ±20	13.6 ± 1.2	BDL	360,841	BDL

Distance = Distance from the MHWM (negative values to seaward; positive values to landward)
LOI = Loss on Ignition
BDL = Below Detection Limit Detection Limit for ^{134}Cs = 0.6 Bq kg^{-1}, ^{241}Am = 1.5 Bq kg^{-1}
NA = Total Weight Not Available

Table 3.13 Radionuclide Concentrations and Inventories for the 15-30 cm Depth Intervals from Kippford Transect T1, Collected 28/8/90

DISTANCE (m)	LOI (%)	^{137}Cs (Bq kg^{-1})	^{134}Cs (Bq kg^{-1})	^{241}Am (Bq kg^{-1})	^{137}Cs (Bq m^{-2})	^{241}Am (Bq m^{-2})
-5	5.8	BDL	BDL	BDL	417,377	BDL
0	4.8	1080 ± 12	2.1 ± 0.3	563 ± 11	340,301	217,577
20	5.8	870 ± 10	1.7 ± 0.4	BDL	122,903	BDL
40	6.3	350 ± 5	BDL	BDL	103,049	BDL
60	7.3	350 ± 5	1.2 ± 0.3	BDL	64,276	BDL
80	8.4	280 ± 4	1.8 ± 0.6	BDL	61,000	BDL

Distance = Distance from the MHWM (negative values to seaward; positive values to landward)
LOI = Loss on Ignition
BDL = Below Detection Limit Detection Limit for ^{137}Cs = 0.6 Bq kg^{-1}, ^{134}Cs = 0.6 Bq kg^{-1}, ^{241}Am = 1.5 Bq kg^{-1}

Table 3.14 Radionuclide Concentrations and Inventories for the 0-15 cm Depth Intervals from Carse Bay Transect T1, Collected 15/8/91

DISTANCE (m)	LOI (%)	^{137}Cs (Bq kg^{-1})	^{134}Cs (Bq kg^{-1})	^{241}Am (Bq kg^{-1})	^{137}Cs (Bq m^{-2})	^{241}Am (Bq m^{-2})
-90	5.2	968 ± 12	4.9 ± 0.9	320 ± 8	168,758	55,788
-80	6.5	850 ± 11	5.1 ± 1.0	353 ± 11	89,363	37,112
-70	5.2	1,070 ± 13	4.0 ± 0.9	248 ± 9	166,087	38,495
-60	6.3	1,110 ± 14	10.5 ± 1.6	388 ± 7	169,840	59,367
-50	6.2	992 ± 12	8.4 ± 1.2	317 ± 11	158,544	50,664
-40	7.3	1,090 ± 14	9.6 ± 1.4	431 ± 13	109,965	43,481
-30	8.2	1,380 ± 16	13.8 ± 1.7	526 ± 9	199,673	76,107
-20	8.6	1,620 ± 19	16.5 ± 1.8	637 ± 11	242,283	95,268
-10	9.7	1,580 ± 18	13.3 ± 2.1	590 ± 16	136,887	51,116
0	10.7	2,160 ± 25	14.8 ± 1.6	901 ± 52	255,568	106,605
10	9.4	2,070 ± 23	9.5 ± 2.0	628 ± 19	287,602	87,253
30	12.4	2,320 ± 26	14.6 ± 2.2	777 ± 20	280,864	94,065
100	30.1	887 ± 12	12.5 ± 2.0	173 ± 6	47,019	9,170

Distance = Distance from the MHWM (negative values to seaward; positive values to landward)
LOI = Loss on Ignition

Table 3.15 Radionuclide Concentrations and Inventories for the 15-30 cm Depth Intervals from Carse Bay Transect T1, Collected 15/8/91

DISTANCE (m)	LOI (%)	^{137}Cs (Bq kg^{-1})	^{134}Cs (Bq kg^{-1})	^{241}Am (Bq kg^{-1})	^{137}Cs (Bq m^{-2})	^{241}Am (Bq m^{-2})
-90	3.0	1280 ± 15	2.9 ± 0.7	365 ± 11	235,611	67,186
-80	4.0	943 ± 12	4.0 ± 0.9	275 ± 9	169,156	49,330
-70	3.7	1120 ± 13	BDL	341 ± 12	170,775	51,995
-60	3.7	1540 ± 18	3.9 ± 0.8	353 ± 11	273,384	62,665
-50	3.9	1520 ± 17	3.2 ± 1.0	463 ± 14	281,805	85,839
-40	3.7	1280 ± 15	5.0 ± 1.0	282 ± 9	228,587	50,361
-30	5.7	1500 ± 18	10.2 ± 1.9	406 ± 12	165,796	44,875
-20	4.7	1680 ± 19	5.4 ± 1.0	324 ± 11	245,161	47,281
-10	4.9	1740 ± 20	5.1 ± 1.0	369 ± 11	301,805	64,003
0	6.3	691 ± 9	BDL	153 ± 6	100,287	22,205
10	6.7	289 ± 5	BDL	67 ± 3	43,145	10,003
30	8.6	148 ± 4	BDL	46 ± 3	20,641	6,457
100	8.9	13 ± 1	BDL	4 ± 1	1,706	523

Distance = Distance from the MHWM (negative values to seaward; positive values to landward)
LOI = Loss on Ignition
BDL = Below Detection Limit Detection Limit for ^{134}Cs = 0.6 Bq kg^{-1}

Table 3.16 Analytical Results for Southwick Water Transect T2 5m Core (T2.5), Collected 24/1/92

SOUTHWICK T2 - 5m CORE				
Depth (cm)	^{137}Cs (Bq kg^{1})	^{241}Am (Bq kg^{-1})	^{137}Cs (Bq m^{-2})	^{241}Am (Bq m^{-2})
0- 5	322 ± 6	209 ± 6	16,000	10,000
5-10	436 ± 7	261 ± 5	22,000	13,000
10-15	831 ± 12	328 ± 10	50,000	20,000
15-20	937 ± 13	345 ± 10	32,000	12,000
20-25	2,670 ± 32	701 ± 12	128,000	33,000
25-30	2,580 ± 31	1,000 ± 16	134,000	52,000
30-35	1,870 ± 24	542 ± 15	46,000	13,000
35-40	1,920 ± 24	843 ± 14	73,000	32,000
40-45	355 ± 7	54 ± 3	26,000	4,000
45-50	916 ± 13	256 ± 7	45,000	13,000
50-55	349 ± 6	102 ± 4	12,000	4,000
55-60	72 ± 3	19 ± 2	4,000	1,000
60-65	437 ± 7	134 ± 4	14,000	4,000
65-70	89 ± 3	25 ± 2	5,000	1,000
70-75	29 ± 2	5 ± 1	1,000	200
75-80	239 ± 5	75 ± 3	14,000	4,000
80-85	42 ± 3	7 ± 1	2,000	400
85-90	7 ± 1	3 ± 1	400	200
90-95	73 ± 3	19 ± 2	5,000	1,000
95-100	4 ± 1	BDL	400	BDL

BDL = Below Detection Limit
Detection Limit for ^{241}Am = 1.5 Bq kg^{-1}

Table 3.17 Analytical Results for Southwick Water Transect T2 10m (T2.10) Core, Collected 24/1/92.

SOUTHWICK T2 10m				
DEPTH (cm)	^{137}Cs (Bq kg^{-1})	^{241}Am (Bq kg^{-1})	^{137}Cs (Bq m^{-2})	^{241}Am (Bq m^{-2})
0- 5	398 ± 7	244 ± 7	16,000	10,000
5-10	951 ± 13	418 ± 10	38,000	17,000
10-15	2,610 ± 31	746 ± 12	113,000	32,000
15-20	2,190 ± 26	645 ± 18	91,000	27,000
20-25	2,680 ± 32	1,250 ± 19	126,000	59,000
25-30	649 ± 10	70 ± 3	30,000	3,000
30-35	1,460 ± 19	470 ± 13	53,000	17,000
35-40	3,020 ± 37	969 ± 24	58,000	19,000
40-45	2,510 ± 32	1,190 ± 19	49,000	23,000
45-50	1,100 ± 15	327 ± 10	51,000	15,000
50-55	420 ± 7	160 ± 6	25,000	9,000
55-60	117 ± 3	15 ± 2	6,000	800
60-65	429 ± 7	134 ± 4	26,000	8,000
65-70	60 ± 3	8 ± 1	3,000	400
70-75	9 ± 1	BDL	600	BDL
75-80	181 ± 4	50 ± 3	11,000	3,000
80-85	30 ± 2	7 ± 1	2,000	400
85-90	19 ± 2	3 ± 1	1,000	100
90-95	97 ± 3	27 ± 3	8,000	2,000
95-100	24 ± 2	BDL	2,000	BDL

BDL = Below Detection Limits
Detection Limit for ^{241}Am = 1.5 Bq kg^{-1}

Table 3.18 Analytical Results from Southwick Transect T2, 20 m Core (T2.20) Collected on 24/1/92.

SOUTHWICK T2 20 m				
Depth (cm)	^{137}Cs (Bq kg^{-1})	^{241}Am (Bq kg^{-1})	^{137}Cs (Bq m^{-2})	^{241}Am (Bq m^{-2})
0- 5	1,820 ± 22	612 ± 16	77,000	26,000
5-10	1,570 ± 20	520 ± 12	51,000	17,000
10-15	181 ± 5	114 ± 2	8,000	5,000
15-20	250 ± 5	74 ± 3	17,000	5,000
20-25	18 ± 2	BDL	900	BDL
25-30	11 ± 2	BDL	800	BDL
30-35	102 ± 3	33 ± 2	7,000	2,000
35-40	5 ± 1	BDL	300	BDL
40-45	5 ± 2	BDL	300	BDL
45-50	33 ± 2	9 ± 1	2,000	500
50-55	23 ± 2	4 ± 1	1,500	300
55-60	3 ± 1	BDL	200	BDL
60-65	94 ± 1	27 ± 1	6,000	2,000
65-70	6 ± 1	BDL	300	BDL
70-75	3 ± 1	BDL	150	BDL
75-80	48 ± 2	16 ± 2	3,000	1,000
80-85	BDL	BDL	BDL	BDL
85-90	BDL	BDL	BDL	BDL
90-95	18 ± 1	7 ± 1	1,500	600
95-100	5 ± 1	BDL	500	BDL

BDL = Below Detection Limits
Detection Limit for ^{137}Cs = 0.6 Bq kg^{-1}, ^{241}Am = 1.5 Bq kg^{-1}

Table 3.19 Analytical Results from Southwick Transect T2, 30 m Core (T2.30) Collected on 24/1/92.

SOUTHWICK T2 30 m				
Depth (cm)	^{137}Cs (Bq kg^{-1})	^{241}Am (Bq kg^{-1})	^{137}Cs (Bq m^{-2})	^{241}Am (Bq m^{-2})
0- 5	946 ± 7.0	122 ± 3	35,000	4,000
5-10	33 ± 1.0	7 ± 0.5	1,800	300
10-15	5 ± 1.0	BDL	200	BDL
15-20	21 ± 0.8	4 ± 0.3	1,000	200
20-25	12 ± 0.7	2 ± 0.3	600	100
25-30	4 ± 0.5	BDL	200	BDL
30-35	16 ± 1.0	3 ± 0.4	900	100
35-40	BDL	BDL	BDL	BDL
40-45	BDL	BDL	BDL	BDL
45-50	BDL	BDL	BDL	BDL
50-55	BDL	BDL	BDL	BDL
55-60	BDL	BDL	BDL	BDL
60-65	BDL	BDL	BDL	BDL
65-70	BDL	BDL	BDL	BDL
70-75	BDL	BDL	BDL	BDL
75-80	BDL	BDL	BDL	BDL
80-85	BDL	BDL	BDL	BDL
85-90	BDL	BDL	BDL	BDL
90-95	BDL	BDL	BDL	BDL
95-100	BDL	BDL	BDL	BDL

BDL = Below Detection Limits
Detection limit for ^{137}Cs = 0.6 Bq kg^{-1}, ^{241}Am = 1.5 Bq kg^{-1}

Table 3.20 Analytical Results from Southwick Transect T3 5 m Core (S3.5), Collected 27/5/92.

SOUTHWICK T3 5m				
Depth (cm)	LOI %	^{137}Cs (Bq kg^{-1})	^{134}Cs (Bq kg^{-1})	^{241}Am (Bq kg^{-1})
Surface	NA	498 ± 10	BDL	463 ± 12
0- 5	5.4	345 ± 3	2 ± 0.3	212 ± 7
5-10	4.3	347 ± 3	2 ± 0.3	219 ± 2
10-15	5.9	469 ± 3	2 ± 0.4	265 ± 9
15-20	6.0	947 ± 5	13 ± 0.7	352 ± 3
20-25	7.0	2,450 ± 7	5 ± 0.6	650 ± 4
25-30	6.7	1,981 ± 8	2 ± 0.5	892 ± 12
30-35	5.2	319 ± 3	BDL	49 ± 2
35-40	4.0	55 ± 1	BDL	5 ± 1
40-45	3.4	25 ± 1	BDL	BDL
45-50	3.5	8 ± 1	BDL	BDL
50-55	4.5	10 ± 1	BDL	BDL
55-60	4.3	33 ± 1	BDL	BDL
60-65	4.8	14 ± 1	BDL	BDL
65-70	4.9	14 ± 1	BDL	BDL
70-75	4.5	8 ± 1	BDL	BDL
75-80	4.9	3 ± 1	BDL	BDL
80-85	4.2	BDL	BDL	BDL
85-90	4.2	BDL	BDL	BDL
90-95	3.9	BDL	BDL	BDL
95-100	3.7	BDL	BDL	BDL

BDL = Below Detection Limits
Detection Limit for ^{137}Cs = 0.6 Bq kg^{-1}, ^{241}Am = 1.5 Bq kg^{-1}
NA = Not Available

Table 3.21 Analytical Results from Southwick Transect T3 10 m Core (S3.10), Collected 27/5/92.

SOUTHWICK T3 10m				
Depth (cm)	LOI %	^{137}Cs (Bq kg^{-1})	^{134}Cs (Bq kg^{-1})	^{241}Am (Bq kg^{-1})
Surface	NA	150 ± 9	BDL	167 ± 12.0
0- 5	6.9	419 ± 3	2.0 ± 0.4	271 ± 8.0
5-10	6.5	783 ± 5	8.0 ± 0.6	426 ± 11.0
10-15	6.4	1,500 ± 17	10.0 ± 0.8	502 ± 8.0
15-20	7.3	3,386 ± 10	5.0 ± 0.6	1,110 ± 15.0
20-25	6.9	1,470 ± 8	1.5 ± 0.5	538 ± 9.0
25-30	5.1	303 ± 4	BDL	9 ± 1.0
30-35	3.6	72 ± 2	BDL	5 ± 1.0
35-40	3.8	35 ± 1	BDL	BDL
40-45	4.2	40 ± 1	BDL	1 ± 0.3
45-50	4.2	52 ± 2	BDL	BDL
50-55	3.8	42 ± 1	BDL	BDL
55-60	3.2	33 ± 1	BDL	BDL
60-65	2.8	27 ± 1	BDL	BDL
65-70	2.7	12 ± 1	BDL	BDL
70-75	3.5	7 ± 1	BDL	BDL
75-80	3.1	5 ± 1	BDL	BDL
80-85	4.0	4 ± 1	BDL	BDL
85-90	3.8	16 ± 1	BDL	BDL
90-95	3.4	56 ± 2	BDL	BDL
95-100	3.0	90 ± 2	BDL	BDL

BDL = Below Detection Limits
Detection Limit for ^{134}Cs = 0.6 Bq kg^{-1}, ^{241}Am = 1.5 Bq kg^{-1}

Table 3.22 Analytical Results from Southwick Transect T3 15 m Core (S3.15), Collected 27/5/92

SOUTHWICK T3 15 m				
Depth (cm)	LOI (%)	^{137}Cs (Bq kg^{-1})	^{134}Cs (Bq kg^{-1})	^{241}Am (Bq kg^{-1})
Surface	NA	302 ± 14	BDL	302 ± 21
0- 5	7.8	587 ± 4	3 ± 0.1	457 ± 31
5-10	8.6	1,647 ± 7	18 ± 0.9	613 ± 10
10-15	8.9	3,775 ± 11	6 ± 0.7	1,314 ± 17
15-20	6.9	768 ± 5	BDL	108 ± 4
20-25	4.3	59 ± 2	BDL	5 ± 1
25-30	4.2	16 ± 1	BDL	BDL
30-35	4.6	19 ± 1	BDL	BDL
35-40	3.5	6 ± 1	BDL	BDL
40-45	2.6	4 ± 1	BDL	BDL
45-50	2.7	3 ± 1	BDL	BDL
50-55	3.0	BDL	BDL	BDL
55-60	3.1	BDL	BDL	BDL
60-65	2.8	BDL	BDL	BDL
65-70	2.7	BDL	BDL	BDL
70-75	2.7	BDL	BDL	BDL
75-80	2.7	BDL	BDL	BDL
80-85	2.6	BDL	BDL	BDL
85-90	2.6	BDL	BDL	BDL
90-95	2.4	BDL	BDL	BDL
95-100	2.5	BDL	BDL	BDL

BDL = Below Detection Limits
Detection Limits for ^{137}Cs = 0.6 Bq kg^{-1}, ^{134}Cs = 0.6 Bq kg^{-1}, ^{241}Am = 1.5 Bq kg^{-1}
NA = Not Available

Table 3.23 Percentage Content of Particle Size Fractions within Core SC1 and Irish Sea Sediment

SOUTHWICK CORE SC1				IRISH SEA
Fraction	0-5 cm	40-45 cm	65-70 cm	Sub-Tidal
Coarse Sand	0.1	0.25	0.25	0.15
Fine Sand	76.0	57.0	63.0	24.0
Silt	12.0	26.0	21.0	37.0
Clay	2.0	6.0	9.0	20.0
Organic Matter	5.0	5.0	4.0	6.0
Total	95.1	94.25	97.25	87.15

Table 3.24 Results of X-ray Diffraction Analysis for Mineralogical Content of Sediment Samples

	SOUTHWICK CORE SC1					IRISH SEA
Bulk (whole rock)	0-5 cm	20-25 cm	40-45 cm	55-60 cm	65-70 cm	Sediment
Major >20%	Quartz	Quartz	Quartz	Quartz	Quartz	Quartz
Minor 5-20%	Chlorite Feldspar (plagioclase & K feldspar)	Chlorite Feldspar (plagioclase & K feldspar)	Chlorite Feldspar (plagioclase & K feldspar)	Chlorite	Feldspar	Feldspar
Trace <5%	Mica/Illite Calcite, possible Kaolin	Mica/Illite probable Calcite, Kaolin	Mica/Illite possible Dolomite, Kaolin	Feldspar, Mica/Illite possible Calcite,	Mica/Illite Chlorite Calcite, Dolomite, possible Kaolin	
Clay (<10 μm)						
Major	Chlorite	Chlorite	Chlorite	Chlorite	Chlorite	Chlorite
Minor	Illite	Illite	Illite	Illite	Illite	Illite
Trace	Kaolin	possible Kaolin	possible Kaolin	possible Kaolin	possible Kaolin	possible Kaolin

Table 3.25 Analytical Results for Sequential Leaching of ^{137}Cs and $^{239+240}Pu$ from Intertidal Sediment from Southwick Water

Leaching Reagent	Intertidal Sediment			
	^{137}Cs (Bq kg^{-1})	%	$^{239+240}Pu$ (Bq kg^{-1})	%
0.05M $CaCl_2$ (Readily Available)	BDL	-	BDL	-
0.5M Acetic Acid (Exchangeable)	BDL	-	1 ± 0.04	-
0.1M Tetra Sodium Pyrophosphate (Chelated with OM)	BDL	-	14 ± 0.20	8
Acid Oxalate (Secondary Fe/Mn Oxides)	BDL	-	149 ± 3.40	89
1M HNO_3 (More Acid Soluble)	2 ± 0.1	2	2 ± 0.05	1
Residual	110 ± 6	98	3 ± 0.06	1

Table 3.26 Analytical Results for Sequential Leaching of ^{137}Cs from Sediment Samples Derived from Southwick Water Core SC1

Depth / Age	0-5 cm (~1 y)		20-25 cm (~9 y)		40-45 cm (~18 y)		55-60 cm (~22 y)		65-70 cm (~28 y)	
Leaching Reagent	^{137}Cs (Bq kg^{-1})	%	^{137}Cs (Bq kg^{-1})	%	^{137}Cs (Bq kg^{-1})	%	^{137}Cs (Bq kg^{-1})	%	^{137}Cs (Bq kg^{-1})	%
0.05M $CaCl_2$ (Readily Available)	BDL	-	BDL	-	13 ± 0.2	1	BDL	-	BDL	-
0.5M Acetic Acid (Exchangeable)	BDL	-	BDL	-	BDL	-	BDL	-	3 ± 0.1	3
0.1M Tetra Sodium Pyrophosphate (Chelated with OM)	BDL	-	3.5 ± 0.1	-	0.7 ± 0.02	-	BDL	-	BDL	-
Acid Oxalate (Secondary Fe/Mn Minerals)	6 ± 0.1	3	37 ± 0.5	4	32.5 ± 0.4	3	4.5 ± 0.1	2	1 ± 0.05	1
IM HNO_3 (Readily Acid Soluble)	29 ± 0.9	13	141 ± 2.4	15	121 ± 2	12	31.0 ± 0.9	14	9 ± 0.5	12
Residual	181 ± 2.8	84	751 ± 8.6	81	822 ± 9.4	83	193.0 ± 2.9	84	67 ± 1.5	85

Table 3.27 Analytical Results for Sequential Leaching of ^{137}Cs from Sediment Samples from Southwick Core T3 10m (S3.10)

Depth / Age	0-5 cm (~2 y)		15-20 cm (~16 y)		25-30 cm (~25 y)	
Southwick T3 10 m	^{137}Cs (Bq kg^{-1})	%	^{137}Cs (Bq kg^{-1})	%	^{137}Cs (Bq kg^{-1})	%
0.05M $CaCl_2$ (Readily Available)	BDL	-	BDL	-	BDL	-
0.5M Acetic Acid (Exchangeable)	BDL	-	BDL	-	BDL	-
0.1M Tetra Sodium Pyrophosphate (Chelated with OM)	BDL	-	BDL	-	BDL	-
Acid Oxalate (Secondary Fe/Mn Oxides)	BDL	-	BDL	-	BDL	-
1M HNO_3 (More Acid Soluble)	6 ± 0.1	2	30 ± 0.3	1	4 ± 0.1	1
Residual	337 ± 11	98	3158 ± 42	99	273 ± 10	99

Table 3.28 Analytical Results for $^{239+240}Pu$ from Sequential Extraction of Sediment Samples from SC1

Depth / Age	0-5 cm (~1 y)		20-25 cm (~9 y)		40-45 cm (~18 y)		55-60 cm (~22 y)		65-70 cm (~28 y)	
Leaching Reagent	$^{239+240}Pu$ (Bq kg^{-1})	%	$^{239+240}Pu$ (Bq kg^{-1})	%	$^{239+240}Pu$ (Bq kg^{-1})	%	$^{239+240}Pu$ (Bq kg^{-1})	%	$^{239+240}Pu$ (Bq kg^{-1})	%
0.05M $CaCl_2$ (Readily Available)	0.1 ± 0.02	-	BDL	-	0.1 ± 0.009	-	BDL	-	BDL	-
0.5M Acetic Acid (Exchangeable)	1.8 ± 0.06	2	0.6 ± 0.04	-	2.2 ± 0.05	1	BDL	-	BDL	-
0.1M Tetra Sodium Pyrophosphate (Chelated with OM)	41.8 ± 1.68	41	80.0 ± 1.5	43	54.7 ± 2.71	24	32.9 ± 0.8	34	3.43 ± 0.2	17
Acid Oxalate (Secondary Fe/Mn Minerals)	40.3 ± 1.2	39	74.6 ± 2.2	40	118.4 ± 2.4	51	44.5 ± 1.4	46	11.3 ± 0.25	57
IM HNO_3 (Readily Acid Soluble)	1.7 ± 0.05	2	1.1 ± 0.04	1	4.0 ± 0.27	2	1.2 ± 0.03	1	0.33 ± 0.03	2
Residual	16.8 ± 0.44	16	30.0 ± 0.7	16	50.9 ± 1.25	22	18.3 ± 0.5	19	4.8 ± 0.16	24

Table 3.29 Analytical Results for Sequential Leaching of $^{239+240}Pu$ from Sediment Samples derived from Southwick Core T3 10 m (S3.10)

Depth / Age	0-5 cm (~2 y)		15-20 cm (~16 y)		25-30 cm (~25 y)	
Southwick T3 10 m	$^{239+240}Pu$ (Bq kg^{-1})	%	$^{239+240}Pu$ (Bq kg^{-1})	%	$^{239+240}Pu$ (Bq kg^{-1})	%
0.05M $CaCl_2$ (Readily Available)	BDL	-	BDL	-	BDL	-
0.5M Acetic Acid (Exchangeable)	1 ± 0.03	-	1 ± 0.05	-	BDL	-
0.1M Tetra Sodium Pyrophosphate (Chelated with OM)	90 ± 1.40	44	256 ± 11.70	39	13.5 ± 0.4	43
Acid Oxalate (Secondary Fe/Mn Minerals)	74 ± 1.30	36	266 ± 4.70	41	12.4 ± 0.3	40
1M HNO_3 (More Acid Soluble)	4 ± 0.10	2	5 ± 0.10	1	BDL	-
Residual	34 ± 0.50	17	127 ± 1.50	19	5.2 ± 0.1	17

Table 3.30 Sequential Extraction of $^{239+240}$Pu from Marine Sediments and Terrestrial Soils Compiled from McDonald *et al.*, (1990; 1992)

% of $^{239+240}$Pu in Irish Sea and Solway Sediments						
SAMPLE	% Carbon	Readily Available	Exchangeable	Organically Bound	Secondary Fe/Mn Minerals	Residual
Core A (Marine)	8.0	<0.05	0.50 ± 0.05	31 ± 3	47 ± 4	22.0 ± 2.0
Core E (Marine)	5.2	<0.05	0.70 ± 0.04	40 ± 1	37 ± 2	23.0 ± 2.0
Kippford (Sediment)	5.3	<0.05	<0.05	32 ± 2	56 ± 3	11.0 ± 1.0
Culkeist (Sediment)	15.2	5.60 ± 0.1	3.60 ± 0.40	66 ± 6	17 ± 2	8.6 ± 0.9

Table 3.31 Analytical Results for the Flow Desorption Experiment, Leaching ^{137}Cs from the 0-5 cm Interval SC1 (sediment conc. 406Bq kg^{-1}) with Freshwater (Mains)

DESORPTION EXPERIMENT 0-5 cm FRESHWATER		
Volume (l)	^{137}Cs (Bq l^{-1})	K_D (l kg^{-1})
0- 110	0.004 ± 0.0001	1.0×10^5
111- 260	0.003 ± 0.0002	1.4×10^5
261- 330	0.003 ± 0.0001	1.4×10^5
331- 420	0.002 ± 0.0001	2.0×10^5
421- 560	0.003 ± 0.0001	1.4×10^5
561- 663	0.003 ± 0.0001	1.4×10^5
664- 885	0.003 ± 0.0001	1.4×10^5
886-1055	0.005 ± 0.0001	8.1×10^4
1056-1105	0.002 ± 0.0002	2.0×10^5
1106-1130	BDL	NA
1131-1168	0.002 ± 0.0003	2.0×10^5
1169-1205	BDL	NA
1206-1216	BDL	NA
1217-1250	0.002 ± 0.0003	2.0×10^5
1251-1310	0.0004 ± 0.0002	1.0×10^6
1311-1320	BDL	NA

BDL = Below Detection Limits
Limits of Detection = 0.028 Bq (^{137}Cs)
NA = Not Available

Table 3.32 Analytical Results for the Flow Desorption Experiment leaching ^{137}Cs from the 40-45 cm Interval SC1 (sediment conc. 1450 Bq kg^{-1}) with Freshwater (Mains)

DESORPTION EXPERIMENT 40-45 cm FRESHWATER		
Volume (l)	Concentration (Bq l^{-1})	K_D (l kg^{-1})
0- 40	0.005 ± 0.0003	2.9×10^5
41-120	0.006 ± 0.0002	2.4×10^5
121-271	0.010 ± 0.0003	1.4×10^5
272-300	0.004 ± 0.0004	3.6×10^5

Table 3.33 Analytical Results for the Flow Desorption Experiment, Leaching ^{137}Cs from the 0-5 cm Interval SC1 (sediment conc. 406 Bq kg^{-1}) with Field Drain Water (Ground Water)

DESORPTION EXPERIMENT 0-5 cm FIELD DRAIN		
Volume (l)	^{137}Cs (Bq l^{-1})	K_D (l kg^{-1})
0- 57	0.001 ± 0.0002	4.1×10^5
58- 80	BDL	NA
81-140	0.002 ± 0.0005	2.0×10^5
141-162	BDL	NA
163-220	0.001 ± 0.0002	4.1×10^5
221-300	0.001 ± 0.0001	4.1×10^5

BDL = Below Detection Limits
Limits of Detection = 0.028 Bq (^{137}Cs)
NA = Not Available

Table 3.34 Analytical Results for the Flow Desorption Experiment,Leaching ^{137}Cs from the 0-5cm Interval SC1(sediment conc. 1450 Bq kg^{-1}) with Field Drain Water (Ground Water)

DESORPTION EXPERIMENT 40-45 cm FIELD DRAIN		
Volume (l)	^{137}Cs (Bq l^{-1})	K_D (l kg^{-1})
0- 65	0.01 ± 0.0002	1.5×10^5
66-125	0.007 ± 0.0002	2.1×10^5
126-150	0.004 ± 0.0005	3.6×10^5
151-175	0.008 ± 0.0005	1.8×10^5
176-290	0.003 ± 0.0001	4.8×10^5
290-300	BDL	NA

BDL = Below Detection Limits
Limits of Detection = 0.028 Bq (^{137}Cs)
NA = Not Available

Table 3.35 Analytical Results for the Flow Desorption Experiment Leaching ^{137}Cs from the 0-5 cm Interval SC1 (sediment conc. 406 Bq kg^{-1}) with Seawater

DESORPTION EXPERIMENT 0-5 cm SEAWATER		
Volume (l)	^{137}Cs (Bq l^{-1})	K_D (l kg^{-1})
0- 65	0.0008 ± 0.0008	5.1×10^5
66-100	0.006 ± 0.0003	6.7×10^4
101-202	0.002 ± 0.0001	2.0×10^5
203-300	0.001 ± 0.0001	4.1×10^5

Table 3.36 Analytical Results for the Flow Desorption Experiment Leaching ^{137}Cs from the 40-45 cm Interval SC1 (sediment conc. 1450 Bq kg^{-1}) with Seawater

DESORPTION EXPERIMENT 40-45 cm SEAWATER		
Volume (l)	^{137}Cs (Bq l^{-1})	K_D (l kg^{-1})
0-105	0.02 ± 0.0002	7.3×10^4
106-300	0.01 ± 0.0001	1.5×10^5
301-340	0.009 ± 0.0003	1.6×10^5

Table 3.37 Analytical Results for the Leaching of ^{137}Cs from the 0-5 cm Interval SC1 (sediment conc. 406 Bq kg^{-1}) with Competing Cations

DESORPTION EXPERIMENT 0-5 cm COMPETING CATIONS			
Media	Volume (l)	^{137}Cs (Bq l^{-1})	K_D (l kg^{-1})
KCl	50	0.008 ± 0.0003	5.1×10^4
NH_4Cl	50	0.002 ± 0.0002	2.2×10^5

Table 3.38 Analytical Results from Batch Desorption Experiment (sediment conc. 421 Bq kg^{-1})

BATCH DESORPTION EXPERIMENT		
Volume (l)	^{137}Cs (Bq l^{-1})	K_D
0-10	0.006 ± 0.0011	7.0×10^4
11-25	0.009 ± 0.0008	4.7×10^4

Table 3.39 Analytical Results from Neutron Activation Analysis of Sediment Samples

NAA of Sediment Samples				
Sample	Cs (ppm)	Na (ppm)	Cr (ppm)	Fe (ppm)
SC1 2.5 cm	0.37 ± 0.027	12120 ± 362	0.50 ± 0.017	0.23 ± 0.006
SC1 7.5 cm	0.43 ± 0.031	12791 ± 383	0.57 ± 0.019	0.27 ± 0.007
SC1 12.5 cm	0.32 ± 0.021	10884 ± 324	0.45 ± 0.014	0.21 ± 0.005
SC1 17.5 cm	0.35 ± 0.024	11946 ± 357	0.50 ± 0.016	0.23 ± 0.006
SC1 22.5 cm	0.44 ± 0.027	11624 ± 348	0.55 ± 0.018	0.27 ± 0.007
SC1 27.5 cm	0.52 ± 0.033	11967 ± 358	0.60 ± 0.019	0.31 ± 0.008
SC1 32.5 cm	0.42 ± 0.025	11656 ± 347	0.52 ± 0.016	0.26 ± 0.006
SC1 37.5 cm	0.44 ± 0.028	11234 ± 335	0.52 ± 0.016	0.258 ± 0.007
SC1 42.5 cm	0.39 ± 0.024	11258 ± 336	0.51 ± 0.016	0.242 ± 0.006
SC1 47.5 cm	0.49 ± 0.031	10848 ± 324	0.59 ± 0.019	0.31 ± 0.008
SC1 52.5 cm	0.50 ± 0.032	16525 ± 484	0.62 ± 0.019	0.31 ± 0.008
SC1 57.5 cm	0.50 ± 0.031	14789 ± 443	0.61 ± 0.019	0.30 ± 0.007
SC1 62.5 cm	0.42 ± 0.028	11404 ± 335	0.50 ± 0.015	0.27 ± 0.006
SC1 67.5 cm	0.46 ± 0.032	12046 ± 355	0.51 ± 0.016	0.28 ± 0.007
River Sed	0.26 ± 0.020	12810 ± 376	0.47 ± 0.015	0.18 ± 0.005
T3 10 m 2.5 cm	0.41 ± 0.027	8726 ± 258	0.57 ± 0.017	0.27 ± 0.007
T3 10 m 17.5 cm	0.82 ± 0.049	10282 ± 304	0.83 ± 0.025	0.45 ± 0.011
T3 10 m 27.5 cm	0.54 ± 0.035	10144 ± 299	0.58 ± 0.018	0.33 ± 0.008

Table 3.40 Analytical results from NAA of sediment samples

NAA of SEDIMENT SAMPLES				
Sample	Co (ppm)	Br (ppm)	Rb (ppm)	Sb (ppm)
SC1 2.5 cm	0.33 ± 0.012	39.1 ± 6.01	0.49 ± 0.038	0.56 ± 0.147
SC1 7.5 cm	0.37 ± 0.013	48.7 ± 7.54	0.55 ± 0.042	0.40 ± 0.102
SC1 12.5 cm	0.28 ± 0.009	26.6 ± 4.32	0.48 ± 0.029	0.31 ± 0.084
SC1 17.5 cm	0.32 ± 0.011	36.8 ± 5.72	0.52 ± 0.034	0.52 ± 0.123
SC1 22.5 cm	0.36 ± 0.014	47.0 ± 7.39	0.55 ± 0.041	0.52 ± 0.158
SC1 27.5 cm	0.42 ± 0.015	50.9 ± 7.88	0.61 ± 0.046	0.52 ± 0.144
SC1 32.5 cm	0.35 ± 0.011	40.8 ± 6.28	0.55 ± 0.033	0.42 ± 0.105
SC1 37.5 cm	0.37 ± 0.012	35.2 ± 5.52	0.566 ± 0.034	BDL
SC1 42.5 cm	0.33 ± 0.011	35.2 ± 5.48	0.52 ± 0.032	0.44 ± 0.110
SC1 47.5 cm	0.40 ± 0.014	49.1 ± 7.64	0.61 ± 0.042	0.65 ± 0.164
SC1 52.5 cm	0.38 ± 0.013	54.9 ± 10.63	0.64 ± 0.048	0.56 ± 0.124
SC1 57.5 cm	0.41 ± 0.013	46.8 ± 9.06	0.59 ± 0.039	0.80 ± 0.152
SC1 62.5 cm	0.35 ± 0.012	22.8 ± 4.78	0.58 ± 0.038	0.54 ± 0.121
SC1 67.5 cm	0.37 ± 0.013	25.1 ± 5.13	0.58 ± 0.039	0.58 ± 0.135
River Sed	0.24 ± 0.009	13.0 ± 2.70	0.46 ± 0.031	0.34 ± 0.09
T3 10 m 2.5 cm	0.36 ± 0.012	37.8 ± 7.34	0.51 ± 0.035	0.57 ± 0.112
T3 10 m 17.5 cm	0.60 ± 0.020	77.3 ± 14.76	0.77 ± 0.054	0.91 ± 0.200
T3 10 m 27.5 cm	0.43 ± 0.014	51.85 ± 9.97	0.63 ± 0.041	0.74 ± 0.156

Table 3.41 Analytical Results from NAA of Sediment Samples (contd)

NAA OF SEDIMENT SAMPLES				
Sample	La (ppm)	Ce (ppm)	Eu (ppm)	Sm (ppm)
SC1 2.5 cm	19.3 ± 0.92	0.38 ± 0.011	0.40 ± 0.036	3.12 ± 0.099
SC1 7.5 cm	22.1 ± 1.08	0.44 ± 0.013	0.46 ± 0.039	3.85 ± 0.116
SC1 12.5 cm	18.2 ± 0.77	0.35 ± 0.01	0.39 ± 0.031	3.16 ± 0.094
SC1 17.5 cm	18.8 ± 0.80	0.37 ± 0.011	0.40 ± 0.038	3.23 ± 0.097
SC1 22.5 cm	20.9 ± 0.93	0.41 ± 0.012	0.42 ± 0.047	3.63 ± 0.111
SC1 27.5 cm	21.9 ± 0.95	0.45 ± 0.013	0.48 ± 0.038	3.92 ± 0.118
SC1 32.5 cm	21.58 ± 0.87	0.38 ± 0.011	0.42 ± 0.032	3.57 ± 0.103
SC1 37.5 cm	19.4 ± 0.75	0.39 ± 0.011	0.44 ± 0.036	3.45 ± 0.101
SC1 42.5 cm	19.2 ± 0.83	0.37 ± 0.011	0.43 ± 0.037	3.38 ± 0.099
SC1 47.5 cm	22.3 ± 0.87	0.43 ± 0.012	0.48 ± 0.041	4.02 ± 0.117
SC1 52.5 cm	33.8 ± 1.57	0.44 ± 0.012	0.45 ± 0.035	7.31 ± 0.348
SC1 57.5 cm	28.4 ± 1.54	0.44 ± 0.012	0.44 ± 0.031	5.89 ± 0.302
SC1 62.5 cm	18.6 ± 1.19	0.37 ± 0.011	0.37 ± 0.030	3.64 ± 0.23
SC1 67.5 cm	20.8 ± 1.41	0.40 ± 0.012	0.36 ± 0.033	3.38 ± 0.253
River Sed	17.9 ± 1.20	0.35 ± 0.009	0.35 ± 0.029	3.00 ± 0.290
T3 10 m 2.5 cm	19.3 ± 1.05	0.42 ± 0.012	0.44 ± 0.032	3.56 ± 0.216
T3 10 m 17.5 cm	30.9 ± 1.99	0.57 ± 0.016	0.58 ± 0.046	5.59 ± 0.325
T3 10 m 27.5 cm	22.9 ± 1.40	0.45 ± 0.013	0.45 ± 0.034	3.88 ± 0.245

Table 3.42 Analytical Results from NAA of Sediment Samples (contd)

NAA OF SEDIMENT SAMPLES			
Sample	Tb (ppm)	Lu (ppm)	Hf (ppm)
SC1 2.5 cm	0.35 ± 0.068	0.53 ± 0.034	1.25 ± 0.052
SC1 7.5 cm	0.42 ± 0.08	0.59 ± 0.037	1.22 ± 0.051
SC1 12.5 cm	0.28 ± 0.048	0.47 ± 0.028	1.20 ± 0.048
SC1 17.5 cm	0.31 ± 0.063	0.49 ± 0.03	1.19 ± 0.049
SC1 22.5 cm	0.40 ± 0.096	0.58 ± 0.041	1.29 ± 0.054
SC1 27.5 cm	0.48 ± 0.103	0.63 ± 0.038	1.28 ± 0.055
SC1 32.5 cm	0.40 ± 0.068	0.53 ± 0.029	1.19 ± 0.048
SC1 37.5 cm	0.39 ± 0.076	0.51 ± 0.034	1.12 ± 0.047
SC1 42.5 cm	0.36 ± 0.064	0.51 ± 0.029	1.13 ± 0.046
SC1 47.5 cm	0.33 ± 0.081	0.55 ± 0.035	1.13 ± 0.048
SC1 52.5 cm	0.51 ± 0.079	0.66 ± 0.04	1.39 ± 0.057
SC1 57.5 cm	0.42 ± 0.064	0.65 ± 0.038	1.28 ± 0.052
SC1 62.5 cm	0.38 ± 0.069	0.57 ± 0.035	1.12 ± 0.046
SC1 67.5 cm	0.43 ± 0.066	0.58 ± 0.037	1.17 ± 0.049
River Sed	0.36 ± 0.054	0.52 ± 0.032	1.51 ± 0.061
T3 10 m 2.5 cm	0.38 ± 0.062	0.64 ± 0.039	1.27 ± 0.052
T3 10 m 17.5 cm	0.65 ± 0.116	0.774 ± 0.049	1.28 ± 0.055
T3 10 m 27.5 cm	0.38 ± 0.057	0.56 ± 0.037	1.20 ± 0.05

Table 3.43 Analytical Results from NAA of Sediment Samples

NAA OF SEDIMENT SAMPLES		
Sample	Ta (ppm)	Th (ppm)
SC1 2.5 cm	0.54 ± 0.089	0.34 ± 0.01
SC1 7.5 cm	0.54 ± 0.078	0.41 ± 0.012
SC1 12.5 cm	0.52 ± 0.073	0.31 ± 0.009
SC1 17.5 cm	0.55 ± 0.086	0.35 ± 0.01
SC1 22.5 cm	0.55 ± 0.102	0.41 ± 0.012
SC1 27.5 cm	0.68 ± 0.101	0.40 ± 0.012
SC1 32.5 cm	0.54 ± 0.066	0.36 ± 0.012
SC1 37.5 cm	0.60 ± 0.089	0.37 ± 0.012
SC1 42.5 cm	0.49 ± 0.069	0.36 ± 0.012
SC1 47.5 cm	0.58 ± 0.079	0.43 ± 0.012
SC1 52.5 cm	0.49 ± 0.061	0.46 ± 0.013
SC1 57.5 cm	0.49 ± 0.064	0.43 ± 0.012
SC1 62.5 cm	0.47 ± 0.058	0.37 ± 0.01
SC1 67.5 cm	0.46 ± 0.061	0.41 ± 0.011
River Sed	0.43 ± 0.053	0.38 ± 0.01
T3 10 m 2.5 cm	0.48 ± 0.06	0.42 ± 0.012
T3 10 m 17.5 cm	0.66 ± 0.085	0.57 ± 0.016
T3 10 m 27.5 cm	0.46 ± 0.061	0.44 ± 0.012

Table 3.44 Concentrations of ^{137}Cs and K_D Values from NAA of Desorption Media.

NAA OF WATER SAMPLES		
Desorption period (days)	Concentration ($\mu g\ ml^{-1}$)	K_D ($l\ kg^{-1}$)
8	9.20×10^{-6}	4.69×10^{6}
22	2.42×10^{-5}	1.78×10^{6}
60	2.28×10^{-5}	1.89×10^{6}
64	2.96×10^{-5}	1.46×10^{6}

Table 3.45 Analytical Results from Desorption Experiment involving Neutron Activation Analysis of Water Samples in Contact with Contaminated Sediment (SC1 0-5 cm)

Period Samples In Contact With Water			
8 Days	22 Days	60 Days	64 Days
0.02 ± 0.003	0.42 ± 0.035	0.40 ± 0.032	0.65 ± 0.054
NA	NA	NA	NA
0.02 ± 0.001	0.53 ± 0.018	0.31 ± 0.014	0.52 ± 0.023
0.01 ± 0.002	0.11 ± 0.003	0.16 ± 0.005	0.27 ± 0.008
0.01 ± 0.001	0.20 ± 0.010	0.27 ± 0.010	0.45 ± 0.020
NA	NA	NA	NA
0.01 ± 0.002	0.30 ± 0.030	0.30 ± 0.060	0.50 ± 0.060
0.21 ± 0.040	1.50 ± 0.260	1.51 ± 0.260	2.52 ± 0.430
NA	NA	NA	NA
0.01 ± 0.001	0.06 ± 0.007	0.10 ± 0.008	0.17 ± 0.013
0.02 ± 0.005	0.12 ± 0.030	0.21 ± 0.030	0.35 ± 0.050
NA	NA	NA	NA
NA	NA	NA	NA
NA	NA	0.17 ± 0.03	0.28 ± 0.05
0.01 ± 0.002	0.13 ± 0.020	0.31 ± 0.030	0.51 ± 0.040
NA	NA	NA	NA
0.01 ± 0.001	0.11 ± 0.010	0.15 ± 0.010	0.24 ± 0.010

NA = Not Available

CHAPTER 4
DISCUSSION

4.1. RADIONUCLIDE VERTICAL PROFILES AND TRANSPORT MECHANISM TO FLOODPLAIN DEPOSITS AT SOUTHWICK WATER

4.1.1 Vertical Profiles

The radionuclide concentration profiles for sections SC1 and SC2 from Southwick Water are illustrated in Figs 4.1 and Figs 4.2 respectively. The concentration profiles exhibit distinct sub-surface maxima and bear a qualitative resemblance to the Sellafield discharge pattern. The profiles for SC1 (Fig 4.1) showed distinct sub-surface maxima for ^{137}Cs, ^{241}Am and $^{239+240}Pu$ concentrations, with the maximum concentrations for ^{137}Cs (1,880 Bq kg^{-1}) and ^{241}Am (687 Bq kg^{-1}) at 35-40 cm, while the $^{239+240}Pu$ maximum (386 Bq kg^{-1}) was at 30-35 cm. The ^{134}Cs profile also exhibits a sub-surface maximum but is confined to the 5-10 cm interval.

The profiles for SC2 (Fig 4.2) again showed distinct sub-surface maxima, however, the depth of penetration in this case was confined to 20 cm. The maximum concentrations of ^{137}Cs (1,138 Bq kg^{-1}) and $^{239+240}Pu$ (250 Bq kg^{-1}) were found in the 10-15 cm interval, while the ^{241}Am maximum (730 Bq kg^{-1}) was at 15-20 cm.

It is possible to identify clearly the particular source of plutonium contamination using the $^{238}Pu/^{239+240}Pu$ activity ratio. The Sellafield effluent exhibited an activity ratio of about 0.3 between 1978-82 (BNFL 1979-1983) compared with 0.03 for weapons testing fallout (Hardy *et al.*, 1973). The accident at Chernobyl produced a characteristic $^{134}Cs/^{137}Cs$ activity ratio of 0.6 (Clarke and Smith, 1988) compared with a 0.07 ratio for Sellafield waste discharges in 1986. In addition the presence of ^{241}Am in such concentrations in both cores clearly demonstrates that the principal source of the contamination was from Sellafield derived radionuclides and not weapons fallout which produced inventories of 12 Bq m^{-2} (Perkins and Thomas, 1980).

Fig 4.1 Concentration profiles of radionuclides for sediment core SC1 collected from Southwick merse 8/12/89.

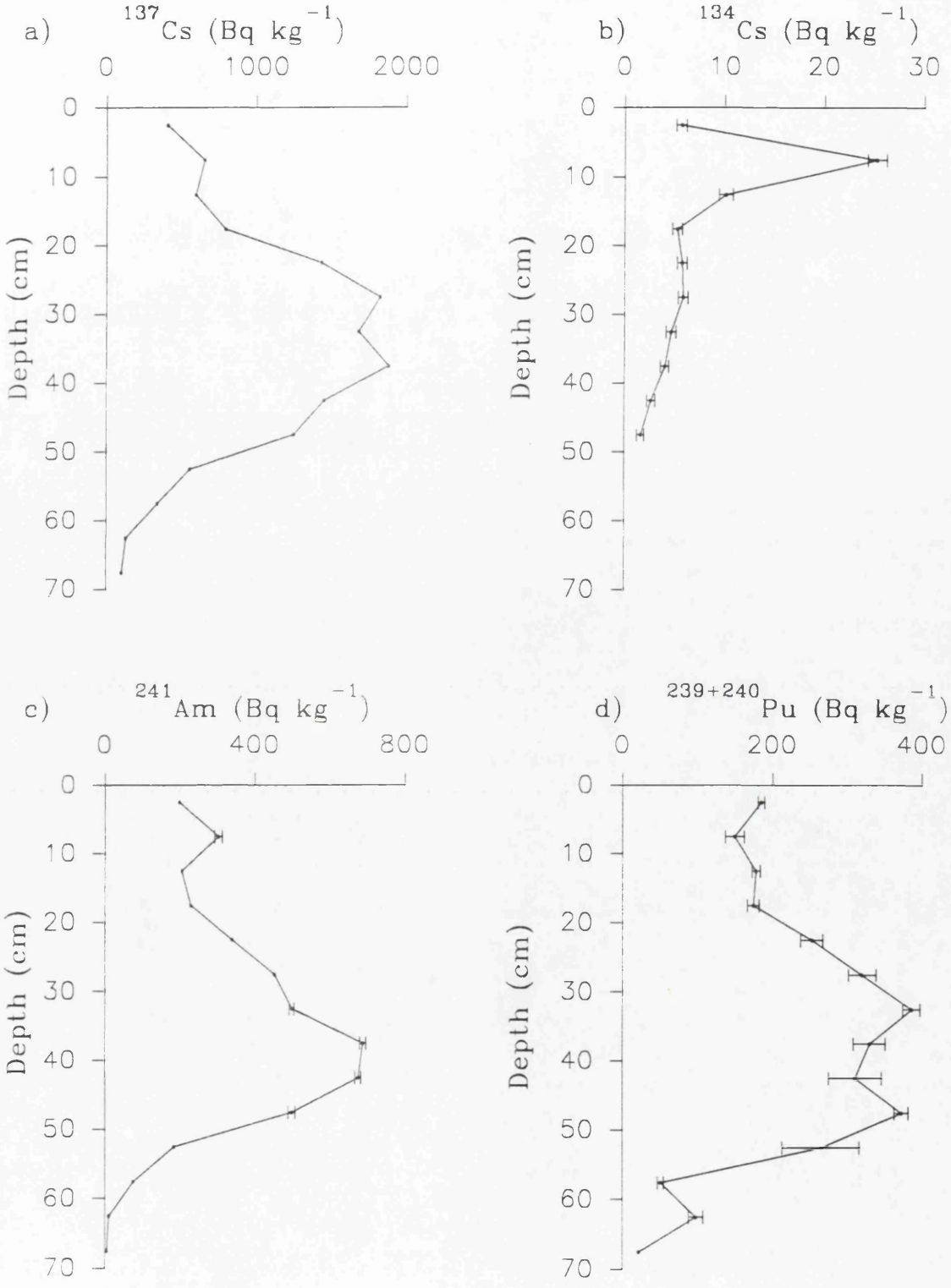

Fig 4.2 Concentration profiles of radionuclides for sediment core SC2 collected from Southwick merse 21/3/90.

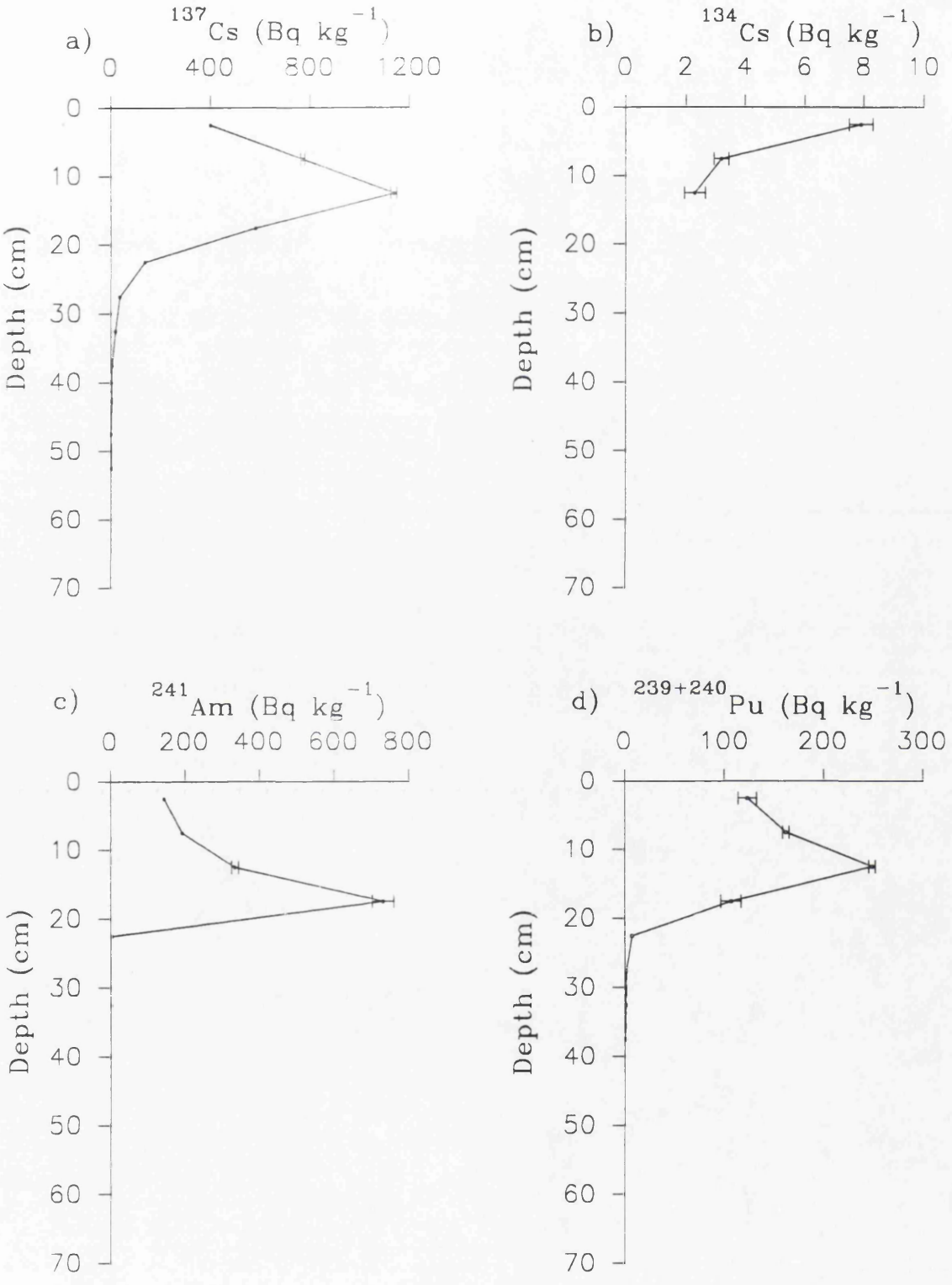

From the difference in depth of penetration of the radionuclides it can be concluded from the profiles that section SC2 probably has a lower sedimentation rate than section SC1 and this reflects the location of each section. SC1 was located 800 m upriver from the sea, on a slightly curving section of the river bank, which experiences longer and more frequent tidal inundation than section SC2 which was located some 1,200 m upriver from the sea. In addition there is a series of meanders in the river between the locations of SC1 and SC2. The incoming tide dissipates its energy on the river banks and silt/sand bars as it moves up river, with an energy loss in proportion to distance travelled (Selby, 1985). The meanders in the river increase the distance travelled and change the direction of flow, further reducing the energy and therefore the sediment carrying capacity of the incoming tide before it reaches the site of section SC2.

The vertical concentration profiles suggest that these sites have experienced some accumulation in recent years. If the accumulation has been continuous, the profiles will provide a record of radionuclide deposition at these sites. The profiles are similar to those interpreted as being directly related to the Sellafield annual discharge (Aston and Stanners, 1979, 1981a; Hamilton and Clarke, 1984; Ben-Shaban, 1989 and Kershaw *et al.,* 1990). However, as outlined in Section 1.1.2 and Section 1.4.4.3, this approach may not be valid and the following discussion attempts to relate sediment concentrations and activity ratios as a function of depth to temporal variations in the Sellafield discharge.

In order to model the radiological impact of the Sellafield discharge adequately and to predict future trends in critical group exposure, it is essential to identify and quantify the processes governing the environmental dispersion of radionuclides (MacKenzie and Scott, 1993) and these vertical concentration profiles for radionuclides in the saltmarsh deposits permit examination of the transportation mechanism of Sellafield radionuclides to this area. The supply mechanism can be considered to involve one (or a combination) of two contrasting transport mechanisms, namely solution transport or particulate transport (MacKenzie *et al.*, 1987). In the case of solution transport, radionuclides can be considered to be transported away from the discharge point in solution in seawater, with continuous removal from solution to the sediment occurring during transport.

In such a process, different radionuclides would be removed from solution differentially with respect to increasing distance from the discharge point according to their K_D values in this system. Operation of this mechanism would mean that, at any point in the Irish Sea where the rate of accumulation of sediment is rapid relative to post-depositional mixing, the surface sediment radionuclide concentrations would be determined by the quantities of radionuclides in immediately preceding discharges and the radionuclide activity ratios would correspondingly be some constant fraction of, though not necessarily equal to, those of the discharge. These are, in fact, the conditions necessary for a sediment profile to preserve a direct record of the Sellafield discharge for all of the (long-lived) radionuclides released into the marine environment.

In the contrasting mechanism of particle transport, the radionuclides are assumed to become partitioned between the aqueous and solid phases almost immediately upon discharge, with soluble species being rapidly removed from the Irish Sea in a time of less than one year (Jefferies *et al.,* 1973), while particle reactive radionuclides are taken up by surface sediments close to the discharge point. Thereafter, the particle associated radionuclides are transported by reworking and dispersal processes influencing the sediment particles to which they are bound. As discussed in detail in Section 1.4.3, it has been well established that particle reactive radionuclides have been dominantly concentrated in the fine sediment close to the Sellafield pipeline and that the main area of contaminated sediment is subject to intense vertical mixing (Kershaw *et al*, 1983,1984). Complete vertical mixing of the sediment over the depth range containing the Sellafield waste would result in the radionuclide concentrations and activity ratios in the sediment being related to those of the time integrated discharge (allowing for radioactive decay and ingrowth where appropriate), rather than to individual discharges. Thus, if re-distribution of such sediment is the dominant mechanism of transport of Sellafield waste radionuclides within the Irish Sea, then radionuclide concentrations in surface sediments should vary spatially in accordance with the extent of dispersion and consequent dilution of the contaminated silt and activity ratios should reflect those of the time integrated discharge. Moreover, in an accumulating intertidal deposit being supplied from this mixed pool of contaminated sediment, radionuclide activity ratios throughout the depth range affected should be a constant fraction of those

of the integrated discharge corresponding to the year of deposition, making appropriate allowances for post-depositional radioactive decay and ingrowth. The sediment section SC1 with its greater depth of penetration and distribution of radionuclides provides a better time resolution for comparison with the historical Sellafield discharge pattern than the restricted distribution of section SC2 which is confined to the upper 20 cm of the profile.

4.1.2 Transportation Mechanism

If the sub-surface maxima in radionuclide concentrations (Fig 4.1) are taken to correspond to the maximum discharges from Sellafield in the period 1973-75 (Fig 4.3) then sediment accumulation rates for each section can be defined, giving values of 2.7 cm y^{-1} using the ^{137}Cs profile, 2.5 cm y^{-1} for ^{241}Am and 2.0 cm y^{-1} for the $^{239+240}Pu$ profile, with a mean value of 2.4 cm y^{-1}. These values for the sedimentation rates are in reasonable agreement with those produced by Ben-Shaban (1989) for cores collected at a nearby location on the bank of the Southwick Water. Ben-Shaban (1989) calculated a sedimentation rate of 4.3 cm y^{-1} for core NCS862 located ~200 m further upriver from the site of section SC1 at the intersection of the path from the entrance and the meander of the Southwick Water (Fig 2.2). This site had been subject to slumping and removal of material at some time prior to the time of collection in March 1986, however, visual observation has since indicated that the site has been subsequently experiencing rapid accumulation of sediment. The sample location therefore, may not have been subject to continuous deposition over the 40 year time scale that Sellafield effluent has been discharged. However, the elevation of the river bank, covered by a rich grass sward, suggests that the site has been subject to accumulation of sediment for a considerable number of years. The dynamic nature of saltmarshes in general creates environments prone to rapid erosion and deposition. The sedimentation rates calculated from the radionuclide concentration profiles are applicable only to their particular sites and cannot be extrapolated to other locations within the merse which could be experiencing different sedimentation conditions.

Fig 4.3 Temporal variations in Annual discharges from Sellafield

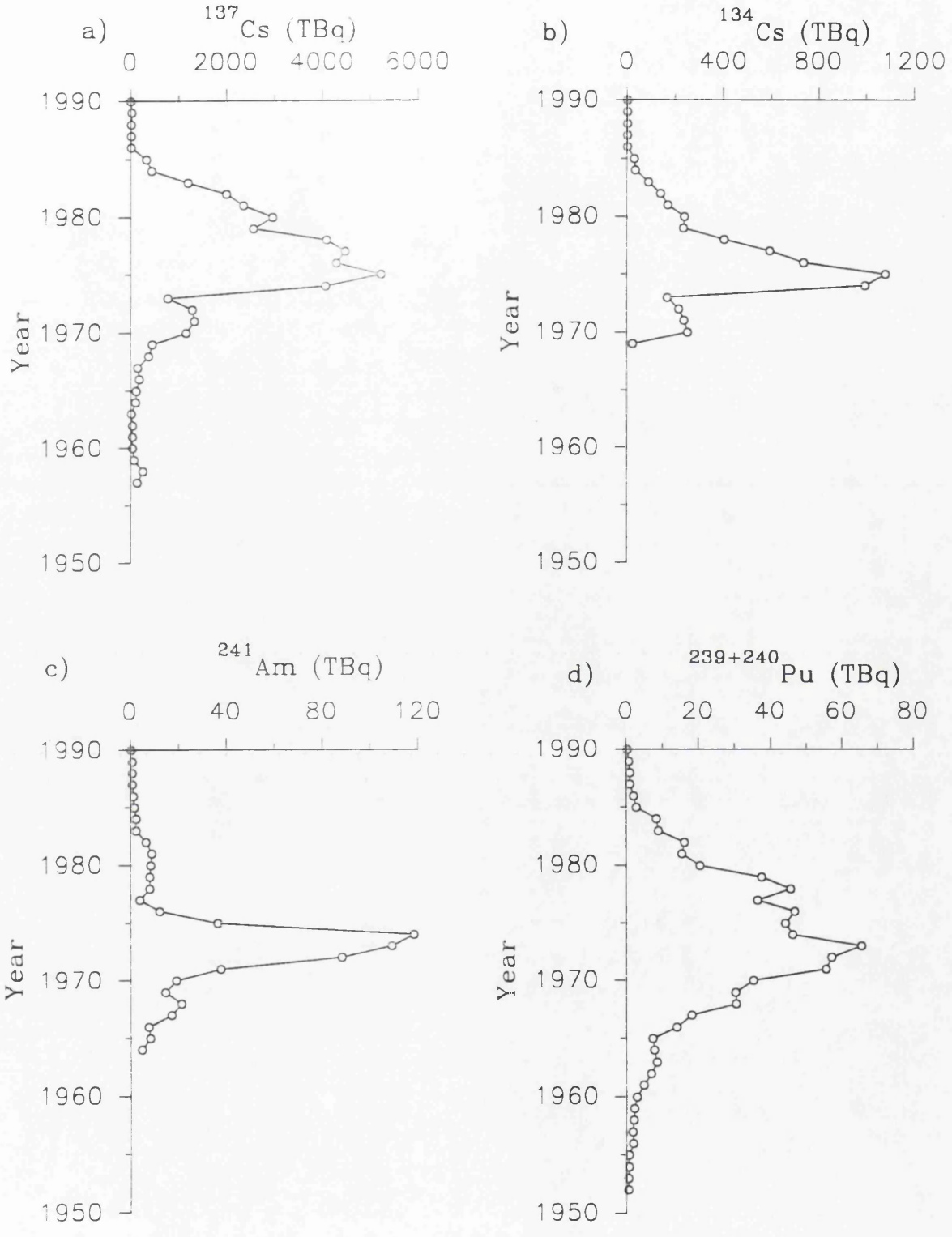

Fig 4.4 Plot of natural log of unsupported ^{210}Pb concentration versus depth in core SC1.

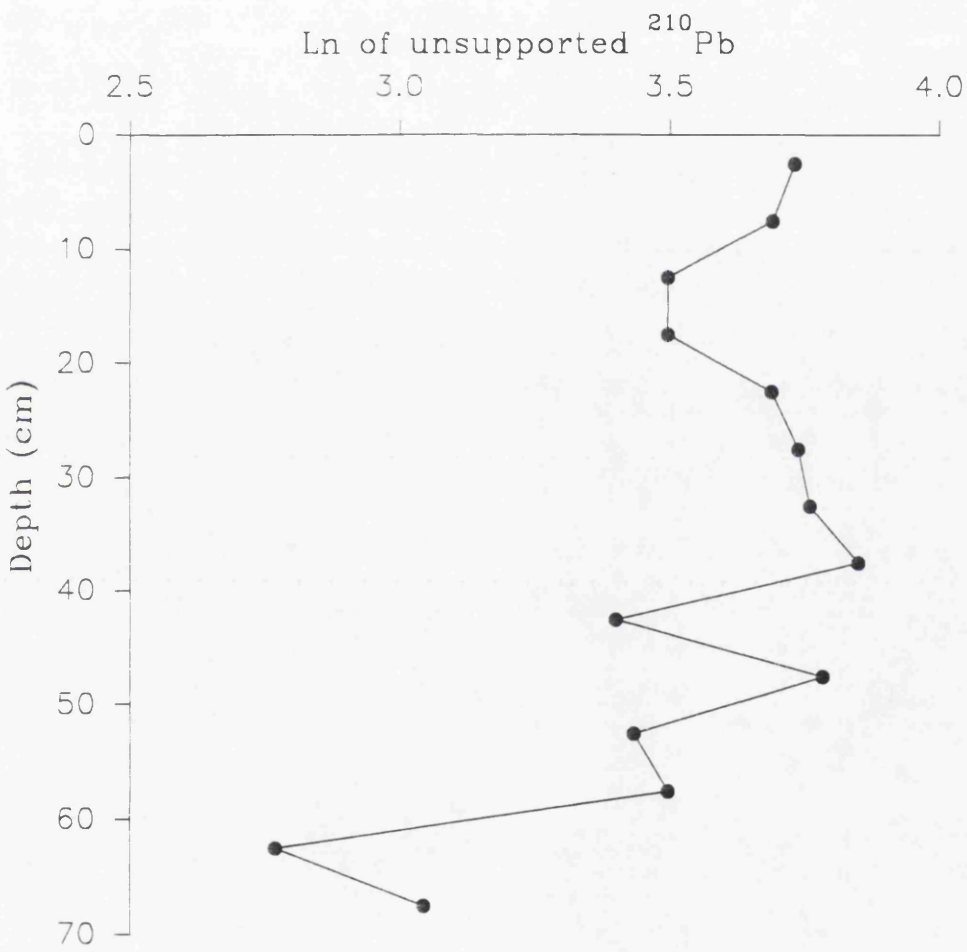

The ^{210}Pb data (Fig 4.4), derived from the analysis of the ^{210}Po grand-daughter, provide an independent chronology which can be compared to the chronology determined by the radionuclide depth profiles above. The ^{210}Pb data are not ideal for this purpose since the decrease in concentration with depth is small and irregular. Nevertheless, linear correlation of the natural log $^{210}Pb_{excess}$ versus depth gives a reasonable straight line ($R^2 = 0.6$), implying a sedimentation rate of 1.3 cm y^{-1}. The irregular shape of the profile probably reflects non steady state deposition of ^{210}Pb at the sample site. There are strong similarities between the chronologies produced by the radionuclide profiles and the ^{210}Pb dating with values ranging from 1.3 to 2.7 cm y^{-1}. However, the use of the independent ^{210}Pb dating chronology is open to uncertainty since it has been established that steady state deposition of ^{210}Pb has been perturbed in the north east Irish Sea by discharges of natural decay series radionuclides from the Albright and Wilson orthophosphate production plant at Whitehaven in Cumbria (McCartney *et al.,* 1990). The ^{210}Pb derived sedimentation rate is therefore subject to considerable uncertainty, but at the limited level of confidence that can be applied, is in reasonable agreement with the chronologies estimated from the Sellafield waste radionuclide distributions in the sediment. The ^{210}Pb profile from SC1 is similar to the profile generated from core NCS862 in 1986 by Ben-Shaban (1989), with the range of values being 16 to 47 Bq kg^{-1} and 19 to 36 Bq kg^{-1} for SC1 and NCS862 respectively. The chronologies obtained from the ^{210}Pb profiles are obviously different (section SC1 1.3 cm y^{-1}, section NCS862 4.3 cm y^{-1}) and the variation is attributable to the site specific nature of the deposition process. The uncertainty attached to the ^{210}Pb data at this site meant that greater reliability was placed on the chronologies from the Sellafield radionuclide profiles which were within the range 2.0 cm y^{-1} to 2.7 cm y^{-1}, giving a mean value of 2.4 cm y^{-1} which was taken as the sedimentation rate for section SC1. Fig 4.5 illustrates the chronology derived from this sedimentation rate, with an estimated error of 15%. The sedimentation rate for section SC2 was determined by the same method as SC1 with the rate calculated as 0.9 cm y^{-1}. As stated above, the restricted distribution of the radionuclides within this core, producing only 5 data points for a 30 year chronology, meant that the profile did not provide sufficient resolution for comparison with temporal variations in the Sellafield discharges and was therefore not used as a tool for investigation of the radionuclide transportation mechanism.

Fig 4.5 Sediment chronology for core SC1 produced by the 2.4 cm y^{-1} sedimentation rate, assuming an error of 15%.

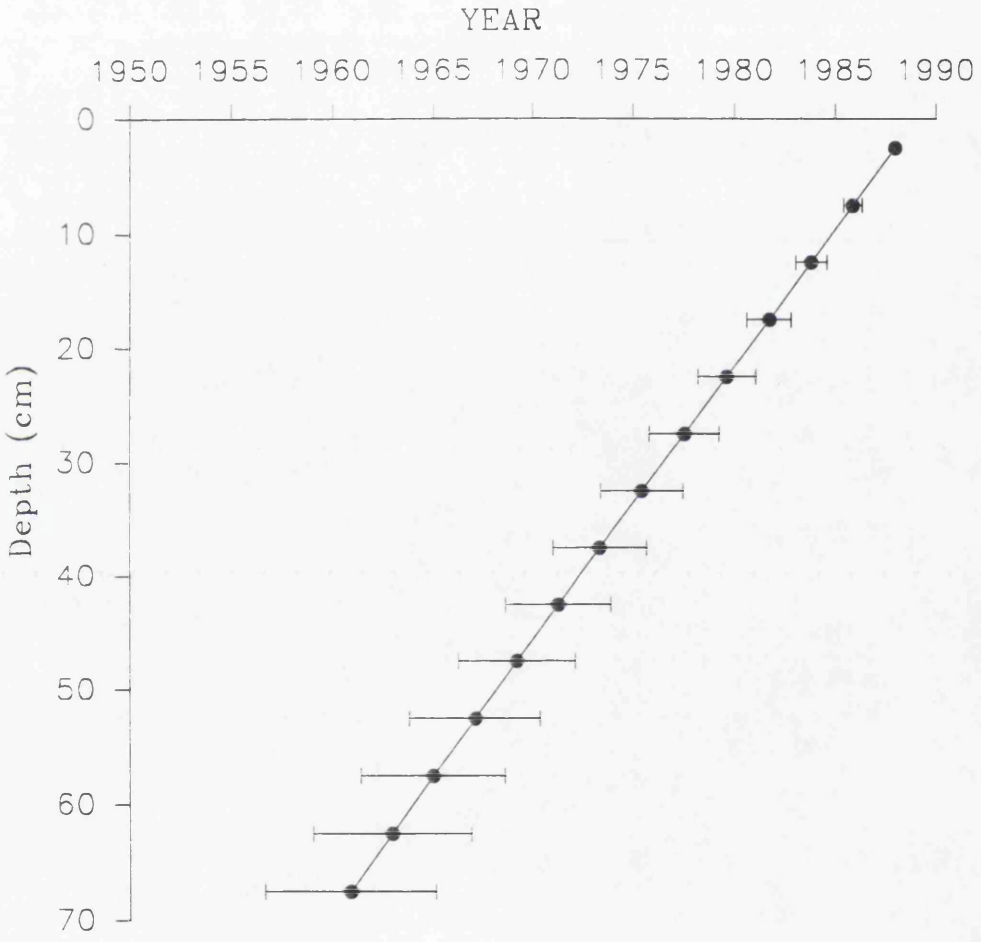

The shapes of the radionuclide concentration profiles for SC1 are similar to the shape of the corresponding Sellafield annual discharge pattern and qualitative comparison of the section profiles and the Sellafield annual discharge data suggests that a simple model can be applied in which radionuclide concentrations in successively deposited layers of accumulating sediment provide a record with variations in direct proportion to temporal variations in the Sellafield discharge. However, quantitative scrutiny of the data reveals that application of such a model generates major inconsistencies between observed variations in radionuclide concentrations and activity ratios at depth in the sediment and corresponding temporal variations in the Sellafield discharge pattern.

The decrease in the Sellafield discharges from the peak values in the mid 1970's to 1989 was much greater than the observed decrease in radionuclide concentrations from the maximum at depth to the surface. This can be illustrated simply by comparison of the ratio of maximum to surface sediment concentrations in SC1 with the ratio of maximum Sellafield discharge to the 1989 value. The ratio of the maximum ^{137}Cs concentration to that of the surface sample has a value of 4.6 for SC1 (Table 3.1, Fig 4.1), whereas the ratio of 1989 to 1975 in the Sellafield discharges has a value of 249.1. Similarly, comparison of the ^{241}Am and $^{239+240}Pu$ concentrations with the Sellafield discharges provides additional evidence of discrepancies between the sediment section profiles and the Sellafield annual discharge. The ratio of the maximum concentration of $^{239+240}Pu$ within section SC1 and the surface deposit is 2.09 compared with 89.77 for the Sellafield annual discharge (Table 1.1). The ratio of the maximum concentration of ^{241}Am to the surface concentration is 3.45 for SC1 compared with 145.99 for the Sellafield annual discharge. The ^{241}Am and $^{239+240}Pu$ annual discharge data indicate that the decrease in the Sellafield discharges from the mid 1970's to the late 1980's has been between one and two orders of magnitude greater than the corresponding decrease in the sediment radionuclide concentrations in SC1.

The above evidence indicates that the radionuclide concentrations in different layers of the sections are not linearly related to the radionuclide discharges from Sellafield for corresponding years on the basis of the chronology used (2.4 cm y^{-1}). The concentrations of radionulides deposited within the sediment section since the mid

1970s have been greater than would have been expected if there had been a direct relationship between the annual discharge and the sediment section concentrations.

This basic comparison demonstrates that a simple model involving continuous accumulation of sediment, contaminated in proportion to immediately preceding Sellafield discharges, cannot adequately account for the observed radionuclide distribution in the sediment section.

4.1.2.1 Comparison of the Isotope Activity Ratio Profiles

Comparison of the sediment isotope activity ratios with those of the Sellafield effluent provides further evidence of the difficulty in attempting to describe the sediment profiles in terms of a simple model. Differences in geochemical and biogeochemical behaviour can obviously give rise to fractionation of different elements during environmental processes, with the result that activity ratios for radionuclides of different elements can vary between different environmental materials and between environmental materials and the Sellafield effluent. Such limitations do not apply to isotope activity ratios since isotopic fractionation during chemical or biological processes is negligible. The isotope activity ratios for SC1 were decay corrected to the time of deposition using the mean sedimentation rate of 2.4 cm y^{-1}. The isotope activity ratios at any given depth in the sediment (decay corrected to the time of deposition) should be equal to those of the Sellafield discharge for the appropriate year if a simple mechanism involving accumulation of sediment with radionuclide contamination in proportion to effluent releases is operating. Deviations from this situation would imply mixing of waste of different ages before deposition of the sediment, provided the level of post-depositional mixing is low. There was no evidence of bioturbation by soil organisms such as worm burrows which implied that post depositional mixing was low. In addition, the sharply defined peaks with distinct sub-surface maxima in the radionuclide profiles (Fig 4.1 a,b,c,d) indicate that disturbance by soil fauna has not resulted in the post depositional mixing of the soil profile.

The $^{238}Pu/^{239+240}Pu$ activity ratios for section SC1, decay corrected to the time of deposition, are shown in Fig 4.6 together with corresponding activity ratio data for

the Sellafield discharges where available (post 1978). There is a pronounced discrepancy between the sediment activity ratios, which were typically in the range 0.20 to 0.22 (post 1973), and the corresponding discharge values, which were generally greater than 0.3, during the period for which ^{238}Pu results for the effluent have been available. As noted by Kershaw *et al.,* (1990) in discussion of the Maryport core results and by Hunt (1985) when considering surface sediment results, a discrepancy of this sort indicates that the sediment must have undergone some degree of mixing before deposition, resulting in mixing of Sellafield waste plutonium of different ages. It is apparent from the data that some mixing has occurred, however, it is not possible on the basis of the $^{238}Pu/^{239+240}Pu$ data alone to quantify the degree of mixing because of the limited information available on the activity ratio in the discharges.

The observation that lower $^{238}Pu/^{239+240}Pu$ activity ratios are recorded in section SC1 than are present in the Sellafield discharges is not an isolated phenomenon; similar occurrences can be identified in the Maryport cores (collected 1987) and in core NCS862 collected from the bank of the Southwick Water, ~200 m upriver from the location of section SC1, in March 1986 (Ben-Shaban, 1989). Fig 4.7 illustrates the $^{238}Pu/^{239+240}Pu$ activity ratios decay corrected to the time of deposition, for sediment section SC1 together with corresponding data for NCS862 (Ben-Shaban, 1989), the Maryport cores (Kershaw *et al.,* 1990), surface sediment from Newbiggin (Hetherington, 1975) and the Sellafield discharges (BNFL, 1977-1989). There is close agreement between the $^{238}Pu/^{239+240}Pu$ activity ratios for the sediment cores and the Newbiggin surface silt, with values in the range 0.20 to 0.22 for the 1978-90 period. In contrast, the Sellafield discharge values for the same period were generally greater than 0.3, reinforcing the argument that some degree of mixing had occurred before on-site deposition. The similarity of the $^{238}Pu/^{239+240}Pu$ values in sediment from different parts of the Irish Sea basin indicates that similar degrees of mixing have occurred in each case and this could indicate a common process, namely mixing of offshore sediment prior to deposition in coastal environments. The similarities between the sediment data for SC1, NCS862 and the Maryport cores provides a considerable degree of confidence in the sedimentation rates and chronologies derived from radionuclide concentration profiles, activity ratios and independent ^{210}Pb dating.

Fig 4.6 Sediment $^{238}Pu/^{239+240}Pu$ activity ratios for SC1 decay corrected to time of deposition plotted with the corresponding annual discharge activity ratios.

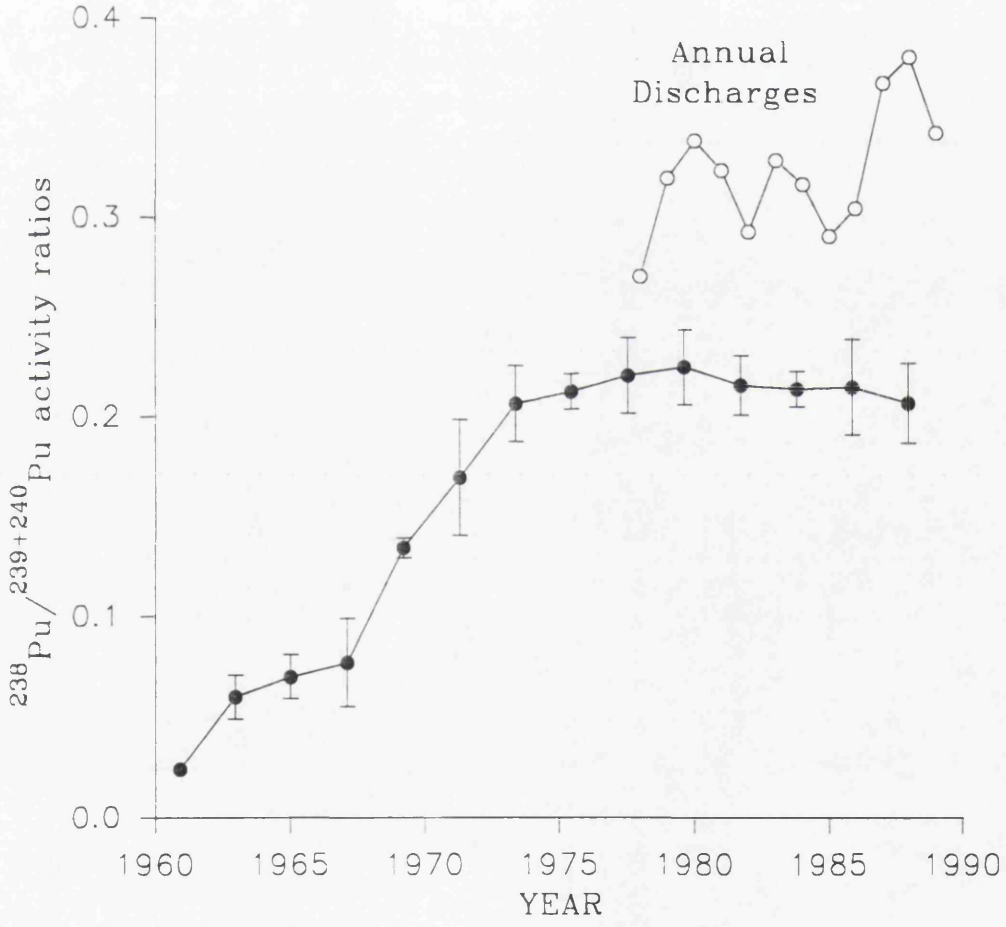

Fig 4.7 $^{238}Pu/^{239+240}Pu$ activity ratios (decay corrected to time of deposition) for sediment sections 1) SC1 and 2) NCS862 along with corresponding data for 3) Maryport Harbour cores (Kershaw *et al.*, 1990) surface sediment from 4) Newbiggin (Hetherington, 1975; Hunt,1985) and 5) the Sellafield discharge (BNFL, . 1977–1989).

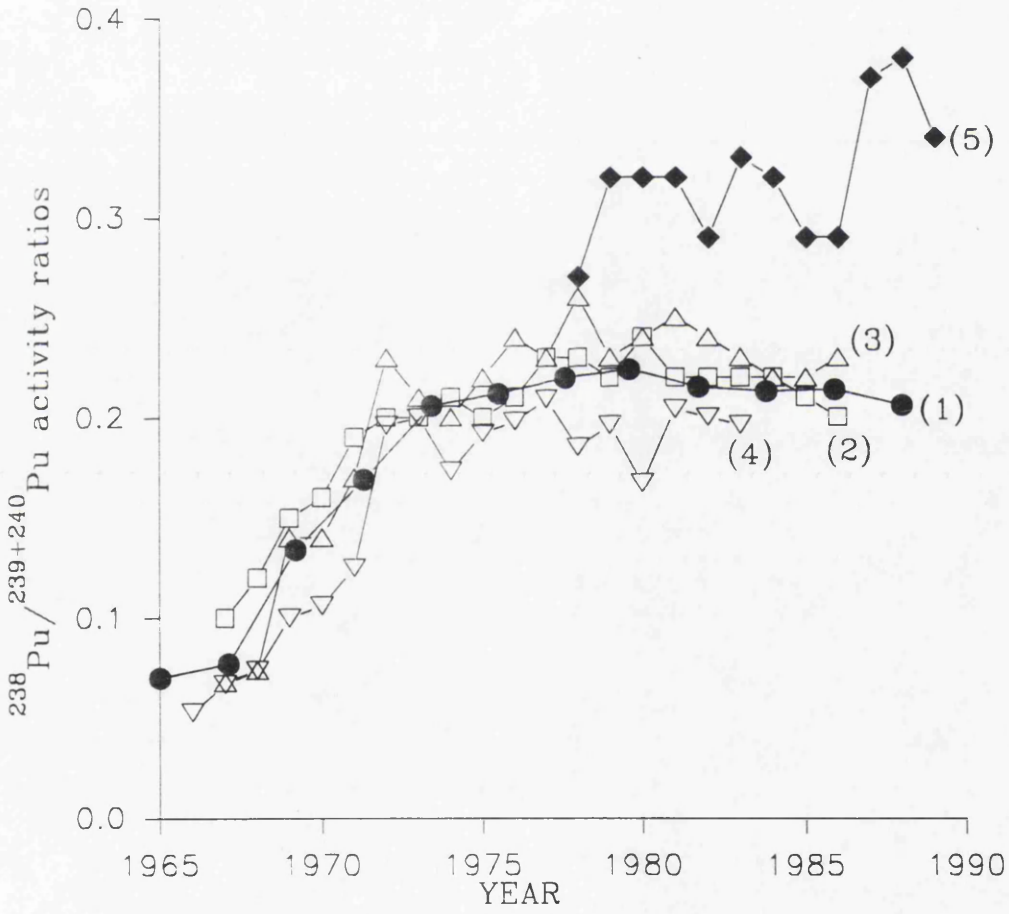

The $^{134}Cs/^{137}Cs$ activity ratio data for section SC1 (Fig 4.8) are generally in very close agreement with the corresponding annual discharge values, a situation which contrasts markedly with that for the $^{238}Pu/^{239+240}Pu$ isotope activity ratios and implies that no mixing is taking place prior to deposition. There are however two anomalous points in the plot, namely 1971 and 1973 which are higher than any observed $^{134}Cs/^{137}Cs$ ratio for the discharge, producing obvious anomalies which can be explained in two ways. Firstly the chronology used for decay correction of the $^{134}Cs/^{137}Cs$ activity ratios in the sediment profile, established from the 2.4 cm y^{-1} sedimentation rate, covers a 16 year period and probably represents a gross over simplification of the sediment history at this site. The chronology fails to account for variations in deposition which may have occurred during this period due to variations in environmental conditions. Secondly, the sedimentation rate adopted has a crucial effect on the decay corrected ratio profile which is generated. If the sedimentation rate is too low, the resultant chronology will overestimate the age of the sediment and the decay correction of the sediment activity ratios will be greater than required, moving the profile closer to or above the discharge profile. In contrast, if the sedimentation rate is too high, the age of the sediment will be underestimated, with the resultant decay corrected profiles being moved below the discharge data curve.

If the sediment chronology is adjusted to make the maximum sediment ratio value (1973) equal to the value for the corresponding year in the discharge activity ratio, the profile produced for the sediment section is below the annual discharge values as illustrated in Fig 4.9. The amended values are all below the annual discharge values except for 1971 and would support a particulate transportation mechanism as argued with the $^{238}Pu/^{239+240}Pu$ activity ratios above. However, the degree of correction required to manipulate the $^{134}Cs/^{137}Cs$ data to produce a similar profile to the $^{238}Pu/^{239+240}Pu$, where all the data points were below the corresponding annual discharge values undermines the validity of using this ratio for the purpose of determining the supply mechanism to this site. The $^{134}Cs/^{137}Cs$ activity ratio profile is too susceptible to distortion due to the problems encountered in applying a suitable sedimentation rate, which is exacerbated by the short half-life of ^{134}Cs and the inherent error on the ratio.

Fig 4.8 $^{134}Cs/^{137}Cs$ activity ratio for core SC1 decay corrected to time of deposition, plotted against the corresponding activity ratios for the Sellafield annual discharges.

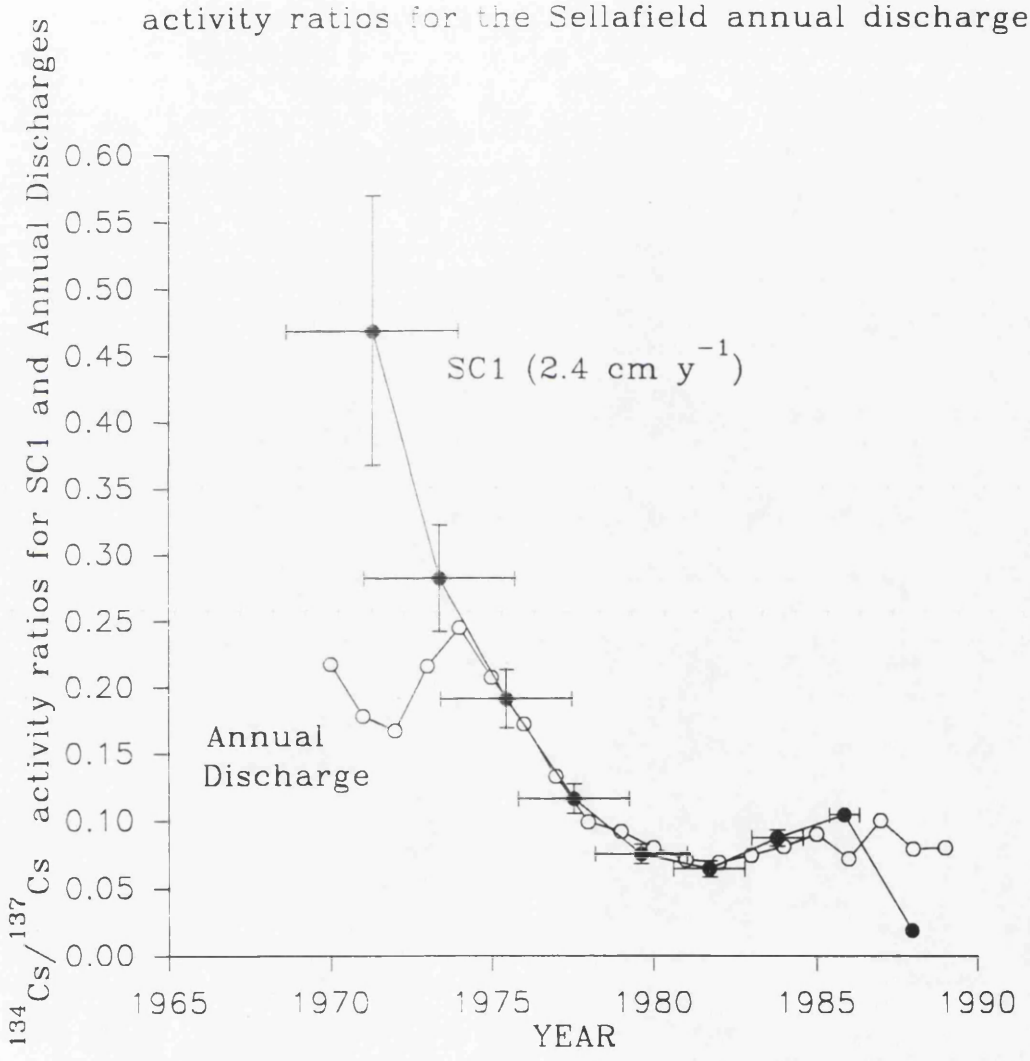

Fig 4.9 $^{134}Cs/^{137}Cs$ activity ratios for core SC1 decay corrected to time of deposition, with corresponding activity ratios in the annual discharge and an amended ratio for SC1 which brings the maximum sediment ratio value into agreement with the corresponding ratio value in the Sellafield discharge.

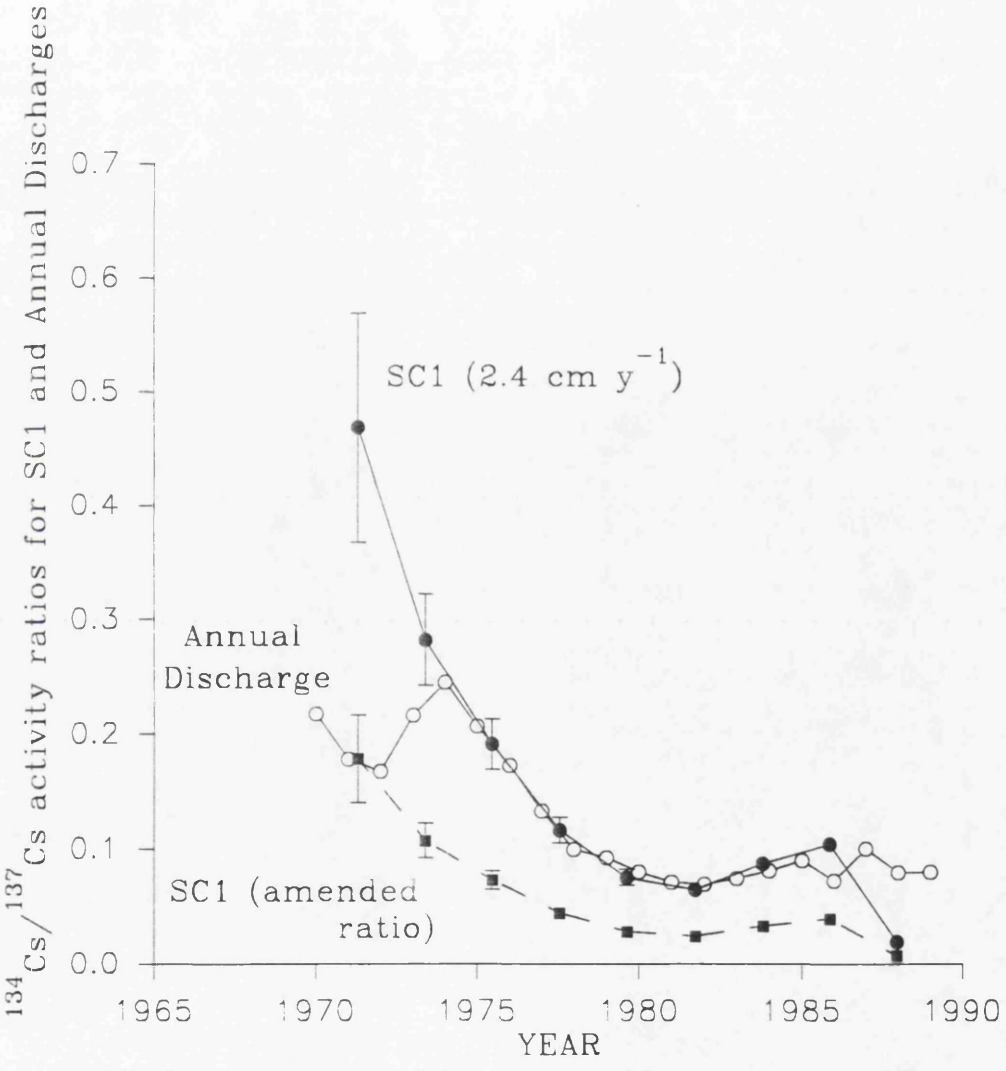

There is one interesting observation evident in both Fig 4.8 and Fig 4.9; the surface activity ratio values (0-5 cm, 1987 to 1988) are systematically below the ratios for corresponding annual discharges. The problems associated with applying sedimentation rates to produce a chronology are not so pronounced in this upper level and despite the adjustment illustrated in Fig 4.9, the sediment values are in very close agreement. The values for the surface layer of the sediment profile and the annual discharges cannot be reconciled and would suggest that these sediments have undergone some degree of pre-depositional mixing.

Despite the potential underestimation of the sedimentation rate within section SC1 it is apparent that the section exhibits a small but distinct response to deposition of Chernobyl fallout radiocaesium in May 1986. The $^{134}Cs/^{137}Cs$ activity ratio for the sediment, decay corrected to time of deposition and normalised to the integrated discharge from Sellafield is illustrated in Fig 4.10 and shows an enhanced value for 1986 (11.55) compared with the adjacent sediment values (4.75,5.12), this enhanced value corresponds to a depth of 5-10 cm.

4.1.2.2 Non-Isotopic Activity Ratio Profiles

The $^{241}Am/^{239+240}Pu$ and $^{137}Cs/^{241}Am$ activity ratios in the sediment can also potentially provide useful information on the mechanism of supply of Sellafield waste to these intertidal areas. Information on the discharge of $^{239+240}Pu$ and ^{241}Am from Sellafield is relatively complete and the $^{241}Am/^{239+240}Pu$ activity ratio in sediment profiles therefore presents considerable potential for investigation of the mechanism of radionuclide transport in this area. Differences in geochemical behaviour between $^{239+240}Pu$ and ^{241}Am clearly have to be considered but, to a first approximation, plutonium and americium can be taken to have similar properties in this system. Moreover, since ^{241}Am is produced *in-situ* in the sediment by decay of ^{241}Pu, the activity ratios observed in the sediment must be compared not only with the annual and time integrated discharges but also with the annual ^{241}Am discharge plus ingrowth of ^{241}Am from the corresponding annual discharge of ^{241}Pu, to allow for a situation involving solution transport and effectively identical environmental behaviour of americium and plutonium. Fig 4.11 shows the $^{241}Am/^{239+240}Pu$ activity ratios for section SC1 normalised to those of the discharge

Fig 4.10 $^{134}Cs/^{137}Cs$ activity ratios for core SC1 decay corrected to time of deposition and normalised to the integrated discharge ratio from Sellafield.

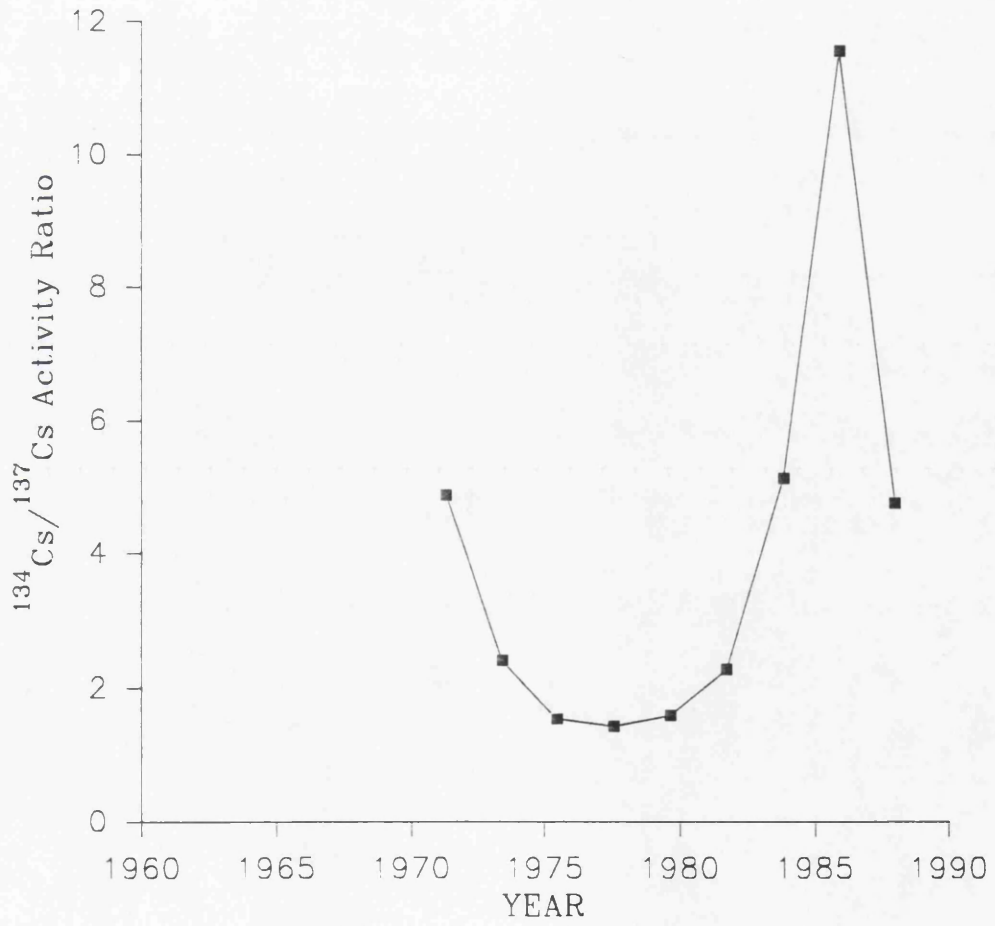

Fig 4.11 $^{241}Am/^{239+240}Pu$ activity ratio for core SC1 normalised to (1) annual discharge, (2) annual discharge plus in-situ ingrowth and (3) integrated discharge plus ingrowth.

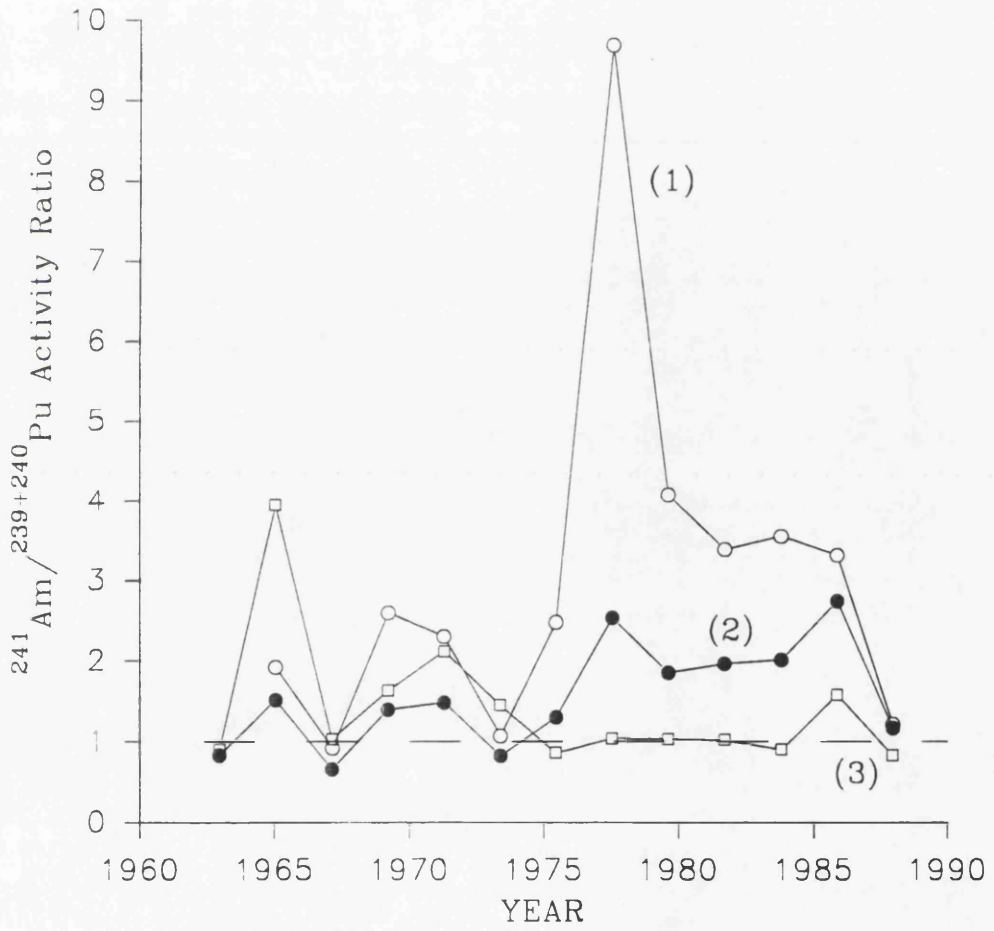

by dividing the sediment ratio by (1) the annual discharge ratio, (2) the annual discharge ratio plus ingrowth of ^{241}Am from ^{241}Pu, and (3) the time integrated discharge, allowing for ingrowth. The sediment $^{241}Am/^{239+240}Pu$ ratio does not bear a fixed relationship to either the annual discharge ratio or the annual discharge ratio compensated for ingrowth, but does approximate well to a constant fraction of the time integrated discharge ratio. Thus, the $^{241}Am/^{239+240}Pu$ ratio normalised to the annual discharge values exhibits a large and irregular distribution with a range of values from 1.07 to 9.68, while the ratio normalised to the annual discharge plus ^{241}Am ingrowth from ^{241}Pu decay exhibits smaller, but distinct, variations in the range 0.7 to 2.7. It is apparent from Fig 4.11 that there is no constant relationship between the sediment activity ratios and those of the annual discharge or annual discharge plus ingrowth, which indicates that the results are incompatible with a solution transport mechanism. In marked contrast, the sediment activity ratio normalised to the time integrated discharge ratio is virtually constant back to 1972, with a mean value of 1.08 $\pm$ 0.4, which is consistent with a particle transport mechanism to the site. As outlined in Section 1.4.2 above, both ^{241}Am and $^{239+240}Pu$ are particle reactive nuclides and are predominantly associated with the fine sediments within the Irish Sea. Particulate transport would entail mixing of various years deposits through physical processes and would therefore produce a ratio which would be lower than any single year's annual contribution. The ratio normalised to the integrated discharge exhibits slightly enhanced values (up to 2.1) in the early 1970's, suggesting that a time of two to three years may be required for complete mixing of americium and plutonium within the sediment which acts as the source of material being deposited at these locations. However, the near unity values observed for this normalised ratio since 1975 (1.07 $\pm$ 0.24) indicate that during this period there has been effectively complete homogenisation of past Sellafield discharges in the sediment before deposition and confirms that plutonium and americium exhibit very similar behaviour in this system. Enhanced values are observed in the ratio normalised to the time integrated discharge and annual discharge plus ingrowth values at a depth of 7.5 cm corresponding to deposition in 1985. This implies a higher concentration of ^{241}Am relative to $^{239+240}Pu$ in sediment deposited at this time. This appears to be an anomalous result and is probably a consequence of experimental error or sample heterogeneity with the 7.5 cm sample being the weighted mean of duplicate analyses (144.8 Bq kg^{-1} $\pm$ 3.4

and 186.9 Bq kg^{-1} ± 10).

Comparison of the $^{241}Am/^{239+240}Pu$ results from SC1 with other Irish Sea intertidal sediment cores provides compelling evidence to support a particle transport mechanism for radionuclide supply to these areas. For example, Fig 4.12a and Fig 4.12b represent the profiles generated from sediment core NCS862 (Ben-Shaban, 1989) and the Maryport cores (Kershaw *et al.*, 1990) respectively. Comparison of the data shows that in terms of the arguments advanced above, at all three sites the dominant supply mechanism is particulate transport. In each case an almost identical pattern is obtained in which the $^{241}Am/^{239+240}Pu$ ratio is effectively a constant fraction of the time integrated discharge ratio.

A significant consequence of the operation of a particle transport mechanism is that radionuclides in any particular discharge from Sellafield will, after mixing with older waste, be re-distributed in a continuous process over an extended time so it is not possible to define a unique value for transit time of radionuclides from the discharge point to any depositional sedimentary environment.

The $^{137}Cs/^{241}Am$ activity ratios may be treated similarly, bearing in mind the major differences in geochemical behaviour of caesium and americium. Fig 4.13 shows the decay corrected $^{137}Cs/^{241}Am$ activity ratios for section SC1 normalised to the Sellafield effluent ratio as described above for the $^{241}Am/^{239,240}Pu$ activity ratios. In this case, the activity ratio observed in the sediment at any given location would be expected to differ from that of the effluent by a factor determined by the relative K_D's of the nuclides but, by the arguments advanced above, solution transport should give sediment activity ratios which are a constant fraction of the annual effluent ratio, or the annual ratio compensated for ingrowth of ^{241}Am from ^{241}Pu. The major variations in the normalised activity ratios corresponding to these two cases in Fig 4.13 clearly indicate that the results are incompatible with a solution transport model. Particle transport would be expected to generate sediment $^{137}Cs/^{241}Am$ activity ratios which are a constant fraction of the time integrated Sellafield discharge and, as shown in Fig 4.13, the activity ratios normalised to time integrated discharge values (allowing for radioactive decay and ingrowth) do exhibit smaller variations than were observed by normalisation to the

Fig 4.12a $^{241}Am/^{239+240}Pu$ activity ratio for core NCS862 normalised to (1) annual discharge, (2) annual discharge plus in-situ ingrowth and (3) integrated discharge plus ingrowth.

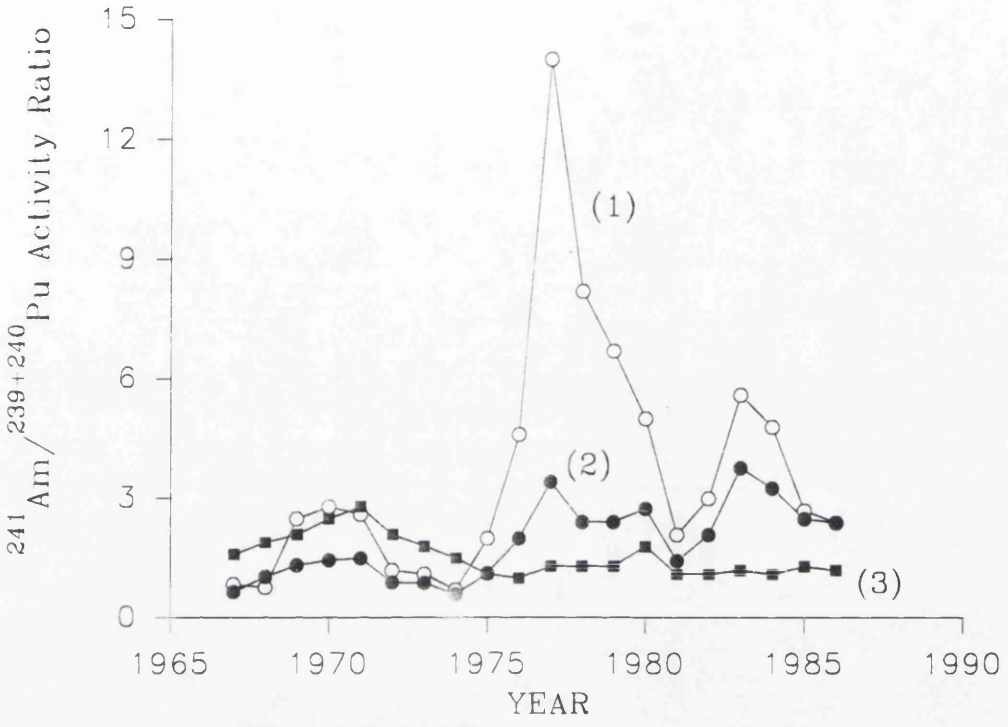

Fig 4.12b $^{241}Am/^{239+240}Pu$ activity ratio for the Maryport core normalised to (1) annual discharge, (2) annual discharge plus in-situ ingrowth and (3) integrated discharge plus ingrowth.

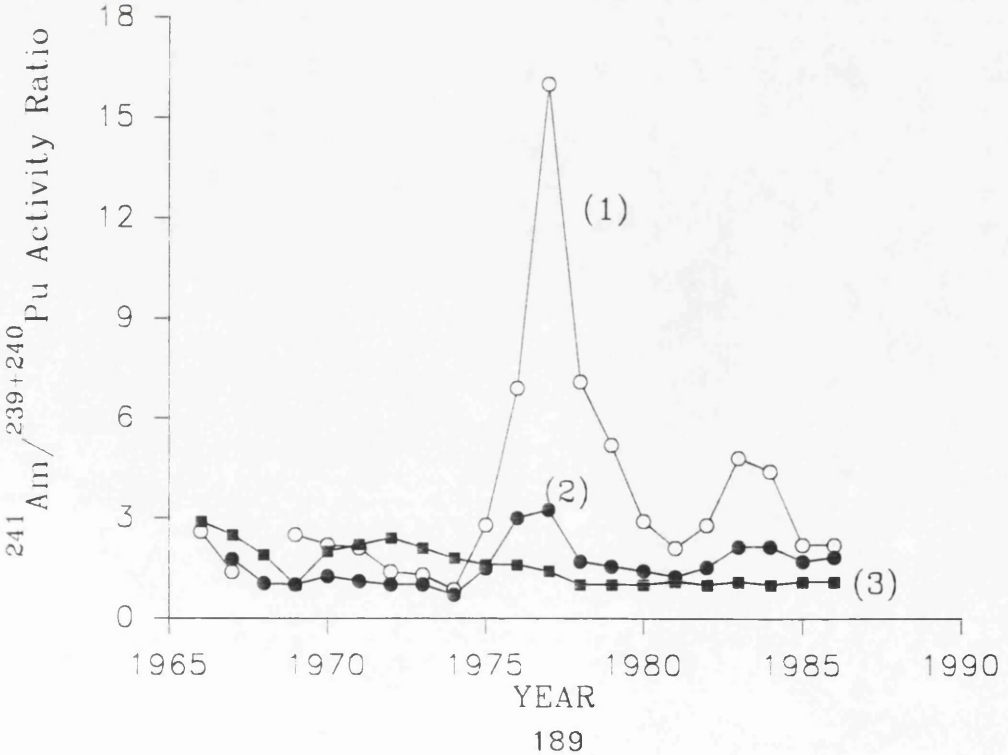

Fig 4.13 $^{137}Cs/^{241}Am$ activity ratio core SC1 normalised to (1) annual discharge, (2) annual discharge plus ingrowth and (3) integrated discharge plus ingrowth.

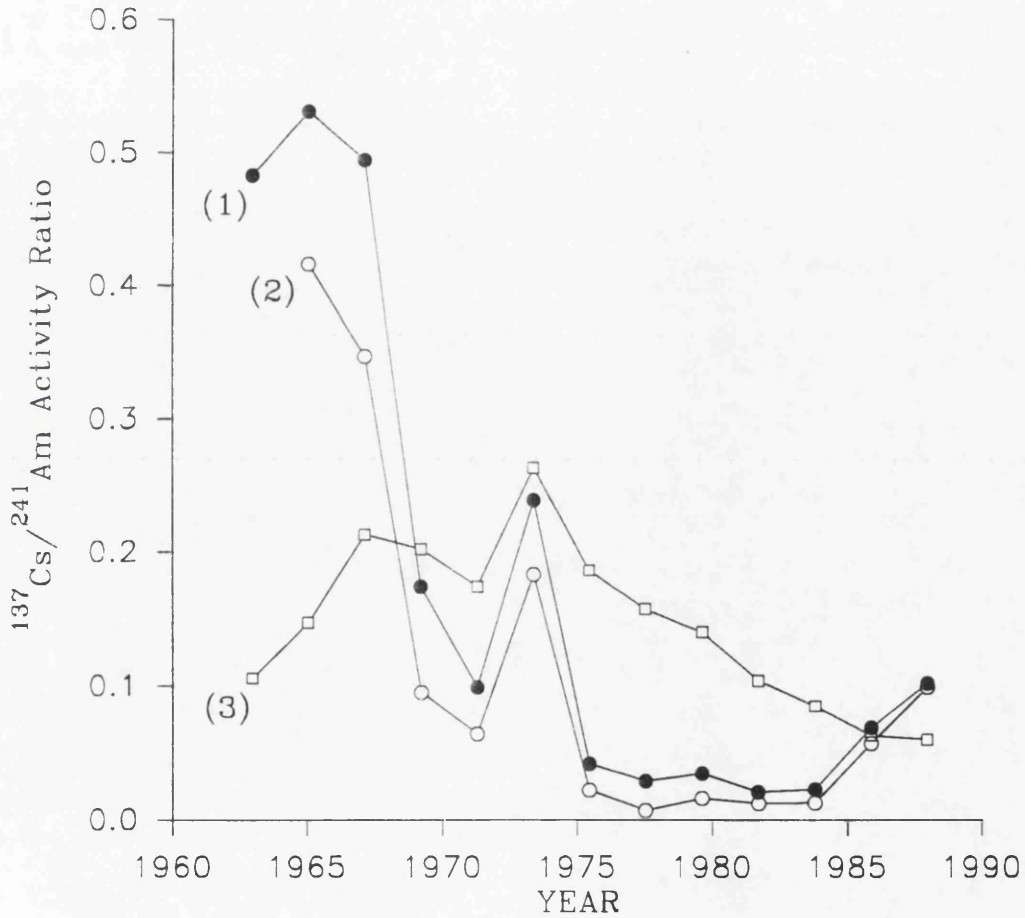

annual discharge ratios. The ratios normalised to the time integrated discharge do not, however, attain a constant value as was observed for the corresponding normalisation of the $^{241}Am/^{239+240}Pu$ activity ratios. The results post 1974 indicate a systematic decrease in the sediment $^{137}Cs/^{241}Am$ activity ratio relative to the time integrated discharge ratio, implying a loss of ^{137}Cs relative to ^{241}Am from the pool of sediment supplying these intertidal areas over this time period. The apparent loss of ^{137}Cs from the sediment can be estimated using the decline in the sediment activity ratio normalised to the integrated discharge and assuming that the concentration of ^{241}Am will be unaffected by re-dissolution. The ratio declines from 0.186 (1975) to 0.06 (1987) indicating a reduction of 68% in the ^{137}Cs concentrations relative to ^{241}Am concentrations since the mid 1970's. Similar reductions of 61% (1986) and 62% (1986) were observed for the decay corrected sediment ratios in the cores collected by Ben-Shaban (1989) and Kershaw (Kershaw *et al.*, 1990). This observed loss of ^{137}Cs is only applicable to sediment which has undergone resuspension and transport to these intertidal areas and cannot be extrapolated to the complete offshore sediment deposit. If it is assumed that the discharged ^{241}Am is totally retained in the Irish Sea sediments, then the decay corrected $^{137}Cs/^{241}Am$ activity ratio data for SC1 compared to the time integrated discharge values for the period around 1975 suggest a maximum retention in the sediment of about 19% of the discharged ^{137}Cs.

4.1.3 Modelling The Processes Affecting Radionuclide Supply

The particle transport mechanism of radionuclide supply from a mixed pool of contaminated sediment is compatible with the observed radionuclide activity ratios in the intertidal sediments. However, it cannot, on its own, account for the shapes of the sediment radionuclide profiles which contain distinct sub-surface maxima in layers deposited in the 1970's. In contrast, the time integrated environmental inventories of Sellafield ^{241}Am and $^{239+240}Pu$ have exhibited a continuous increase with time and the ^{137}Cs integrated inventory has only shown a small decrease in recent years when the output from the discharge has been less than the loss by radioactive decay. Thus, in addition to particle transport and radioactive decay, some other process (or processes) must be operating which has given rise to a decrease in radionuclide concentrations in sediment deposited in these locations

since the mid 1970's.

This effect could be due to re-dissolution of the radionuclides from the sediment, but observations by Hunt and Kershaw (1990) indicate that, for the actinides, any such effect would be small. A more likely cause of the observed decrease in concentrations is physical dispersion and dilution of the contaminated sediment as demonstrated by Hunt (1985) and there is additional evidence that such dispersion and dilution has occurred. Thus, in 1977/78 Pentreath *et al.,* (1984) observed that concentrations of Sellafield waste radionuclides in Irish Sea surface sediments decreased by over two orders of magnitude on moving away from the discharge point to the Solway coast of south west Scotland. In contrast, in 1987, McDonald *et al.,* (1990) found that corresponding variations in radionuclide concentrations in surface sediments of the same area were dominated by sediment composition rather than by distance from Sellafield and that silts exhibited effectively constant radionuclide concentrations over a distance of some 60 km. In addition to lateral dispersion of sediment, vertical mixing as described by Kershaw *et al.,*(1983, 1984) would also result in reduced radionuclide concentrations by downwards mixing of contaminated sediment and upwards mixing of uncontaminated material. The rate of reduction in concentrations due to re-dissolution or dilution/dispersion will depend upon the radionuclide concentration in the sediment and both processes should ideally follow first order kinetics.

Therefore, the major factors giving rise to temporal variations in pollutant radionuclide concentrations in the offshore sediment are, input from the Sellafield discharge, radioactive decay and ingrowth, dispersion/dilution and to a lesser extent, re-dissolution. All of these must be incorporated within any model of radionuclide supply to intertidal areas by re-distribution of contaminated sediment. Despite the apparent complexity of this system, it is possible to set up a simple model which is capable of explaining the general shapes of the observed profiles and predicting future trends in radionuclide concentrations in the sediment, by examining and interpreting the behaviour of the ratio of the radionuclide concentrations to the integrated discharges as a function of depth in the cores, and therefore of time. Thus, Fig 4.14 shows the plot of temporal variations in the natural logarithm of the sediment $^{239+240}Pu$ concentration normalised to the time

Fig 4.14 Natural log of sediment $^{239+240}$Pu concentrations for SC1, decay corrected to time of deposition, divided by the integrated $^{239+240}$Pu discharge from Sellafield.

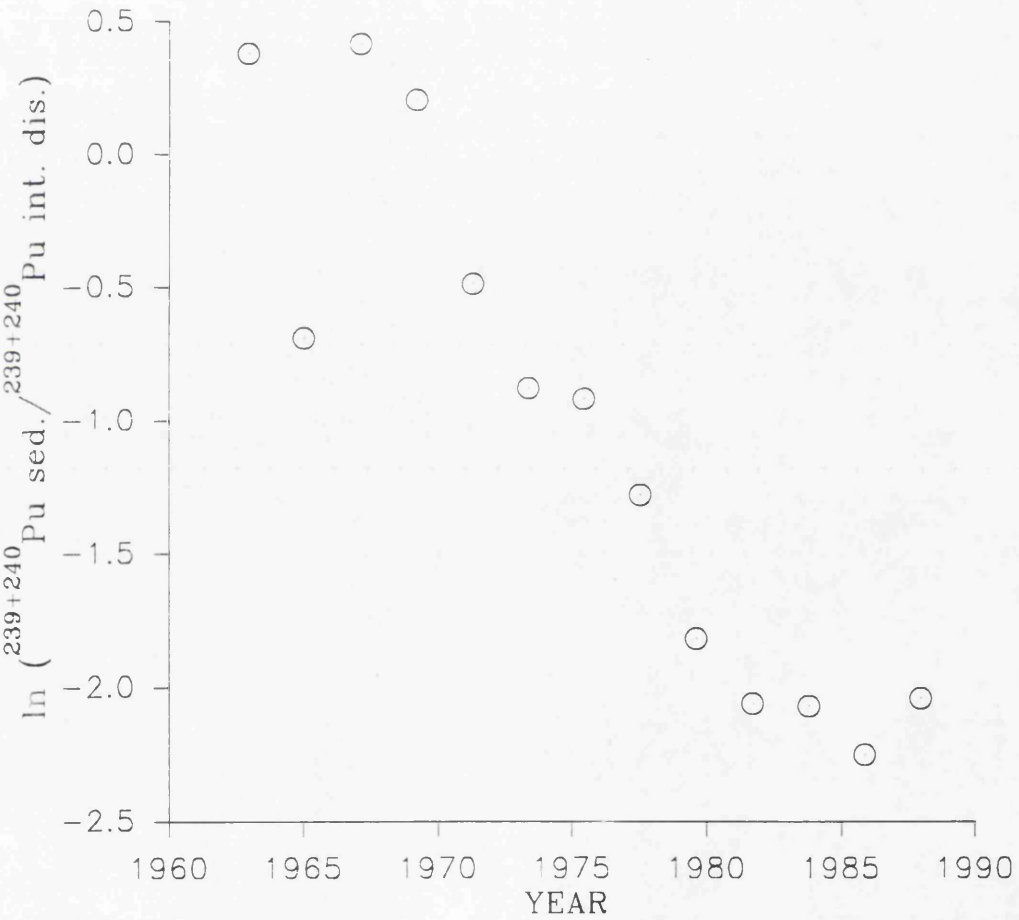

integrated discharge for section SC1. Fig 4.15 and Fig 4.16 show the corresponding plots for ^{241}Am, (allowing for radioactive decay and ingrowth) and ^{137}Cs respectively. In all the graphs there is clear evidence of an initial increase in concentration, which corresponds to the increasing annual discharges from Sellafield prior to 1975, followed by a decrease as a function of time in the sediment radionuclide concentrations relative to the time integrated discharge. The effects of these reductions in radionuclide concentrations are most pronounced after the major period of contamination in the early to mid 1970's, when for example ^{137}Cs losses from the sediments exceeded fresh inputs from Sellafield. The crucial observation, however, is that there is a high degree of linearity, particularly after 1975 within all the graphs. The linear sections of the plots may be accounted for in a simple way by assuming that, in the entire pool of contaminated sediment supplying the material being deposited (or in a notionally discrete volume of sediment within the pool), there is an input of radionuclides governed by the Sellafield discharge and a removal, or dilution, produced by some combination of the above mechanisms which can be described by first order kinetics. Transfer of a small portion of sediment from this pool to an accumulating intertidal deposit thus provides a record in the sediment profile of the temporal variations in sediment radionuclide concentrations produced by the operation of these competing processes. The chain of events determining the radionuclide concentrations in the depositing sediment is clearly complex, but the end result can nevertheless be interpreted according to the simple expression:

$$\frac{dC_t}{dt} = I_t - \Lambda C_t \qquad (4.1)$$

Where C_t is the radionuclide concentration in the depositing sediment at time t, I_t is an input term representing the annual discharge from Sellafield and Λ is a removal factor per unit time which is a constant comprising the sum of the contributions from radioactive decay, dispersion/dilution and re-dissolution, characterised respectively by constants λ_1, λ_2 and λ_3 such that:

$$\Lambda = \lambda_1 + \lambda_2 + \lambda_3$$

The relative importance of these terms will depend upon the radionuclide under

Fig 4.15 Natural log of sediment ^{241}Am concentration SC1, decay corrected to time of deposition, divided by integrated of ^{241}Am plus ingrowth from ^{241}Pu from Sellafield.

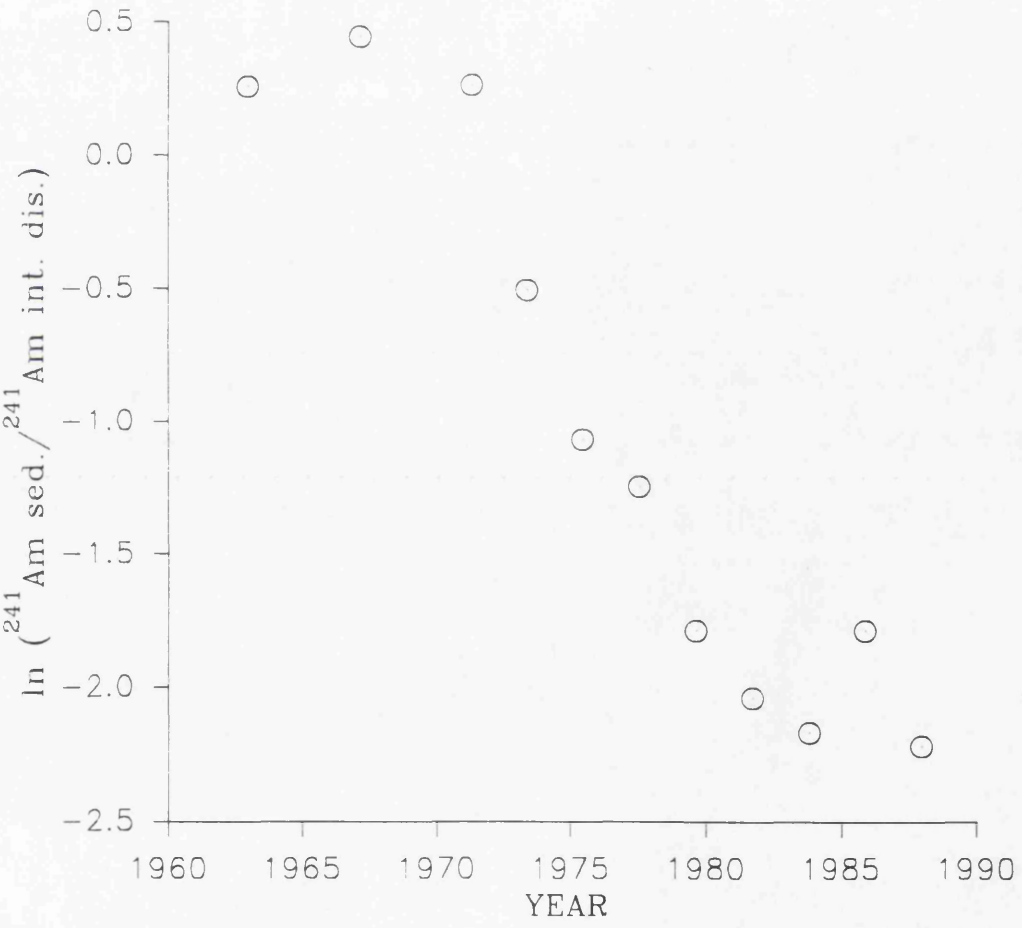

Fig 4.16 Natural log of sediment ^{137}Cs concentration SC1, decay corrected to time of deposition, divided by Integrated ^{137}Cs discharges from Sellafield.

consideration with, for example, decay and re-dissolution being much more important for ^{137}Cs than for ^{241}Am or $^{239+240}Pu$. If I_t falls to zero, as is now almost the case, since annual discharges have declined to such a level that they are a very small fraction of the total environmental inventories, then C_t will show an exponential decrease with time, as will the ratio of C_t to the integrated discharge, consistent with the linearity of the plots in Figs 4.14, 4.15 and 4.16.

Half value periods for reductions in the radionuclide concentrations may be extracted from the linear portions of the plots in Figs 4.14, 4.15 and 4.16. Linear regressions were performed on the points in the linear sections of the functions. The gradient can be substituted within the equation 4.2 to represent the sum of the λ values (Λ). The half period can be calculated using Equation 4.3 below

$$C_t = C_0 \, e^{-\Lambda T} \qquad \textbf{(4.2)}$$

$$Half\ value\ period = \frac{ln2}{\Lambda} \qquad \textbf{(4.3)}$$

The half periods for ^{241}Am and $^{239+240}Pu$, calculated from Figs 4.14 and 4.15 are 4.6 years and 5.3 years respectively, compared with 3.0 years for ^{137}Cs (Fig 4.16). These values show that the rate of reduction of the actinide concentrations, which will effectively result only from sediment dilution/dispersion, will be considerably slower than for ^{137}Cs which will experience re-dissolution as well as dispersion/dilution processes.

The effects of radioactive decay have been removed by normalisation of the sediment concentrations to the time integrated Sellafield discharge. The λ_3 value attributable to re-dissolution of ^{137}Cs can be derived by assuming that the λ_2 value (dispersion/dilution) is the same as that found for the actinides. The half period value minus the λ_2 value will determine the re-dissolution value λ_3 which translates into half value periods for re-dissolution in the range 7 to 9 years. The equation

$$\frac{dC_t}{dt} = I_t - \Lambda C_t \qquad \textbf{(4.4)}$$

as defined above, can be used to calculate the annual change in concentration year by year, using the values for the integrated discharge and the Λ values derived from the gradients of the linear portions of the plots from Fig 4.14, Fig 4.15 and Fig 4.16 to derive values for C_t as a function of time. The resultant plots generated from this calculation for dilution half value periods of 4 and 6 years are illustrated in Fig 4.17, Fig 4.18 and Fig 4.19 for $^{239+240}Pu$, ^{241}Am and ^{137}Cs respectively. The decay corrected total environmental inventories of the radionuclides are also shown to represent the case where no dilution has taken place. In each case, the shapes of the model curves provide a relatively close match with the observed shapes of the concentration profiles in the sediment. An important feature of the predicted concentration trends is that the maximum radionuclide concentrations in the sediment occur at a later date than the year of maximum discharge from Sellafield and this time difference varies between different radionuclides. This observation indicates why lag times had to be invoked in previous studies when attempts were made to match radionuclide concentration trends observed in Irish Sea intertidal sediment with those of the Sellafield discharge (Stanners and Aston, 1981,a,b: Aston and Stanners, 1982) and why these varied between different radionuclides. A further consequence of the temporal offset of the maximum sediment radionuclide concentrations from those of the maximum discharge is that the sedimentation rates calculated by relating the sub-surface maxima to the year of maximum discharge will be too low as has been discussed in Section 4.1.2.1. The sedimentation rate calculated from the ^{137}Cs profile increases from 2.7 cm y^{-1} to 3.1 cm y^{-1} when the 'lag time' is taken into account. Similar increases in sedimentation rates are observed for ^{241}Am (2.5 cm y^{-1} to 2.9 cm y^{-1}) and $^{239+240}Pu$ (2.03 cm y^{-1} to 2.3 cm y^{-1}). The model predictions for a 4 year dilution using the re-calculated mean sedimentation rate of 2.95 cm y^{-1} are illustrated in Fig 4.20, Fig 4.21, and Fig 4.22 for ^{137}Cs, ^{241}Am and $^{239+240}Pu$ respectively. The model profiles for ^{137}Cs, ^{241}Am and $^{239+240}Pu$ are in close agreement with the observed profile. However, any change in chronology will not make any substantial difference to the arguments outlined above. The magnitude of the discrepancies between isotope and radionuclide ratios within the sediment and the discharges cannot be resolved by changing the sedimentation rate. Corrections can be made when the maximum sediment isotope ratio is normalised to the corresponding annual discharge value as performed for the $^{134}Cs/^{137}Cs$ activity ratio (Fig 4.8). However, the requirement

Fig 4.17 Model curves for temporal variations in relative $^{239+240}Pu$ concentrations in Irish Sea sediments.

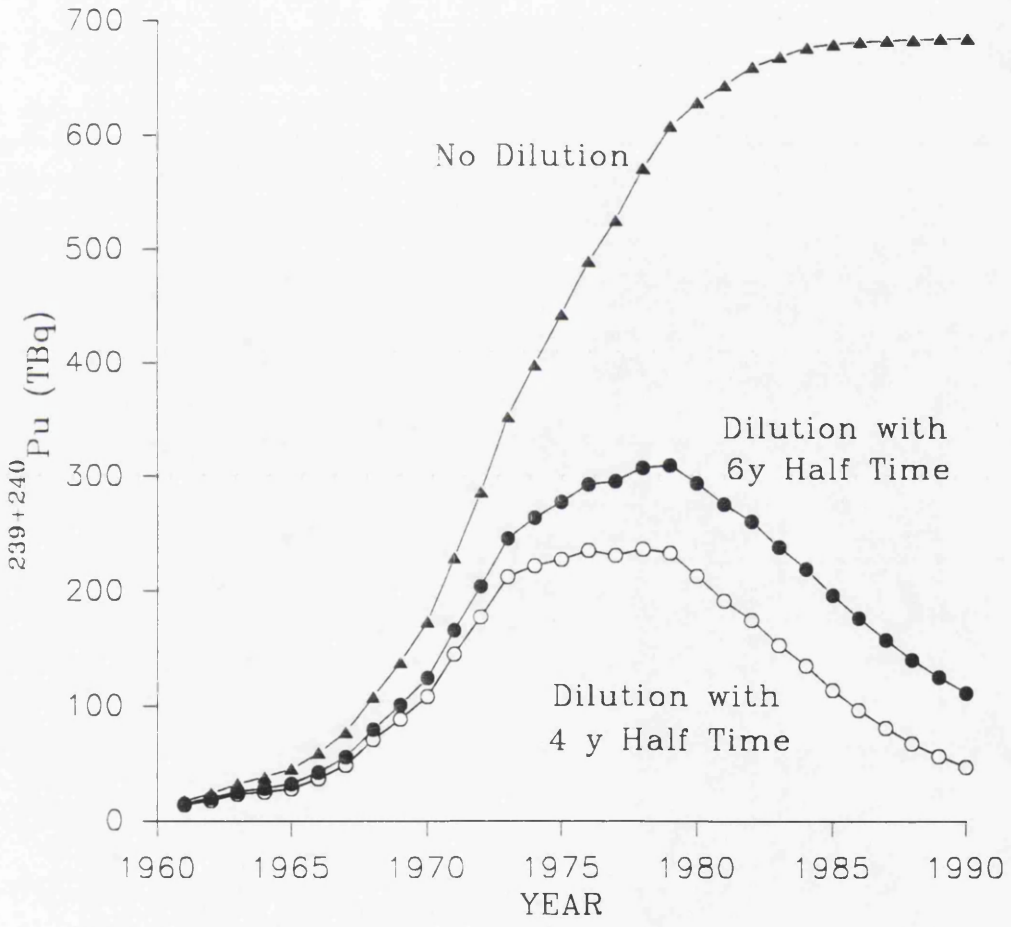

Fig 4.18 Model curves for temporal variations in relative concentrations of ^{241}Am in Irish Sea sediment.

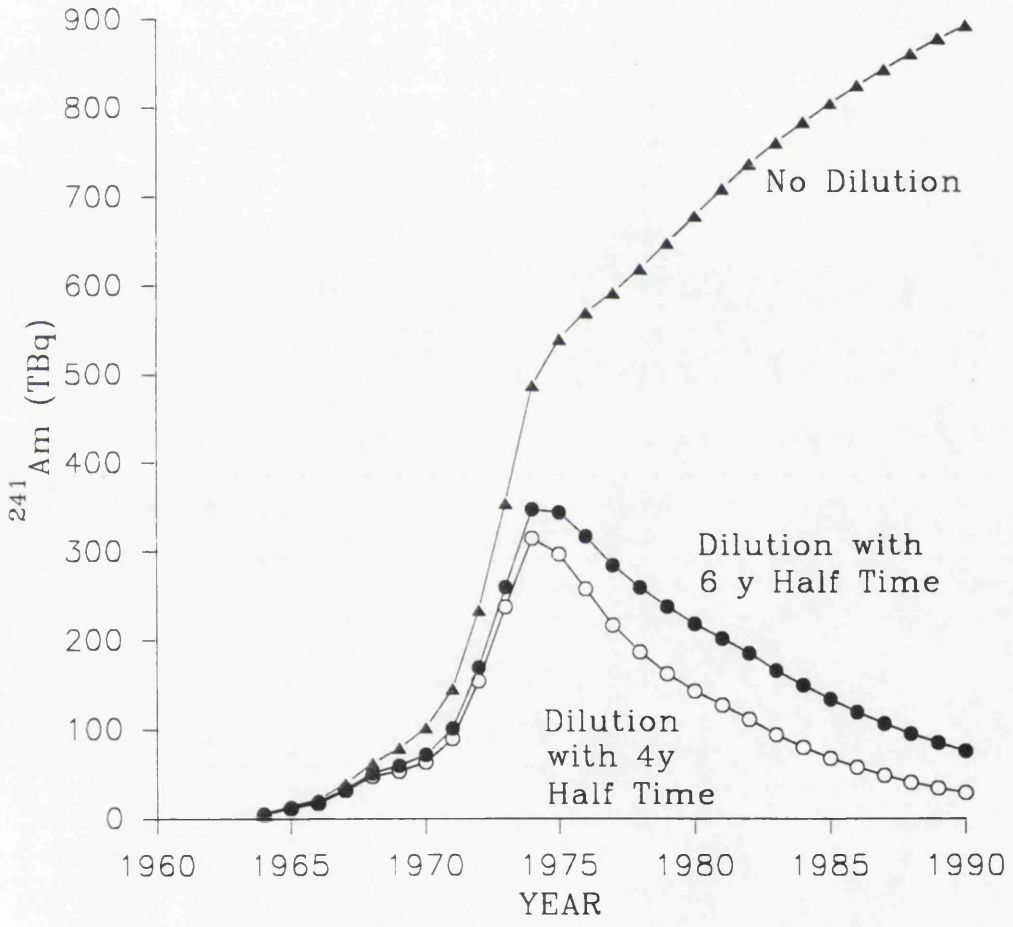

Fig 4.19 Model curves for temporal variations in relative concentrations of ^{137}Cs in Irish Sea sediment.

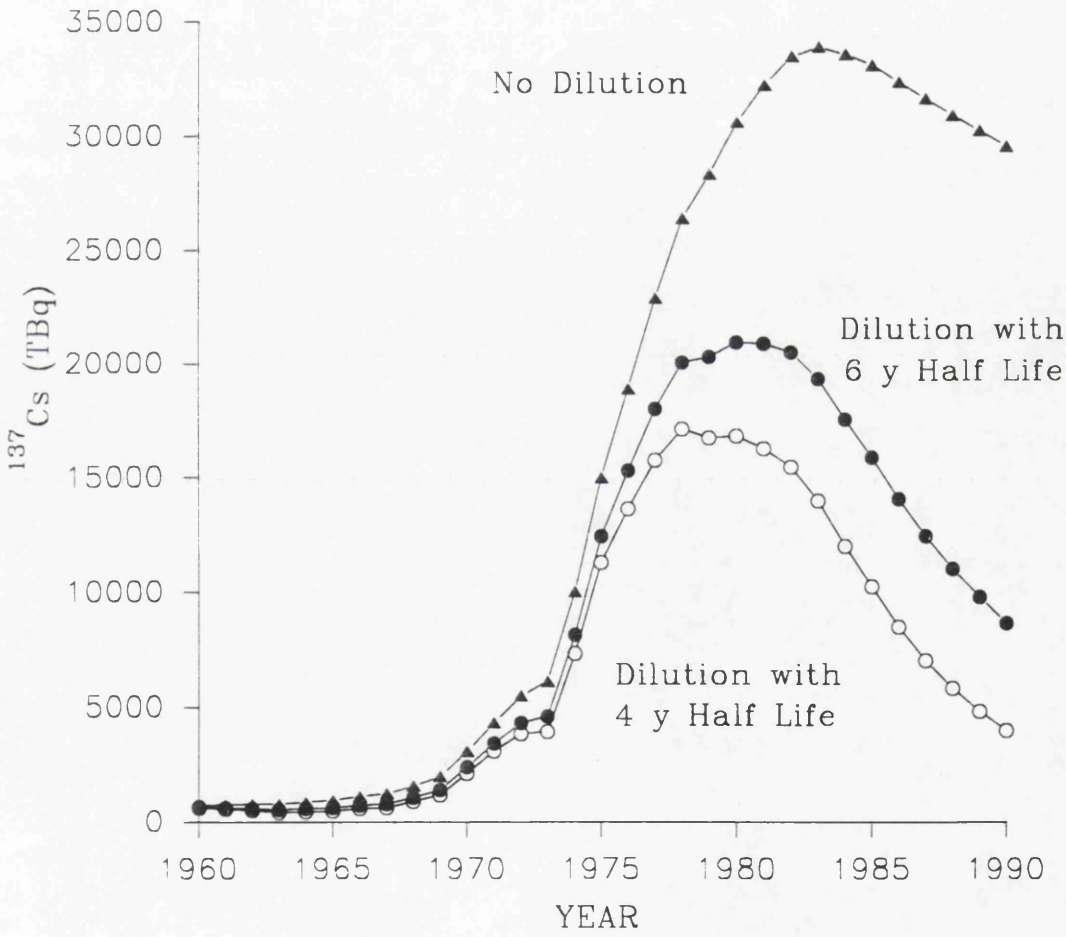

Fig 4.20 Model prediction for ^{137}Cs using re-calculated sedimentation rate 2.95cm y^{-1}, data normalised to 1977 ratio between sediment and model curve.

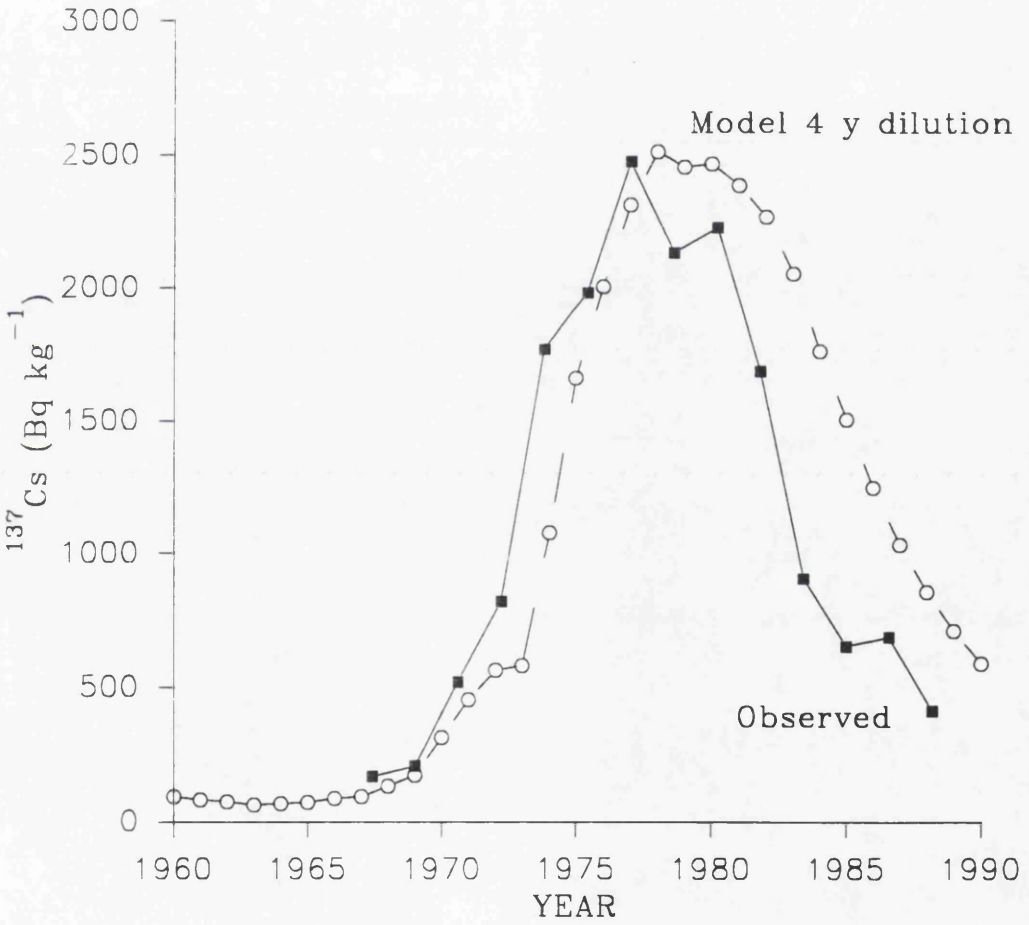

Fig 4.21 Model prediction for ^{241}Am using the re-calculated sedimentation rate 2.95 cm y^{-1}, peak in model curve (1976) normalised to peak in sediment concentration (1974).

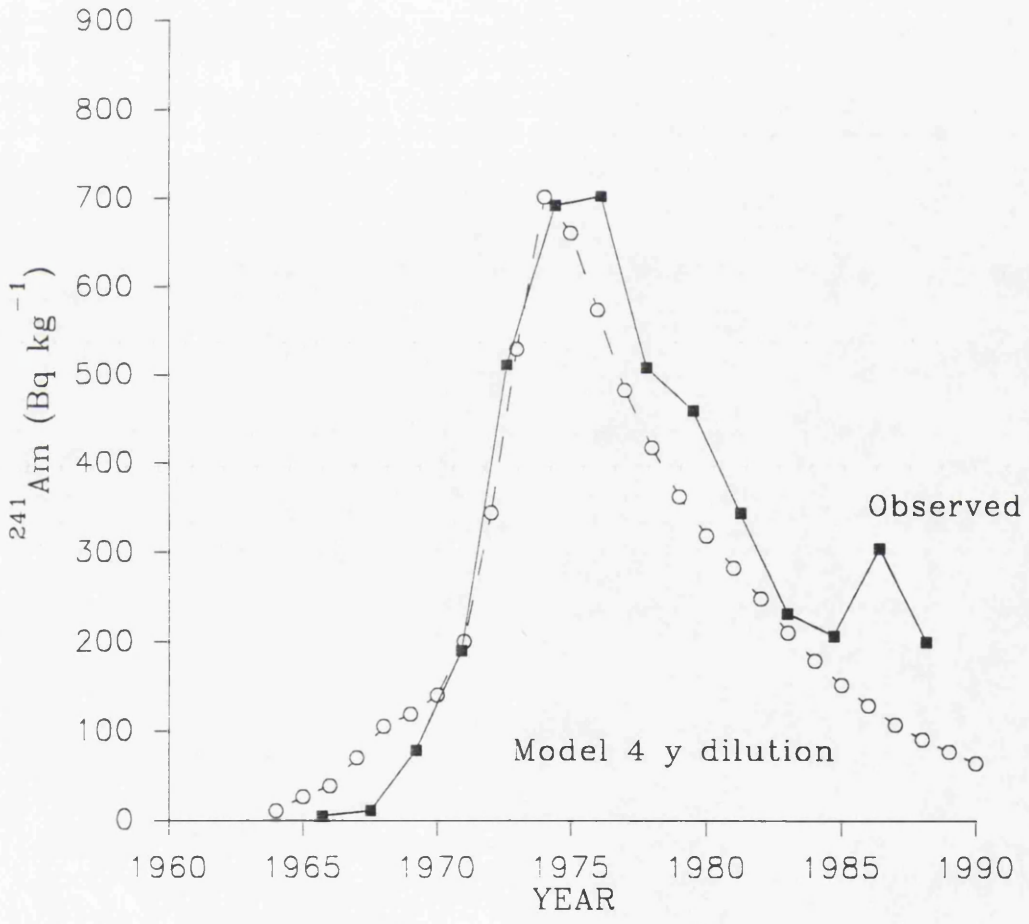

Fig 4.22 Model prediction for $^{239+240}Pu$ using re-calculated sedimentation rate of 2.95 cm y^{-1}, peak in model curve (1978) normalised to peak in sediment curve (1978).

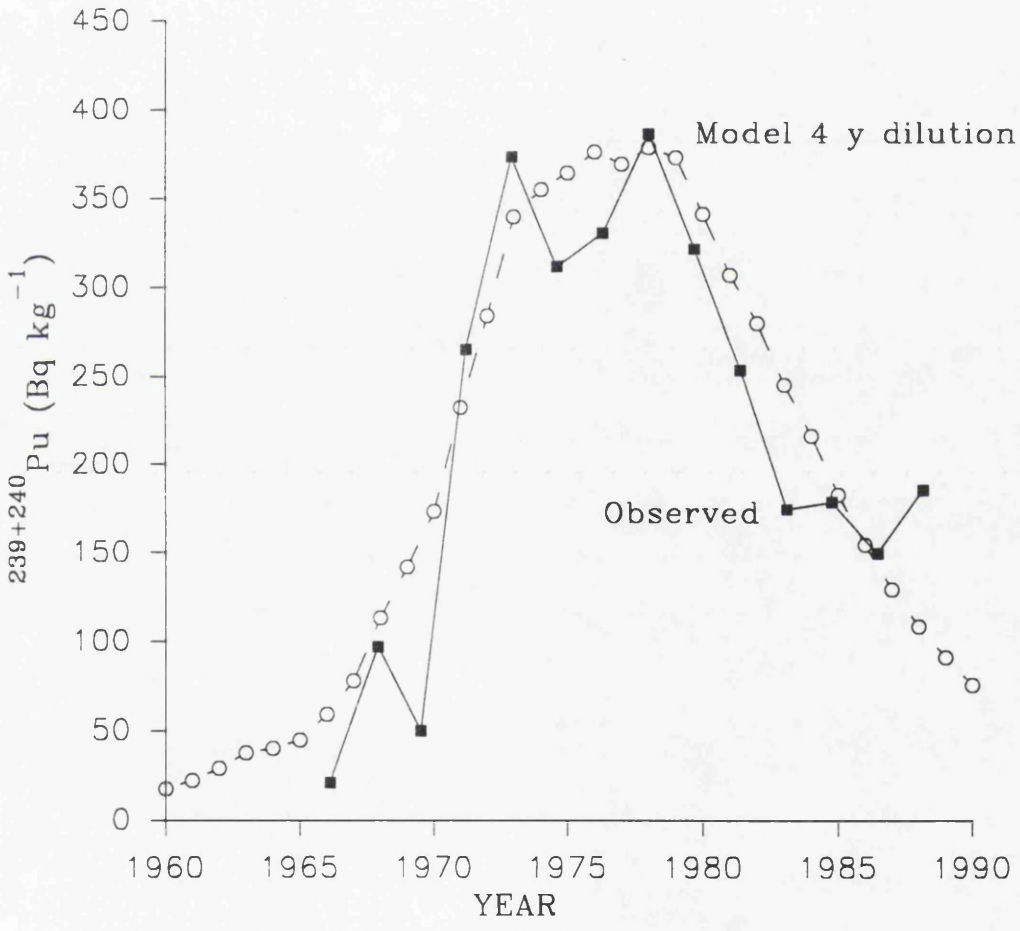

to perform such a correction illustrates the extent of the disparity between the sediment activity ratios and the Sellafield discharges.

In summary, the main observation is that the dominant mechanism for supply of radionuclides to the saltmarsh deposits at Southwick Water involves transport by movement of contaminated particulate material.

The sediment sections exhibit a historical record of the integrated discharges from Sellafield and the radionuclides are transported to the site in a continuous process with maximum radionuclide concentrations in the sediments occurring several years after the maximum discharge from Sellafield. Different temporal displacements of the maxima for individual radionuclides are observed due to the effects of dilution/dispersion, which can account for the apparently variable lag times observed between the release of radionuclides from Sellafield and their deposition. Despite the complexity of the processes operating within the marine environment of the Irish sea the system can be easily modelled using the terms outlined in the equation below

$$\frac{dC_t}{dt} = I_t - \Lambda C_t \qquad (4.5)$$

4.2 LATERAL DISTRIBUTION OF RADIONUCLIDES ACROSS MERSE DEPOSITS

The arguments presented in Section 4.1 establish that the mechanism of Sellafield waste radionuclide supply to the Solway Firth merse deposits is by on-shore transport of contaminated sediment and that this mechanism is likely to operate for the foreseeable future. This means that, even with reduced levels of radionuclide discharges from Sellafield, there will be a chronic radionuclide contamination of these areas and it is consequently of considerable importance to evaluate the magnitude of the contamination and the geochemical behaviour of the radionuclides in this environment. The following section describes an investigation of radionuclide concentrations and inventories in a series of lateral transects across

merse areas, with the aims of establishing radionuclide distributions at individual locations and deriving total inventories for the Solway merse areas. The sampling and analytical methods employed are described in Chapter 2.

4.2.1 Creetown

The sampling location for the Creetown transect is illustrated in Plate 2.5. This open, coastal merse exhibits a low elevation with the stepped edge at the MHWM being less than 0.5 m in height. Radionuclide concentrations for the 0-15 cm and 15-30 cm depth intervals from the Creetown transect T1 are reported in Tables 3.4 and 3.5 respectively and illustrated in Figs 4.23 and 4.25 respectively.

The concentration trends in ^{137}Cs, ^{134}Cs, ^{241}Am, ^{238}Pu and $^{239+240}Pu$ are very similar, with values declining in each case from the intertidal sediments to a distinct minimum below the MHWM (0 m), before increasing again with distance inland across the consolidated merse.

The concentration of ^{137}Cs (Fig 4.23a) in the 0-15 cm depth interval declined from 714 Bq kg^{-1} at 100 m out from the stepped bank of the merse (MHWM), to 74 Bq kg^{-1} on approaching the bank. The concentration then increased inland, reaching 1,680 Bq kg^{-1} at 100 m across the merse. A similar pattern was observed for ^{241}Am (Fig 4.23c) and $^{239+240}Pu$ concentrations (Fig 4.23d) with maximum concentrations recorded 100 m inland from the MHWM (0 m). The trends in the ^{134}Cs concentrations (Fig 4.23b) conform to the trends observed in the ^{137}Cs, ^{241}Am and $^{239+240}Pu$ transects although some of the points within the intertidal zone are below the detection limit (0.6 Bq kg^{-1}).

The radionuclide and isotope activity ratios for the 0-15 cm depth intervals in transect T1 are illustrated in Fig 4.24. The $^{134}Cs/^{137}Cs$ activity ratio (Fig 4.24a) shows a gradual decline from 0.014 at 0 m to 0.008 at 100 m inland. The values from the intertidal section are below the detection limit for ^{134}Cs except the point at -100 m which produces an activity ratio of 0.003. The general trend is one of declining values inland, with the observed range being well below the decay corrected Chernobyl fallout value of 0.14 (McDonald *et al.,* 1992) but above the

Fig 4.23 Radionuclide concentrations for the 0–15 cm samples from Creetown transect T1 collected 28/8/90.

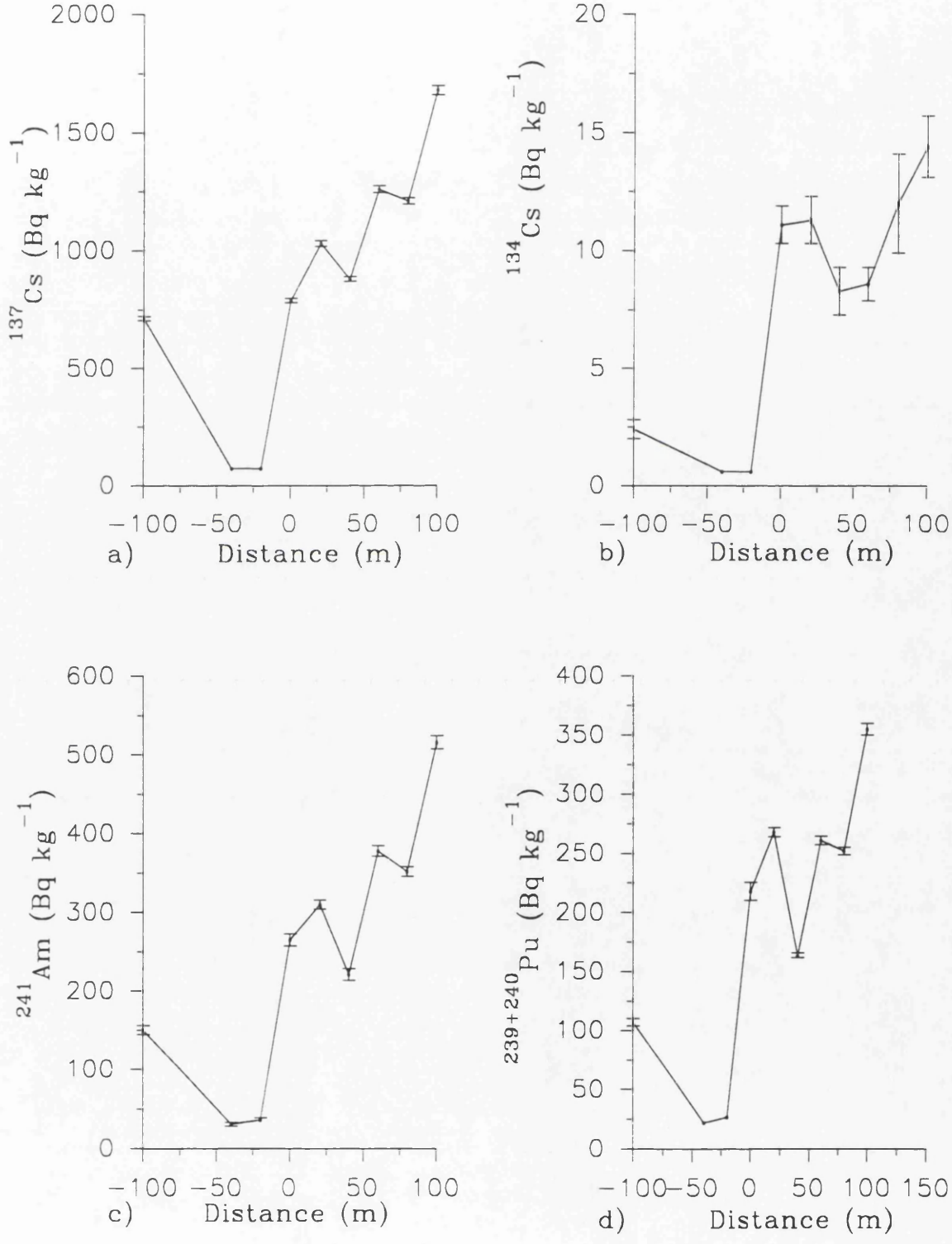

Fig 4.24 Radionuclide and Isotope activity ratios for 0–15 cm samples from Creetown transect T1.

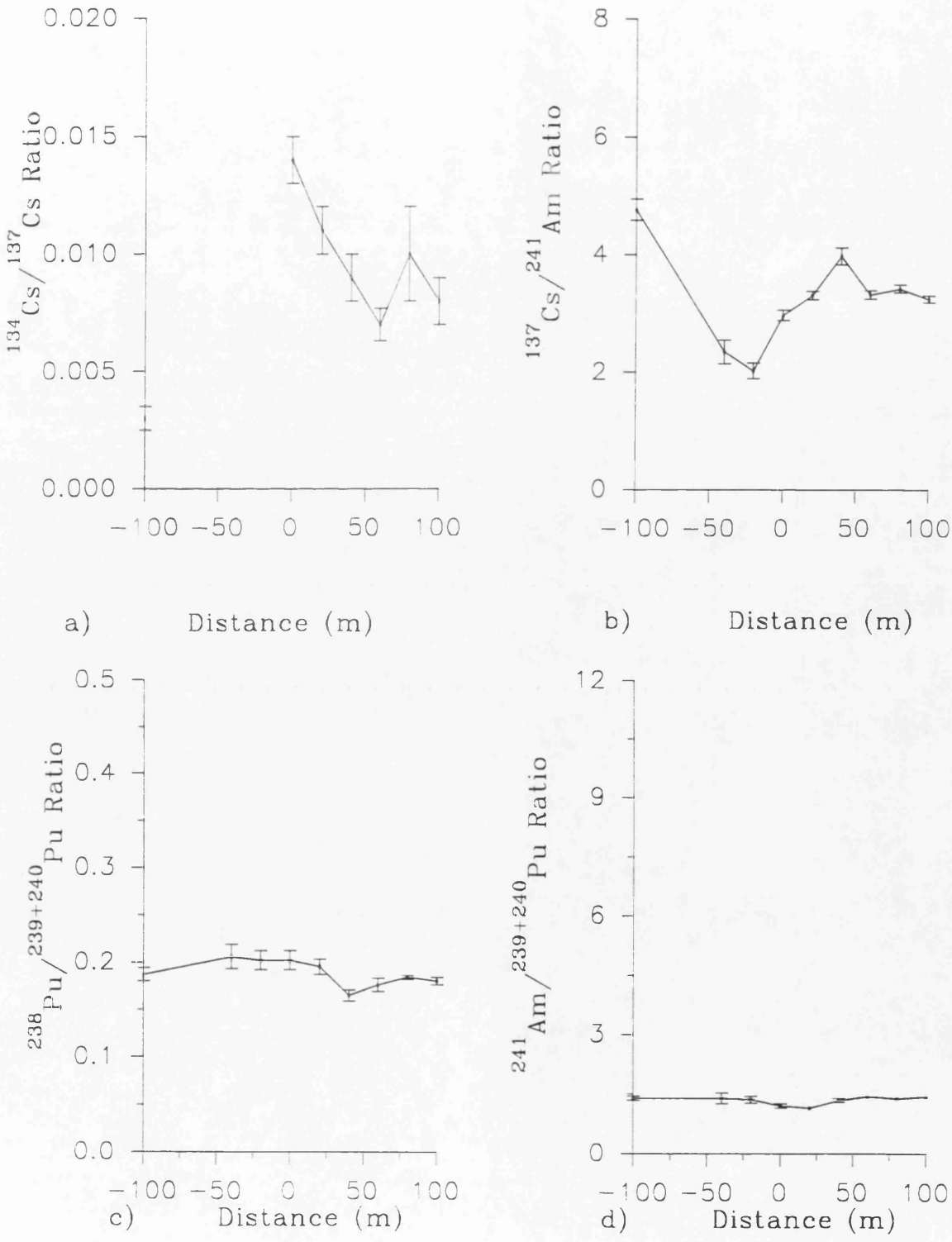

Fig 4.25 Radionuclide concentrations for 15–30 cm samples from Creetown transect T1, collected 28/8/90.

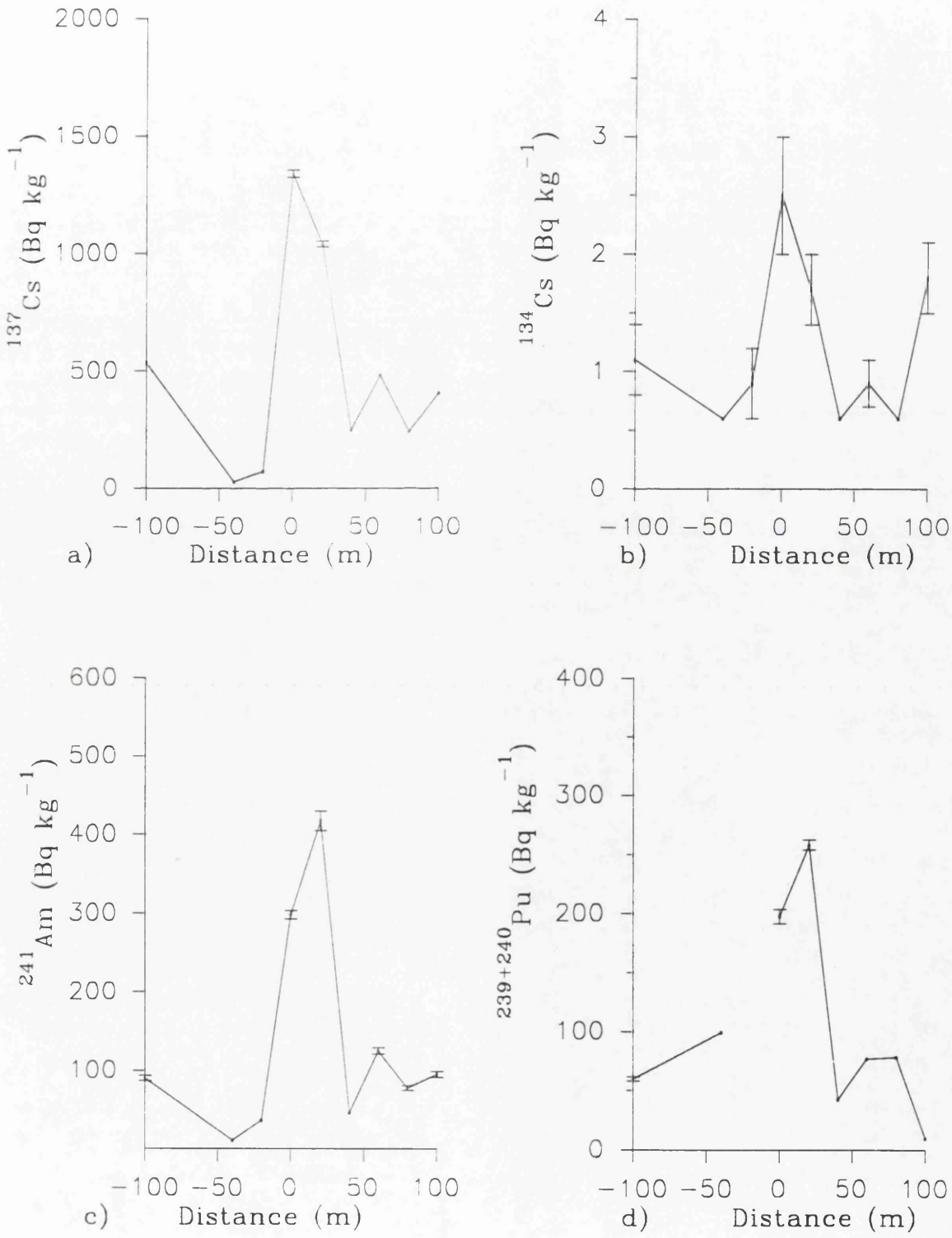

Sellafield integrated value for 1990 of 0.0028.

There are two possible explanations for the decline of the $^{134}Cs/^{137}Cs$ activity ratio inland. Firstly the decline may reflect the presence of older radiocaesium deposited further inland or secondly it could reflect the decreasing influence of Sellafield radiocaesium and an increasing contribution from weapons testing fallout. The first scenario is more likely given that the deposition of radionuclides from Sellafield has occurred over a 40 year period and is controlled by physical processes; as the saltmarsh develops and increases in elevation the frequency and extent of tidal inundation is reduced and therefore deposition of contaminated sediment would be gradually restricted to the seaward side of the floodplain. The increasing elevation would leave previously contaminated areas largely unaffected by tidal inundation except for the highest flood tides. Therefore, radiocaesium deposited at inland locations (100 m plus) would be considerably older and have a correspondingly lower ^{134}Cs content due to radioactive decay, than more recently deposited concentrations observed close to the MHWM. The second possibility of a declining Sellafield influence with a corresponding increase in weapons testing fallout seems less plausible. Cawse and Horrill (1986) estimated that the average ^{137}Cs inventory for UK latitudes was 3,700 Bq m^{-2} in 1977 which is decay corrected to 2,700 Bq m^{-2} (1990). Baxter *et al.*,(1989) reported decay corrected inventories of 2,000 - 7,000 Bq m^{-2} of ^{137}Cs for soils in south west Scotland. These values and the absence of ^{134}Cs data from the fallout suggests that any contribution to the $^{134}Cs/^{137}Cs$ activity ratio would be small compared with the contribution from Sellafield. The decline in the $^{134}Cs/^{137}Cs$ activity ratio with distance inland cannot be attributable to Chernobyl fallout as this would increase the activity ratio. In addition, the activity ratios present in the transect do not exhibit any similarity to the Chernobyl ratio of approximately 0.14. In addition the $^{137}Cs/^{241}Am$ (Fig 4.24b) does not show enhanced values which would be the case if Chernobyl radiocaesium were present. Any Chernobyl fallout deposited at this location would appear to have been removed by tidal inundation. This implies that the Chernobyl radiocaesium was not strongly retained within any soil component.

The $^{241}Am/^{239+240}Pu$ activity ratio (Fig 4.24d) and the $^{238}Pu/^{239+240}Pu$ activity ratio (Fig 4.24c) are virtually constant throughout the whole transect with values of 1.4

and 0.2 respectively. Taken together these observations are consistent with the arguments set out in Section 4.1 advocating a particulate transport mechanism for the supply of radionuclides to the coast of south west Scotland. The integrated Sellafield discharges (decay corrected cumulative discharges) produce an almost constant $^{241}Am/^{239+240}Pu$ activity ratio of ~ 1 during the 1970's and show a gradual increase to 1.325 by 1990. The observed trends in the sediment samples compare favourably with the almost constant trends in the Sellafield integrated discharge.

The radionuclide concentrations for the 15-30 cm depth interval samples are illustrated in Fig 4.25 and all four profiles are similar and differ markedly from the 0-15 cm profiles. The transect generally exhibits very similar trends, with declining concentrations from 100 m out in the intertidal sediments, to pronounced minimum in the intertidal sediments close to the MHWM and with concentrations increasing for up to 20 m inland before declining dramatically at approximately 40 m from the bank (MHWM). The most notable features of the 15-30 cm depth interval data are the minima at the same position as observed for the 0-15 cm samples and the pronounced peaks in concentrations up to 20 m inland. The radionuclide and isotope activity ratios for the 15-30 cm depth intervals are illustrated in Fig 4.26. The $^{134}Cs/^{137}Cs$ activity ratio (Fig 4.26a) shows a decline from 0.012 (-20 m) to 0.002 inland, again suggesting the presence of older radiocaesium at depth further inland. The $^{137}Cs/^{241}Am$ activity ratio exhibits a greater degree of variation than the corresponding ratios in the 0-15 cm depth intervals, however the values only range between 2 and 5.9.

The $^{241}Am/^{239+240}Pu$ activity ratios for the 15-30 cm depth interval (Fig 4.26c) are virtually constant, except for the pronounced increase at 100 m (9.6) which implies a dominance of ^{241}Am over $^{239+240}Pu$ at this site. The $^{238}Pu/^{239+240}Pu$ activity ratio declines from 0.19 to 0.09 (100 m) with distance and suggests the presence of older Sellafield waste on moving inland. Information on the ^{238}Pu and $^{239+240}Pu$ discharges from Sellafield prior to 1979 is not readily available. However, information on the $^{238}Pu/^{239+240}Pu$ activity ratio has been extrapolated from Hetherington *et al.*, (1976) who analyzed surface scrapings of intertidal sediments

Fig 4.26 Radionuclide and Isotope activity ratios for 15–30 cm samples from Creetown transect T1.

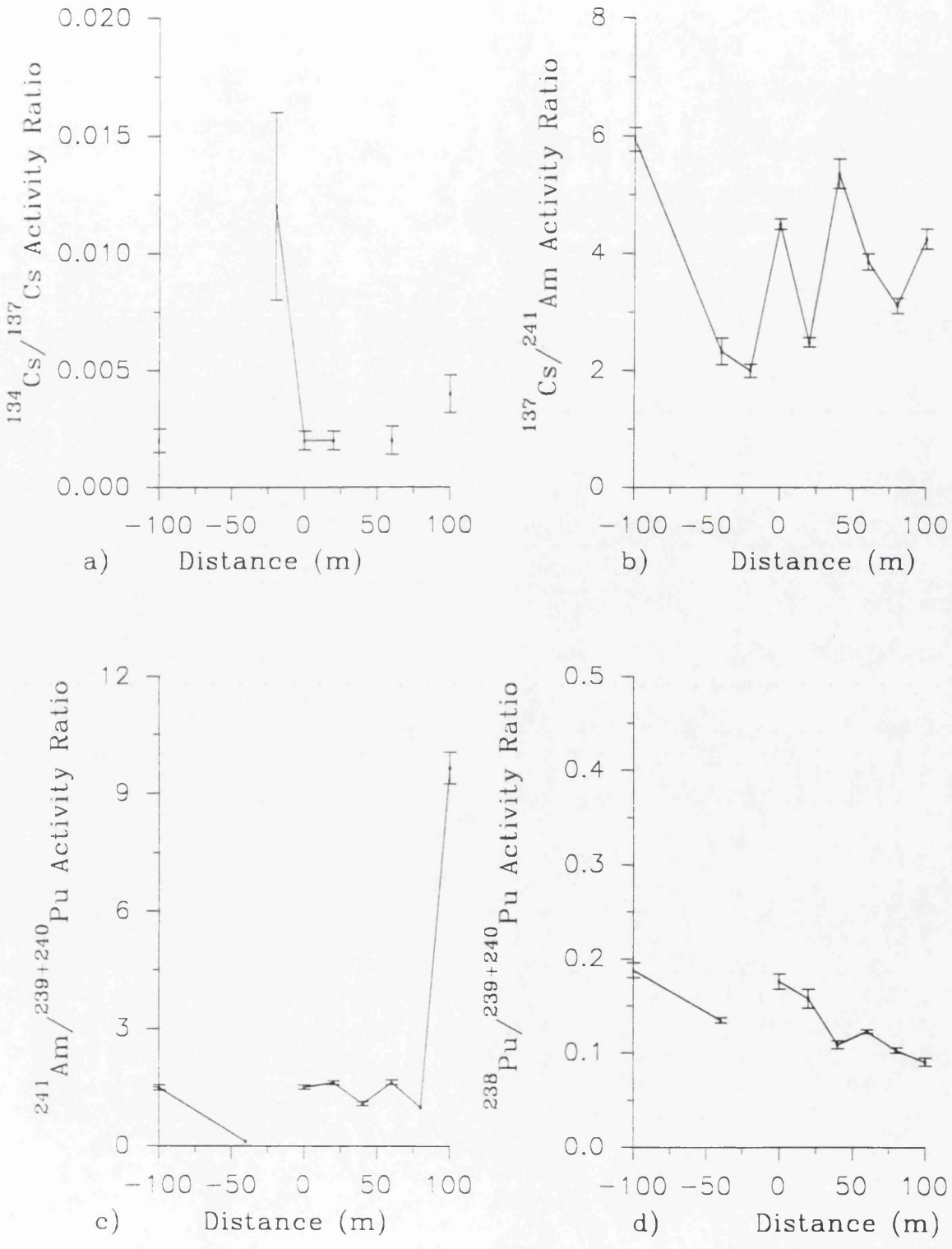

from the River Esk estuary between 1966 and 1975. Hetherington's data is reproduced in Fig 4.7 and exhibits an activity ratio for 1966 of 0.053 supporting the suggestion that early Sellafield discharges exhibited low $^{238}Pu/^{239+240}Pu$ activity ratios.

If the radionuclide concentration profiles for the 0-15 cm and 15-30 cm depth intervals are superimposed, as illustrated in Fig 4.27 for ^{137}Cs, it is evident that there is a sub-surface maximum at a distance of up to 20 m inland across the merse. The figure also shows the total ^{137}Cs concentrations in the 0-30 cm depth interval which exhibit a pronounced peak up to 20 m inland with concentrations declining and then gradually increasing towards the 100 m mark. This illustrates the influence of the sub-surface maximum recorded at the edge of the merse, as observed for Southwick Core No. 1 (SC1) in Section 4.1, combined with a decreasing depth distribution of ^{137}Cs on moving inland across the merse. The increasing concentrations inland can probably be attributed to the association of radionuclides with the finest sedimentary particles which are transported furthest inland as the incoming tide dissipates its energy on the elevated surface of the merse.

The radionuclide concentrations within the merse are strongly correlated with each other when linear regression analysis is undertaken. For example, linear regression of ^{137}Cs and ^{241}Am concentrations in the 0-15 cm depth interval produces an R^2 value of 0.95 and similar results are obtained for ^{137}Cs and $^{239+240}Pu$ ($R^2 = 0.79$) and ^{241}Am and $^{239+240}Pu$ ($R^2 = 0.91$). The concentrations in the 15-30 cm interval have lower correlation values; 0.78 for ^{137}Cs and ^{241}Am, 0.74 for ^{137}Cs and $^{239+240}Pu$ and 0.92 for ^{241}Am and $^{239+240}Pu$. These correlations suggest (but do not prove) that the different radionuclides are associated with some specific component of the sediment, most probably, the fine sediment and that the variations in the lateral distribution of this component affect ^{137}Cs, ^{241}Am and $^{239+240}Pu$ in the same way. The fact that the correlations occur in samples which contain sediment of different ages suggests that this process has been operating in this way for some time.

The loss on ignition (LOI) data for the 0-15 cm interval samples exhibit a correlation

Fig 4.27 The lateral distribution pattern of ^{137}Cs within the 0–15 cm, 15–30 cm and the combined total in the 0–30 cm depth interval for the Creetown transect T1.

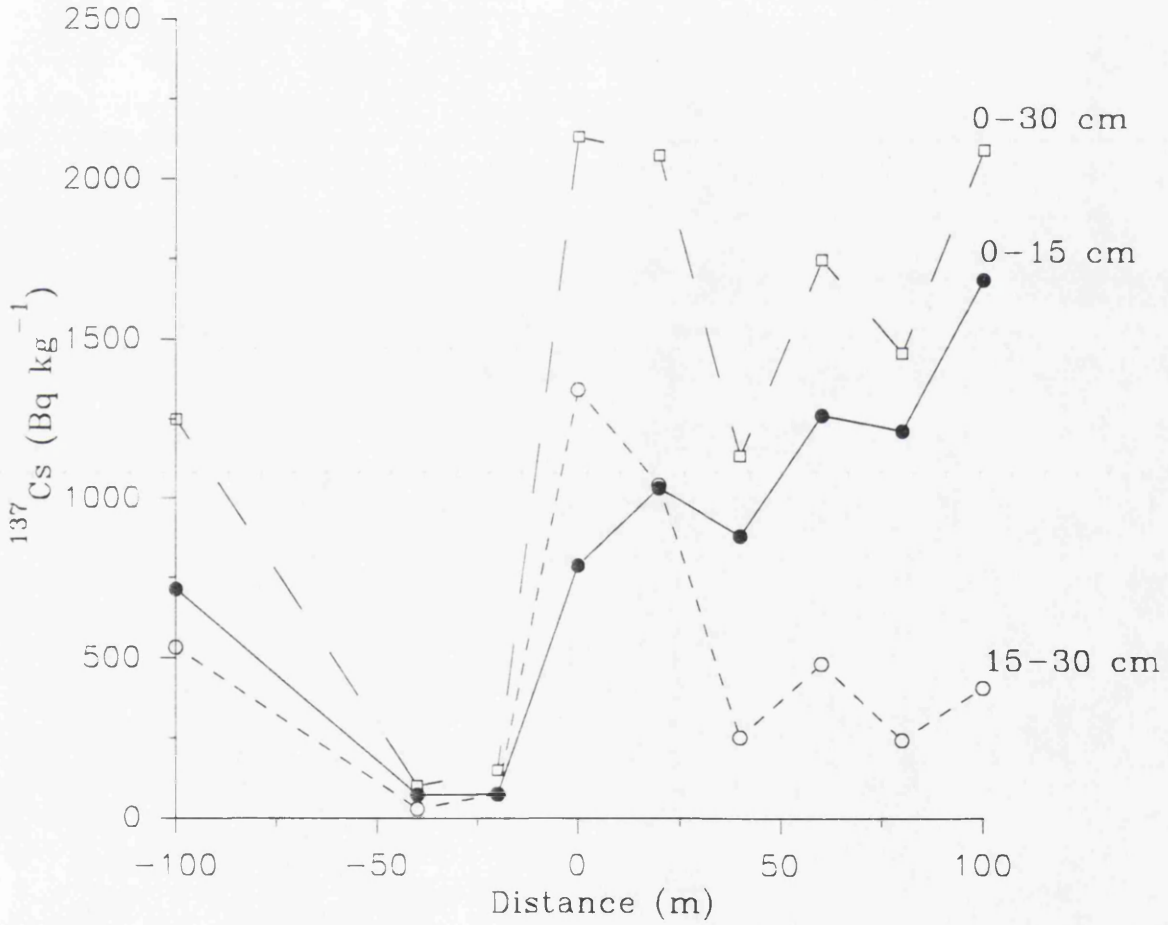

with distance, producing an R^2 value of 0.88. The LOI data for the 15-30 cm depth interval produce an R^2 value of 0.45, indicating a much poorer correlation. These results are not surprising since organic content will increase inland as flora colonise the sediments and alter the soil conditions. The poor correlation between LOI data in the 15-30 cm interval and distance could reflect the absence of root penetration and soil fauna at this depth.

The radionuclide concentrations in the 0-15 cm interval exhibit a reasonable correlation with the LOI data with R^2 values of 0.58, 0.70 and 0.69 for ^{137}Cs, ^{241}Am and $^{239+240}Pu$ respectively. While these R^2 values indicate some relationship between LOI data and radionuclide concentrations the linear regression analysis do not establish a causal link. For example, organics can increase on-shore due to plant development, while radionuclide concentrations may also increase on-shore, not through association with organic content, but through deposition of the finest particulate material further inland. Linear regression analysis could thus indicate a relationship where no physical link between the two variables may exist.

The radionuclide inventories for the transect are also reported in Table 3.4 and Table 3.5 and are illustrated in Fig 4.28. The trends in the inventories along the transect are effectively the same as those observed for the radionuclide concentrations. These inventories are almost one order of magnitude greater than those observed by McDonald *et al.,* (1992) along a transect across terrestrial soils at Carsluith further down river from the present sample site. The transect collected by McDonald *et al.,* produced ^{137}Cs inventories which declined from a maximum of 86,580 Bq m^{-2} at 0 m to 28,210 Bq m^{-2} at 125 m inland. In contrast, the present work illustrates an increase with distance inland to 456,000 Bq m^{-2} at 100 m. The contrast between the present work and the transect collected by McDonald *et al.,* clearly illustrates the variation in inventories observed between the inland terrestrial soils and the saltmarsh deposits. The observation of increasing radionuclide concentrations inland has previously been reported by Ben-Shaban (1989) who observed similar trends in the Solway floodplain during the mid 1980s.

Fig 4.28a. The ^{137}Cs inventories in the 0–15 cm, 15–30 cm and 0–30 cm depth intervals for the Creetown transect T1.

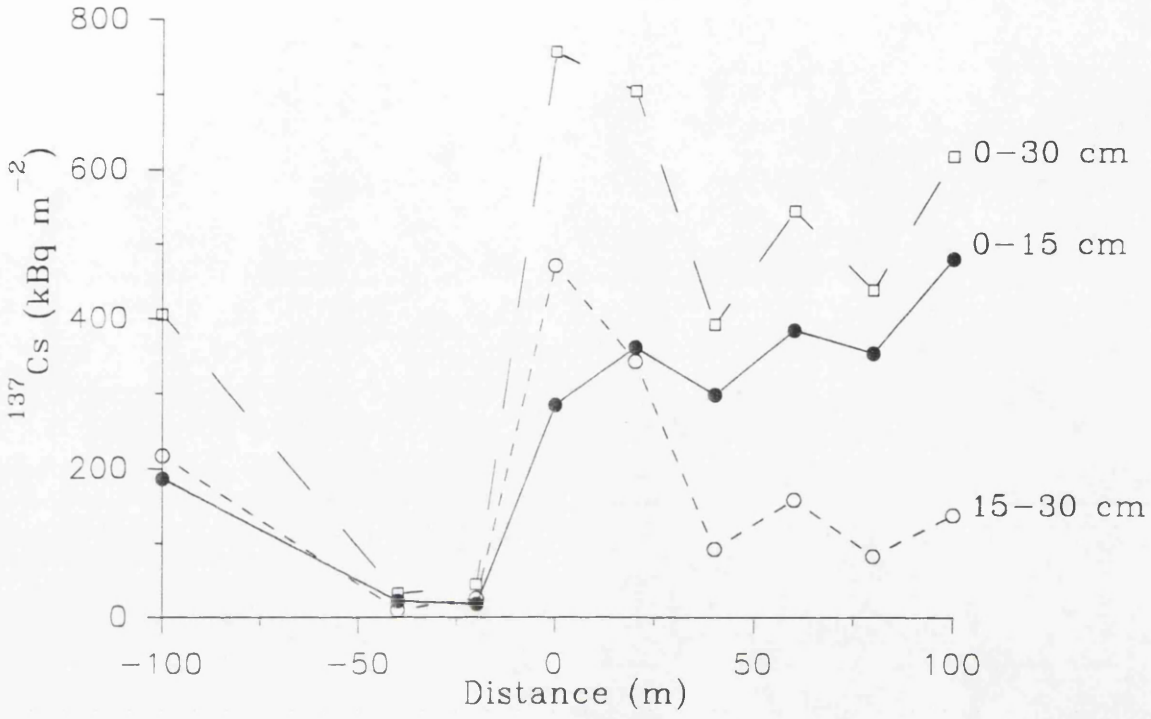

Fig 4.28b. The ^{241}Am inventories in the 0–15 cm, 15–30 cm and 0–30 cm depth intervals for the Creetown transect T1.

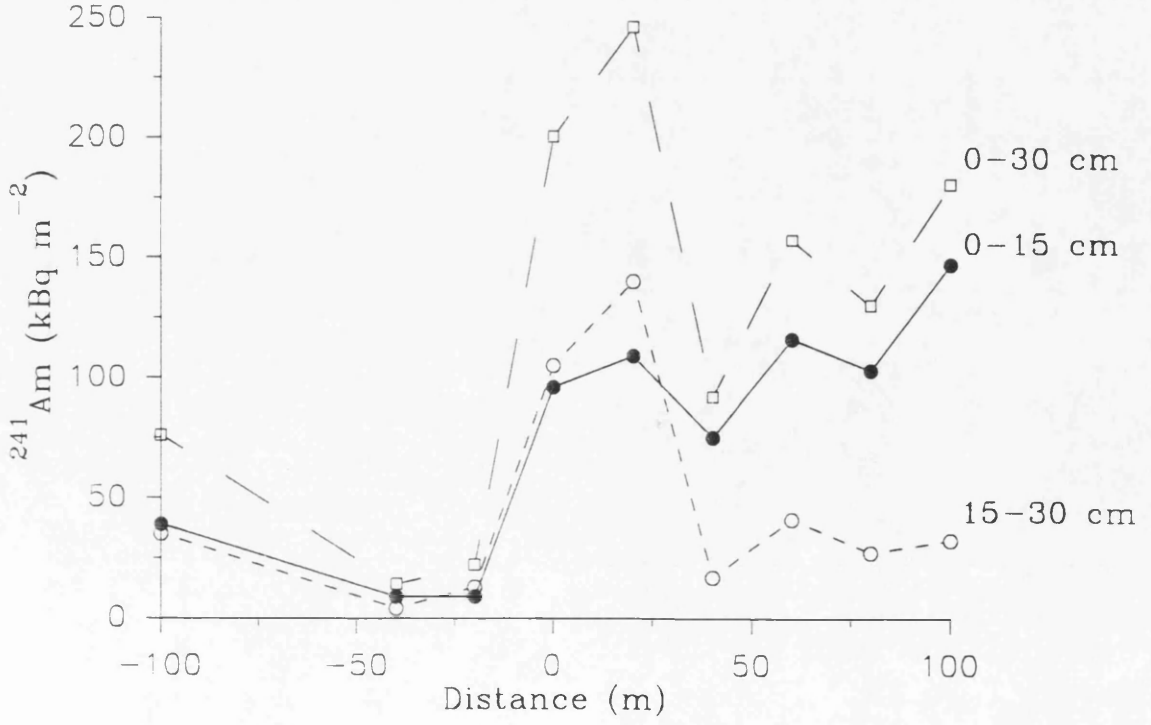

Fig 4.28c. The $^{239+240}$Pu inventories in the 0–15 cm, 15–30 cm and 0–30 cm depth intervals for the Creetown transect T1.

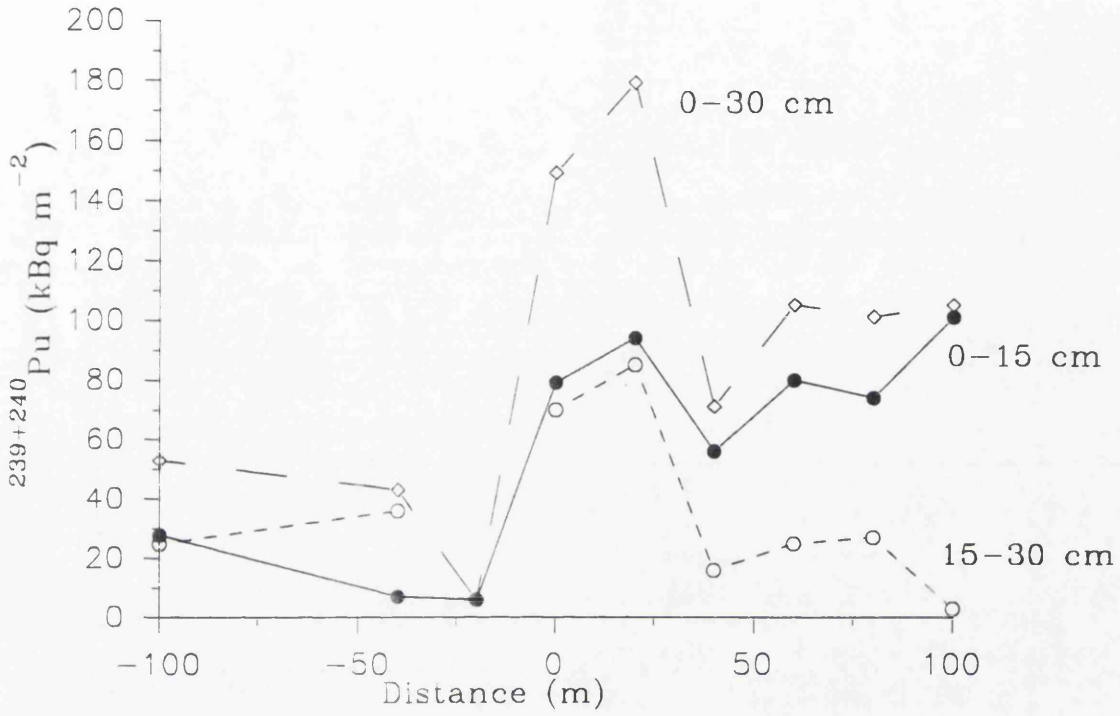

4.2.2 Wigtown

The Wigtown merse is illustrated in Plates 2.3 and 2.4 and exhibits a higher elevation than the Creetown transect, with the stepped edge of the merse at the MHWM being approximately 1.5 m high. The radionuclide concentrations for the 0-15 cm and 15-30 cm depth intervals from the Wigtown transect T1 are reported in Table 3.6 and Table 3.7 respectively and illustrated in Fig 4.29 and Fig 4.31 respectively. The concentrations in the Wigtown transect are noticeably lower for sites in the consolidated merse (above the MHWM) than the corresponding values in the Creetown transect.

Concentrations of ^{137}Cs (Fig 4.29a) in the 0-15 cm interval decline from 582 Bq kg^{-1} at -40 m i.e. 40 m out from the MHWM, to 30 Bq kg^{-1} at the MHWM (0 m) before systematically increasing to over 700 Bq kg^{-1} at 80 m inland. A similar trend is observed for ^{241}Am (Fig 4.29c), with concentrations in the intertidal zone declining from approximately 300 Bq kg^{-1} to 19 Bq kg^{-1} at the MHWM. The activity then increases gradually, but to only 176 Bq kg^{-1} at the 80 m site, and does not exceed the maximum concentration recorded in the intertidal sediments. The ^{134}Cs concentrations (Fig 4.29b) exhibit a similar trend with a decline from the intertidal zone towards the MHWM, where the concentrations were below the limit of detection, before increasing inland. These trends are essentially very similar to those observed at Creetown with a pronounced minimum in the intertidal sediments close to the MHWM.

The results from the 15-30 cm depth intervals show a general similarity to the 0-15 cm profiles. The concentrations of both ^{137}Cs and ^{241}Am exhibit very similar trends, with values declining from the intertidal end of the transect towards the MHWM and then increasing gradually inland across the merse. The enhanced concentrations reported for the sampling point at 40 m out from the MHWM can be explained by the fact that this location consisted of an 'island' of consolidated grass covered merse which was gradually being eroded and was obviously different from the surrounding unconsolidated intertidal sediment. The results for ^{137}Cs and ^{241}Am clearly show enhanced concentrations at this site in comparison with the intertidal sediment (-20 m). There were insufficient ^{134}Cs data above the limits of

Fig 4.29 ^{137}Cs, ^{134}Cs and ^{241}Am concentrations from the 0–15 cm samples from Wigtown transect T1 collected 27/8/90.

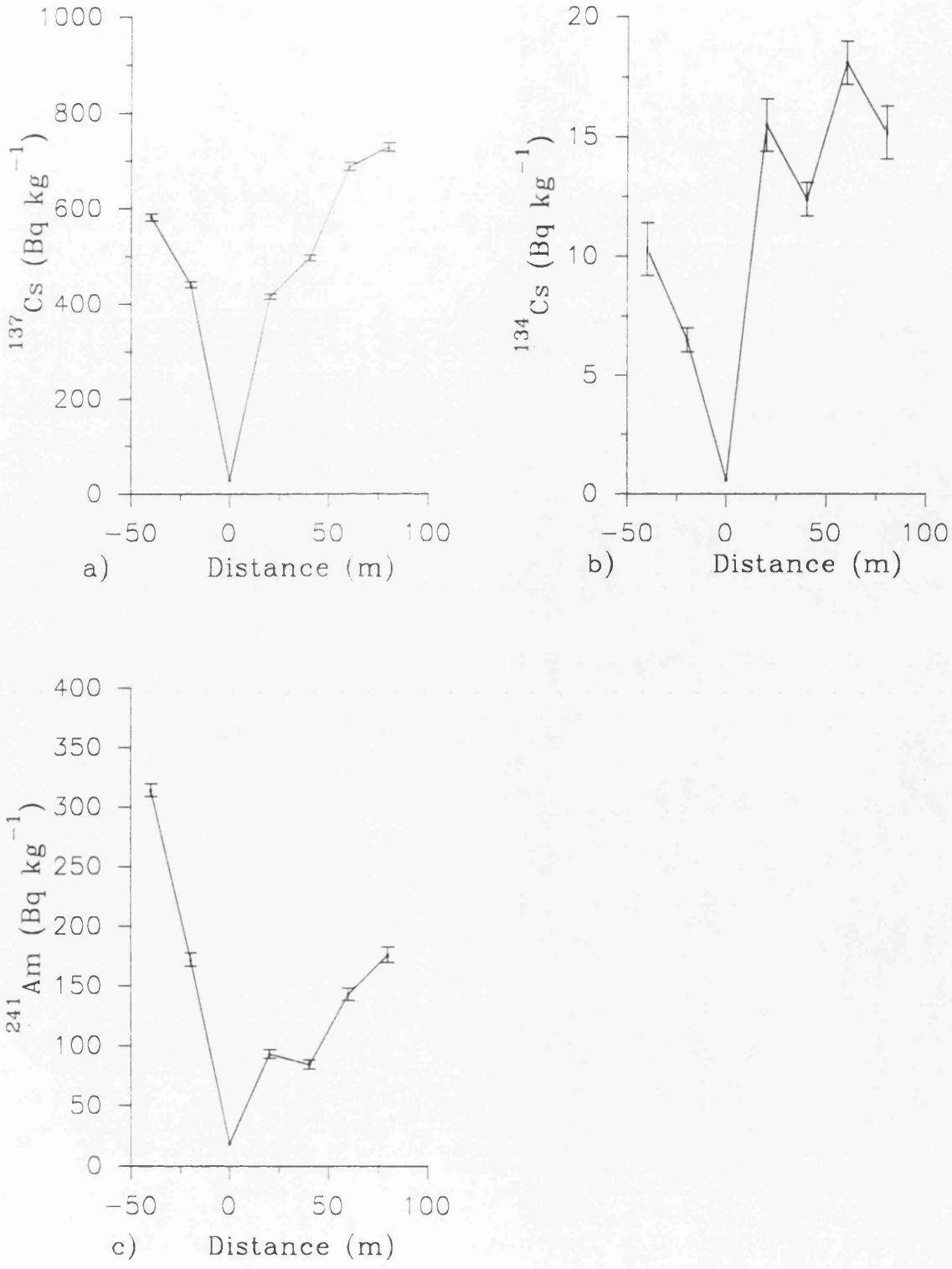

Fig 4.30 $^{134}Cs/^{137}Cs$ and $^{137}Cs/^{241}Am$ activity ratios of 0–15 cm samples from Wigtown transect T1.

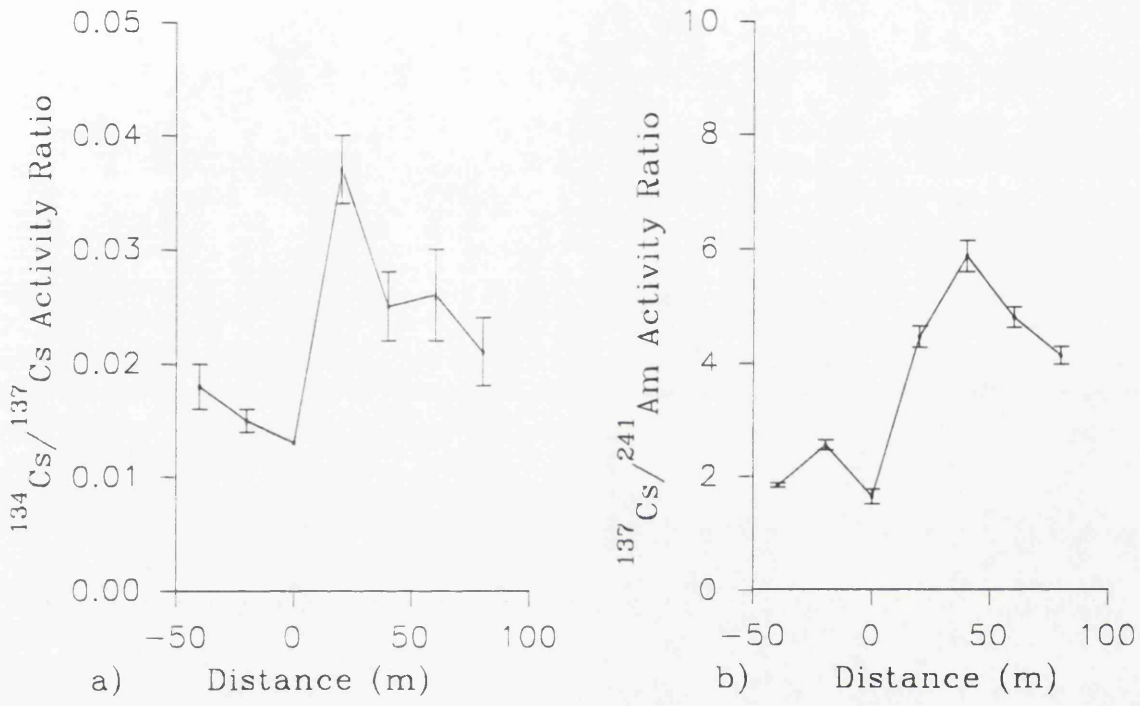

Fig 4.31 Radionuclide concentrations and activity ratios for 15-30 cm samples from Wigtown transect T1.

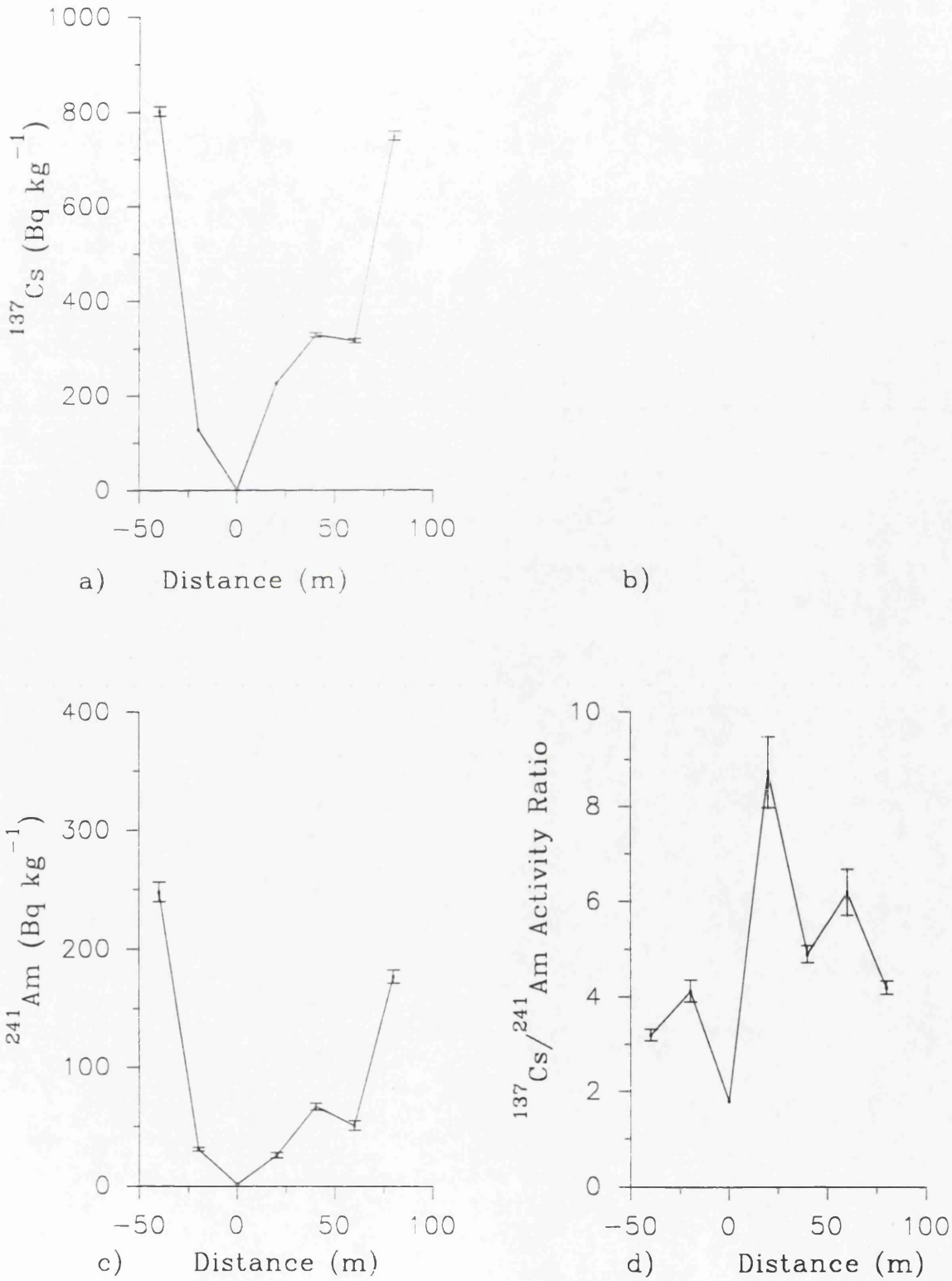

detection to enable construction of a graph.

Linear regression analysis of ^{137}Cs and ^{134}Cs concentrations and ^{137}Cs and ^{241}Am in the 0-15 cm depth intervals produce R^2 values of 0.83 and 0.93 respectively. As for Creetown, caution is required in the interpretation of these linear regression values. The R^2 values suggest that the radionuclides are associated with some component of the sediment, most probably the fine sediment, and that the lateral distribution of that component affects the radionuclides in the same way.

The absence of maximum concentrations at depth in the Wigtown transect compared with Creetown can be attributed to two factors; the sampling strategy and the topography of the merse. The sampling strategy with samples collected from the top 30 cm of the merse, at 20 m intervals could fail to identify maximum concentrations below this depth. For example, Ben-Shaban (1989) reported a sub-surface maximum at a depth of 35-40 cm within a section obtained from the 'cliff' face at the MHWM from an area of merse close to the present transect location. The topography of the merse will influence the deposition pattern at each particular location within the floodplain. The elevation of Wigtown merse at the MHWM is approximately 1.5 m above the intertidal sediments, in contrast the cliff at the MHWM of the Creetown merse is less than 0.5 m high. Therefore, it is quite probable that Wigtown merse is less frequently inundated by the sea than the Creetown merse, resulting in different deposition trends at this location. In addition, the topography of Wigtown merse does not display the characteristic stepped features observed at Creetown. These stepped features are relics of previous MHWM's where the vertical cliff face has slumped and has been partially filled in with sediment. These features are susceptible to rapid accumulation of sediment, leading to a gradual increase in the elevation of the merse. Stepped edges caused by slumping and infilling were observed within the drainage channels (plate 2.5) but, when traversing inland along the transect, no stepped features were observed. Thus, deposition of contaminated material would primarily be confined to locations around the drainage channels, with only periodic inundation of inland areas of grass covered sward which involves deposition and removal of material from the surface during the flow and ebb tides. Therefore, sub-surface maxima are unlikely to be created at inland locations because of the increased elevation of the

merse except at the stepped edges of minor drainage channels. In addition the frequency of inundation is insufficient to bury the grass covered sward. Support for this hypothesis is found in the Creetown transect where values beyond the 20 m site exhibit surface maxima.

The $^{134}Cs/^{137}Cs$ and $^{137}Cs/^{241}Am$ activity ratios for the Wigtown transect T1 are illustrated in Fig 4.30 and Fig 4.31. The $^{134}Cs/^{137}Cs$ activity ratio (Fig 4.30a) for the 0-15 cm samples has a point below the limits of detection (0 m) but the general trend is one of decline from the intertidal to the MHWM with an increase up to 20 m inland and then declining as the merse is traversed. The $^{134}Cs/^{137}Cs$ activity ratio exhibits enhanced values compared with those in the Creetown transect (Fig 4.24a). The Wigtown values decline from a maximum of 0.037 at 20 m to 0.021 at 80 m, compared with a maximum of 0.014 at Creetown. The Wigtown values are however, greater than the integrated $^{134}Cs/^{137}Cs$ activity ratios from Sellafield ($\sim$0.0028) at the time of sample collection in 1990, but below the corresponding decay corrected isotope ratio for Chernobyl fallout (0.14). There is a systematic decrease in the $^{134}Cs/^{137}Cs$ activity ratio with distance across the merse which suggests the presence of older radiocaesium from Sellafield at these inland sites.

The $^{137}Cs/^{241}Am$ activity ratios for the 0-15 cm and 15-30 cm depth intervals exhibit very similar trends, trends which have also been observed at Creetown which suggests that the ^{137}Cs and ^{241}Am concentrations are from the same source term, have been well mixed and that they are associated with similar components of the sediment. Further comparison between the Wigtown and Creetown transects indicates that the maximum $^{137}Cs/^{241}Am$ activity ratio recorded within the merse at both sites is at $\sim$40 m and that the minimum value of 2 was recorded close to the MHWM. This minimum value observed in the intertidal sediments close to the MHWM implies that in this zone the sediment is susceptible to a high degree of mixing by tidal action.

The concentrations reported for the Wigtown and Creetown transects compare favourably with results reported by Ben-Shaban (1989) for a transect across Wigtown merse. Ben-Shaban observed increasing concentrations for up to 500 m

inland across the consolidated merse.

The radionuclide inventories for the Wigtown transect are also reported in Tables 3.6 and 3.7 and are illustrated in Fig 4.32. The inventories in the present study are similar to the corresponding values reported by Ben-Shaban (1989). The ^{137}Cs inventories (0-15 cm) have values of 9,000 Bq m^{-2} (0 m), 234,000 Bq m^{-2} (60 m) and 188,000 Bq m^{-2} (80 m) compared with 8,000 Bq m^{-2} (0 m), 140,000 Bq m^{-2} (50 m) and 200,000 Bq m^{-2} (100 m) for the corresponding values reported by Ben-Shaban.

The inventories are generally lower for intertidal sites than for consolidated merse and this reflects the mixing of the offshore/intertidal sediments by the tides. These offshore sediments are predominantly coarse grained sands, in contrast to the finer textured particles in the consolidated merse.

4.2.3 Southwick

The sample site at Southwick (Plate 2.7) is located within an enclosed riverine environment bounded to the north by the outcropping cliffs of the Criffel pluton and to the south by the extensive tidal flats of Mersehead Sands. The lower reaches of the Southwick Water are tidal and the merse deposits are therefore subject to tidal inundation on a regular basis. The radionuclide concentrations for the Southwick transect T1 are reported in Table 3.8 and Table 3.9 and are illustrated in Fig 4.33 and Fig 4.35 for the 0-15 cm and 15-30 cm depth intervals respectively.

In each case, the transect exhibits a pronounced maximum in concentration at ~ 20 m, with values decreasing systematically from this in each case, except ^{134}Cs which increases again on moving inland from a minimum at 40 m.

Concentrations of ^{137}Cs in the 0-15 cm depth interval (Fig 4.33a) increased inland from the intertidal deposit within the river channel at -3 m (239 Bq kg^{-1}), to a maximum of 2,070 Bq kg^{-1} at 20 m before falling by an order of magnitude to 230 Bq kg^{-1} at a distance of 40 m from the stepped edge of the merse. The ^{137}Cs

Fig 4.32a The ^{137}Cs inventories for the 0–15 cm, 15–30 cm and 0–30 cm depth intervals from Wigtown transect T1.

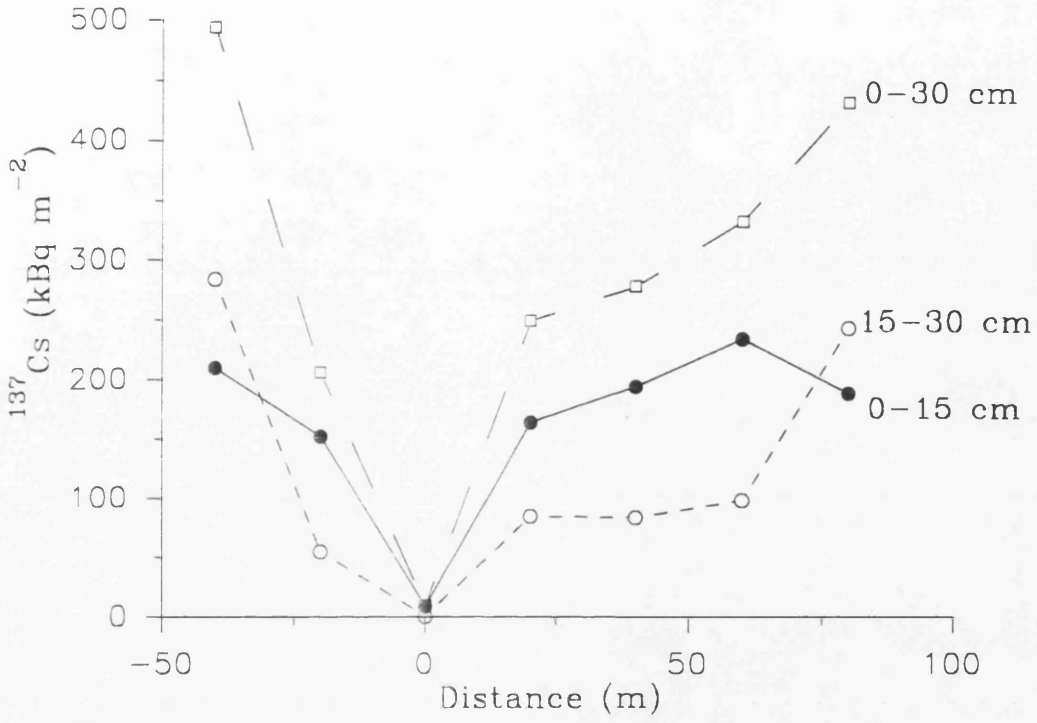

Fig 4.32b The ^{241}Am inventories for the 0–15 cm, 15–30 cm and 0–30 cm depth intervals from Wigtown transect T1.

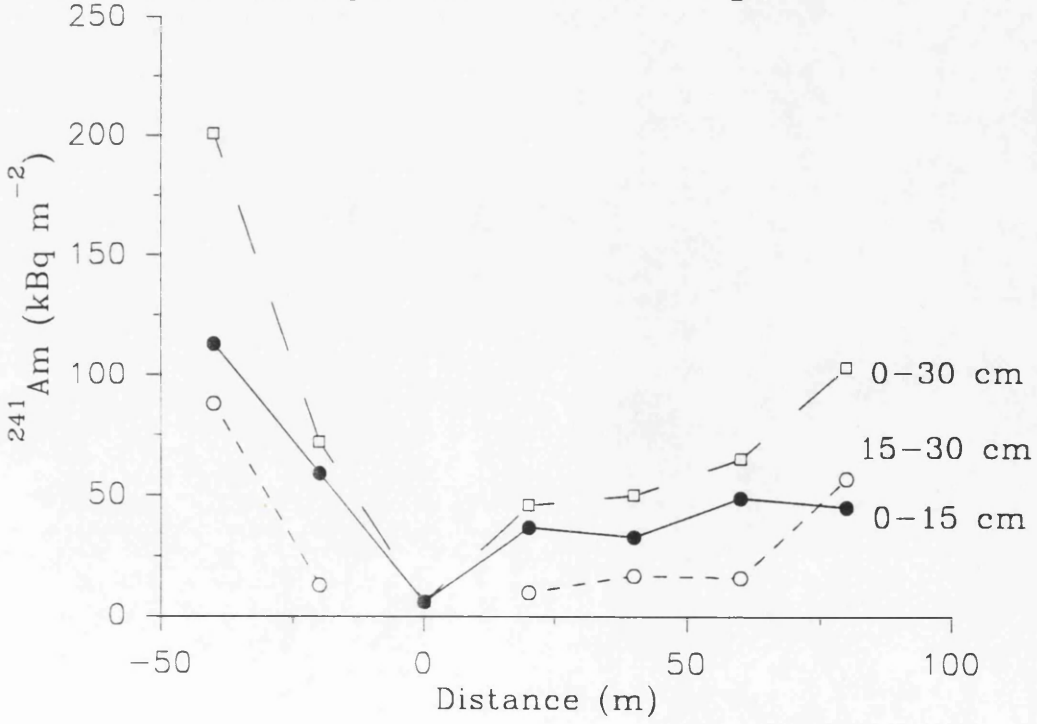

Fig 4.33 Radionuclide concentrations for 0–15 cm samples from Southwick transect T1, collected 25/7/91.

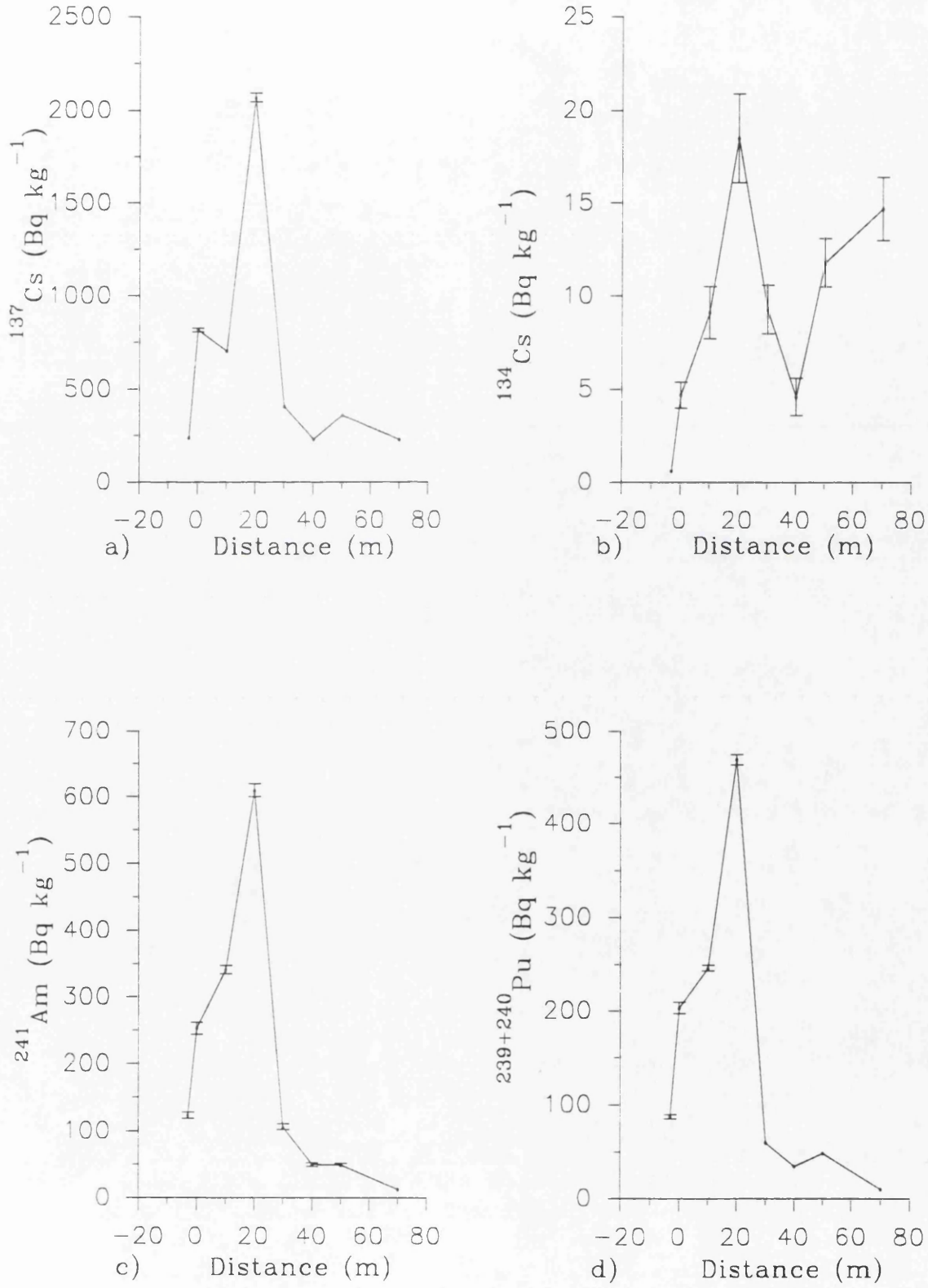

Fig 4.34 Radionuclide and Isotope activity ratios for 0–15 cm samples from Southwick transect T1.

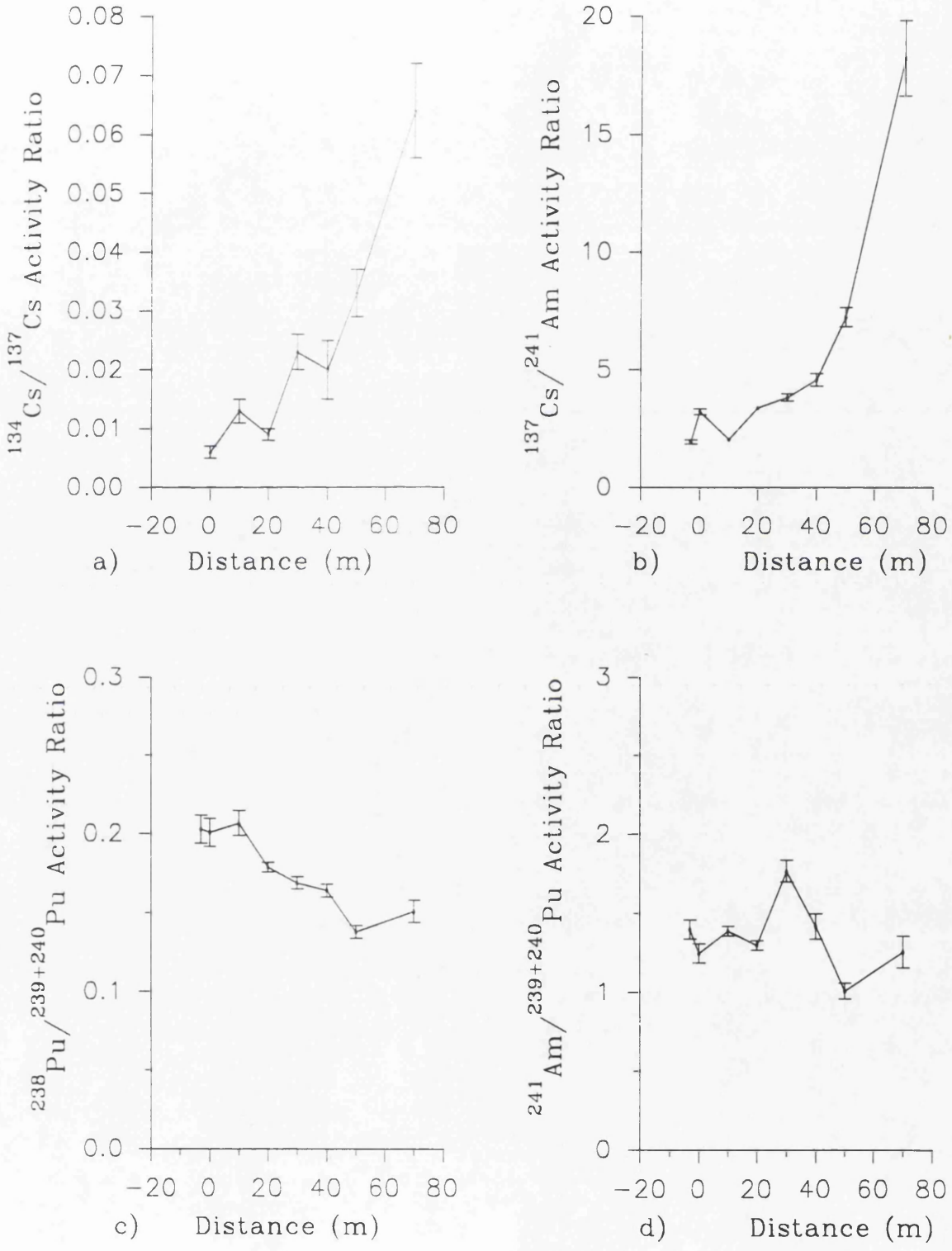

Fig 4.35 Radionuclide concentrations for 15–30 cm samples from Southwick transect T1, collected 25/7/91.

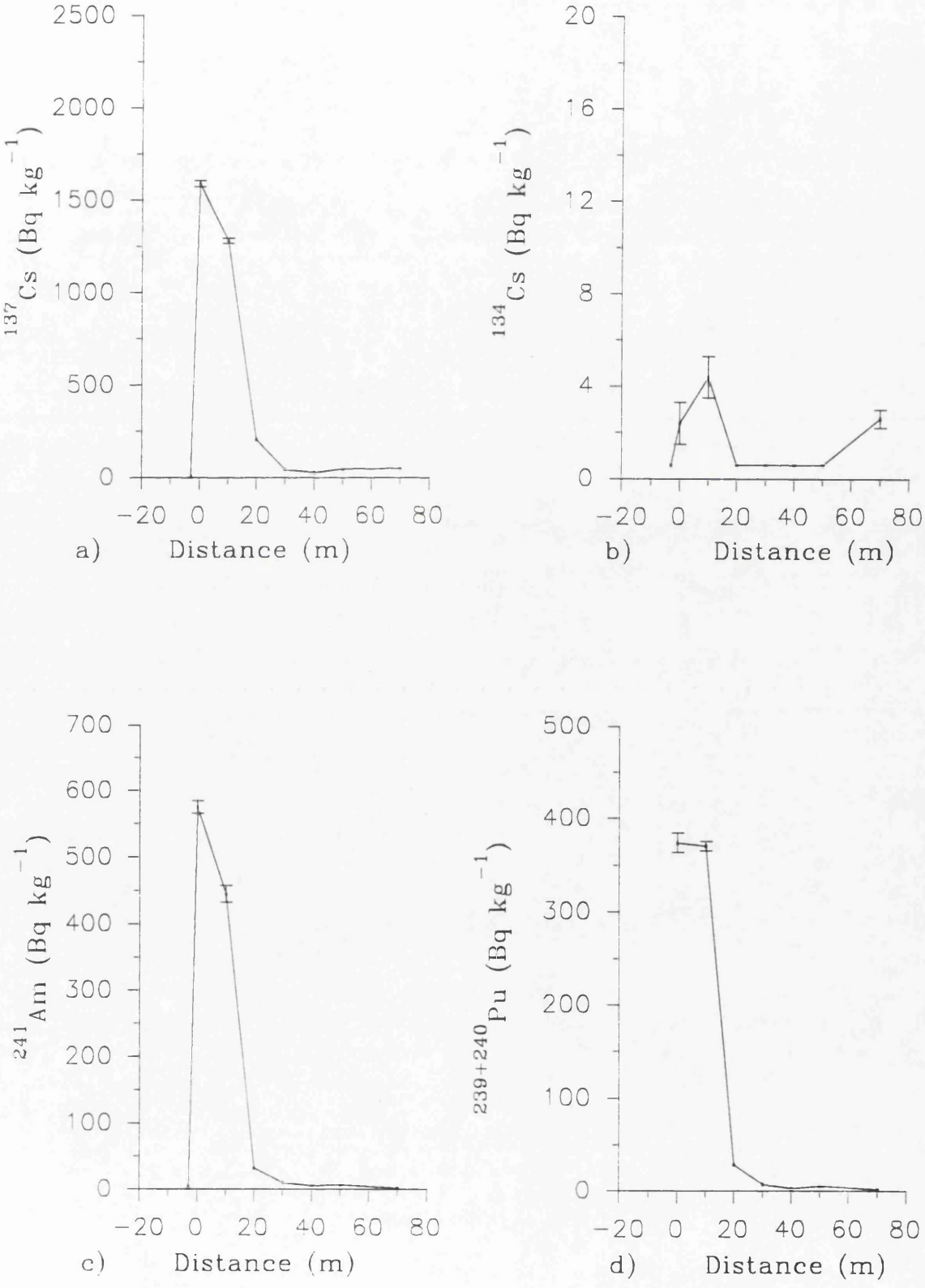

concentrations in the 15-30 cm depth interval (Fig 4.35a) exhibit similar trends to the 0-15 cm interval. Concentrations increase from the intertidal deposits to a maximum concentration at the MHWM (0 m) before declining rapidly from a distance of 10 m inland. The 15-30 cm data produce a sub-surface maximum for distances up to 10 m inland from the MHWM. Surface concentrations dominate beyond 10 m inland, in general being an order of magnitude greater than the corresponding 15-30 cm data. Similar trends are observed in the ^{241}Am and $^{239+240}Pu$ data (Fig 4.33c, d and Fig 4.35 c, d), with concentrations producing sub-surface maxima as far as 10 m inland.

The ^{134}Cs concentrations for the 0-15 cm depth interval samples illustrated in Fig 4.33b exhibit a different profile. The data set is incomplete, with the intertidal value (-3 m) being below the limits of detection, however, the general trend is one of increasing concentrations inland, similar to ^{137}Cs but with a rapid decline inland beyond 20 m followed by a pronounced increase beyond 40 m. This profile suggests that beyond 40 m, the ^{134}Cs concentrations have been enhanced by deposition of Chernobyl fallout.

The radionuclide concentrations are well correlated with each other. For example the concentrations in the 0-15 cm depth interval from the merse produce R^2 values of 0.92 for ^{137}Cs and ^{241}Am, 0.93 for ^{137}Cs and $^{239+240}Pu$ and 0.99 for ^{241}Am and $^{239+240}Pu$. Similar results are obtained for linear regression analysis of the 15-30 cm radionuclide concentrations.

Thus, both Creetown and Southwick transects exhibit sub-surface maxima close to the MHWM, whereas Wigtown does not. In addition, concentrations increase inland at Creetown and Wigtown (0-15 cm) but at Southwick there is a pronounced decline after 20 m. This variation in radionuclide concentration trends reflects the topography at each location. Creetown is a wide, open, low lying merse which is subject to direct inundation by the sea. Wigtown exhibits generally similar topography but has a higher elevation than Creetown. Southwick, on the other hand, is an enclosed riverine location which is only periodically inundated. The pronounced sub-surface maxima up to at least 10 m inland can be attributed to the topography of the merse at Southwick. Visual observation recorded that at 20 m

inland there was a small 'step' in the merse, approximately 10 cm in height. This feature could be a former stepped edge of the merse which has been subsequently filled in with sedimentary material. This relic of previous merse development would have gradually filled up with sediment until the level eventually reached the height of the more consolidated deposits behind the stepped edge. Therefore it is conceivable that radionuclides would have been concentrated at this feature over a period of years. Evidence to support this hypothesis is provided by the concentration profiles and sedimentation rates of Southwick Core No. 1 (SC1) and Core No. 2 (SC2) which were collected from the stepped edge of the bank of the Southwick Water. In addition Ben-Shaban (1989) collected a section from an area of merse in 1986 which had been subject to slumping but at the time of sample collection was experiencing rapid accretion.

The present radionuclide distribution pattern at Southwick is still influenced by the 'step' feature at 20 m inland. The sample sites located closer to the tidal reaches of the Southwick Water will be subjected to more frequent and prolonged tidal inundation than sites located further inland. The 'step' feature, together with the vegetation cover, will limit the progression of suspended particulates brought on-shore by the incoming tide. Thus, as the tide dissipates its energy over the merse, the carrying capacity will be reduced and suspended material will be deposited. During inundation, as the tide progresses inland, the depth of water covering the merse will be limited by the gradient of the surface over which it flows and as the depth of water declines the energy of the system is reduced, therefore reducing the carrying capacity of the water. This results in deposition of material through physical sorting of particles with the finest particles inland and the coarsest material closer to the sea. The sample sites from 30 m and beyond will be subjected to tidal inundation but less frequently and for shorter periods than locations closer to the river. Concentrations of radionuclides in sediment deposited during these ingresses could have been relatively high due to the association of radionuclides with the finest particle sizes (Aston and Stanners, 1981b; Jones *et al.*, 1984 and Hamilton and Clarke, 1984) and the influence of vegetation on the entrapment of this very fine sediment.

Ben-Shaban (1989) also undertook collection of surface samples (< 1 cm depth)

along a 55 m transect located some 50 m upriver from the present sample location and observed increasing concentrations inland to 45 m, beyond which they declined. Obviously, the sample collection methods were different for each transect and the results cannot be directly compared. However, the Ben-Shaban data provide substantial support for the argument advocating the influence which topography exerts on the radionuclide deposition pattern at this location.

The radionuclide inventories for Southwick (Fig 4.37) are considerably lower than those for Creetown and Wigtown, although the maximum concentrations observed are higher. This variation reflects the location and physical topography of each site. The weights of the samples collected at Southwick were lower than the Creetown or Wigtown transects suggesting that more fine grained material was present at Southwick. Fine grained silts and clays comprise 14% of the sediment fractions present at Southwick, however the predominant component is fine sand (Section 4.4). This particle size distribution pattern combined with the topography and elevation of Southwick merse produces larger radionuclide concentrations close to the MHWM than more inland locations. Tidal inundation is less extensive in the upper reaches of the Southwick merse due to the increased elevation and terrestrial influence within this riverine location compared with the more open coastal merse at Creetown and Wigtown.

The radionuclide and isotope activity ratios are illustrated in Fig 4.34 and Fig 4.36. The $^{134}Cs/^{137}Cs$ activity ratio for the 0-15 cm interval (Fig 4.34a) increases from 0.006 at the MHWM to 0.064 at 70 m inland. The results for the corresponding values in the 15-30 cm depth interval (Fig 4.36a) are incomplete because most ^{134}Cs values are below the limit of detection and are only included to illustrate the variation between the values at the MHWM and the enhanced value at 70 m. The variation in $^{134}Cs/^{137}Cs$ activity ratios implies that an additional source of radiocaesium is present, most probably Chernobyl fallout. The $^{137}Cs/^{241}Am$ activity ratio (4.34b) exhibits a very similar trend to the $^{134}Cs/^{137}Cs$ activity ratio. This enhancement of the ratio on moving inland supports the argument for the presence of Chernobyl fallout. The $^{137}Cs/^{241}Am$ activity ratio for the 15-30 cm interval (Fig 4.36b) exhibits a smaller range of values but shows a general increase. This illustrates the effects of topography on deposition trends; beyond the 20 m 'step',

Fig 4.36 Radionuclide and Isotope activity ratios for 15–30 cm samples from Southwick transect T1.

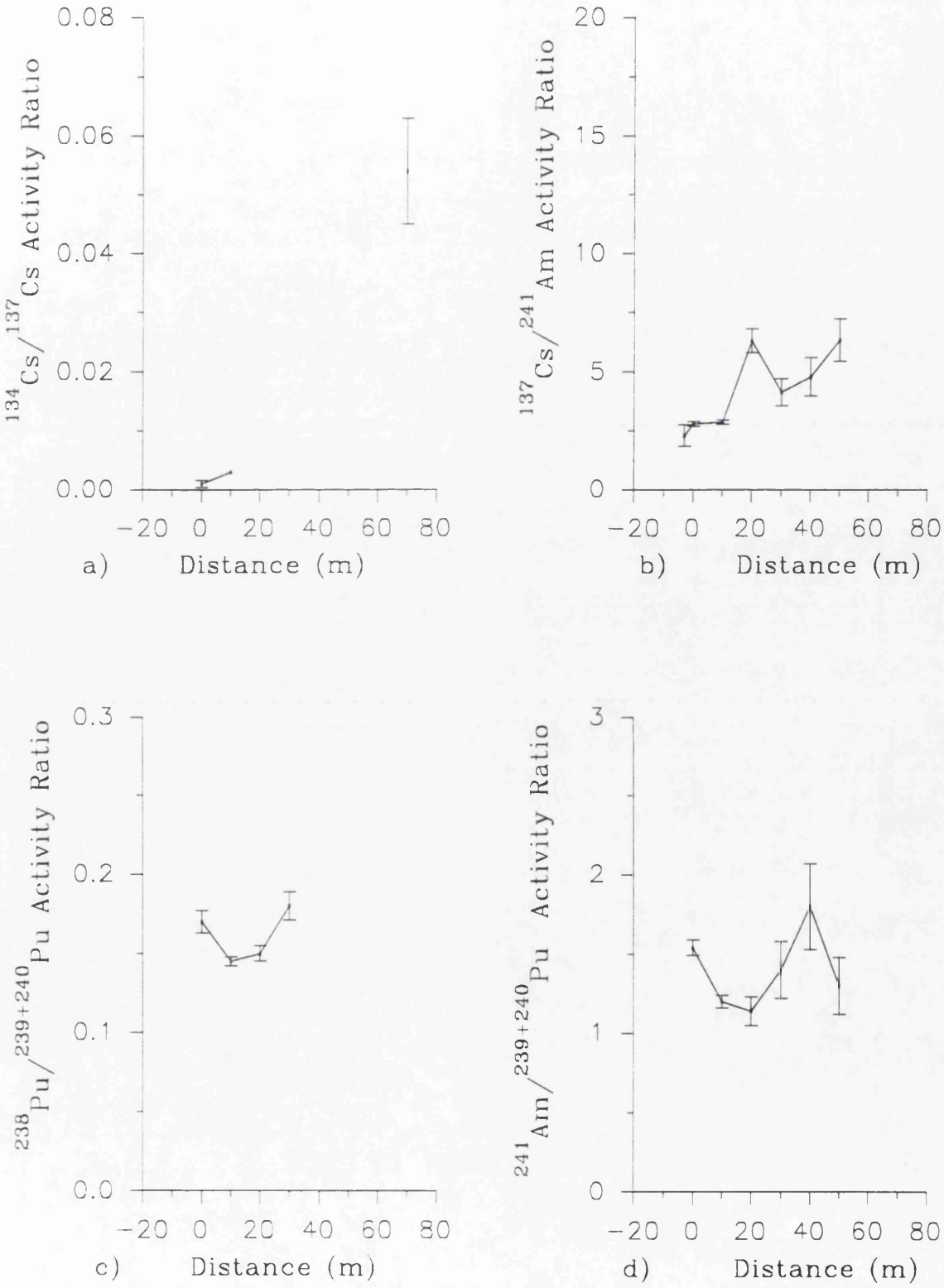

Fig 4.37a The ^{137}Cs inventories for the 0–15 cm, 15–30cm and 0–30 cm depth intervals from Southwick transect T1.

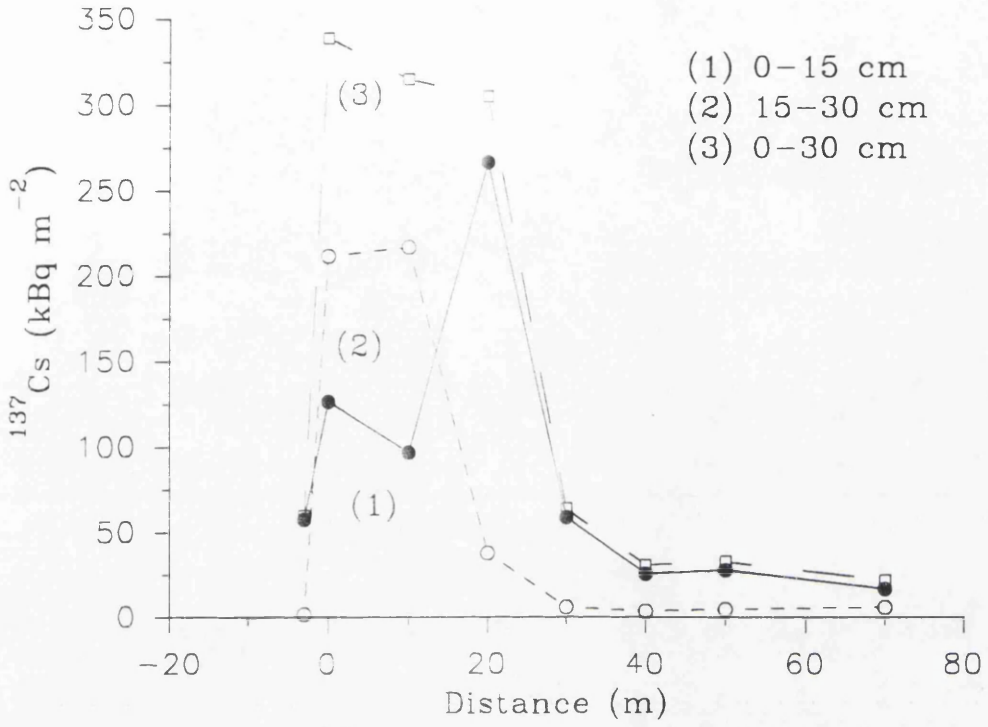

Fig 4.37b The ^{241}Am inventories for the 0–15 cm, 15–30 cm and 0–30 cm depth intervals from Southwick transect T1

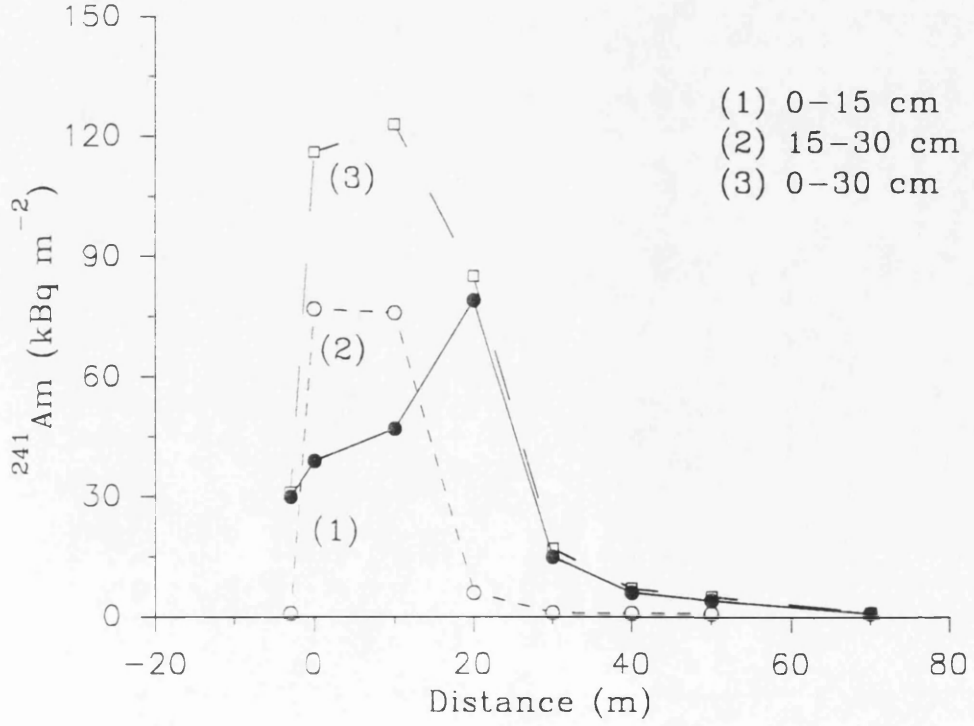

Fig 4.37c The $^{239+240}$Pu inventories in the 0–15 cm, 15–30 cm and 0–30 cm depth intervals for Southwick transect T1.

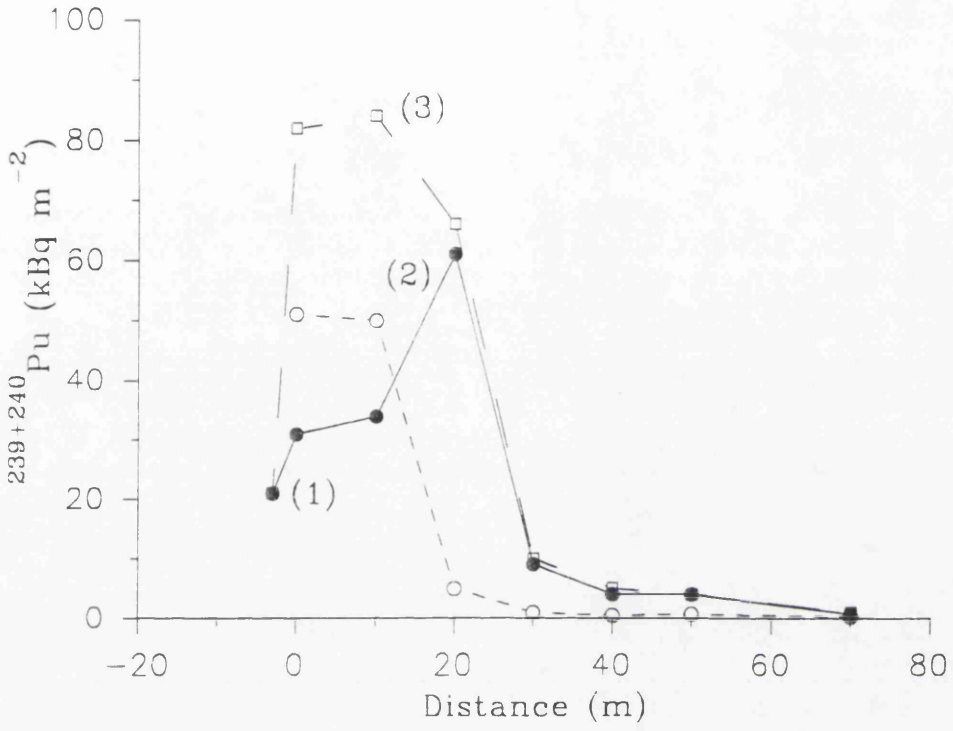

tidal inundation is more limited and the presence of enhanced $^{134}Cs/^{137}Cs$ activity ratios inland which are attributable to Chernobyl suggests a reduction in marine influence and an increasing terrestrial influence.

The $^{238}Pu/^{239+240}Pu$ isotope activity ratios for 0-15 cm (Fig 4.34c) decline from 0.20 at the MHWM to 0.15 at 70 m inland, the values for the 15-30 cm interval (Fig 4.36c) range from 0.17 to 0.15 suggesting the presence of older Sellafield effluent. The $^{238}Pu/^{239+240}Pu$ and $^{241}Am/^{239+240}Pu$ activity ratios for both depth intervals exhibit very limited variations despite samples having been deposited at different times over a 40 year period. This supports the argument for offshore mixing of material prior to deposition. In addition, the small range of values within the $^{238}Pu/^{239+240}Pu$ and $^{241}Am/^{239+240}Pu$ activity ratios compared with $^{137}Cs/^{241}Am$ and $^{134}Cs/^{137}Cs$ activity ratios reinforces the observation that the inland samples have been influenced by Chernobyl fallout.

The Creetown transect exhibits generally similar radionuclide and isotope activity ratios to the Southwick Water transect except for the observed presence of Chernobyl fallout at Southwick Water. The $^{134}Cs/^{137}Cs$ activity ratio for Creetown does not exhibit a systematic increase as reported for the Southwick transect due to the absence of Chernobyl radiocaesium. In addition, the $^{137}Cs/^{241}Am$ activity ratio does not exhibit enhanced values inland as reported for the Southwick transect. However, the $^{238}Pu/^{239+240}Pu$ and $^{241}Am/^{239+240}Pu$ activity ratios are essentially very similar with any variation being accounted for by the effects of topography on deposition patterns. The $^{238}Pu/^{239+240}Pu$ activity ratio for Creetown is almost constant while the Southwick ratio gradually declines with distance. The $^{241}Am/^{239+240}Pu$ activity ratio for Creetown exhibits limited variation and despite the apparent fluctuations in the profile generated by the Southwick transect, the values also produce a very limited range.

4.2.4 Orchardton

The transect at Orchardton started in the intertidal sediment of the Orchardton Burn/Pottleland Lane and extended inland across an area covered in salt tolerant vegetation and dissected by minor drainage channels before ending in improved

pasture land which was elevated above the merse and displayed a rich grass sward in contrast to the salt tolerant vegetation colonizing the rest of the transect. This pasture land formed a distinct change in ground.

The radionuclide concentrations for this transect are listed in Tables 3.10 and 3.11 and are illustrated in Fig 4.38 (0-15 cm) and Fig 4.40 (15-30 cm). The concentration trends indicate minimum values at the MHWM. The concentration trends of ^{137}Cs and ^{241}Am in the 0-15 cm depth interval are very similar and exhibit pronounced maxima at 125 m inland. The ^{134}Cs profile exhibits more variation, however, the maximum value is also observed at 125 m. The 15-30 cm depth interval samples produce different patterns from the 0-15 cm interval samples, however, the minimum and maximum values are observed at the MHWM and 125 m inland respectively. The transects for the 0-15 cm and 15-30 cm intervals indicate that beyond 125 m there is a dramatic decline in concentration at the change in ground from salt tolerant vegetation to improved grassland (180 m).

The observation of a dramatic decline in concentration inland was not observed at other transect locations with the exception of Southwick. Compared with Creetown and Wigtown, which traversed similar distances ($\sim$200 m), the observation at Orchardton of very low inland concentrations requires explanation. The trends at Orchardton can be related to the location, the topography of the merse and the sampling strategy. Orchardton merse is located at the head of a bay and is formed on top of raised beach deposits. This is a relatively low energy environment compared with the open expanses of merse at Creetown and Wigtown. The transect at Orchardton traverses three distinct zones; the intertidal zone, the merse and improved grassland. The concentration trends can be directly related to these zones. The intertidal zone exhibits lower concentrations than the merse, similar to the trends observed at all of the transect locations. The merse deposits have a gappy turf formed by clumps of vegetation and not the rich grass sward observed at other transects. In addition, this area is dissected by numerous drainage channels. The improved grassland located on a slightly elevated platform forms a distinct change in ground and due to the distance inland and elevated position is less frequently inundated by the tides. Not surprisingly, this location exhibits relatively low concentrations. The transect at Orchardton traverses the

Fig 4.38 Radionuclide concentrations for 0–15 cm samples from Orchardton transect T1 collected 29/8/90.

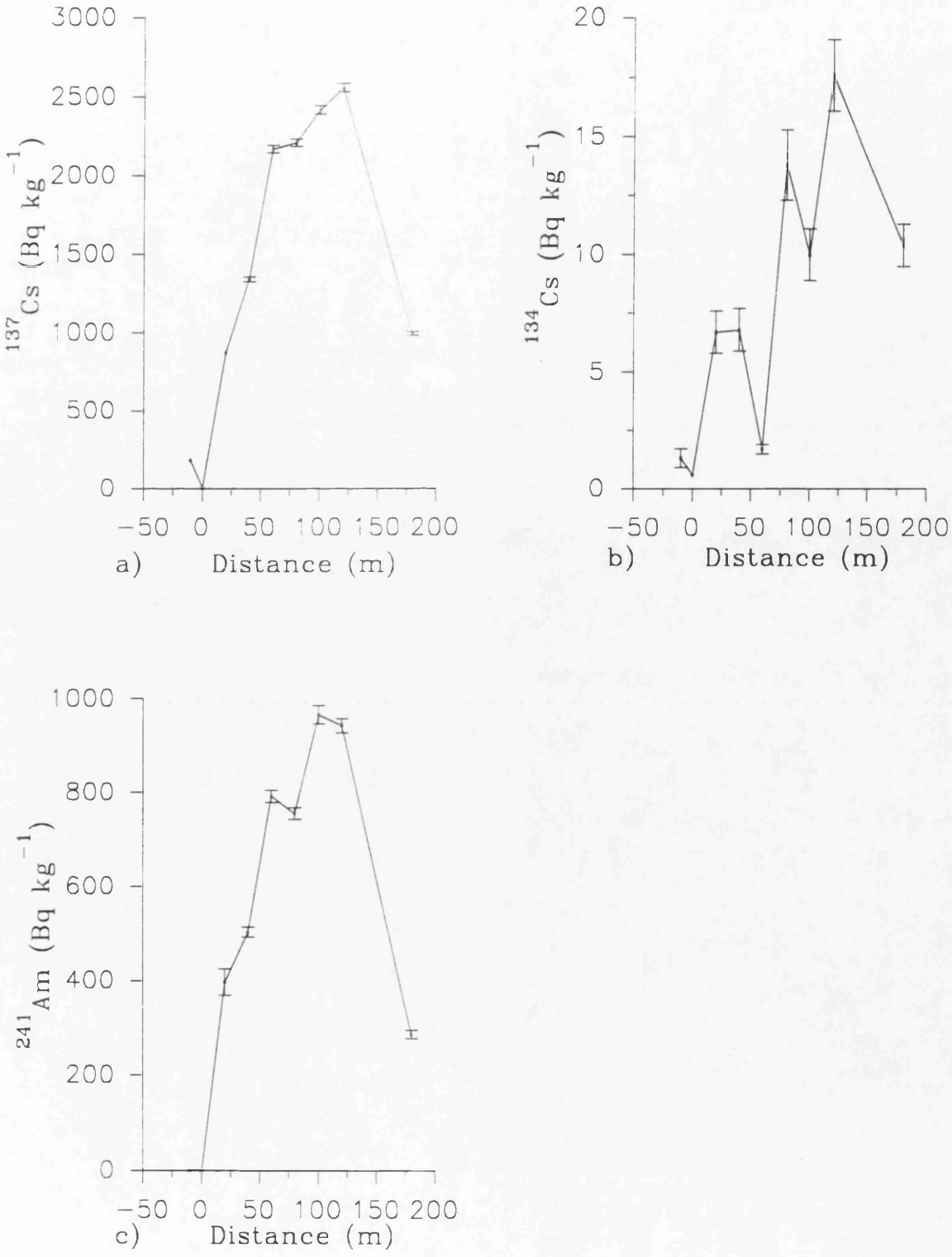

Fig 4.39 Radionuclide and Isotope activity ratios of 0–15 cm samples from Orchardton transect T1.

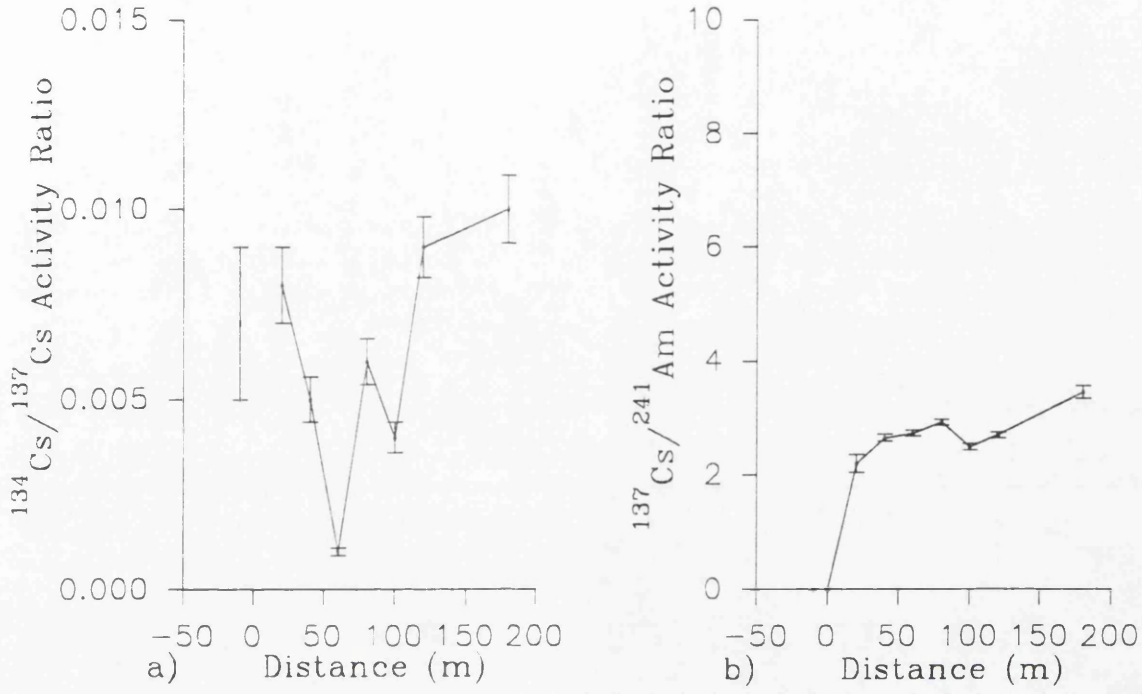

Fig 4.40 Radionuclide concentrations for 15-30 cm samples from Orchardton transect T1.

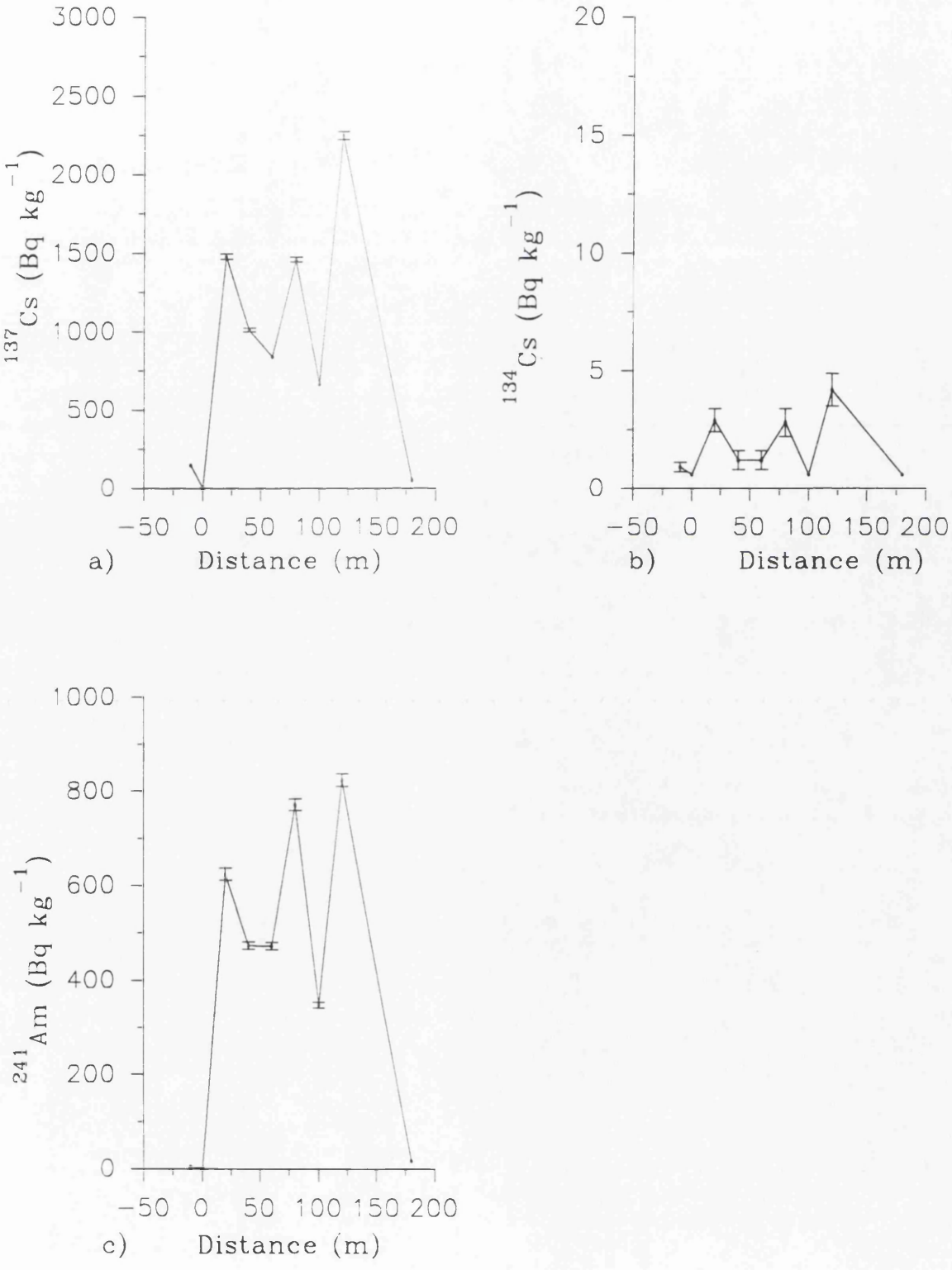

entire merse deposits (~200 m) unlike the transects at Wigtown and Creetown which traversed approximately the same distance of intertidal and merse deposits but did not cover the entire merse (less than 50% of the merse deposits). Ben-Shaban (1989) undertook a transect which traversed the entire breadth of the merse at Wigtown and reported that the largest inventories occurred furthest inland. The variations between the Orchardton results and Ben-Shaban's Wigtown results can be explained in terms of topography. There is no distinct increase in elevation of the merse inland at Wigtown, in contrast to the elevated site at the inland edge of Orchardton merse.

The radionuclide inventories for the transect are listed in Tables 3.10 and 3.11 and illustrated in Fig 4.42. These show levels of ^{137}Cs of up to 804,000 Bq m^{-2} within the top 15 cm of the merse before falling to 279,000 Bq m^{-2} within the improved pasture. These inventories are larger than those observed at the other transect locations. The total inventories (0-30 cm) are illustrated in Fig 4.42 and show levels of ^{137}Cs of over 1,300,000 Bq m^{-2} at 120 m declining to 382,000 Bq m^{-2} at 180 m.

The $^{134}Cs/^{137}Cs$ activity ratio for the 0-15 cm depth interval (Fig 4.39a) exhibits a gradual decrease from 20 m to 60 m before increasing inland to the 180 m site. The ratios up to 60 m inland, decline from 0.007 (20 m) to 0.0008 (60 m) and are below the integrated ratio values from Sellafield of ~0.0028 (1990). The distinct increase in the ratios beyond 60 m would suggest the presence of Chernobyl radiocaesium. This $^{134}Cs/^{137}Cs$ activity ratio transect is quite different from the corresponding transects at other locations where the ratios either increased or declined with distance inland due to the presence or absence of Chernobyl fallout. The trend at Orchardton suggests a declining influence of Sellafield effluent up to 60 m inland, with a corresponding increase in Chernobyl influence beyond this. However, the contribution from Chernobyl fallout at these sites is less than 31,000 Bq m^{-2} and therefore has a minimal effect on the magnitude of the inventories. These inventories must therefore be attributable to Sellafield effluent. The range of values for the $^{134}Cs/^{137}Cs$ activity ratio is lower for this transect than for the other locations especially at the seaward end. The $^{134}Cs/^{137}Cs$ activity ratios for the 15-30 cm interval (Fig 4.40a) are incomplete and cannot be interpreted

Fig 4.41 Radionuclide and Isotope activity ratios for 15–30 cm samples from Orchardton transect T1.

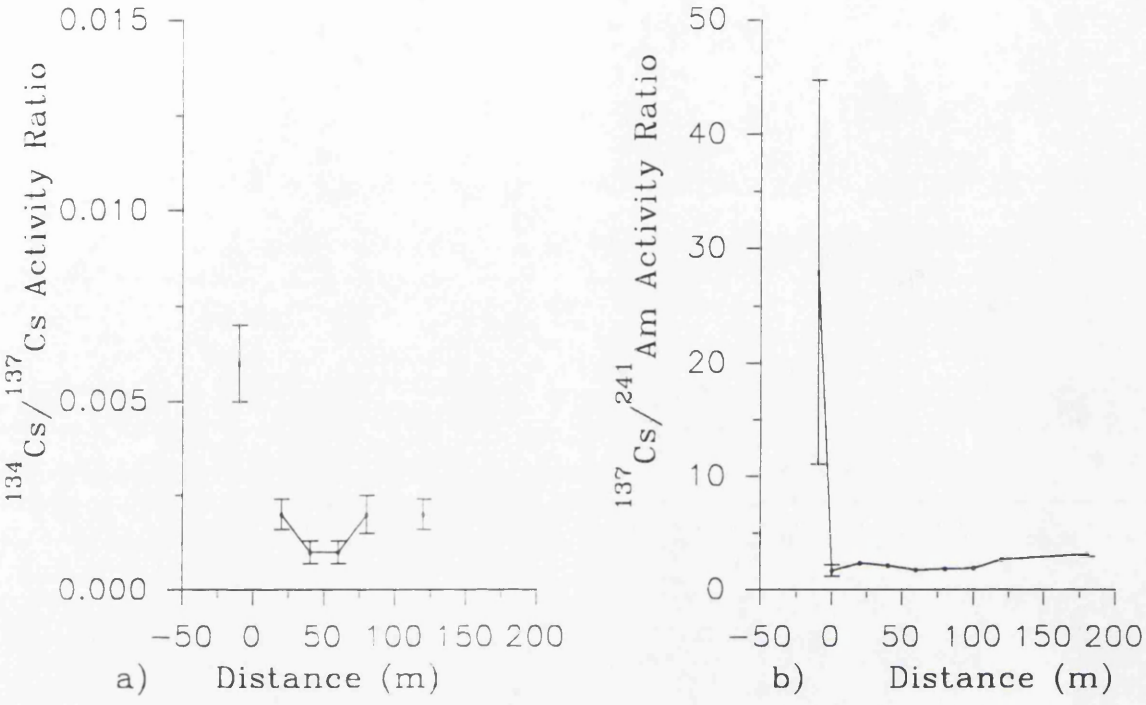

Fig 4.42a The ^{137}Cs inventories for the 0–15 cm, 15–30 cm and 0–30 cm depth intervals for Orchardton transect T1.

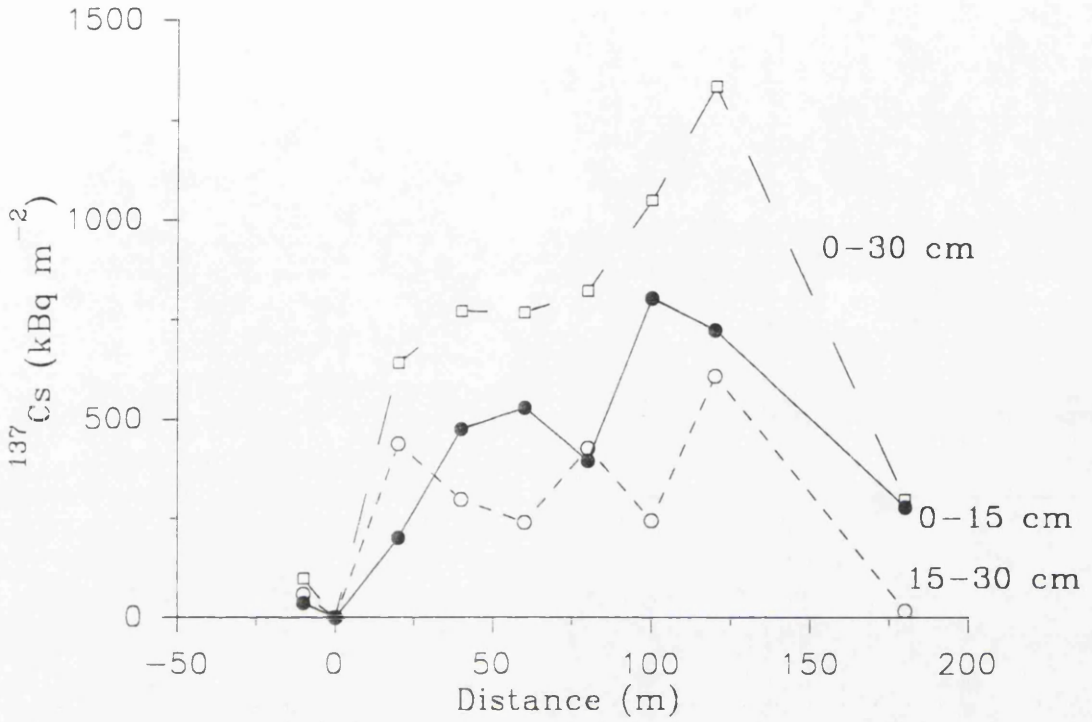

Fig 4.42b The ^{241}Am inventories from the 0–15 cm, 15–30 cm and 0–30 cm depth intervals for Orchardton transect T1.

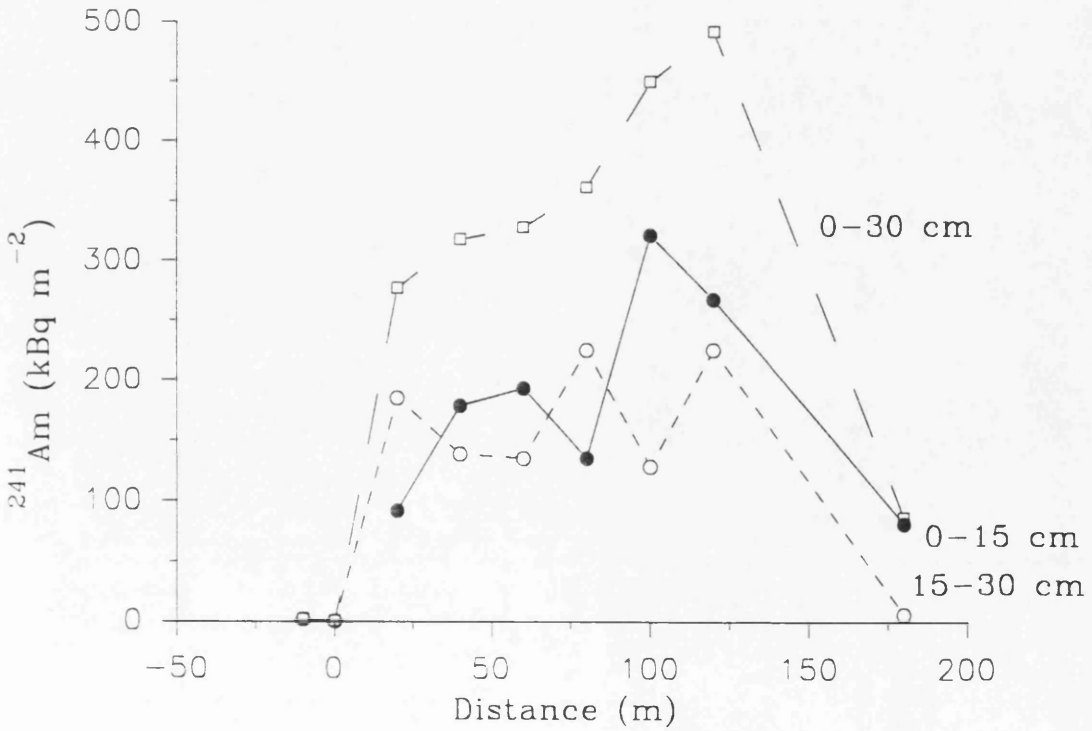

The $^{137}Cs/^{241}Am$ activity ratio (Fig 4.39b) increases to 80 m, dips slightly then increases to a maximum at 180 m. This indicates an enhancement of the ^{137}Cs values at this site which is consistent with the presence of Chernobyl fallout on moving inland. The 15-30 cm interval $^{137}Cs/^{241}Am$ activity ratio (Fig 4.40b) exhibits a general increase inland.

4.2.5 Kippford

The merse at Kippford has a relatively low elevation with the height of the stepped edge at the MHWM being approximately 0.3 m. The radionuclide concentrations for the Kippford transect are listed in Tables 3.12 and 3.13 for the 0-15 cm and 15-30 cm depths respectively and illustrated in Figs 4.43 and 4.45. The concentrations of ^{137}Cs and ^{134}Cs increase inland to a maximum at 60 m before declining. In contrast, the ^{241}Am concentrations were limited to 20 m inland, with a maximum value in the 0-15 cm interval of 626 Bq kg^{-1} at 20 m. There were insufficient ^{241}Am data above the limit of detection within the 15-30 cm transect to enable construction of a graph. The transects show maximum concentrations inland which are similar to the other transects investigated, however, the variation between the location of the maximum concentrations of ^{137}Cs (60 m) and ^{241}Am (20 m) would indicate that there are two sources of radionuclide supply to this site. If the presence of ^{241}Am up to 20 m inland is assumed to mark the limit of Sellafield influence then the ^{137}Cs and ^{134}Cs concentrations up to 80 m would indicate the presence of Chernobyl fallout. However, the concentrations of ^{137}Cs observed at Kippford produce inventories which are significantly larger than any previously reported inventory attributable to Chernobyl (38,700 Bq m^{-2}, McDonald *et al.*, 1992). The ^{137}Cs inventories minus the Chernobyl component range between 341,000 Bq m^{-2} - 591,000 Bq m^{-2}. These values are far too large to be attributable to Chernobyl fallout and would therefore indicate the presence of Sellafield effluent. This is inconsistent with the observation that the presence of ^{241}Am is restricted to only 20 m inland. Given that a particulate transport mechanism has been advocated for this location, the only rational explanation centres on the deposition of older radiocaesium discharged during the 1960's and early 1970's before the ^{241}Am discharges increased. Sub-surface maxima were not observed at Kippford which indicates generally low sedimentation rates.

Fig 4.43 Radionuclide concentrations for 0–15 cm samples from Kippford transect T1, collected 28/8/90.

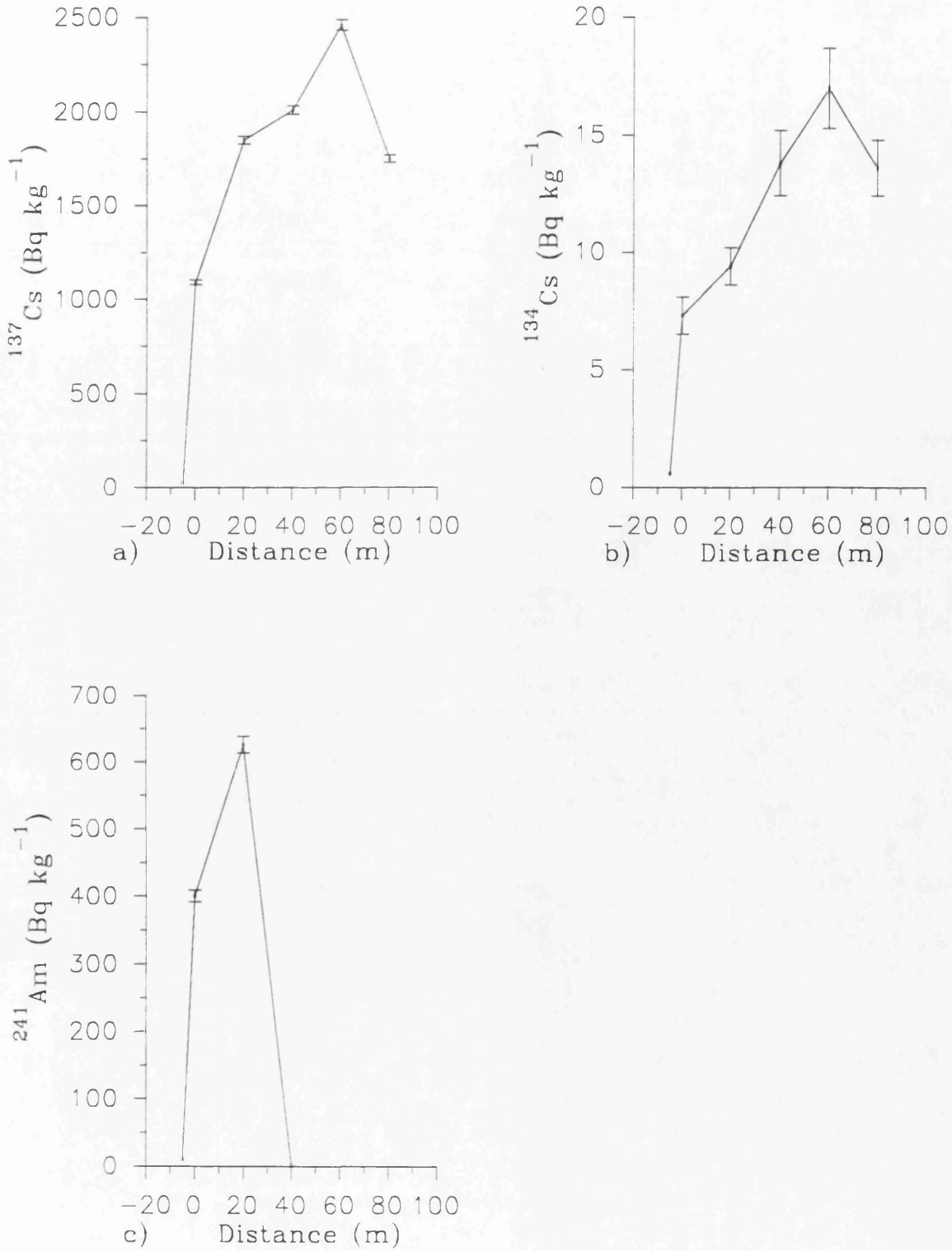

Fig 4.44 Radionuclide and Isotope activity ratios of 0–15 cm samples from Kippford transect T1.

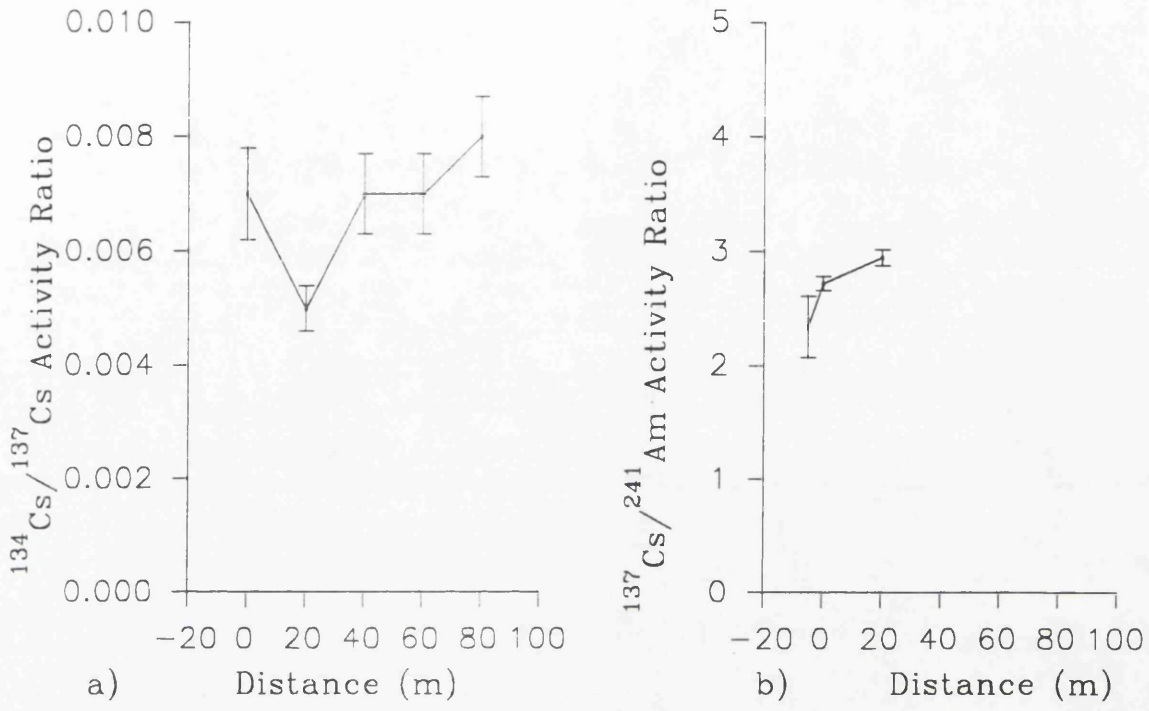

Fig 4.45 Radionuclide concentrations and isotope activity ratios for 15–30 cm samples from Kippford transect T1.

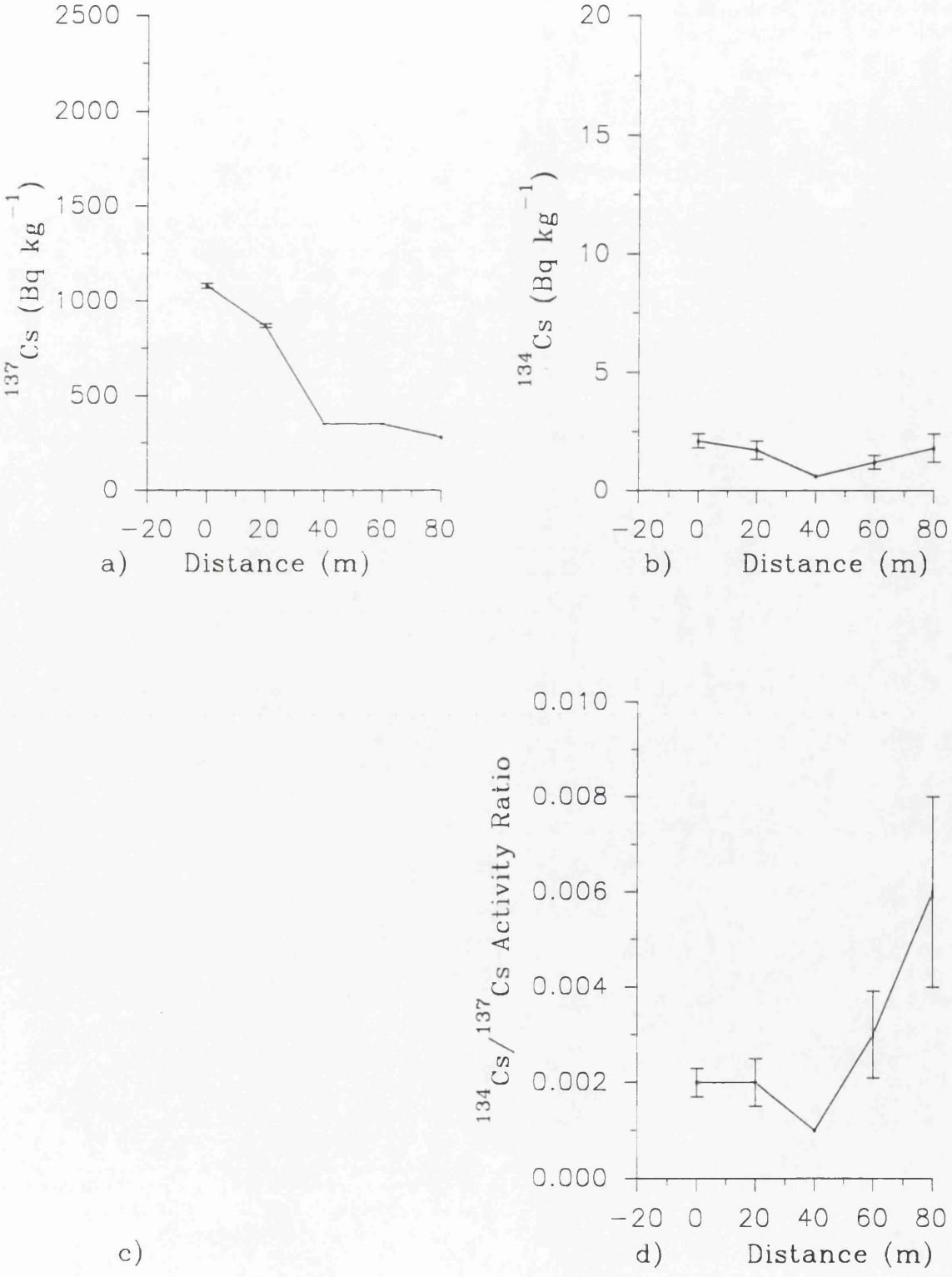

Fig 4.46a The ^{137}Cs inventories in the 0–15 cm, 15–30 cm and 0–30 cm depth intervals for Kippford transect T1.

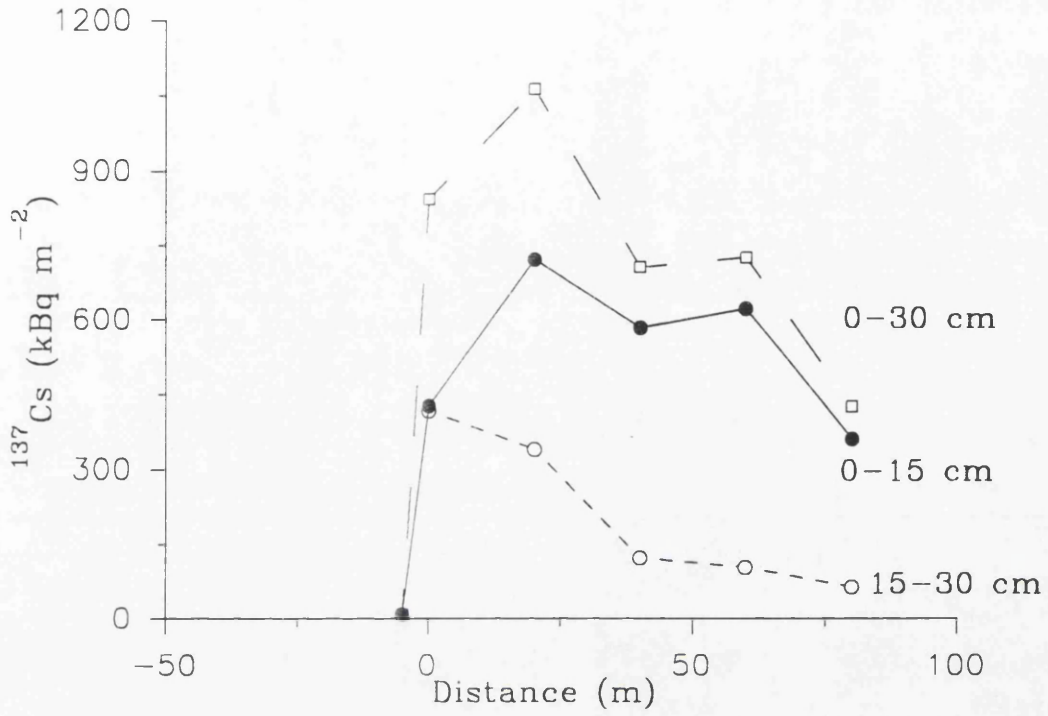

Fig 4.46b The ^{241}Am inventories in the 0–15 cm, 15–30 cm and 0–30 cm depth intervals for Kippford transect T1.

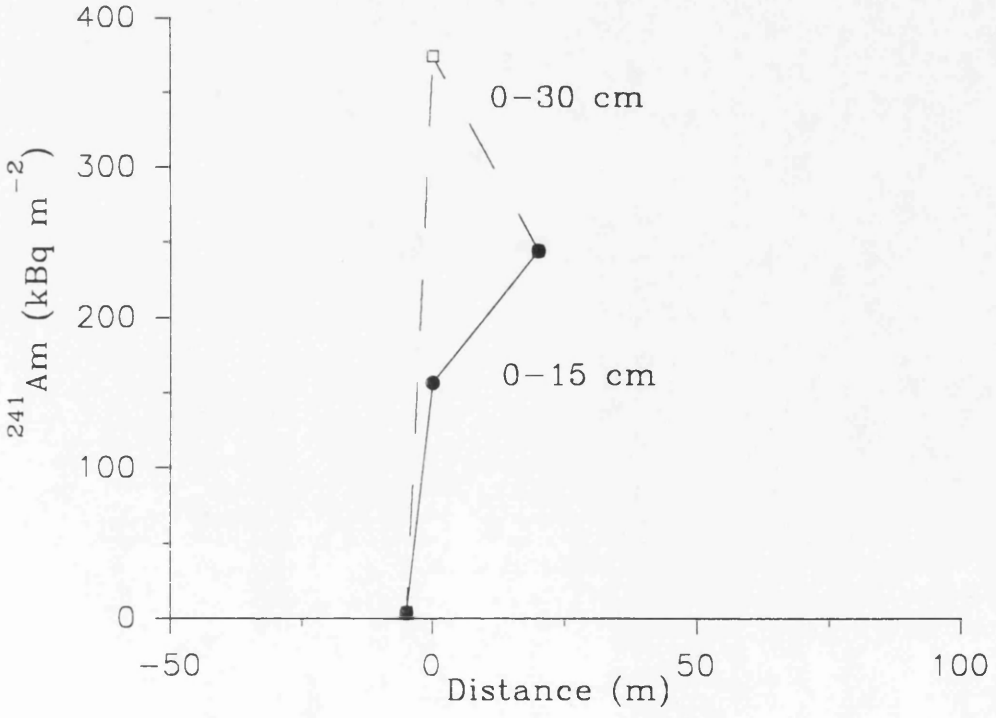

The inventories for the Kippford transect (Fig 4.46) are high in comparison with the Creetown, Wigtown and Southwick transects. The magnitude of the inventories in the 0-15 cm depth interval are very similar to the Orchardton data, with ^{137}Cs values increasing to 722,000 Bq m^{-2} at 20 m before declining to 361,000 Bq m^{-2} at 80 m. The ^{241}Am concentrations produce a maximum inventory of 244,000 Bq m^{-2} at 20 m. The total inventories are illustrated in Fig 4.46 and show an increase inland to 20 m before declining. The $^{134}Cs/^{137}Cs$ activity ratios are illustrated in Fig 4.44a for the 0-15 cm interval samples and show similarities to the Orchardton transect. The ratio at Kippford declines from the MHWM to 20 m inland which suggests the presence of older radiocaesium from Sellafield. The 15-30 cm activity ratio (Fig 4.45d) supports this observation with a ratio of ~0.002 up to 20 m inland. Both activity ratios increase from beyond 20 m which combined with the absence of ^{241}Am data indicates the presence of Chernobyl fallout. However, as discussed above the magnitude of the inventories are far too large to be attributable to Chernobyl.

4.2.6 Carse Bay

The merse at Carse Bay is less extensive than at the other locations, forming a small fringe beyond the sand and mudflats. The radionuclide concentrations recorded at Carse Bay are listed in Tables 3.14 and 3.15 and illustrated in Figs 4.47 and 4.49. The concentrations produce sub-surface maxima for ^{137}Cs within the intertidal section (-90 m to 0 m) of the transect, while inland from the MHWM, surface concentrations dominate. The ^{241}Am data produce sub-surface maxima only for sites located between 90 m and 40 m out from the MHWM, thereafter surface concentrations dominate. The concentration trends within the transect show an increase inland towards the MHWM (0 m) before declining across the consolidated merse. The ^{137}Cs concentrations in the 0-15 cm interval produce a maximum value at 30 m inland from the MHWM. In contrast, the maximum ^{241}Am value is located at the MHWM, however, the general trend is very similar.

The pronounced variations in the ^{241}Am and ^{134}Cs concentrations indicate that this transect is different from the others. The transect also has sub-surface maxima within the 'intertidal' zone, unlike previous transects. In addition, the transect

Fig 4.47 Radionuclide concentrations of 0–15 cm samples from Carse Bay transect T1. collected 15/8/91.

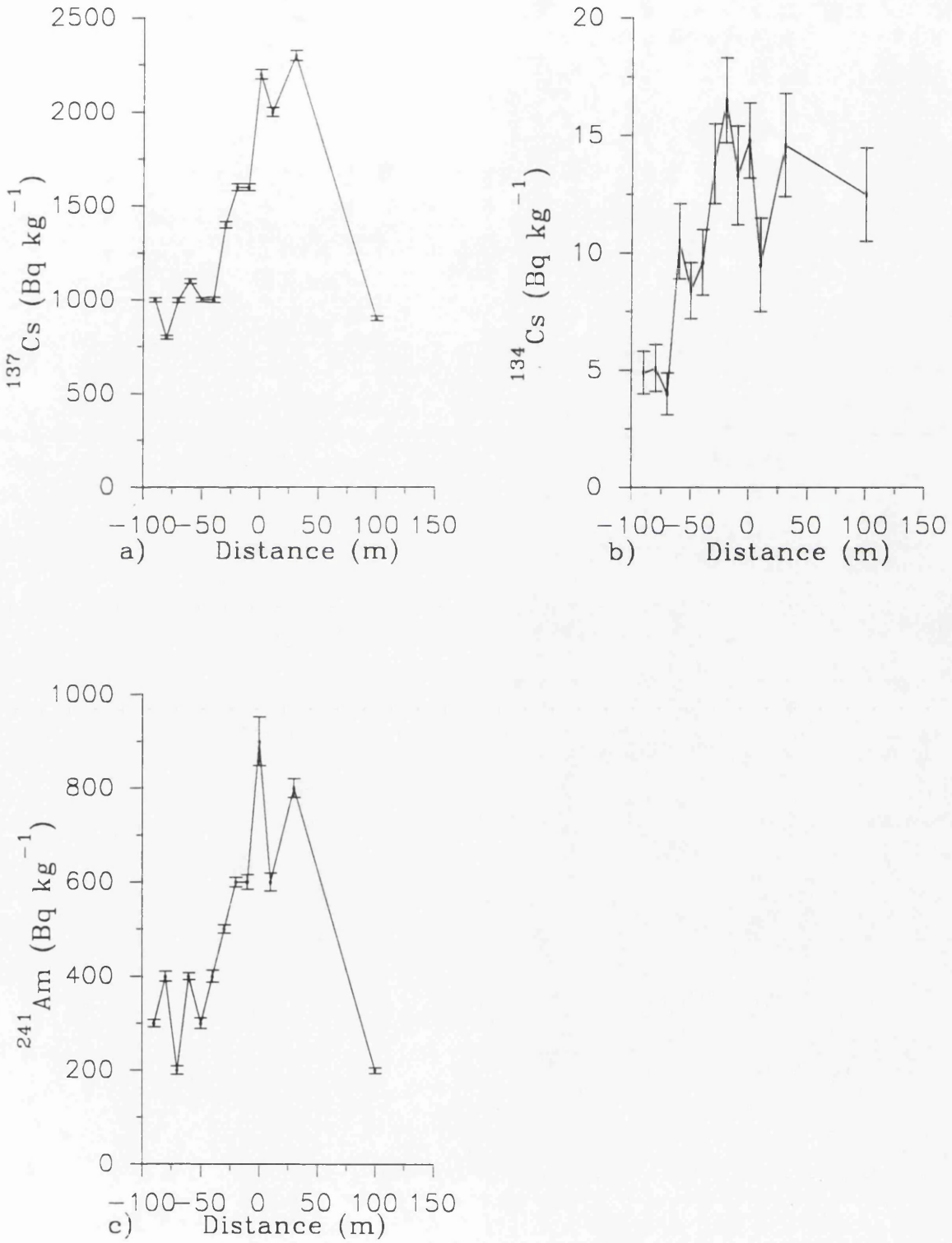

Fig 4.48 Radionuclide and Isotope activity ratios of 0–15 cm samples from Carse Bay transect T1.

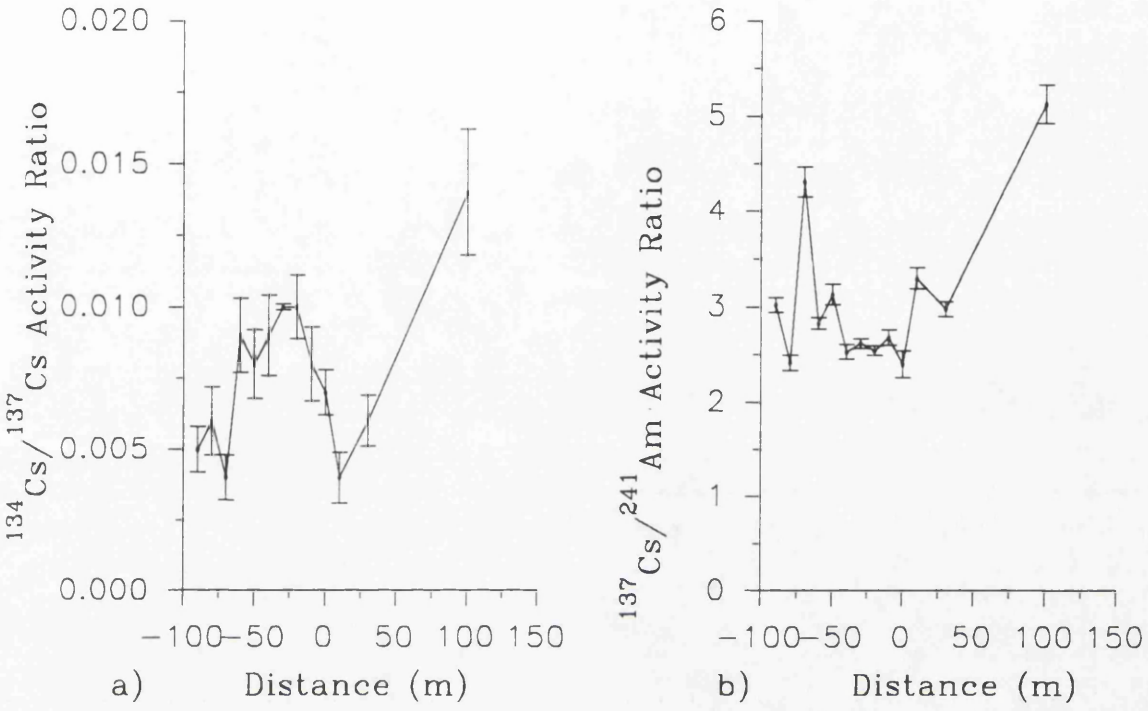

Fig 4.49 Radionuclide concentrations in 15–30 cm samples from Carse Bay transect T1.

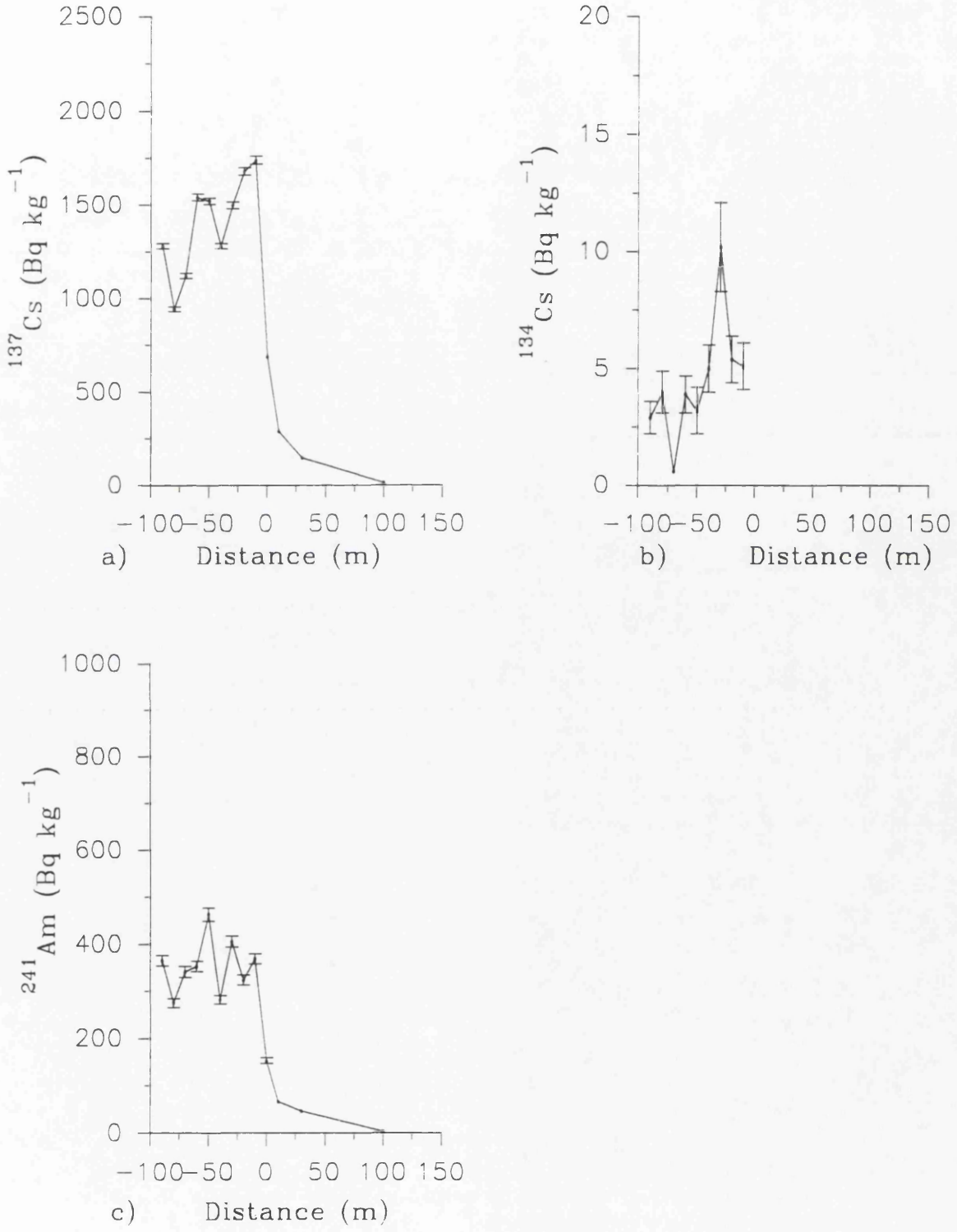

displays similar trends to the Southwick transect where concentrations in both the 0-15 cm and 15-30 cm depth intervals declined dramatically due to the influence of a topographic feature, the 'step' at 20 m. The variation in concentration within the intertidal zone can be accounted for by the sampling strategy. Samples were collected along the transect which traversed across an area consisting of small 'islands' of merse surrounded by intertidal sediment. The variations observed relate to the type of material sampled, in that the merse 'islands' produced slightly higher concentrations than the adjacent sediment as has been observed at Creetown.

The Carse Bay transect beyond the MHWM displays a pronounced similarity to the Southwick transect values from beyond the step at 20 m inland, with the 0-15 cm concentrations being one order of magnitude greater than the corresponding 15-30 cm values.

The $^{134}Cs/^{137}Cs$ activity ratio for the 0-15 cm interval (Fig 4.48a) increases inland to 80 m out from the MHWM before declining to 0.004 at 10 m inland, the ratio then increases to 0.014 at 100 m. The presence of an increasing $^{134}Cs/^{137}Cs$ activity ratio would argue for the influence of Chernobyl fallout, however, this is difficult to rationalise with the position within the intertidal zone. However, the fact that 'islands' of consolidated merse were sampled along with unconsolidated sediment would suggest that Chernobyl radiocaesium could have been deposited on these islands before they were as severely affected by erosion as they are at present. The increasing ratio beyond the MHWM would imply the presence of Chernobyl fallout. The $^{134}Cs/^{137}Cs$ activity ratio for the 15-30 cm interval are incomplete but display a low range of values indicating older deposits.

The $^{137}Cs/^{241}Am$ activity ratio fluctuates but generally increases inland with a range of values from 2.4 to 5.1 while the range is small a large excess of ^{137}Cs over ^{241}Am at 100 m (5.13) is observed which would support the observation of the presence of Chernobyl fallout at this inland location. The 15-30 cm activity ratio (Fig 4.48b) displays similar fluctuations within the intertidal zone but declines inland suggesting the presence of older effluent.

Fig 4.50 Radionuclide and Isotope activity ratios for 15–30 cm samples from Carse Bay transect T1.

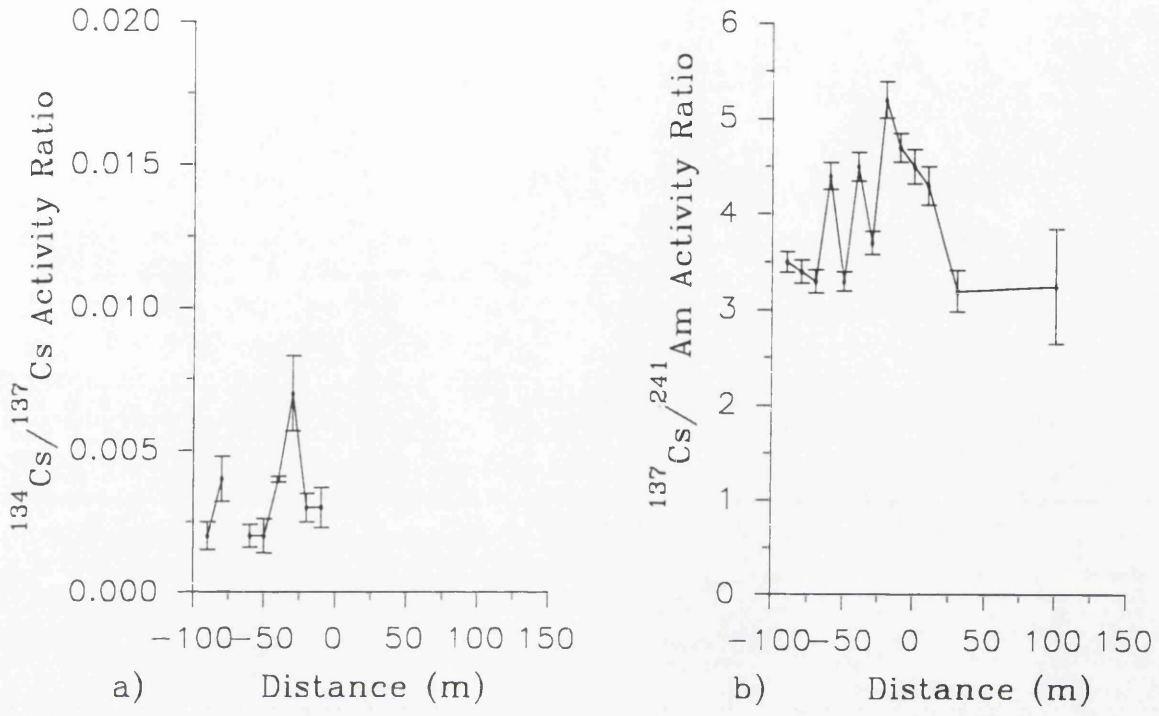

Fig 4.51a The ^{137}Cs inventories for the 0–15 cm, 15–30 cm and 0–30 cm depth intervals from Carse Bay transect T1.

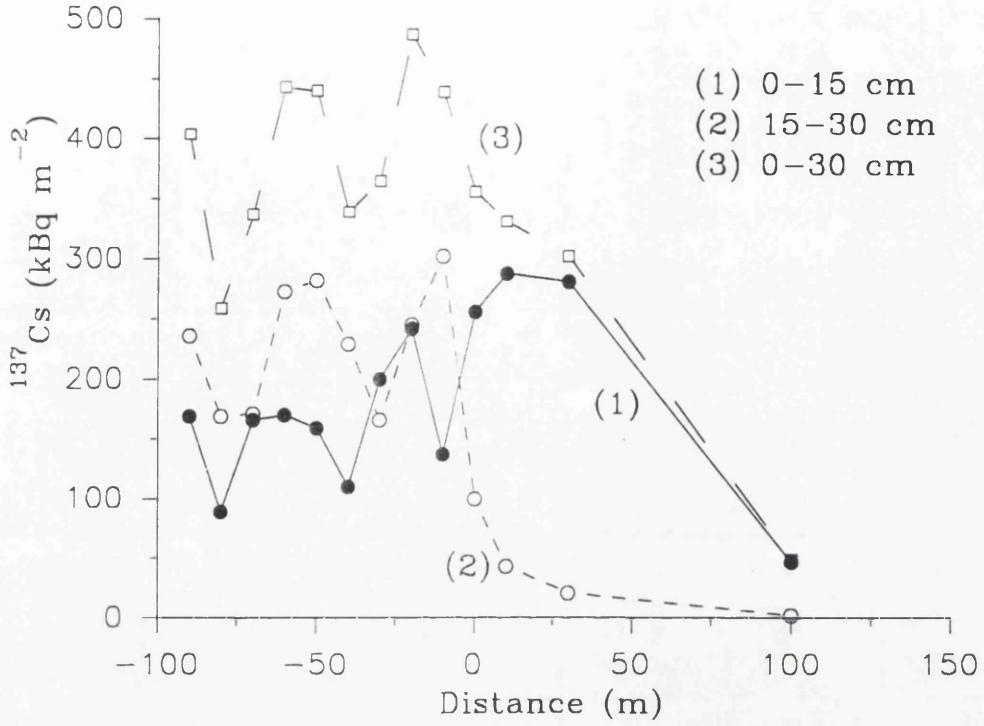

Fig 4.51b. The ^{241}Am inventories for the 0–15 cm, 15–30 cm and 0–30 cm depth intervals from Carse Bay transect T1.

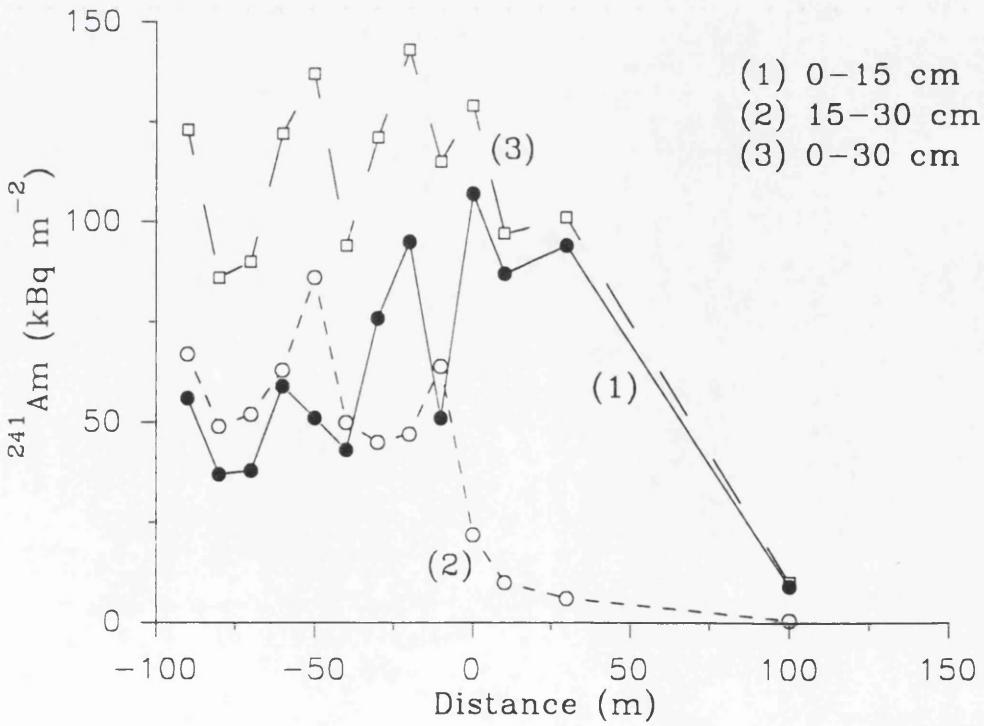

The total inventories for the Carse Bay transect are illustrated in Fig 4.51 and show generally lower inventories than recorded at other locations, except Southwick, with a pronounced decline inland across the consolidated merse.

4.2.7 Overview of Radionuclide Distribution in Merse Transects

There are a few general comments which can be made regarding the transect data outlined above. The results show large lateral variations in radionuclide concentrations within the merse deposits and indicate an increasing depth of distribution towards the MHWM. Table 4.1 lists the maximum, mean and minimum ^{137}Cs and ^{241}Am concentrations recorded at each site with the transects listed in accordance to their westward location on the coast of the Solway Firth. These results are illustrated in Fig 4.52 for ^{137}Cs and Fig 4.53 for ^{241}Am. The results clearly show the large concentration range within each transect, and also show the pronounced differences in concentrations recorded at the different transect locations which are separated by up to 60 km. There are generally strong similarities between the trends in the ^{137}Cs and ^{241}Am graphs with a distinct trend east to west. The maximum concentrations of ^{137}Cs at Carse Bay, Southwick, Kippford and Orchardton are very similar, however, there is a distinct decline further west at Creetown with the lowest maximum concentration at Wigtown which is located some 60 km west of Carse Bay. The ^{241}Am data display more variation but the general trend is the same. The transect at Southwick displays the lowest maximum and mean values of the four most eastward locations which are separated by a distance of approximately 20 km. This is probably due to the enclosed riverine location at Southwick which may experience less frequent and prolonged tidal inundation than other locations. The variation in concentration within each transect, together with the increasing depth distribution towards the MHWM clearly presents problems for evaluating a total inventory and for monitoring radionuclide levels. Samples collected from the 0-30 cm depth interval from the area closest to the MHWM on the seaward side of the merse would effectively underestimate the total radionuclide inventory while samples from further inland would result in an overestimation of the total inventory within the merse areas.

Table 4.1 Maximum, Minimum And Mean ^{137}Cs And ^{241}Am Concentration Values In The 0-15 cm Interval For The Merse At Each Transect.

	Maximum Concentration		Minimum Concentration		Mean Concentration	
	^{137}Cs (Bq kg^{-1})	^{241}Am (Bq kg^{-1})	^{137}Cs (Bq kg^{-1})	^{241}Am (Bq kg^{-1})	^{137}Cs (Bq kg^{-1})	^{241}Am (Bq kg^{-1})
Wigtown	729	176	30	19	472	103
Creetown	1680	516	789	221	1142	340
Orchardton	2560	966	4	287	1572	580
Kippford	2460	626	1090	400	1832	513
Southwick	2070	610	228	13	687	203
Carse Bay	2320	901	887	173	1859	619

Fig 4.52 The maximum, minimum and mean ^{137}Cs concentrations within the 0–15 cm depth intervals of the transects collected along the coast of the Solway Firth.

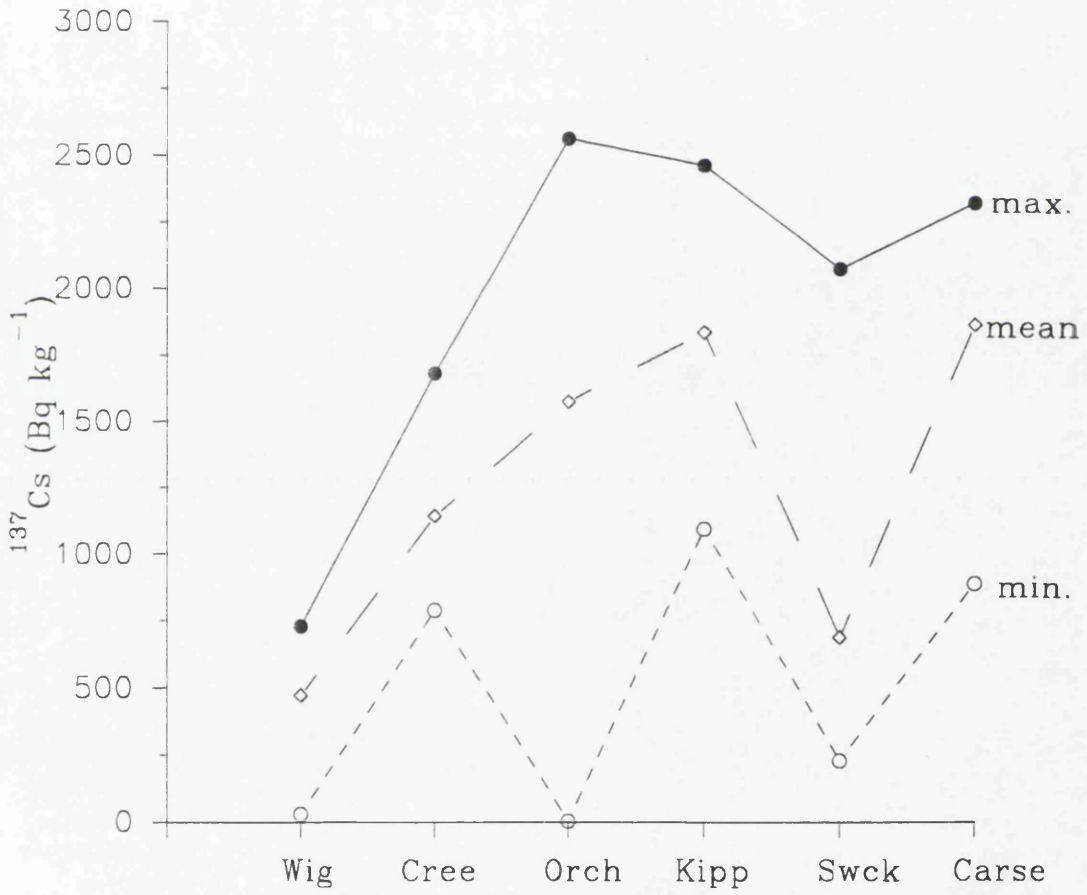

Fig 4.53. The maximum, minimum and mean ^{241}Am concentrations in the 0–15 cm depth intervals from the transects collected along the coast of the Solway Firth.

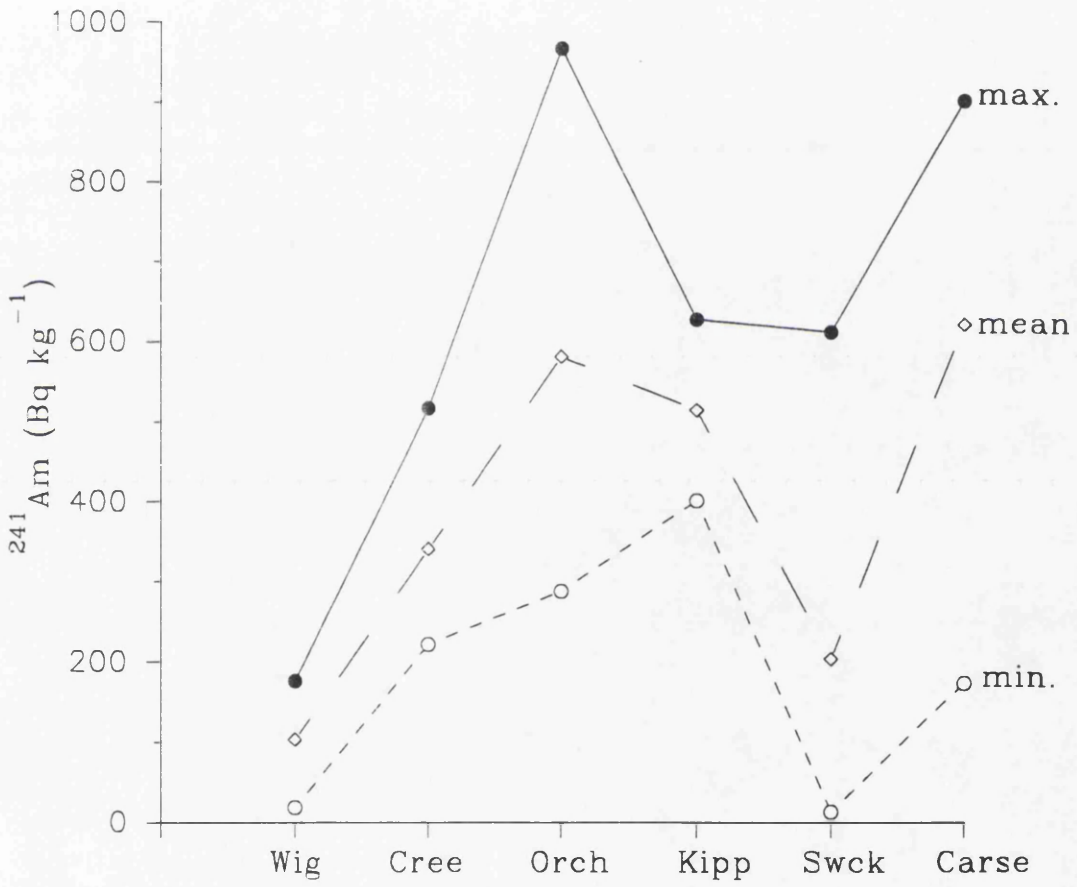

Thus, when calculating the total radionuclide inventory of the merse areas, the deposition pattern with maximum concentrations at depth (> 30 cm) near the edge of the merse (MHWM) as illustrated by Southwick Core No. 1 (SC1) and Ben-Shaban (1989) in Section 4.1, together with the lateral distribution of radionuclides which exhibit increasing concentrations in the surface layers inland, must be taken into account. Table 4.2 lists the maximum, mean and minimum inventories for the transects and these results are illustrated in Figs 4.54 and 4.55. The variation in inventories within each transect, evident from Table 4.2 illustrates the problems associated with sample collection strategies for environmental monitoring purposes. Failure to recognise and sample the distinct depositional zones will effectively lead to an erroneous estimate of the total inventory of the merse. In addition, in view of the presence of sub-surface maxima near the MHWM (below 30 cm), collection of samples from the 0-15 cm and 15-30 cm depth intervals may be underestimating the inventories near the edge of the merse.

Similar problems regarding the lateral and spatial distribution of radionuclides within merse areas are encountered when addressing the determination of human radiation exposure. Data for the dose calculation must be collected across the whole merse area, paying particular attention to the high surface concentrations observed up to 180 m inland from the MHWM (0 m). Failure to undertake this will result in inaccuracy in estimating the radiation dose to humans in this area. These locations close to the banks of the merse are popular areas for recreational pursuits such as bird watching, fishing, wildfowling, mooring boats and walking. In addition, the myriad of drainage channels within the saltmarsh will also produce their own 'deposition' zones with high concentrations although on a much smaller scale. Therefore, the estimation of inventories and human radiation exposure doses have to account for the distinct depositional trends within merse environments if the calculations are truly to reflect the significance of environmental distribution and human occupancy characteristics.

The total inventories for each transect location using the maximum, mean and minimum inventory values in Table 4.2 and the merse areas calculated by the NCC (1989) are listed in Table 4.3. The results clearly show the variation in inventories produced through using these values and emphasises the need to adopt a suitable

Table 4.2 Maximum, Minimum And Mean ^{137}Cs And ^{241}Am Inventories For 0-30 cm Interval From The Merse Area Within Each Transect

	Maximum Inventory		Minimum Inventory		Mean Inventory	
	^{137}Cs (kBq m^{-2})	^{241}Am (kBq m^{-2})	^{137}Cs (kBq m^{-2})	^{241}Am (kBq m^{-2})	^{137}Cs (kBq m^{-2})	^{241}Am (kBq m^{-2})
Wigtown	431	103	10	6	260	54
Creetown	756	246	392	92	575	168
Orchardton	1,335	491	2	84	711	330
Kippford	1,063	374	425	244	752	309
Southwick	339	123	22	1	158	51
Carse Bay	356	129	49	10	260	84

Table 4.3 Total ^{137}Cs And ^{241}Am Inventories (0-30 cm) Observed At Each Transect Location, With The Areas Determined From NCC(1989)

Total Radionuclide Inventories							
		^{137}Cs			^{241}Am		
Location	Area (ha)	Maximum	Minimum	Mean	Maximum	Minimum	Mean
Wigtown	180	7.8×10^{11}	1.8×10^{10}	4.7×10^{11}	1.9×10^{11}	1.1×10^{10}	9.7×10^{10}
Creetown	370	2.8×10^{12}	1.4×10^{12}	2.1×10^{12}	9.1×10^{11}	3.4×10^{11}	6.2×10^{11}
Orchardton	54	7.2×10^{11}	1.1×10^{9}	3.8×10^{11}	2.7×10^{11}	4.6×10^{10}	1.8×10^{11}
Kippford	57	6.0×10^{11}	2.4×10^{11}	4.3×10^{11}	2.1×10^{11}	1.4×10^{11}	1.8×10^{11}
Southwick	56	1.9×10^{11}	1.2×10^{10}	8.8×10^{10}	6.8×10^{10}	5.6×10^{8}	2.9×10^{10}
Carse Bay	35	1.2×10^{11}	1.7×10^{10}	9.1×10^{10}	4.5×10^{10}	3.5×10^{9}	2.9×10^{10}

Fig 4.54 The maximum, minimum and mean ^{137}Cs inventories within the transects collected along the coast of the Solway Firth.

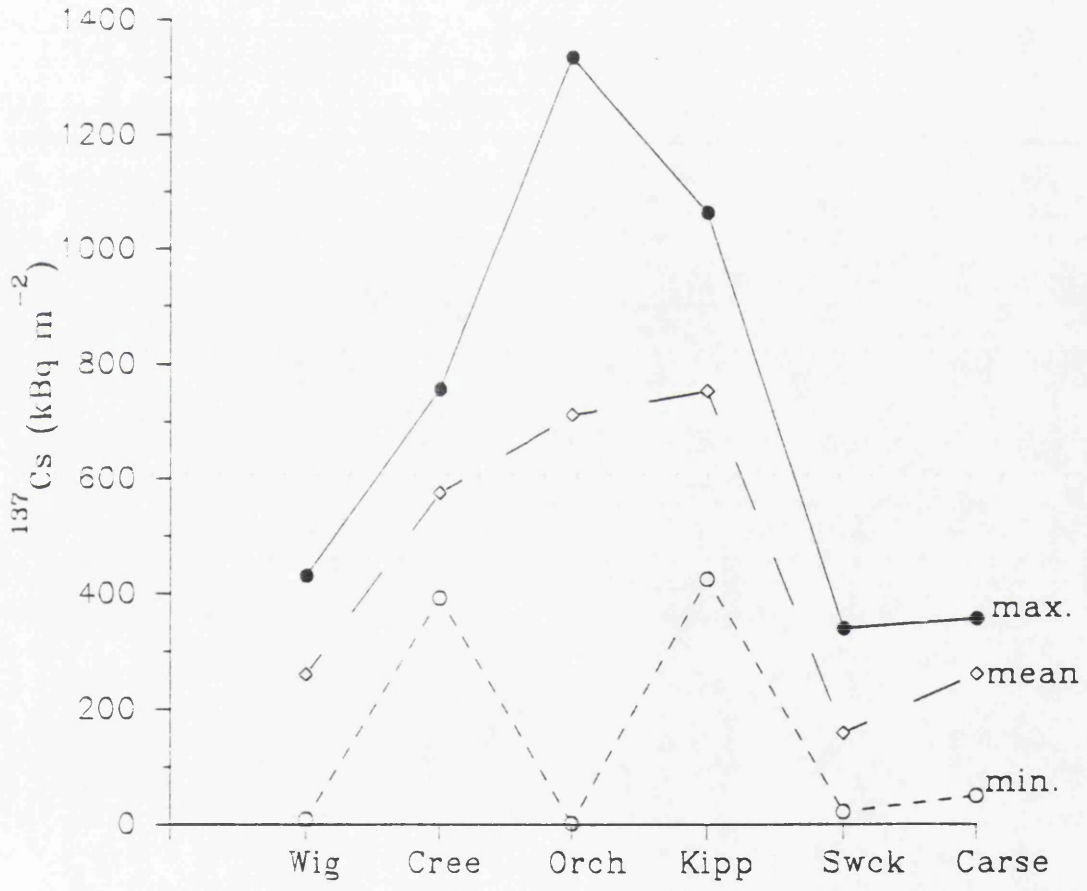

Fig 4.55 The maximum, minimum and mean ^{241}Am inventories for the merse transects collected along the coast of the Solway Firth.

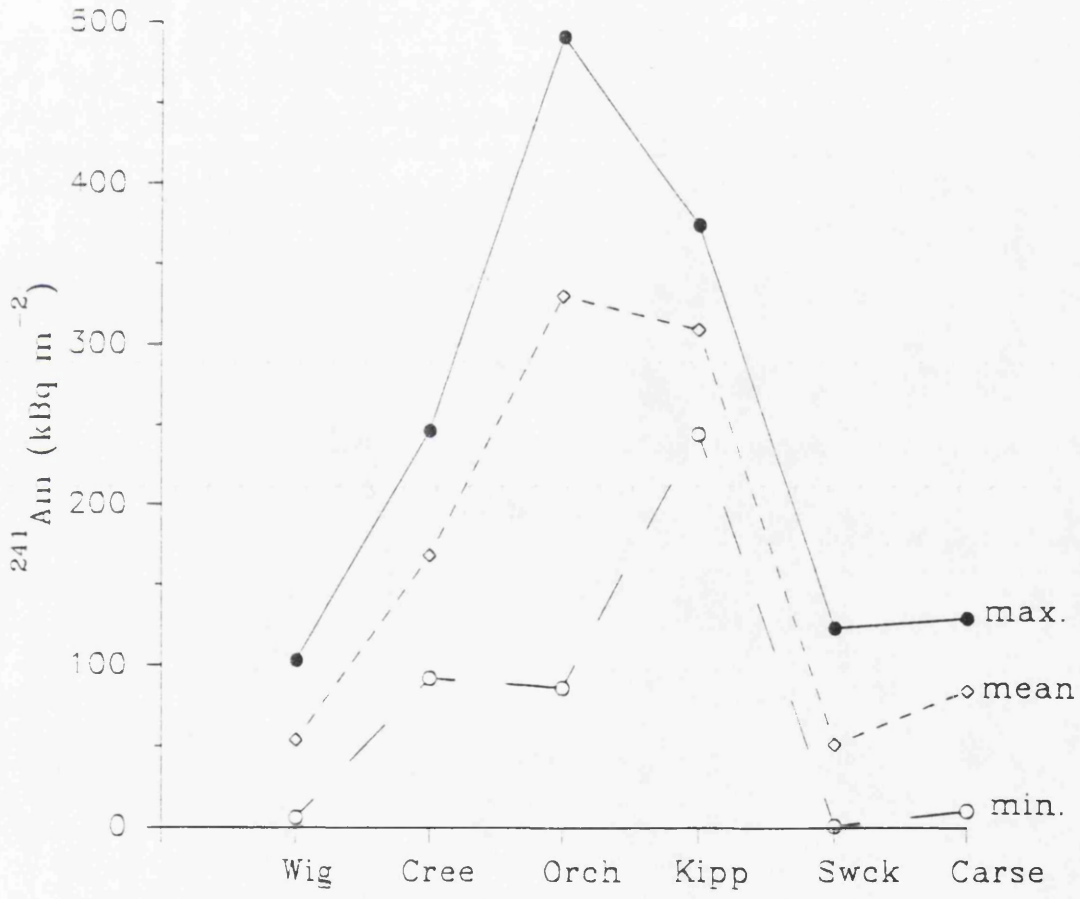

sampling strategy to enable realistic environmental monitoring.

A major feature of the transects is the pronounced minima observed at or near the MHWM (0 m). At the Wigtown and Orchardton transects, the minima values are observed at the MHWM, however, at the other transects the minimum concentrations are observed in the intertidal sediments close to the MHWM. The most likely cause of the minima are deposition of coarse grained sediment with correspondingly lower concentrations than fine grained sediment or the erosion of the merse exposing relatively uncontaminated sediment. Deposition of coarse grained sediment is highly plausible given that the MHWM is a high energy environment where a high degree of mixing and turbation occurs. The second possibility of erosion of the merse at the MHWM exposing uncontaminated sediments is also highly plausible, Allen and Pye (1993) observed retreat of the vertical cliff face of the saltmarsh in the Blackwater Estuary by up to 5 m during storm surge events during the period 1987-90. In summary both explanations are plausible and perhaps a combination of buried sediment which is exposed through erosion combined with deposition of coarse grained material could be responsible for the minimum values observed at the transect locations.

This section has highlighted the very high inventories which are present within the merse environments of south west Scotland. These inventories are generally at least one order of magnitude greater than the highest Chernobyl inventory (38,700 Bq m^{-2}) recorded by McDonald *et al.,* (1990) within the same area. In addition the inventories are considerably higher than the inventories attributable to weapons fallout of 3,700 Bq m^{-2} of ^{137}Cs (Cawse and Horrill, 1986) and 55 Bq m^{-2} of $^{239+240}Pu$ (Pierson *et al.,* 1982). There is a distinct trend east to west in the data, with the highest concentrations being recorded at the more eastward sample locations. The westward locations at Wigtown and Creetown exhibit concentrations which are almost one order of magnitude lower than the eastern transects. This reflects the effects of distance from Sellafield, with contaminated sediment being diluted and homogenized during transportation to the sample sites. Within the transects there are also distinct depositional patterns with pronounced minima in concentrations at or close to the MHWM before levels increase inland, with the area of merse (> 20 m) adjacent to the MHWM exhibiting sub-surface maxima

beyond which surface concentrations dominate.

4.3 VERTICAL DISTRIBUTION OF RADIONUCLIDES IN MERSE ENVIRONMENTS

It is apparent from the results of the previous section dealing with the lateral distribution of radionuclides across the merse deposits, that additional information on the vertical distribution of contaminant radionuclides is required to provide data for evaluation of total radionuclide inventories in these deposits. It is also clear that radionuclide vertical distributions vary with position in the merse and it is necessary to characterise such variations in order to evaluate the accuracy of monitoring techniques using either a limited number of discrete samples or fieldwork gamma spectroscopy. A series of soil cores and sections was therefore sampled at selected locations at Southwick Water to provide such information.

The radionuclide concentrations for a set of 1 m cores extracted along transect T2 at 5 m, 10 m, 20 m and 30 m inland from the edge of the merse (MHWM), are set out in Tables 3.16-3.19 and are illustrated in Figs 4.56-4.59. Transect T2 was located close to the site of Southwick Core No. 1 and the 1 m cores were extracted using the Farnel Corer as described in Section 2.1.2. Southwick Core No. 1, discussed in detail in Section 4.1, was extracted from the 70 cm cliff face at the stepped edge of the merse. Samples were extracted in blocks with a surface area of 10 x 15 cm in 5 cm depth intervals. The profile produced sub-surface maxima of 1,880 Bq kg^{-1} of ^{137}Cs and 687 Bq kg^{-1} of ^{241}Am at a depth of 35-40 cm with concentrations below the maxima declining rapidly and consistently with depth.

I Southwick Transect T2 5 m Core (T2.5)

It is evident from Fig 4.56a that the concentrations of ^{137}Cs in the core from the 5 m position exhibited a sub-surface maximum of 2,670 Bq kg^{-1} at a depth of 20-25 cm, below which they declined in a regularly fluctuating pattern. The ^{137}Cs and ^{241}Am (Fig 4.56b) concentrations observed for this core are larger than those reported for section SC1 and the sub-surface maxima occur some 10-15 cm closer to the surface. The upper sections of the profiles are similar to the features

Fig 4.56 Concentrations of radionuclides in Southwick T2 5m

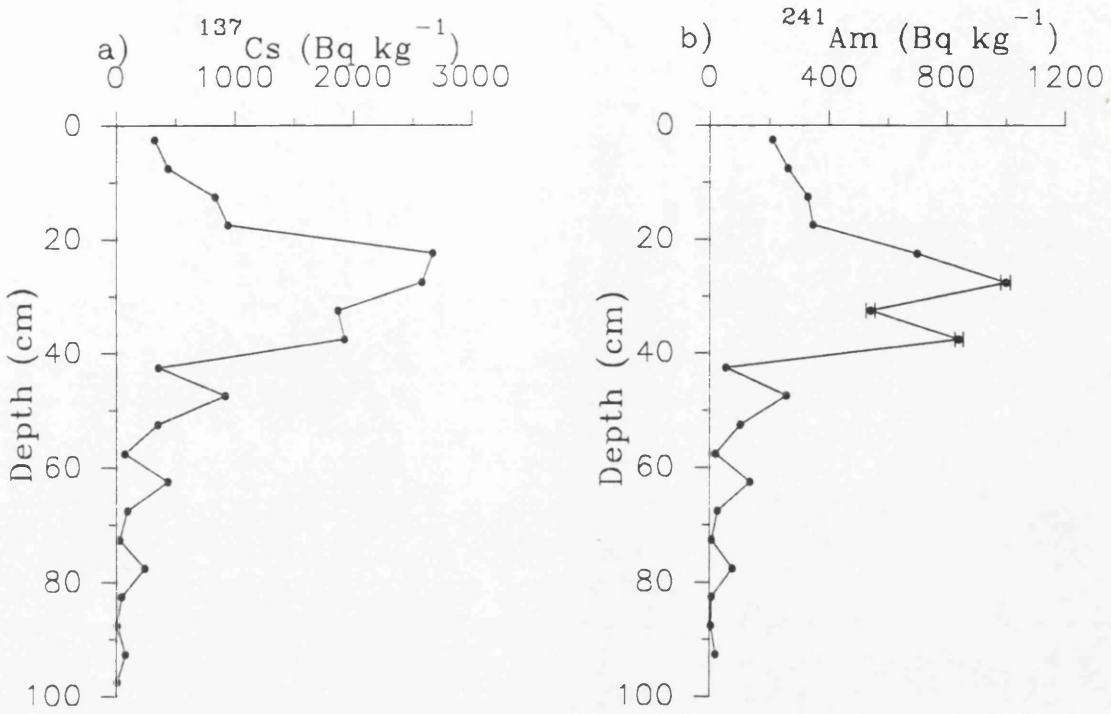

Fig 4.57 Concentrations of radionuclides in Southwick T2 10m

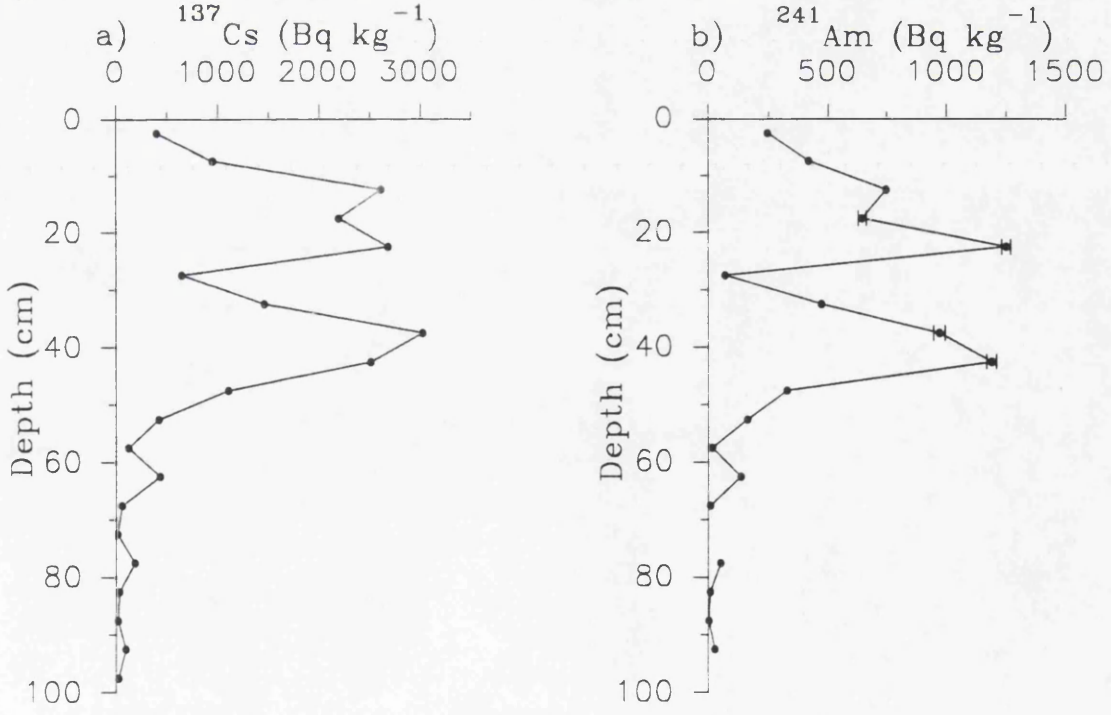

observed for SC1 but the fluctuations in concentration at depth contrast with the consistent decline with depth observed in SC1. The concentrations in core T2.5 cannot be directly compared with a corresponding sampling point in transect T1, because one was not collected due to the 10 m sampling interval adopted for that transect. However, the values may be compared with the mean of the concentrations in the 0 m and 10 m sampling points from transect T1. The concentrations in T2.5 would appear to be in good agreement with those for the corresponding transect samples from T1, with T2.5 having mean ^{137}Cs concentrations of 530 Bq kg^{-1} and 2,062 Bq kg^{-1} for the 0-15 cm and 15-30 cm intervals respectively while the T1 samples had corresponding values of 900 Bq kg^{-1} and 1,400 Bq kg^{-1}. The radionuclide inventories for the total core are 631,000 Bq m^{-2} of ^{137}Cs and 220,000 Bq m^{-2} of ^{241}Am, however, due to the absence of a corresponding sampling point in transect T1 these inventories cannot be compared. The ^{137}Cs profile for core T2.5 has a sub-surface maximum at 20-25 cm, but 45% of the total ^{137}Cs occurs below this depth. Thus, it is apparent that only 55% of the radiocaesium concentrations within the core will be sampled if 0-15 cm and 15-30 cm strategy is adopted and analysis of these samples, as carried out in transect T1, will significantly underestimate radionuclide inventories in this case.

Core T2.5 exhibits sub-surface maxima at 20-25 cm and 25-30 cm in the ^{137}Cs and ^{241}Am profiles, which have qualitatively similar trends to those of the Sellafield annual discharge data.

Treatment of the results in detail, as carried out in Section 4.1 for the section SC1, using the ratio of maximum to surface sediment concentrations in T2.5 compared to the ratio of the maximum Sellafield discharge to the 1990 value indicates discrepancies between the sediment core profiles and the Sellafield discharge. For example the ratio of maximum concentration of ^{137}Cs to the surface concentration was 8.3 compared with 222.6 for the Sellafield annual discharge. Similar results were obtained for the ^{241}Am data and this indicates that the distributions do not bear a quantitative relationship to the Sellafield annual discharge. The $^{137}Cs/^{241}Am$ activity ratio for the core samples ranges between 1.5-6.5 compared with 7.0-1218 for the Sellafield values, again revealing that the radionuclide distribution in the core does not bear a quantitative relationship to the discharge. On the basis of

the model set out in Section 4.1 the sedimentation rates for this core were calculated as 1.6 cm y^{-1} on the basis of ^{137}Cs and 1.5 cm y^{-1} for ^{241}Am, with a mean value of 1.6 cm y^{-1}.

The trends in the T2.5 ^{137}Cs and ^{241}Am profiles (Fig 4.56a, b) match exactly, even down to the fine structure, giving a strong linear correlation (R^2 = 0.92) between the two. A correlation of this type did not occur in the Sellafield annual discharge which showed an R^2 value of 0.05. The pronounced fluctuations in concentrations lower in the core are distinctly different from the trends observed for SC1 and those observed by Ben-Shaban at a nearby location (Ben-Shaban,1989). The fluctuations apparent at depth in T2.5 produce regular trends in the data, with maxima every 15 cm within the profile which corresponds to the depth of insertion of the metal sheath used in the Farnel Corer. This suggests that the fluctuating radionuclide concentrations at depth are attributable to the sample collection procedure and that the results from this core (T2.5) are somewhat anomalous.

II Southwick Transect T2 10 m (T2.10)

The radionuclide concentration profiles for the core T2.10, collected 10 m inland from the MHWM, are illustrated in Fig 4.57. The mean ^{137}Cs concentrations of 1,320 Bq kg^{-1} (0-15 cm) and 1,840 Bq kg^{-1} (15-30 cm) can be compared with 703 Bq kg^{-1} and 1,280 Bq kg^{-1} for the corresponding depth intervals for the sample from the 10 m position in transect T1. Similarly the mean ^{241}Am concentrations of 469 Bq kg^{-1} (0-15 cm) and 655 Bq kg^{-1} (15-30 cm) for T2.10 can be compared with 341 Bq kg^{-1} and 445 Bq kg^{-1} for the corresponding intervals in the transect T1 10 m site.

The total radionuclide inventories for the core are 711,000 Bq m^{-2} of ^{137}Cs and 246,000 Bq m^{-2} for ^{241}Am, with the 0-30 cm intervals producing an inventory of 414,000 Bq m^{-2} of ^{137}Cs and 147,000 Bq m^{-2} of ^{241}Am. These values compare with 315,000 Bq m^{-2} and 123,000 Bq m^{-2} for ^{137}Cs and ^{241}Am inventories in transect T1. Thus, the radionuclide inventories obtained for corresponding depth intervals of the transect and the core are very similar, but the total inventories for the core suggest that the transect values only give 44-50% of the true inventories because of the

failure to sample below 30 cm.

Both radionuclide concentration profiles exhibit similar trends with sub-surface maxima which are separated into two distinct peaks at depths of 20-25 cm and 40-45 cm. The concentrations below the maxima decline rapidly but exhibit the regularly fluctuating pattern that was observed in the core T2.5. The double maximum observed in the T2.10 core ^{137}Cs and ^{241}Am profiles does not match either the trends in the Sellafield discharges or the profiles for section SC1 or core T2.5. Linear regression analysis of the ^{137}Cs and ^{241}Am concentrations produced an R^2 value of 0.91, consistent with the observation for core T2.5 but not with the temporal trends in the discharge.

The $^{137}Cs/^{241}Am$ activity ratio for the 10 m core has a range of values between 1.6 and 9.3 which are very similar to the 5 m core but contrasting markedly with the range of values in the Sellafield annual discharges. Thus, the cores T2.5 and T2.10 exhibit anomalous profiles, with trends that are difficult to relate to each other or to the sediment profiles or the Sellafield discharge.

III Southwick Transect T2 20 m (T2.20)

The radionuclide concentration profiles for core T2.20 collected 20 m inland from the MHWM, are illustrated in Fig 4.58. The radionuclide concentrations reported in Table 3.18 are lower than the values observed for the 5 m and 10 m cores but the mean ^{137}Cs values of 1,190 Bq kg^{-1} (0-15 cm) and 93 Bq kg^{-1} (15-30 cm) compare reasonably favourably with those of 2,070 Bq kg^{-1} and 205 Bq kg^{-1} for the corresponding depth intervals for the sample from 20 m in transect T1. The ^{241}Am concentrations exhibit very similar results for the 0-15 cm interval with mean concentrations of 469 Bq kg^{-1} (T2) compared with 610 Bq kg^{-1} in transect T1. The concentrations of ^{241}Am in the 15-30 cm are very similar with a mean T2 core value of 24 Bq kg^{-1} compared to 32 Bq kg^{-1} for transect T1. The variation between the inventories calculated from the core data and the transect data is more pronounced at the this site with the core producing an inventory of 179,000 Bq m^{-2} of ^{137}Cs compared with 305,000 Bq m^{-2} from the transect. The $^{137}Cs/^{241}Am$ activity ratio ranges between 2.5 and 12.6 which is a slightly greater range of

Fig 4.58 Radionuclide concentrations in Southwick T2 20 m

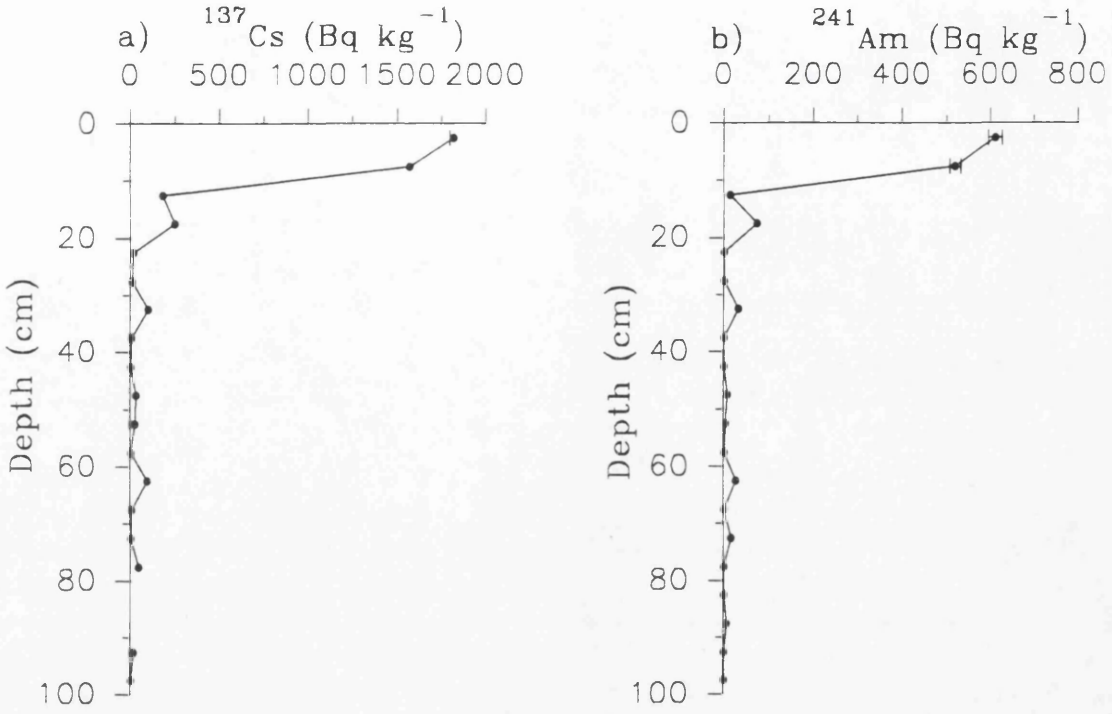

Fig 4.59 Radionuclide concentrations in Southwick T2 30 m.

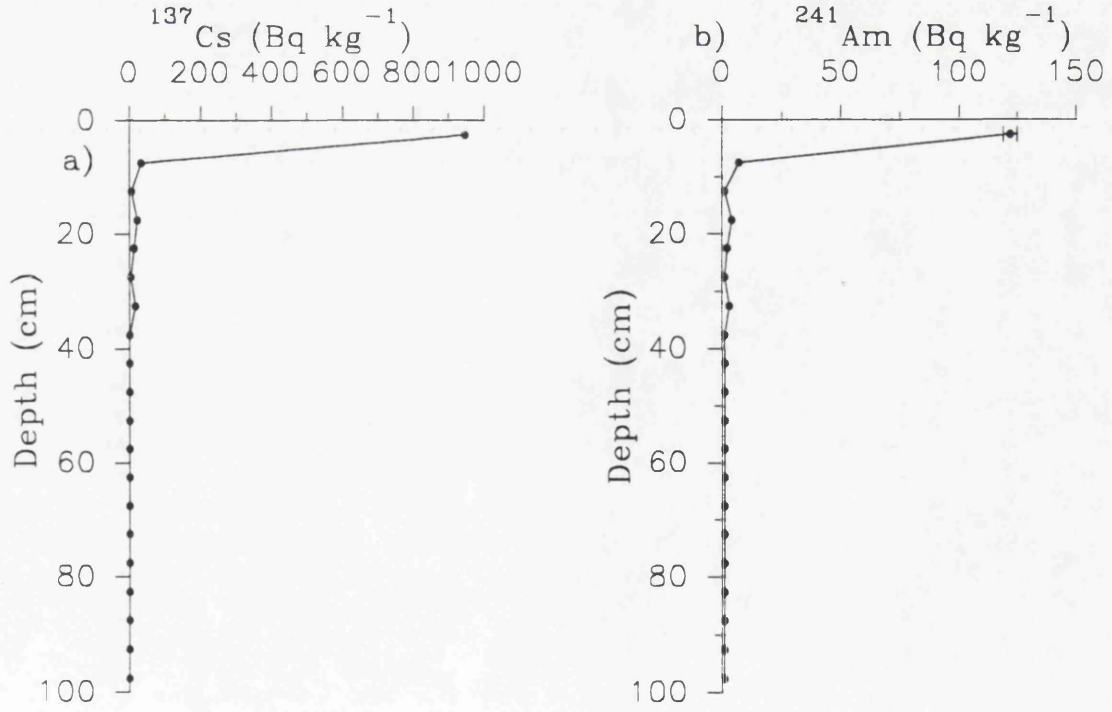

values than those recorded in the other cores. The profiles for core T2.20 (Fig 4.58) show that the radionuclides are predominantly confined to the surface layers of the 0-15 cm interval, with no sub-surface maxima and indicate a decreasing depth of penetration of the radionuclides into the sediments on moving inland. This observation is consistent with the increased elevation and surface topography of the merse on moving inland, producing lower sedimentation due to the reduced frequency of inundation. The decrease in radionuclide penetration agrees with the trends reported for transect T1 where sub-surface maxima were confined to areas less than 20 m from the MHWM. The core profiles (Fig 4.58a, b) produce irregular fluctuations to considerable depths. If the maximum Sellafield discharges are confined to the 0-5 cm depth interval then a sedimentation rate of approximately 0.18 cm y^{-1} can be determined. Therefore the presence of radionuclides at depths approaching 100 cm is not reasonable and suggests contamination. On the evidence of the cores collected in transect T2 it appears that the technique of coring to depths in 15 cm increments does produce reasonable agreement for radionuclide inventories with the T1 transect samples distribution but anomalies of regular fluctuations in concentrations and variations in the depth of penetration are observed.

IV Southwick Transect T2 30 m

The results from Southwick T2 30 cm are illustrated in Fig 4.59 and show a shallow depth of penetration of the radionuclides with no sub-surface maxima. The trend in the concentrations fluctuates with depth and again the presence of radionuclides at such depth is unexpected. In comparison with the corresponding data from transect T1, the total inventories for the core are 39,000 Bq m^{-2} of ^{137}Cs and 5,000 Bq m^{-2} of ^{241}Am which are in reasonable agreement with the transect T1 data of 64,000 Bq m^{-2} of ^{137}Cs and 17,000 Bq m^{-2} of ^{241}Am.

The use of the Farnel Corer thus gives results for the 0-15 cm and 15-30 cm depth intervals that are generally in reasonable agreement with the T1 transect data. However, fluctuations at depth and anomalous depth of penetration are less easily explained. Examination of the data reveals regular trends in the results, with maxima at every 15 cm within each data set, corresponding to the depth of

insertion of the metal sheath used in the Farnel Corer. This suggests that the regularly fluctuating radionuclide concentrations at depth are attributable to the sample collection procedure and that the practice of re-inserting the metal sheath into the hole excavated by the previous sections led to the transmission of sediment from the higher concentrations of the surface layers down the core despite considerable efforts to avoid this.

In order to test this hypothesis, a further set of samples was obtained from the Southwick site by extracting sections as described below.

SOUTHWICK TRANSECT T3

Samples were obtained as discussed in Section 2.1.4 from a series of soil pits dug at 5 m, 10 m and 15 m inland from the stepped edge of the merse near the site of SC1.

I Southwick Transect T3 5 m Section (S3.5)

The radionuclide concentrations for this section are listed in Table 3.20 and illustrated in Fig 4.60. It is evident from Fig 4.60a that the sub-surface maximum for ^{137}Cs was at 20-25 cm with a concentration of 2,450 Bq kg^{-1}. The concentrations declined relatively smoothly and rapidly after the 30-35 cm depth interval from 319 Bq kg^{-1} to 3 Bq kg^{-1} at a depth of 75-80 cm. Figure 4.61 shows the ^{137}Cs profiles for S3.5 and the corresponding core sample T2.5 and reveals reasonably close agreement between the two profiles from the surface to the maximum at 20-25 cm. Below the maximum however, variations are apparent between the profiles, with the pronounced, regular fluctuation in concentration in the T2.5 profile being absent from section S3.5. This clearly illustrates the effects of the sample collection techniques and supports the argument that the Farnel Corer generates spurious results if used to collect sequential depth increments and should not be used through repeated insertions of the metal sheath.

The concentrations of ^{134}Cs (Fig 4.60b) and of ^{241}Am (Fig 4.60c) produced very similar profiles with distinct sub-surface maxima in the top 30 cm of the section

Fig 4.60 Concentrations of radionuclides in Southwick T3 5m

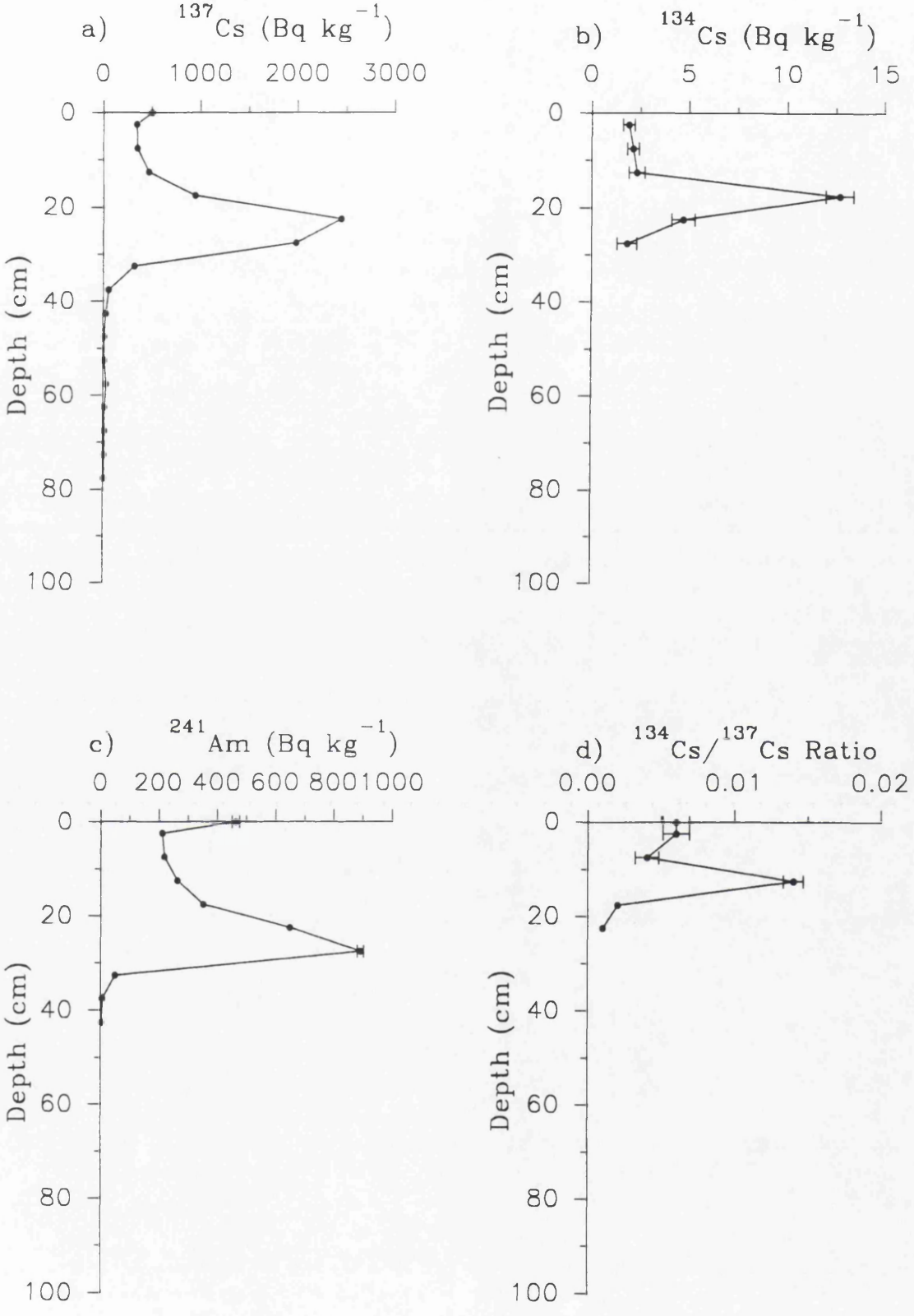

and confirm the absence of regularly varying concentrations at depth. The radionuclide concentrations in this section are directly comparable with the SC1 concentrations. The surface grass concentrations exhibit slightly enhanced values over the adjacent sediment values but since corresponding concentrations were not recorded for SC1 they cannot be compared. These values appear to be high for grass however, the grass had not been washed and therefore would contain a percentage of entrained silt. This observation lends support for the role that vegetation plays in promoting fine sediment accumulation in saltmarsh environments.

The ^{137}Cs and ^{241}Am concentrations observed in the top 5 cm of S3.5 exhibit slightly lower values than were observed for the corresponding section of SC1 from the stepped edge of the merse (0 m). The sub-surface maxima are however larger than those reported for SC1 and the depth of occurrence of the maxima is lower at 20-25 cm (S3.5) compared with 30-35 cm (SC1).

The sedimentation rate calculated using the procedure described for SC1 (Section 4.1) was 1.57 cm y^{-1}, which matches the value derived from core T2.5 and is lower than that for SC1 (mean 2.95 cm y^{-1}). The ^{137}Cs concentration profile is matched to the 4 year dilution model (cf Section 4.1) in Fig 4.62 and shows reasonable agreement between the shapes of the observed and predicted values, with a slight off-set due to errors in the chronology and difficulty in accurately matching the sediment data with the model due to the relatively large time span encompassed in each section (3.2 y).

The total inventories for the section are 286,000 Bq m^{-2} for ^{137}Cs and 107,000 Bq m^{-2} for ^{241}Am. The radionuclides are predominantly confined to the top 30 cm of the section, with inventories recorded for this depth interval of 270,000 Bq m^{-2} and 106,000 Bq m^{-2} for ^{137}Cs and ^{241}Am respectively. The ^{137}Cs inventory is lower than the corresponding inventories observed in transect T1 (310,000 Bq m^{-2}) and transect T2 (364,000 Bq m^{-2}). However, the ^{241}Am inventory is in close agreement with the transects T1 and T2 values 113,000 Bq m^{-2} and 134,000 Bq m^{-2} respectively. This observation of close agreement between the radionuclide inventories suggests that at this site sampling the 0-30 cm interval produces

Fig 4.61 Comparison of the ^{137}Cs concentration profiles for transect T2 (core) and transect T3 (section) at a location of 5 m inland from the MHWM at Southwick Water.

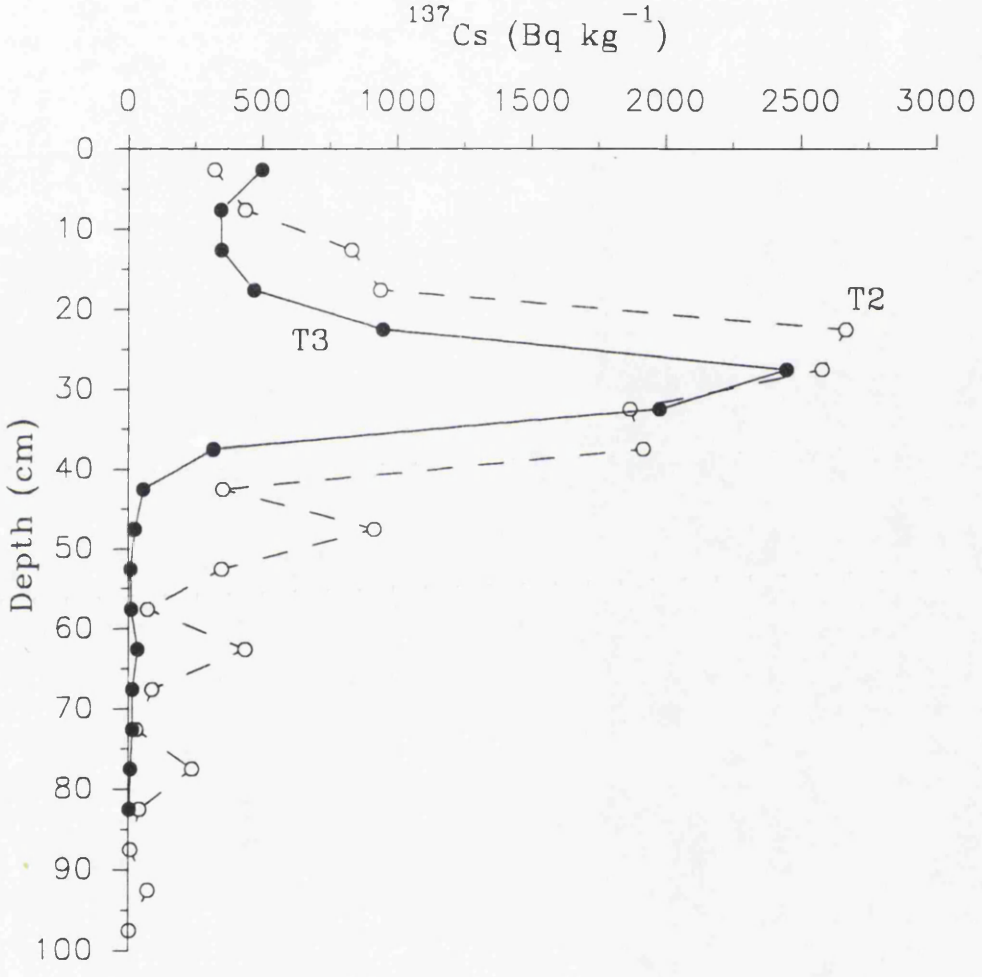

Fig 4.62 Model prediction for ^{137}Cs in Southwick section T3 5 m (T3.5) using mean sedimentation rate of 1.57 cm y^{-1} data normalised to ratio between sediment (1977) and model (1980).

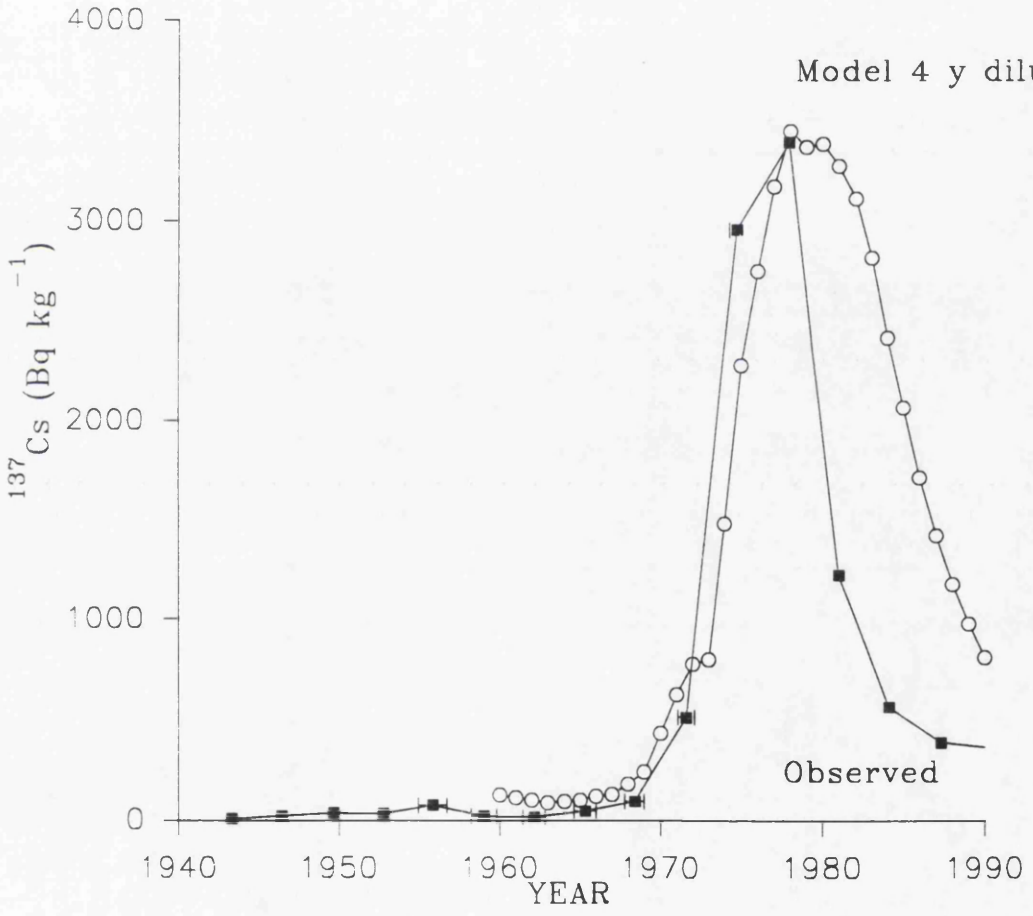

acceptable results in contrast to the conclusion inferred from the core data. The $^{137}Cs/^{241}Am$ activity ratio increases systematically with depth from 1.1 at 5 cm to 12.6 at 45 cm. Similar trends are not as easily identified in SC1 where the values exhibit slight fluctuations between 2.0 and 4.5 down to a depth of 60 cm before increasing to 20.6 at 70 cm.

The $^{134}Cs/^{137}Cs$ activity ratio illustrated in Fig 4.60d indicates that the principal source term for the radiocaesium isotopes is Sellafield although there is evidence of a contribution from Chernobyl fallout. The activity ratio values range from 0.004 to 0.014 which are well below the Sellafield annual discharge ~0.05 but above the integrated values of ~0.0021 for 1991, the most recent integrated value available from Sellafield. The trend in the profile shows a sub-surface maximum with a decrease between 5 cm and 10 cm before increasing again towards the surface. The enhanced values near the surface are almost certainly attributable to Chernobyl fallout. On the basis of the sediment chronology (1.57 cm y^{-1}) the ^{134}Cs and ^{137}Cs concentrations were decay corrected. The decay corrected $^{134}Cs/^{137}Cs$ activity ratio shows a gradual increase with depth from 0.009 (0-5 cm,1990) to 0.44 (15-20 cm,1980) with a slight decline to 0.24 (25-30 cm,1974). This variation in the activity ratio does not reflect variations in the Sellafield annual or integrated discharges. The 1990 and 1980 values are considerably larger than the annual discharge values of 0.05 and 0.08 or the integrated discharge value of 0.0028 (1990) and 0.0459 (1980) respectively. However, the 1974 value is in close agreement with the annual discharge value of 0.245.

SOUTHWICK TRANSECT T3 10 m SECTION (S3.10)

The analytical results for section S3.10 collected 10 m inland from the MHWM are listed in Table 3.21 and illustrated in Fig 4.63, which indicate that ^{137}Cs, ^{134}Cs and ^{241}Am were all confined to the top 25 cm of the sediment profile. The maximum concentration of ^{137}Cs in Fig 4.63a was 3,386 Bq kg^{-1} compared with 2,450 Bq kg^{-1} for the section S3.5 and 1,880 Bq kg^{-1} for SC1. The concentrations of ^{241}Am also exhibit similar trends, with a maximum concentration in S3.10 of 1,110 Bq kg^{-1} compared with 892 Bq kg^{-1} and 687 Bq kg^{-1} for the sections S3.5 and SC1 respectively. The maximum concentrations thus increase on moving inland, but the

Fig 4.63 Concentrations of radionuclides in Southwick T3 10m

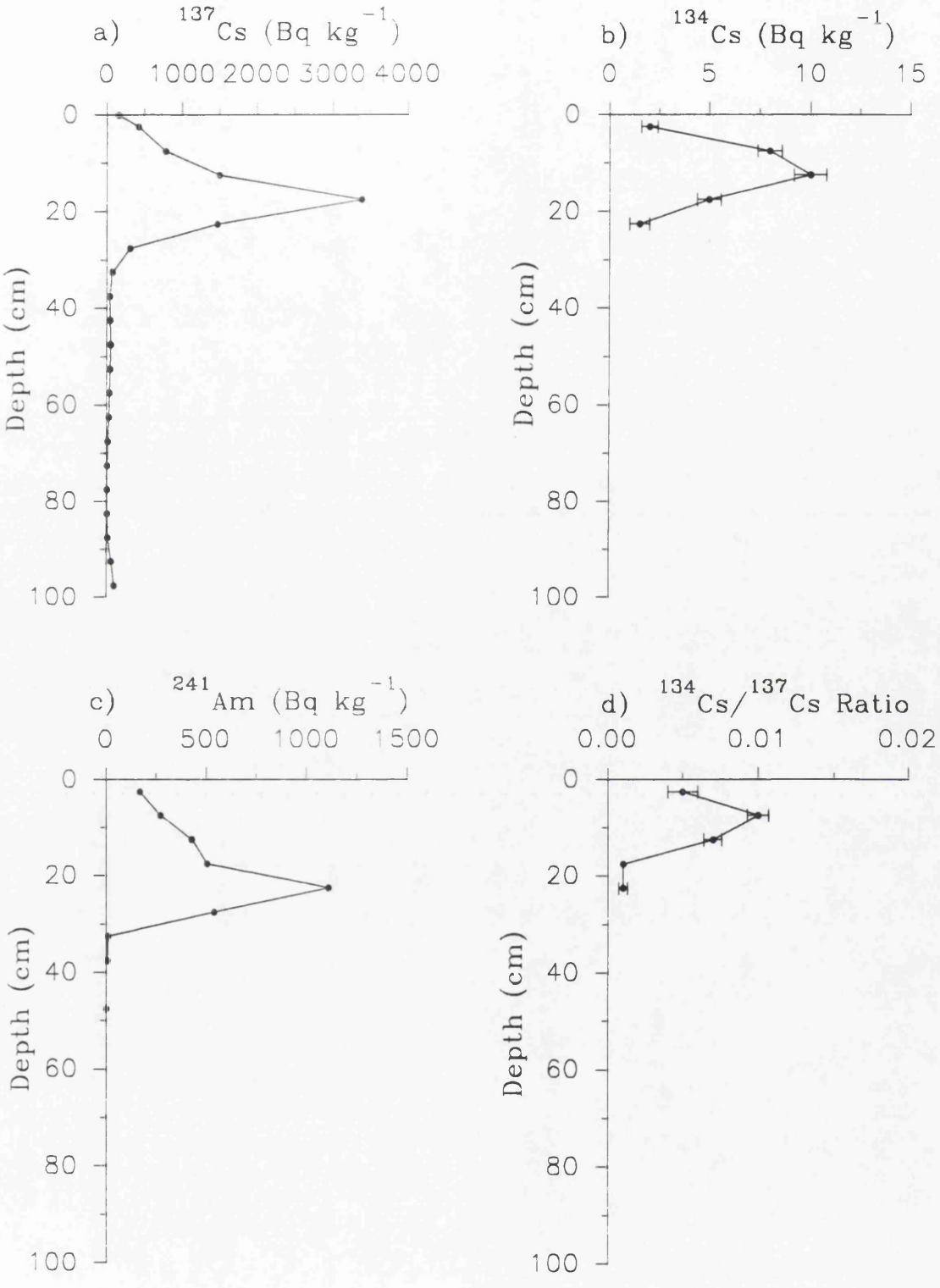

Fig 4.64 Comparison of the concentration profiles produced by transect T2 (core) and transect T3 (section) at a location of 10 m inland from the MHWM at Southwick Water.

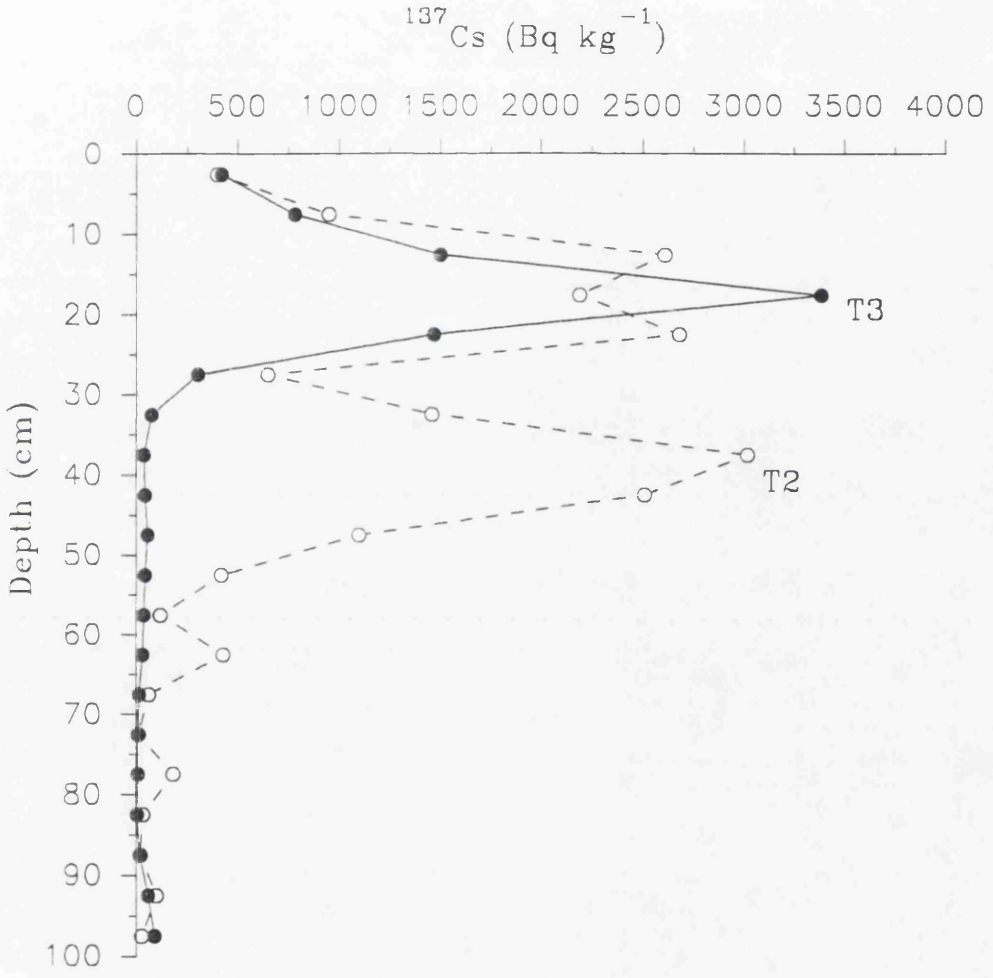

depth of occurrence of the sub-surface maxima decreases from 35-40 cm at SC1to 20-25 cm (S3.5) and 15-20 cm for S3.10. The ^{137}Cs concentration profile from section S3.10 is compared with the corresponding profile for T2.10 in Fig 4.64, which illustrates considerable differences between the two. The profile derived from the section does not exhibit the variability or sharp fluctuations observed in the core profile. The section maximum matches reasonably well with the upper peak for the core but there is no evidence of a lower peak in the section. It can be concluded that a major artefact has been produced in this core by the coring procedure. This reinforces the arguments advanced for restricting the use of the Farnel Corer to collection of samples from the surface layers or from within the limited depth of penetration of the metal sheath (15 cm).

The sedimentation rates calculated from the model (Section 4.1) and the sub-surface maxima range between 0.97 cm y^{-1} (^{241}Am) and 1.25 cm y^{-1} (^{137}Cs) which are lower than those for the 5 m section, confirming a decreasing trend in sedimentation rate on moving inland, consistent with increased elevation resulting in a decrease in frequency of tidal inundation. The model prediction for ^{137}Cs in section T3 10 m using the mean sedimentation rate of 1.11 cm y^{-1} is illustrated in Fig 4.65. The model is normalised to the ratio between 1980 which represents the peak in the sediment concentrations and 1978 the peak in the model curve. The profile illustrates the reasonably close agreement between the model predictions and the observed concentrations. Again the off-set between the observed and predicted values is attributable to errors within the chronology.

Total inventories of 510,000 Bq m^{-2} of ^{137}Cs and 168,000 Bq m^{-2} of ^{241}Am were obtained for S3.10, reflecting the increasing concentrations inland and are considerably higher than the inventories from the 5 m and SC1 sections. This is consistent with deposition of fine particulate material on moving inland.

The $^{137}Cs/^{241}Am$ activity ratios increase with depth from 0.89 at the surface to 33.67 at a depth of 25-30 cm. The range of values is greater than for the 5 m section and for SC1. The decay corrected activity ratio increases from 1.6 (0-5 cm) to 59.0 at 25-30 cm depth, this increase suggests a greater time integration

Fig 4.65 Model prediction for ^{137}Cs in Southwick section T3 10 m (T3.10) using the sedimentation rate of 1.46 cm y^{-1}, data normalised to ratio between sediment (1980) and the model (1978).

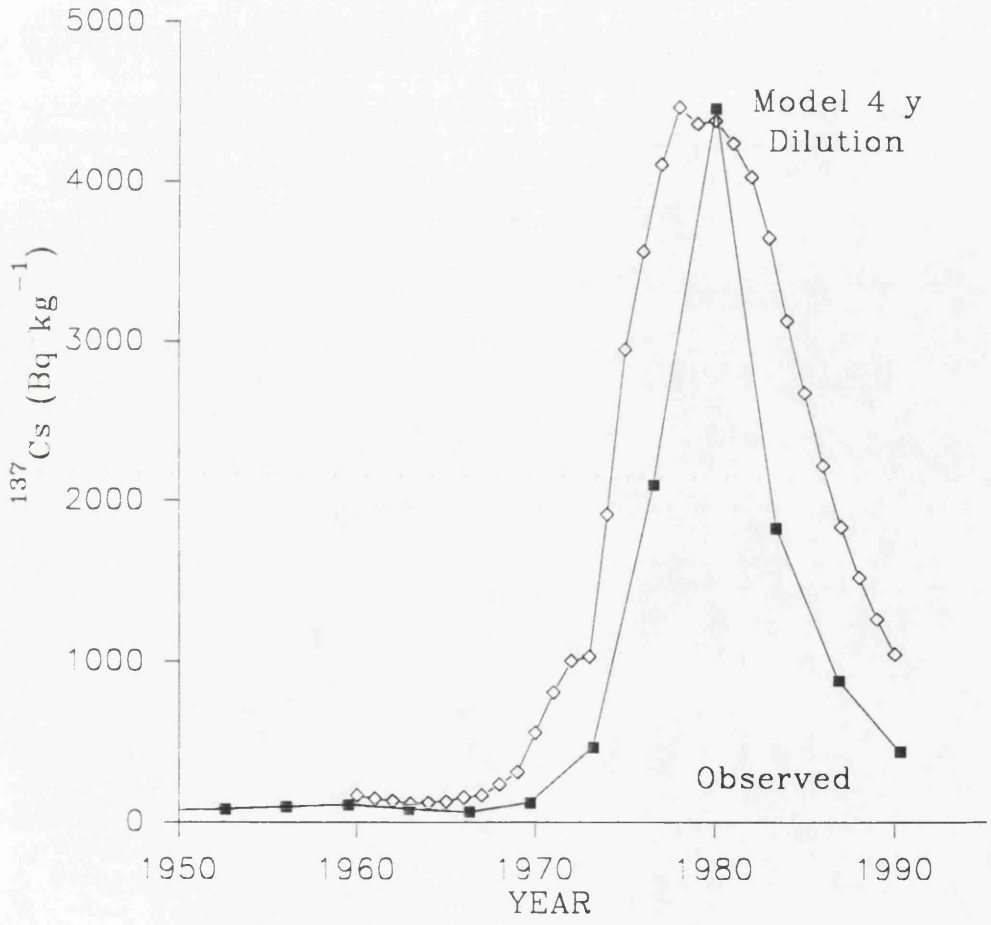

at depth. $^{134}Cs/^{137}Cs$ activity ratio (Fig 4.63d) shows a sub-surface maximum with a decline towards the surface. In contrast with the 5 m section, where Chernobyl fallout was observed, no contribution from this source was apparent. The decay corrected $^{134}Cs/^{137}Cs$ activity ratio increases from 0.009 to 0.582 at a depth of 25-30 cm.

SOUTHWICK TRANSECT T3 15 m SECTION (S3.15)

The radionuclide concentrations for the section S3.15 are set out in Table 3.22 and illustrated in Fig 4.66. The ^{137}Cs, ^{134}Cs and ^{241}Am activities were all confined to the top 20 cm of the profile. The maximum specific activity of the radionuclides are higher than that for the 5 m, 10 m and SC1 sections, with ^{137}Cs increasing to 3,775 Bq kg^{-1} and ^{241}Am to 1,314 Bq kg^{-1}. The trend of decreasing depth of occurrences of the sub-surface maxima was also continued, with the maximum in this case occurring at 10-15 cm. A core was not collected from this site therefore preventing any comparison of the results.

The sedimentation rate calculated from the model developed in Section 4.1 and the ^{137}Cs and ^{241}Am sub-surface maxima were 0.89 cm y^{-1} and 0.69 cm y^{-1} respectively. These values produce a mean sedimentation value of 0.79 cm y^{-1}, again reflecting a systematic decrease in sedimentation rate with increasing distance inland, consistent with a decreasing frequency of inundation by the sea. As with the other sections within this transect the radionuclide concentrations are well correlated, with linear regression analysis producing R^2 values of 0.98 for ^{137}Cs and ^{241}Am, indicating that the radionuclides are associated with a similar component within the sediment namely the fine particles and this has occurred over the time scale of the Sellafield discharges. The total inventories for this section were lower than those of the 5 m section, with a ^{137}Cs inventory of 329,000 Bq m^{-2} and a ^{241}Am inventory of 114,000 Bq m^{-2}. The reduced inventory at this location, 15 m inland from the MHWM, reflects the limited vertical distribution of the radionuclides within the profile, breaking the trend of increasing inventories inland despite increasing concentrations. This suggests that there is less contaminated sediment present at this inland location which reflects the presence of very fine particulate material.

The $^{137}Cs/^{241}Am$ activity ratio exhibits similar trends to the previous sections with values ranging between 1.0 at the surface to 11.8 at 20-25 cm. The $^{134}Cs/^{137}Cs$ activity ratio produces a profile which is very similar to those reported for the 5 m and 10 m sections.

There are a few general points which can be made regarding the vertical distribution of radionuclides within the merse deposits. The Farnel Corer does not provide valid results if it is re-inserted into the sediment. The depth of occurrence of the radionuclide sub-surface maxima declined inland as Fig 4.67 illustrates. The maximum concentrations increased inland from the MHWM. The increasing concentrations and the reduced depth of penetration are consistent with decreasing energy on moving inland. Within this lower energy environment the processes of erosion and deposition are less dynamic and result in the deposition of the finer particles inland. (Aston and Stanners 1981b and 1982b, Aston *et al.,* 1981, 1985, and Hamilton and Clark 1984).

The vertical distributions observed within the merse deposits have major implications for inventory assessment, environmental monitoring and airborne or other field gamma spectrometry. The presence of sub-surface maxima at depths below 30 cm means that if a single sample of 0-30 cm was obtained using a coring technique this could fail to record up to 45% of the inventory within the sediment at the MHWM. Environmental monitoring of merse areas must take into account the depth distribution close to the MHWM which would require sampling down to a depth of at least 0.5 m. Samples should preferably be obtained from an exposed section excavated in the merse, however, the Farnel Corer could be used if the metal sheath is extended to the appropriate length to enable a continuous core to be extracted. The variations in the vertical distribution of radionuclides combined with significant concentration variations over relatively short distances creates fundamental problems for calibration in airborne or other field gamma spectrometry.

Fig 4.66 Concentrations of radionuclides in Southwick T3 15m

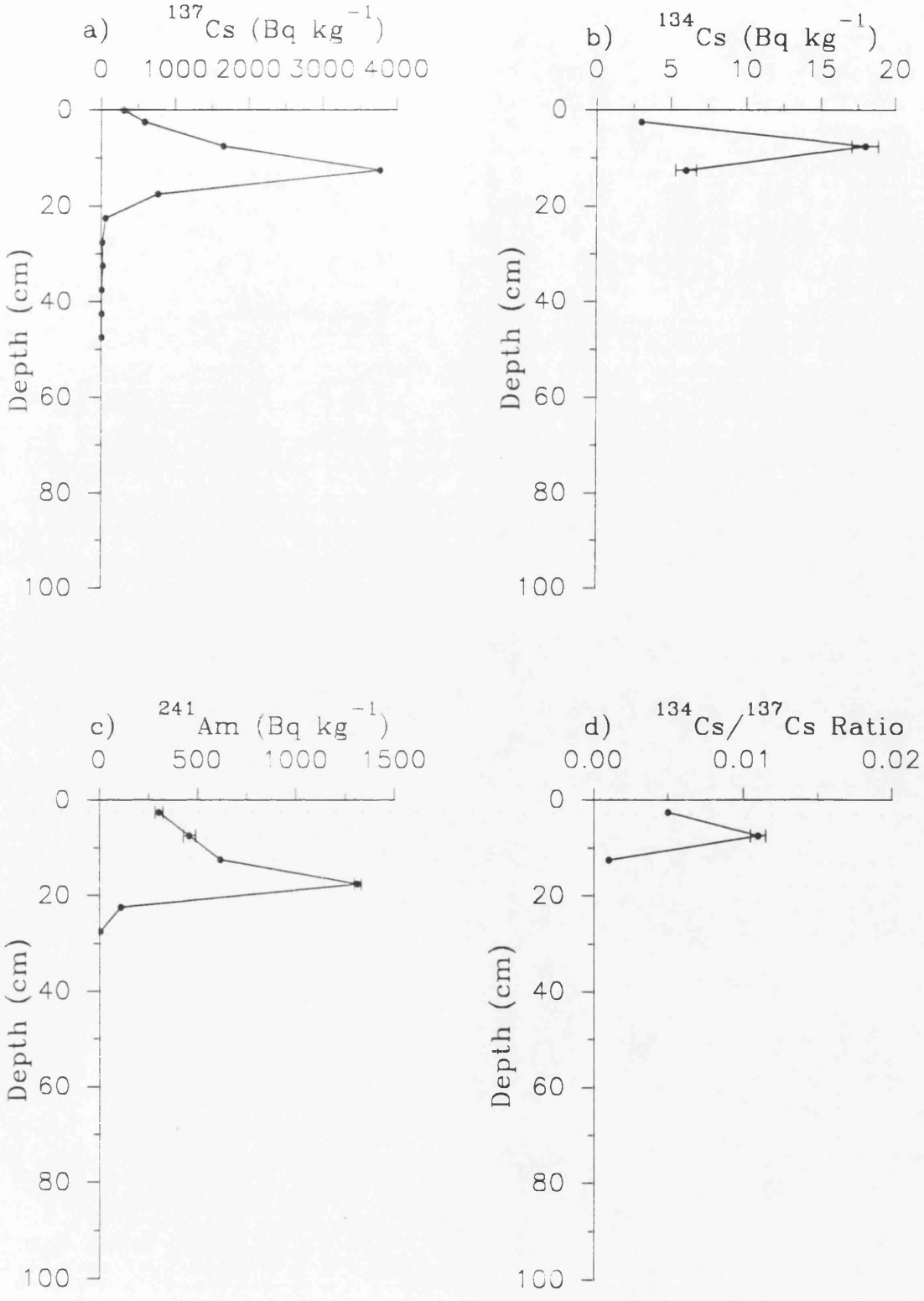

Fig 4.67 Depth of occurrence of ^{137}Cs sub-surface maxima from Southwick transect T3.

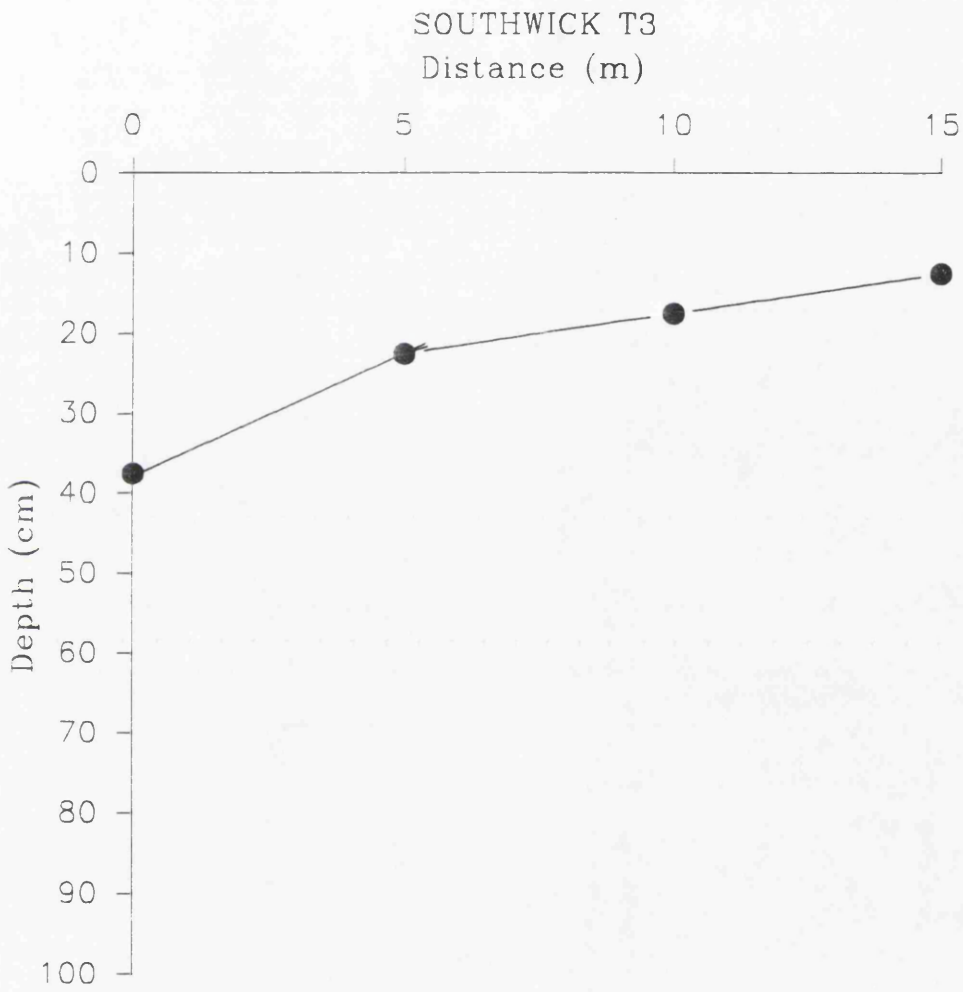

The observed trends of decreasing depth of radionuclide penetration on moving inland from the MHWM has implications for environmental monitoring. If a strategy is adopted using a limited number of samples or a remote sensing method such as airborne γ spectrometry, sub-surface maxima will produce a degree of attenuation of γ photons when they interact with the sediment particles. This phenomenon will make accurate calibration of airborne/field detectors extremely difficult. The degree of attenuation for ^{137}Cs and ^{241}Am in Si has been determined and the results are listed in Table 4.4. The choice of Si was adopted as it replicates the major particle component of the sediment. The results indicate that 14% of the γ photons emitted from ^{137}Cs at a depth of 10 cm will reach the surface. In contrast the γ emissions from ^{241}Am will be virtually totally absorbed by the sediment particles.

Table 4.4 Fraction of γ Photons for ^{137}Cs and ^{241}Am in Si which reach the Surface After Emmission from Different Depths within a Sediment Profile

	Fraction of γ Photons Reaching Surface	
Depth (cm)	^{137}Cs	^{241}Am
10	14%	0.09%
20	1.8%	8×10^{-5}%
30	0.25%	8×10^{-8}%
40	0.03%	6.9×10^{-11}%

The radionuclide concentration profiles from transect T3 together with transect data and the SC1 profile exhibit trends which permit the formulation of a schematic model of the merse.

4.4 CONCEPTUAL MODEL OF THE MERSE

The above observations regarding the lateral and vertical distribution of radionuclides permit the creation of a conceptual model of the merse comprising three zones as illustrated in Fig 4.68. The model is asymmetric when applied to rivers and reflects the topography of the merse at the lower energy sections of the river banks, particularly the convex inner edges of meanders. Similar processes will

occur on the opposite (higher energy) bank but the extent of the component zones will vary according to the topography and the energy of the river. Zone A is intertidal and is an extension of the Irish Sea sediment. Area B, the dynamic zone, is a relatively high energy environment in which water action results in dynamic cycling of sediment with alternating erosion/deposition during the interaction of the incoming tide with the material of the merse. The surface of the merse is colonised by salt-tolerant vegetation which protects the sediment and also acts as a mechanism for trapping suspended sediment. However, the stepped edge of the merse is exposed to direct tidal action which can result in undercutting and slumping as discussed in Chapter 1. This dynamic zone is characterised by high sedimentation/erosion rates. Zone C, the stable zone, experiences little erosion and is subject to accumulation during high flood tides. This zone is well colonised by vegetation such as the grasses; *Puccinellia Maritima* and *Festuca Ruba* which can trap very fine sediment within their roots (Ranwell, 1972). This area of the saltmarsh exhibits a greater degree of floral diversity than the dynamic zone.

A box model of the merse can be constructed on the basis of the model illustrated in Fig 4.69. The intertidal zone A, is a continuation of the general Irish Sea sediment system which supplies material to this zone and during ebb tides, material can be eroded and returned to the offshore sediments. Zone B can be supplied directly from the Irish Sea or from the intertidal Zone A and during the ebb tide or during storm surge events, material can be returned to the intertidal zone or directly to the Irish Sea. The stable zone (C) is supplied from the Irish Sea directly and the intertidal sediments during tidal inundation. The merse is defined as the area covered by vegetation therefore in both Zone B and C the vegetation can trap fine sediment. In contrast the higher energy environment of the intertidal zone results in the re-suspension and transport of the fine sediment. Therefore, the lower energy environment of the merse combined with the vegetative cover results in the preferential deposition of fine sediment resulting in the observed higher radionuclide concentrations in the merse relative to the intertidal areas.

The extent of the dynamic zone will vary depending on the topography of the saltmarsh. In areas close to a relatively large tidal river, such as the River Cree which has a width of approximately 200 m at Creetown, this zone may be 10-15m

Fig 4.68 Schematic model of the component zones within the merse.

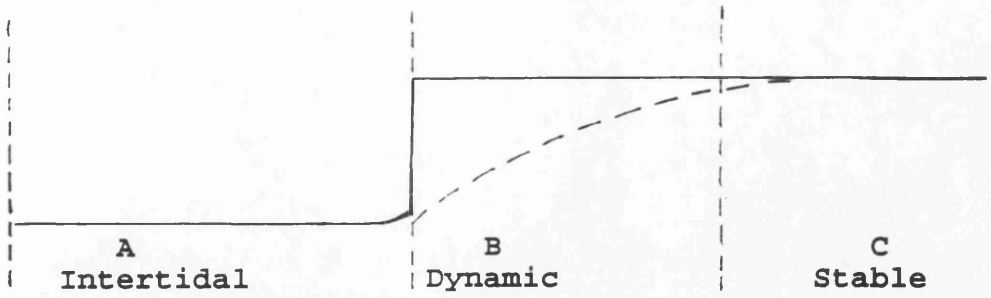

Fig 4.69 Box model of supply routes of sediment to the merse deposits.

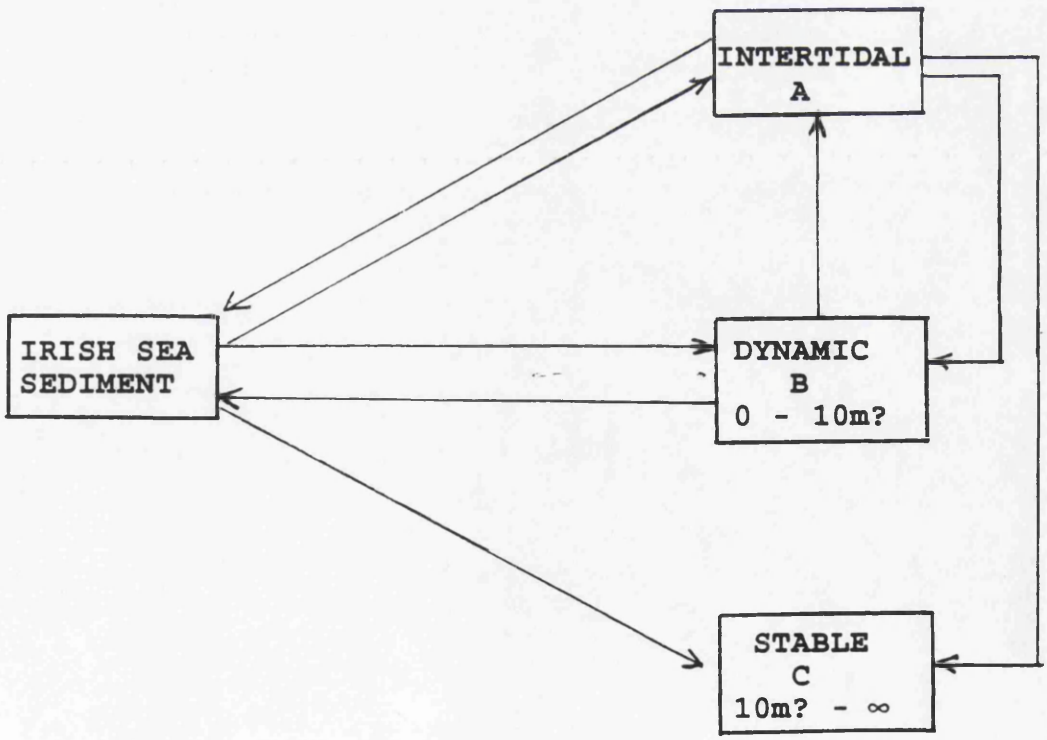

in extent. In addition the high energy environments at the outer edges of meanders within the rivers can create large dynamic zones. In contrast, minor drainage channels, which criss-cross the saltmarsh deposits, will produce less extensive dynamic zones of possibly 1 m or less. Within these zones, rapid deposition can occur, whilst during storm surge events, massive scouring of river banks can result in rapid loss of up to several metres of consolidated material. As a consequence of the drainage pattern within saltmarshes, the multitude of streams or creeks which wind their way across the floodplain offers the potential for contaminated particulate material to be transported further inland on a regular basis than would be the case if the incoming tide were faced with an impenetrable shoreline. Thus, the conceptual model of the merse must take into consideration the micro drainage pattern of these saltmarsh environments where each drainage channel will make a contribution to the spatial distribution of the radionuclides.

More work is required, especially on the vertical and horizontal distribution of radionuclides along these drainage channels, however, the basis of the model is in place. It remains to be refined before it can be used to accurately predict the presence of sub-surface concentrations at drainage channels within the merse.

4.4.1 Radionuclide Inventories for the Coast of South West Scotland

The radionuclide analyses of the merse deposit cores and sections collected along the various transects within the Solway floodplain, combined with the conceptual model, permit estimation of a total inventory of the radionuclides present in this area.

The ^{137}Cs inventories in the 0-15 cm depth interval range from maximum values of 234,000 Bq m^{-2} at Wigtown to 804,000 Bq m^{-2} at Orchardton. The distance inland at which maximum surface concentrations occur varies with location and is site specific due to the topography of the merse. The physical features which affect the surface topography and therefore the radionuclide distribution patterns have been discussed in Section 4.2.

A brief outline of certain relevant features emphasises the site specific nature of the

inventories. At Wigtown, the elevated merse, combined with the absence of step features (relics of former MHWM) within this saltmarsh suggests that the location is subject to only periodic tidal inundation which will result in deposition of the finest grained material furthest inland. This suggestion is supported by the observation that the largest inventories are found at 60 m inland. The generally lower inventories observed at the Wigtown transect are probably due to the distance of this site from Sellafield, which has resulted in the dilution of contaminated sediment before deposition on the merse. In contrast, the enclosed riverine location of Southwick Water, approximately 50 km to the east, exhibits the largest inventories within 20 m of the MHWM. The maximum inventory is observed at 20 m, at which point there is a 10 cm 'step' in the merse, a relic of previous merse development. This feature acts as a partial barrier to the incoming tide which reduces the frequency of inundation for points further inland and also corresponds with the change in vegetation from short cropped grass cover to more tussocky grasses and reeds. As a result the tide dissipates its energy on the seaward side of the merse. This area of merse is a relatively high energy environment compared with more inland locations and is inundated by the tide on a more regular basis. At Orchardton, the maximum inventory is observed at 100 m inland across an area of sparsely colonised merse dissected by meandering drainage channels. A further distance of some 80 m is covered before the change in ground to improved pasture is reached at 180 m, with a corresponding decline in the inventory. The 120 m site produced a very similar but slightly lower inventory to the 100 m site but the general trend of largest inventories further inland is easily identified.

Vegetation cover can also play a significant role in producing large inventories. Oldfield *et al.,* (1993) investigated the contribution that the reed, *Spartina anglica* Hubbard made to entrapment of contaminated sediment. The authors observed large inventories at the sites colonised by this species, with values up to 1,038,000 Bq m^{-2} of ^{137}Cs in the Urr Estuary, near Kippford. These inventories are larger than previously reported for the Galloway coast (McDonald *et al.,* 1992; Garland *et al.*, 1989) and are in reasonably close agreement with the present work. For example, Oldfield's data produces a ^{137}Cs inventory of 576,000 Bq m^{-2} for a stand of *Spartina sp.* located less than 10 m from the slipway at Kippford and very close to

the location of transect T1 which produced a mean inventory for the 0-15 cm of the merse of 516,000 Bq m^{-2}.

A general budget can be estimated for the merse locations along the Solway coast. A conventional sampling programme with a restricted number of samples and limited information on the lateral and vertical distributions of radionuclides would be restricted to taking the total area of merse and multiplying it by the highest inventory recorded to estimate an upper limit for the inventory. Conversely using the lowest inventories establishes a lower limit for the budget. The results for this exercise are reported in Table 4.5. For example using the area of merse taken from the NCC maps (Fig 1.11) and multiplying by the highest inventory recorded in the T1 transects (0-15 cm) an upper limit of the budget is estimated (804,000 Bq m^{-2} of ^{137}Cs, 321,000 Bq m^{-2} of ^{241}Am).

This method of calculating a budget represents a gross over-simplification of the spatial distribution of radionuclides within the saltmarsh environments. However, the budget reported in Table 4.5 can be compared with the Sellafield discharges to estimate the percentage of the effluent returned on-shore. By 1990 Sellafield discharges had generated a decay corrected environmental inventory of approximately 30,000 TBq of ^{137}Cs and 906 TBq of ^{241}Am (allowing for ingrowth) into the Irish Sea. On the basis of these figures it can be estimated that only 0.05% of ^{137}Cs and 0.71% of the ^{241}Am discharged from Sellafield has been returned on-shore. In contrast the minimum percentage returned on-shore was 9.0×10^{-5}% of ^{137}Cs and 1.9×10^{-6}% of ^{241}Am.

Table 4.5 Maximum and Minimum Radionuclide Inventories (0-15 cm) Estimated for the Floodplain Deposits of the Solway Coast.

Radionuclide	Inventory (Bq)	
	Maximum	Minimum
^{137}Cs	1.6×10^{13}	2.7×10^{10}
^{241}Am	6.5×10^{12}	1.8×10^{7}
$^{239+240}Pu$	2.1×10^{12}	1.4×10^{7}

Determination of the budget using the total inventory (0-30 cm) from the T1 transect data set produces a more realistic assessment than relying only on the 0-15 cm interval. Previous discussion on the validity of using the 15-30 cm data in relation to possible contamination by the coring procedure has to be recognised, however, the 15-30 cm data compares reasonably well with corresponding values collected from sections T3. The same procedure as described above for the determination of the maximum and minimum inventory in the 0-15 cm interval was repeated for the 15-30 cm interval and the results combined to produce a total inventory with the results listed in Table 4.6.

Table 4.6 Maximum and Minimum Radionuclide Inventories (0-30 cm) Estimated for the Floodplain Deposits of the Solway Coast.

Radionuclide	Inventory (Bq)	
	Maximum	Minimum
^{137}Cs	2.7×10^{13}	4.1×10^{10}
^{241}Am	1.0×10^{13}	2.0×10^{10}
$^{239+240}Pu$	3.6×10^{12}	2.0×10^{10}

By these calculations the percentage of the Sellafield discharges returned on-shore increases to 0.09% for ^{137}Cs and 1.10% for ^{241}Am. These figures provide a very

crude estimate of the total merse inventories but they fail to account for the variations in the deposition trends which were identified earlier in this Section (4.2). They only provide an estimate of the maximum and minimum levels of contamination in the 0-30 cm depth intervals of these merse areas.

A more suitable approach, which incorporates variations in the sedimentation patterns, involves the determination of the areas of the dynamic and stable zones at each saltmarsh location.

The maps used for this exercise were the Ordnance Survey 1: 50,000 scale which provided sufficient detail of the merse areas to permit calculation of the dynamic zone around rivers (both banks). Although the model is asymmetric, for the ease of calculating a budget for the merse, it was assumed that deposition of contaminated particulate material was symmetrical on both banks. This assumption is based on the fact that the majority of saltmarsh creeks are relatively small and meander across the floodplain which results in a decrease in energy inland promoting deposition of suspended material on the banks which in places can be only centimetres apart. The extent of the dynamic zone has been taken to be 10 m and the inventories of ^{137}Cs from transect T3 used to determine the maximum inventory at depth within this zone. The 10 m section (S3.10), with a maximum inventory of 500,000 Bq m^{-2}, was assumed to be the upper limit of inventories in the dynamic zone. The inventory in the stable zone was estimated to be 200,000 Bq m^{-2} of ^{137}Cs. Table 4.7 illustrates the area of merse attributable to the dynamic and stable zones for the major areas of saltmarsh deposits on the Solway coast of south west Scotland.

Table 4.7 Dynamic and Stable Zone Areas within the Merse Deposits of South West Scotland.

	Zone B	Zone C
	m^2	m^2
Caerlaverock	45,000	855,000
Carse Bay	5,000	95,000
Southwick	50,000	350,000
Kippford	40,000	240,000
Orchardton	25,000	375,000
Kirkcudbright	10,000	40,000
Creetown	30,000	300,000
Wigtown	190,000	456,000
Total	405,000	6,815,000

This method of calculating the budget for the Solway Firth floodplain probably underestimates the contribution within the stable zone by failing to account for the contribution of the myriad of drainage channels within the saltmarsh, but it does provide a more realistic estimate of the budget than assuming that all of the saltmarsh deposits are uniformly contaminated to the same degree. The ^{137}Cs budget calculated at 1.5×10^{12} Bq represents less than 0.005% of the integrated Sellafield discharges and is almost one order of magnitude lower than that calculated using the data in Table 4.5. This budget has been determined for an area from which a large data set has been amassed. Extension of the technique to similar locations outwith the Solway Firth would require a major fieldwork effort, however, it is apparent that this would be necessary in order to provide a realistic budget for the Irish Sea basin.

The inventories produced from this research range up to 1,300,000 Bq m^{-2} which are two orders of magnitude greater than the largest inventory attributable to

Chernobyl fallout in this area of 38,700 Bq m^{-2} (McDonald *et al.*,1990). The magnitude of these inventories combined with the land use of these merse areas makes it essential that the mobility and availability of the radionuclides within these environments is understood to enable a comprehensive assessment of potential doses to man. In the next section the speciation of ^{137}Cs and $^{239+240}Pu$ within the estuarine environment of the Solway Firth is investigated.

4.5 GEOCHEMICAL ASSOCIATIONS OF SELLAFIELD DERIVED RADIONUCLIDES IN MERSE LOCATIONS

The previous sections within this chapter have focused on the supply mechanism of radionuclides to the merse, their vertical and lateral distributions, development of sediment chronologies and estimation of radionuclide budgets for the total merse areas of the Solway Firth. This section aims to investigate the speciation of the radionuclides within the merse environment and any changes in speciation with age (depth) or changing environmental conditions. Despite the fact that only a small percentage of the total Sellafield discharge is involved in on-shore transfer, significant radionuclide inventories (up to 1,300,000 Bq m^{-2}) are produced in the merse sediment. In the light of the magnitude of these inventories speciation studies are necessary to determine the potential mobility and availability of the radionuclides which are of importance in evaluating their potential contribution to human radiation exposure.

Sequential chemical extraction (described in Section 2.6) was used to investigate radionuclide speciation within sediments from Southwick merse. The extraction scheme utilised was based on the scheme developed by McLaren and Crawford, (1973) and modified for radionuclide speciation studies by Cook *et al.*, (1984a,b), Livens and Baxter (1988) and McDonald *et al.*, (1990; 1992), so direct comparisons can be made with these works.

Surface sediment samples from the intertidal area of the estuary at Southwick Water, along with sediment from sections located at the MHWM (SC1) and from 10 m inland across the consolidated merse (S3.10) were subjected to speciation studies. The analysis of the samples from the various locations; intertidal,

riverbank (MHWM) and consolidated merse provided the opportunity to investigate the changes in geochemical behaviour in relation to both the age (depth) and varying geochemical conditions on moving from the marine environment of the Irish Sea to the terrestrial environment of the merse. In Section 4.1 it was demonstrated that the radionuclides discharged from Sellafield become associated with offshore sediments, which then undergo on-shore transport. During this on-shore transfer, the geochemical conditions affecting the radionuclides are altered, from the well oxygenated, alkaline (pH 6 - 8) marine environment of the Irish Sea, (McDonald *et al.,* 1992), to a terrestrial location with slightly acidic conditions (pH 3-6), (Baxter *et al.*, 1989 ; McDonald *et al.,* 1992), variable Eh with more reducing conditions at depth within the sediments and an increasing influence of freshwater (water table and rainfall). Samples from several depth intervals were collected from SC1 and S3.10 and analyzed to establish variations in geochemical association with depth (age) and with distance inland.

The particle size distribution, determined as described in Section 2.9, and mineralogy determined by x-ray diffraction (by the Geology and Applied Geology Department, University of Glasgow) of the sediment samples from SC1 and a sample of surface sediment, obtained from the mud patch off Sellafield, are set out in Tables 3.23 and 3.24 respectively. The major component of the samples from SC1 was fine sand (57-76%), with the percentage of silt and clay ranging between 14% and 30%, while in the Irish Sea sediment, silt and clay are the major fractions (57%). The recoveries of 87-95%, obtained suggest a loss of 5-10% of the material during sieving and this probably consisted mostly of fine material.

The mineralogical analyses (Table 3.24) indicated that the dominant component of all the samples was quartz, which is to be expected from samples comprising up to 76% fine sand. The presence of clay mineral fractions within each sample indicates the potential for retention of radionuclides. The clay minerals identified in Table 3.24, chlorite and illite, are considered to be non expanding clays. The major component is chlorite with the illite forming the minor component. Both types of clay exhibit surface and planar sites where Cs^+ is generally exchangeable through ion exchange mechanisms. The layers within the chlorite mineral are bonded by $MgOH_2$, the bonds are incomplete and may produce channels along

which ions may diffuse into the interlayer sites. Illites exhibit slightly different properties at the edges of their structures, which involves ionic exchange at these edge sites and permits diffusion inwards forming wedge sites where exchange is sterically limited to cations of similar size and charge.

4.5.1 ^{137}Cs Leaching Studies

The analytical results for the sequential extraction of ^{137}Cs from the intertidal sediment from Southwick Water are set out in Table 3.25. The results indicate that 98% of the ^{137}Cs is associated with the residual phase and only 2% in the more acid soluble component. In contrast the analytical results for SC1 located at the MHWM are set out in Table 3.26. It is evident that, independent of the age of sediment, negligible quantities of ^{137}Cs were dissolved by reagents selected to remove it from the available, exchangeable, organic bound and secondary Fe/Mn bound components of the sediment. In each case at least 80% of the ^{137}Cs was tightly bound within the residual phase and between 12% and 15% was relatively tightly bound within the more acid soluble component. There was no discernable variation in geochemical association with depth and hence with age of sediment. It is well recognized that the ^{137}Cs associated with both these phases is unlikely to be removed to solution or be available for plant uptake (Swanhey, 1972).

The analytical results from the sequential extraction of ^{137}Cs from sediment samples collected from the section located 10 m inland from the MHWM (S3.10) are illustrated in Table 3.27. The results indicate that for all three depth intervals and irrespective of age of sediment, that over 98% of the ^{137}Cs was associated with the residual phase.

The variations in geochemical associations of ^{137}Cs within the intertidal and merse sediments could be due to the geochemical conditions experienced in each environment. Section 4.1 demonstrated that the^{137}Cs was transported to the Solway Firth through association with particulate sedimentary material. It is feasible that a proportion of the ^{137}Cs discharged from Sellafield may undergo rapid initial fixation onto the sediment surfaces followed by slow diffusion into the interlayer sites over prolonged periods as Evans *et al.,* (1983) observed for

sediment in freshwater reservoirs in the USA. During the period that the contaminated sediment is transported to the Solway Firth a high proportion, up to 75%, is desorbed (Hunt and Kershaw,1990; McCartney *et al.*,1993). This desorption process will remove the more accessible ^{137}Cs from the sediment leaving the most tightly bound components in the residual phase. Sequential extraction analysis of the intertidal sediment from Southwick Water indicated that 98% was associated with the residual phase which lends support to the above hypothesis of re-dissolution of more available radiocaesium leaving a tightly bound residual component.

The variation between the speciation of ^{137}Cs in the intertidal sediment and SC1 suggests that as a consequence of the on-shore transfer of the radionuclides there is a slight change in association with an increase in the percentage associated with the more acid soluble phase and the secondary Fe/Mn minerals. This variation may be due to changing geochemical conditions at the MHWM with increased exposure to air and limited freshwater leaching through rainfall. However, this location at the MHWM will be subject to regular incursions of seawater which could introduce competing cations. These cations may permit limited displacement of Cs^+ within interlayer sites and restrict ionic bonding to the clay edge sites. Rhodes (1957) and Aston and Duursma (1973) showed that retention of caesium was reduced in the presence of sodium chloride.

In addition, the intertidal sediment will be affected by percolation of brackish water within the bed of the Southwick Water followed by incursion of saline water. This incursion may produce a wedge of saltwater which flows below the freshwater of the river introducing brackish water to the sediment pore water. These conditions may be such that competing cations are not as readily available as for the location at SC1 which experiences predominantly saline inundation at the MHWM. Therefore the ^{137}Cs is almost totally associated with the residual phase.

The variation in speciation between the samples from SC1 and the inland section (S3.10) may be due to the presence of competing cations at SC1 which are absent from the inland location, which experiences predominantly brackish water drainage. Therefore producing relatively similar geochemical conditions to the intertidal

sediment.

The observation regarding the speciation of ^{137}Cs within the floodplain deposits where the primary association is with the more resistant components of the sedimentary samples is broadly similar to the trends observed by Cook *et al.,* (1984b) in an investigation of the geochemical associations of ^{137}Cs and $^{239+240}Pu$ in terrestrial soils at Dounreay in north west Scotland. The authors reported that 55% of the ^{137}Cs was in the residual phase, with 29% in the clay lattice edges (more acid soluble) and 14% in the insoluble organic complexes. The difference between the results of Cook *et al.,* (1984b) and the present work can be explained through the on-shore transfer of ^{137}Cs in spume and sea spray which resulted in a proportion of the ^{137}Cs being in a more available form for the Caithness soil, in contrast to the radiocaesium from Sellafield which is associated with the clay particles of the Irish Sea and floodplain deposits. Livens and Baxter (1988) investigated the ^{137}Cs content of the surface layer (0-5 cm) of a sand sample collected 25 m above the MHWM on the Cumbrian coast (SD 073 966). The results of their investigation showed some similarities to the observations in the present study with up to 71% of the ^{137}Cs being associated with the residual phase, 12% with the oxide, 5% with the organic and 11% with the exchangeable component. There are differences between the results of Livens and Baxter (1988) and the present work which can be attributed to the effects of Chernobyl deposition of ^{137}Cs which would have been in solution during wet deposition and therefore more labile than the radiocaesium from Sellafield which has had more time to diffuse into the interlayer sites of the clay minerals (Livens and Baxter, 1988). Within the present study no evidence of Chernobyl fallout was found within the surface layers of either the SC1 or S3.10 profiles as has been discussed in Sections 4.1 and 4.3.

The strong association of ^{137}Cs with the residual phase and the fact that the mild reagents do not affect dissolution indicates a very low degree of potential mobility and availability. This suggests that at present, the dominant radiological hazard posed by ^{137}Cs in this environment will be by external irradiation. The results imply that groundwater transport and biological uptake will be very small. The observations of re-dissolution of ^{137}Cs from the sediments of the Irish Sea (Hunt

Fig 4.70 Major plutonium associations in section SC1

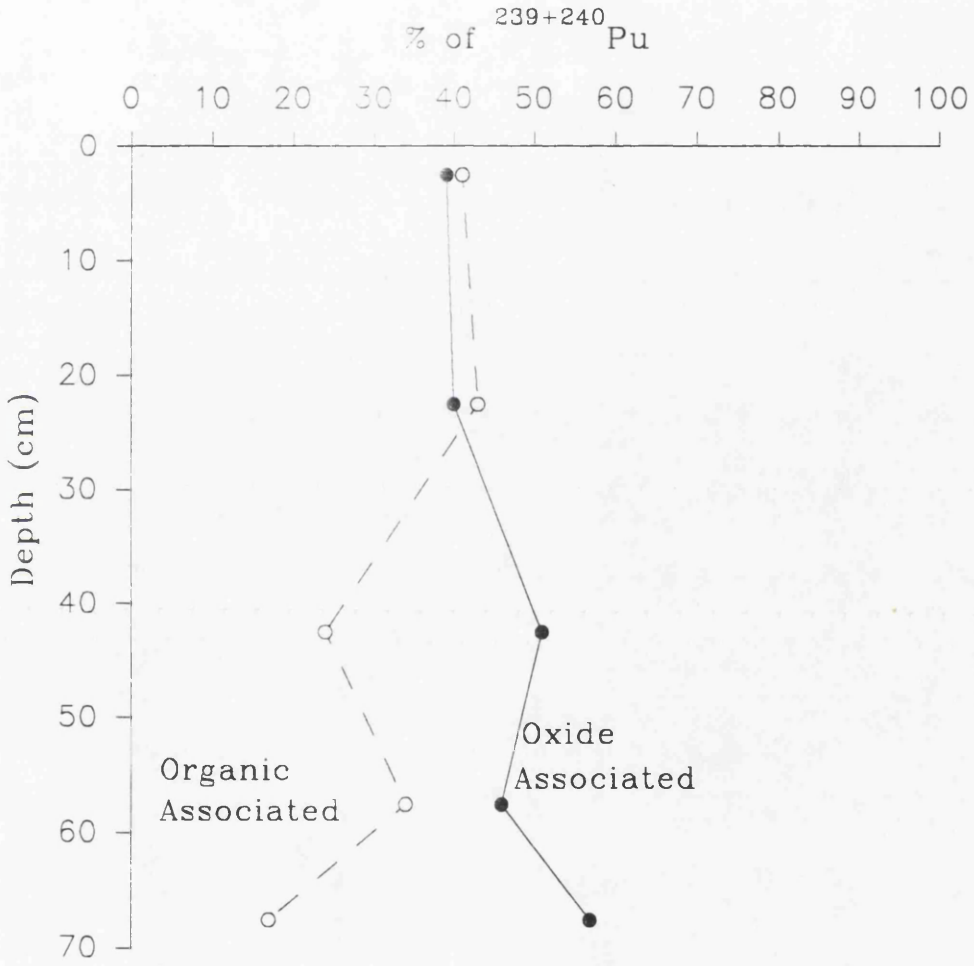

and Kershaw,1990; McCartney *et al.*, 1993) are supported by the findings in Section 4.1 that the $^{137}Cs/^{241}Am$ activity ratio suggests a loss of up to 68% of ^{137}Cs from the sediment deposited in SC1. The sequential extraction results provide strong evidence that this has occurred prior to on-site deposition.

4.5.2 $^{239+240}Pu$ Leaching Studies

The analytical results for the sequential extraction of $^{239+240}Pu$ in the intertidal sediment from Southwick Water are set out in Table 3.25. The results indicate that the $^{239+240}Pu$ is almost totally associated with the secondary Fe/Mn mineral phase (89%) with only a minor contribution from the organic phase (8%). The analytical results for the $^{239+240}Pu$ leaching studies for SC1 are set out in Table 3.28. In the surface sediments (0-5 cm), about 41% of the $^{239+240}Pu$ was associated with the organic extract, 39% was in the secondary Fe/Mn mineral phase, 16% associated with the residual phase, with minor quantities in the other components. A systematic variation in the major associations was observed as a function of depth (age) as illustrated in Fig 4.70, with the organic component containing progressively less $^{239+240}Pu$ and the secondary Fe/Mn and residual fractions containing correspondingly more. This observation is compatible with recent work on the abundance of functional groups in humic acids (in particular -COOH) contained in this sediment by Graham *et al.*, (1993) who have shown through the use of FTIR spectra that there is a pronounced decrease in the carboxyl group content with increasing depth in the sediment. The importance of the oxygen containing ligands is apparent in the strong nature of the binding between hard ligand and hard metal ions. The decrease in the functional groups with depth therefore removes potential binding sites for radionuclides.

The analytical results from the sequential extraction of $^{239+240}Pu$ from S3.10 are illustrated in Table 3.29. The results indicate that the $^{239+240}Pu$ is primarily concentrated in the organic, secondary Fe/Mn mineral and residual phases with virtually no discernable variation in association with depth.

The geochemical associations of $^{239+240}Pu$ within the intertidal sediment are similar to the observations by Aston and Stanners (1981a,c) who reported that between

Fig 4.71 Variation in LOI content within sediment cores SC1 and S3.10 collected from Southwick merse.

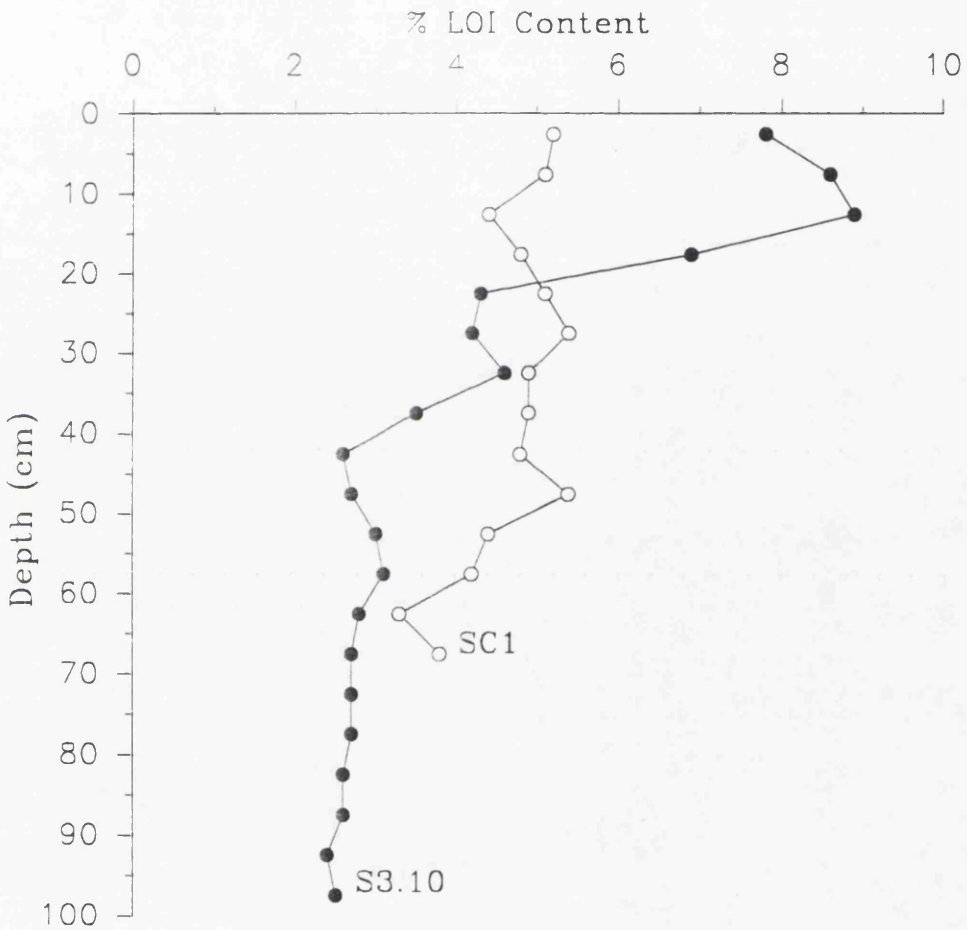

75% and 100% of the $^{239+240}Pu$ in samples of intertidal sediments from the Ravenglass estuary was associated with the non detrital Fe/Mn phases and was removed using an acid reducing reagent. In addition, the results support the observations by McDonald *et al.,* (1990) who investigated the geochemical associations of $^{239+240}Pu$ in a suite of marine cores taken along a transect from Sellafield to Kirkcudbright Bay. Their results indicated that the $^{239+240}Pu$ is predominantly associated with the secondary Fe/Mn minerals, followed by organic and then the residual phases, with similar results for different cores despite the spatial diversity of the sample locations.

The geochemical associations of $^{239+240}Pu$ within both sediment sections SC1 and S3.10 showed strong similarities. The percentages of $^{239+240}Pu$ associated with the organic, secondary Fe/Mn mineral and residual phases are very similar with the order of association in the top 30 cm of both cores being organic $\simeq$ secondary Fe/Mn minerals $>$ residual. Below 30 cm SC1 exhibits a pronounced change in association from organic to secondary Fe/Mn minerals. This trend cannot be attributed to degradation of organic matter as more pronounced degradation occurs in S3.10 (Fig 4.71). While there is a slight variation in organic matter content with depth this is not reflected in the geochemical associations of $^{239+240}Pu$ within the section (S3.10). A more logical explanation centres on the presence of marine derived micro-organisms at depth in SC1 which can survive in the tide-stressed environment at the MHWM but which fail to colonise more inland locations prone to leaching by brackish water. The results for the sequential extraction of $^{239+240}Pu$ from the floodplain sediments are supported by previous research using this extraction scheme. Cook *et al.,* (1984a,b) and Livens and Baxter (1988) reported similar geochemical associations of $^{239+240}Pu$ in terrestrial soils from spatially diverse locations in Caithness and Cumbria, overall the observed order of association was:

organic $>$ oxide $>$ residual $>$ adsorbed $>$ exchangeable.

McDonald *et al.,* (1992) investigated $^{239+240}Pu$ associations in the Solway floodplain soils and also observed that the majority of the plutonium was associated with the organic, sesquioxide (secondary Fe/Mn minerals) and residual phases.

A compilation of results from McDonald *et al.,* (1990;1992) is presented in Table 3.30. These clearly illustrate the variation in the order of geochemical associations evident between the marine and terrestial environments. The two marine cores produce a contrasting order of geochemical association with a predominance of secondary Fe/Mn minerals over organics in Core A, a trend which is reversed in Core E. However, the contrast between the marine and the intertidal sediment and the terrestrial samples is more marked. There is a distinct change in association of $^{239+240}$Pu within these samples, with the dominance of the secondary Fe/Mn mineral phase in the Kippford intertidal sediment contrasting with the dominance of the organic phase in the terrestrial soil at Culkeist. The results of the present work indicate that the $^{239+240}$Pu is associated with the secondary minerals within the intertidal zone and that a change in association or re-distribution occurs as a consequence of the on-shore transfer of contaminated particulate material. This re-association during the sea-to-land transfer could be demonstrating the desorption of plutonium via rapid exchange reactions under the influences of increasing hydrogen ion and dissolved organic concentrations (Mudge *et al.*, 1988) or the dissolution of Fe, Mn oxyhydroxides together with lower Eh conditions (Wilkins *et al.*, 1984), followed by chelation by much more abundant organic matter present in the terrestrial particulate matter.

Despite the variations in geochemical associations reported above, the relatively aggressive chemical reagents required to remove the radionuclides from the sediment samples indicates that they are generally in a form which is unlikely to result in their re-dissolution into the aquatic environment or be made available for plant uptake. Radiocaesium is strongly bound within the residual or more resistant soil components, while $^{239+240}$Pu is retained by the organic or secondary Fe/Mn mineral phases. The plutonium displays a greater potential mobility/bioavailability relative to caesium since it is involved in associations with Fe, Mn oxyhydroxides which will be re-dissolved under reducing conditions and humic substances which could become involved in biological processes. However, the results show no evidence of Fe/Mn dissolution with depth and indicate that if any $^{239+240}$Pu is released from the organic phase it will remain in the soil at the same horizon and would appear to be rapidly re-absorbed by other resistant components. However, Hamilton-Taylor *et al.*, (1987) observed, in laboratory experiments, limited

remobilization of plutonium from the exchangeable phase of contaminated sediment from the Esk Estuary which was exposed to low salinity water (4 ‰). The observations in the present study suggest that the small percentages of plutonium associated with this phase would result in very limited remobilization from the sediments of the merse.

The results indicate that ^{137}Cs is strongly bound to the sediment and despite exposure to tidal inundation and variable environmental conditions remains within the residual phase for periods of up to 28 years. Despite the potential for limited desorption from the exchangeable phase, similar conclusions may be drawn from the $^{239+240}Pu$ data, which suggests that irrespective of the age of sediment, that $^{239+240}Pu$ concentrations within inland merse locations will continue to be strongly associated with the organic and secondary Fe/Mn mineral phases. From a radiological viewpoint, the geochemistries of ^{137}Cs and $^{239+240}Pu$ within this merse environment, suggests that they will continue to pose a potential exposure risk to mankind. The results suggest negligible re-dissolution or availability for both ^{137}Cs and $^{239+240}Pu$ within these saltmarsh deposits. The magnitude of the ^{137}Cs inventories and the geochemical behaviour suggests that this γ-emitting radionuclide will continue to pose a potential exposure risk to man. The potential biogeochemical reactions of plutonium merit further investigation given the environmental persistence and long half-lives of plutonium isotopes (^{238}Pu = 87.7 y, ^{239}Pu = 24,300 y and ^{240}Pu = 6,570 y). Investigation of the scale of potential re-dissolution of ^{137}Cs from environmental samples was undertaken in a series of laboratory experiments discussed in the next section.

4.6 FLOW DESORPTION EXPERIMENTS

It is important to evaluate re-dissolution processes in terms of potential transfer of radionuclides in the environment. This was investigated by a series of desorption experiments as described in Section 2.7.

Desorption experiments provide K_D values which are determined by dividing the concentration in the solid phase by the concentration in the aqueous phase. These values are in principle comparable with K_D values derived from radionuclide uptake

experiments under environmental conditions, however, the systems investigated will vary and it must be borne in mind that K_D values generated may differ between each investigation.

The method adopted to investigate the quantity of ^{137}Cs which could be desorbed from contaminated sediment was flow desorption (Section 2.7). This comprises the passage of a large volume (at least 300 l) of an aqueous medium in a continuous process through a small quantity of contaminated sediment. The sediment samples were subject to leaching by freshwater, field drain water (ground water) and seawater, which were assumed to be representative of the fluctuating environmental conditions prevalent within the merse. Batch desorption experiments were also undertaken, however, these presented too many logistical problems and were subsequently abandoned. There are limitations in the use of flow desorption experiments; primarily, the system may not attain equilibrium with respect to the aqueous and solid phase partitioning of caesium. Therefore, the Cs^+ binding sites may not be fully exposed to the leaching media which would only have the potential to remove a portion of the total caesium within the sediment. In addition, the design of the experiment may influence the kinetics of the process, requiring a longer time to establish equilibrium than applies to the contact time between any 'parcel' of water and the sediment in the natural system. It is therefore possible that the experiment may over-estimate the $K_{D,}$ and values obtained should be regarded as upper limits. The values are nevertheless of relevance since the experiment reflects certain environmental conditions affecting the sample site. The experiment deals with sediment which is exposed to the percolation of natural waters and this replicates environmental conditions at Southwick merse where the system is subject to flow through by ground water and brackish/saltwater.

Two depth intervals from Core SC1, 0-5 cm and 40-45 cm, were used to investigate desorption of ^{137}Cs from the stepped edge of the merse MHWM. These samples have an approximate age of 1 y (0-5 cm) and 18 y (40-45 cm) respectively and permit comparison of the ease of desorption of ^{137}Cs from sediments of different ages.

Fig 4.72 K_D values (log scale) derived from the leaching of a) 0–5 cm and b) 40–45 cm sediment samples with freshwater

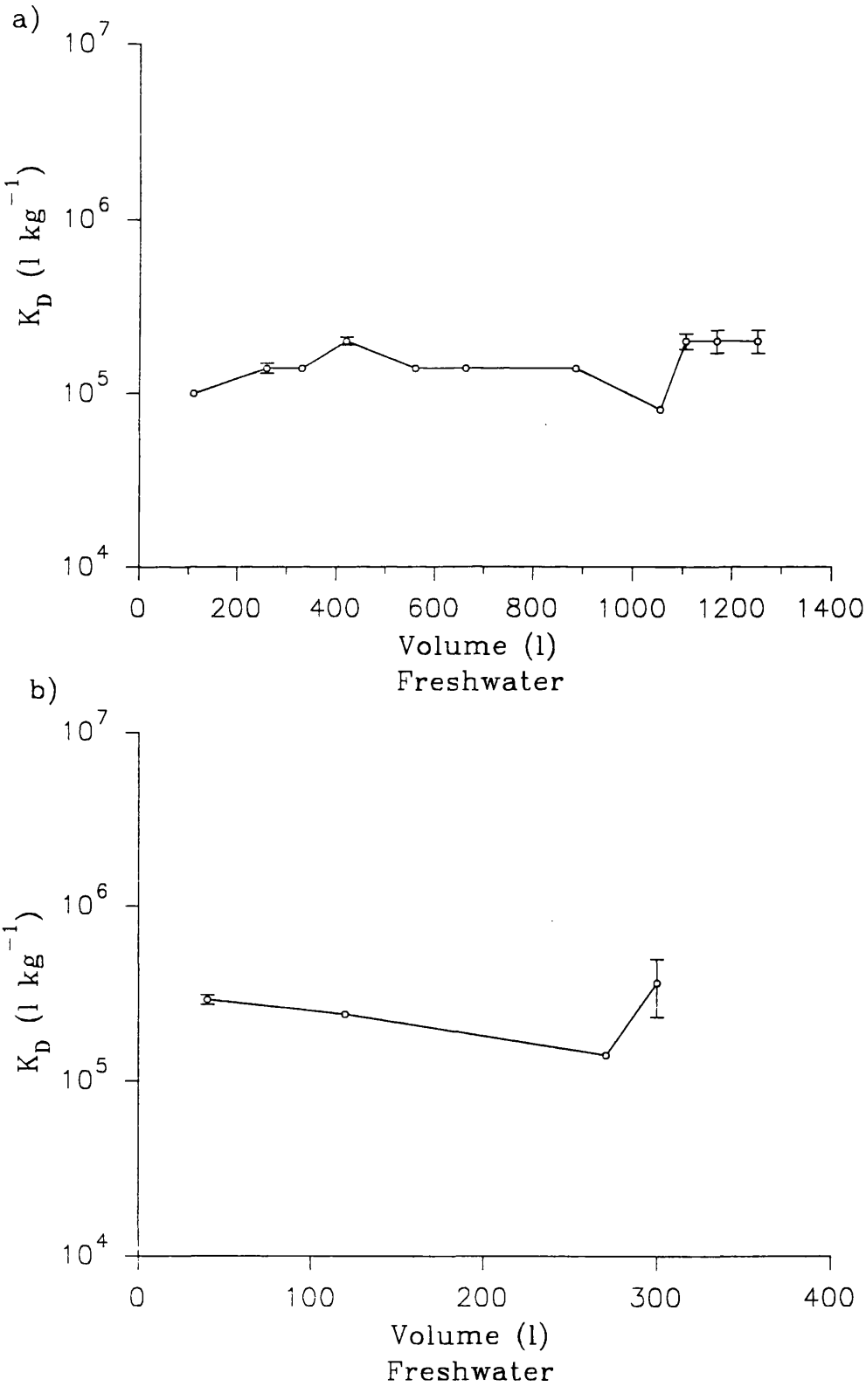

Fig 4.73 K_D values (log scale) derived from the leaching of a) 0–5 cm and b) 40–45 cm sediment samples with ground water (field drain)

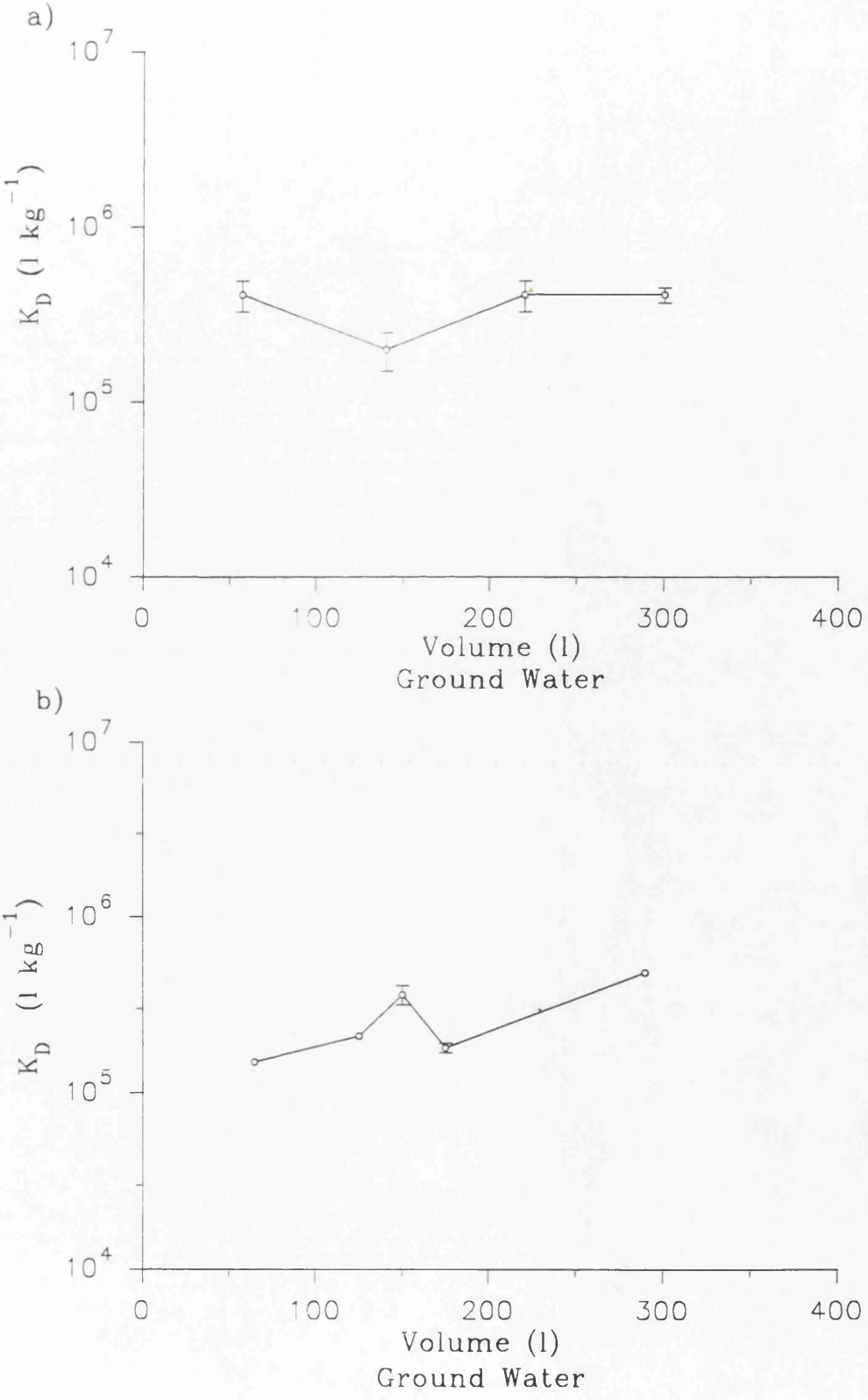

4.6.1 Freshwater

a. 0-5 cm

The results from the experiment are illustrated in Table 3.31. This experiment was begun in January 1990 and ended in May 1992 with over 1,300 l of freshwater being passed through the sediment sample. The results are illustrated in Fig 4.72a and indicate that leaching with up to 1,200 l of freshwater produced an almost constant K_D value of about 10^5 l kg^{-1}, beyond 1,200 l the values are below the detection limit. The results imply that ^{137}Cs is tightly bound to the sediment but that a small quantity can be desorbed by continuous leaching. The total quantity of ^{137}Cs desorbed during the course of this experiment (2 years 4 months) was 4.05 Bq which represents approximately 50% of the total (8.12 Bq) within the 20 g sample. Exposure to freshwater will result in re-dissolution of ^{137}Cs but with a K_D of the order of 10^5 l kg^{-1}. This supports the observations of the geochemical associations of ^{137}Cs in the 0-5 cm interval of SC1 (Table 3.26), where 3% was associated with the secondary Fe/Mn minerals, 13% with the more acid soluble and 84% retained within the residual phase. The K_D values are higher than previously published for the Irish Sea and may suggest that the more labile Cs has been removed, most probably prior to deposition, leaving a more tightly bound residual component within the sediment.

b. 40-45 cm

The results of this experiment are listed in Table 3.32 and illustrated in Fig 4.72b. The K_D values range from 1.4 x 10^5 l kg^{-1} to 3.6 x 10^5 l kg^{-1}, producing a mean value of 2.5 x 10^5 l kg^{-1} which is very similar to the corresponding values for the 0-5 cm depth interval which produces a mean K_D of 1.5 x 10^5 l kg^{-1}.

4.6.2 Field Drain Water

a. 0-5 cm

The leachate for this experiment was collected from the drainage pipe at the entrance of the Scottish Wildlife Trust Nature Reserve at Netherclifton (Southwick Water) and as such was deemed to represent the ground water draining through the merse at this location. The results listed in Table 3.33 and illustrated in

Fig 4.74 K_D values (log scale) derived from the leaching a) 0–5 cm and b) 40–45 cm sediment samples with saltwater

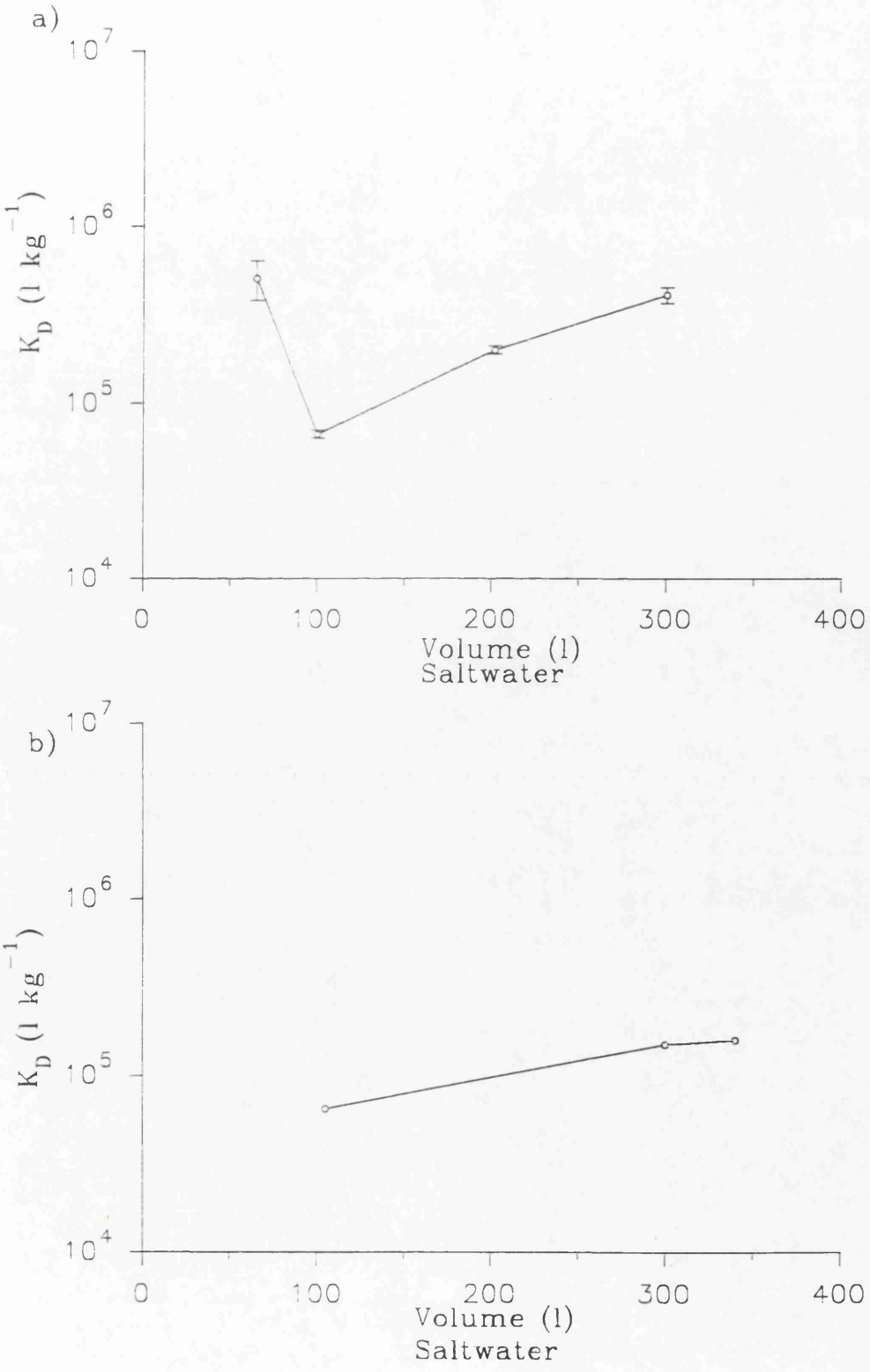

Fig 4.73a exhibit K_D values between 2.0 x 10^5 l kg^{-1} and 4.1 x 10^5 l kg^{-1} producing a mean K_D value of 3.6 x 10^5 l kg^{-1}. These values are slightly higher than the corresponding values for the 0-5 cm sample leached with freshwater which has a mean K_D value of 1.5 x 10^5. These results indicate that greater desorption was observed with the freshwater, with 12.4% of the total ^{137}Cs in the sample mobilized compared with 3.8% in the ground water. This variation would suggest that either some component in the field drain water is inhibiting ^{137}Cs desorption or that some component in the mains water is stimulating it.

b. 40-45 cm

The results are listed in Table 3.34 and illustrated in Fig 4.73b. The results range between 1.5 x 10^5 l kg^{-1} to 4.8 x 10^5 l kg^{-1} with a mean value of 2.7 x 10^5 l kg^{-1}. The mean K_D value is lower than the corresponding value for the 0-5 cm interval. These results indicate that 5.8% of the total sample content was desorbed compared with 3.8% in the 0-5 cm interval. In comparison with the 0-5 cm depth interval results, the K_D values are very similar and taken together the ground water results do not show the range of variation observed for the freshwater (mains) experiments. Despite this apparent variation in range, the K_D values for both leaching solutions are consistently around 10^5 l kg^{-1}.

4.6.3 Seawater

a. 0-5 cm

The results from the leaching of the sediment sample with seawater are listed in Table 3.35 and illustrated in Fig 4.74a. The results show K_D values ranging from 6.7 x 10^4 l kg^{-1} to 5.1 x 10^5 l kg^{-1} with a mean K_D value of 3.0 x 10^5 l kg^{-1}. The seawater results exhibit a greater range of values than the corresponding freshwater results, however, the K_D values are all approximately 10^5 l kg^{-1}. The general trend suggests that as the volume increases a quantity of ^{137}Cs is desorbed before the K_D increases with increasing volume. The total quantity of ^{137}Cs desorbed is 6.8% of the total in the sample which is very similar to the freshwater value.

Fig 4.75 Range of K_D values (log scale) obtained from leaching 0–5 cm depth interval with various aqueous media.

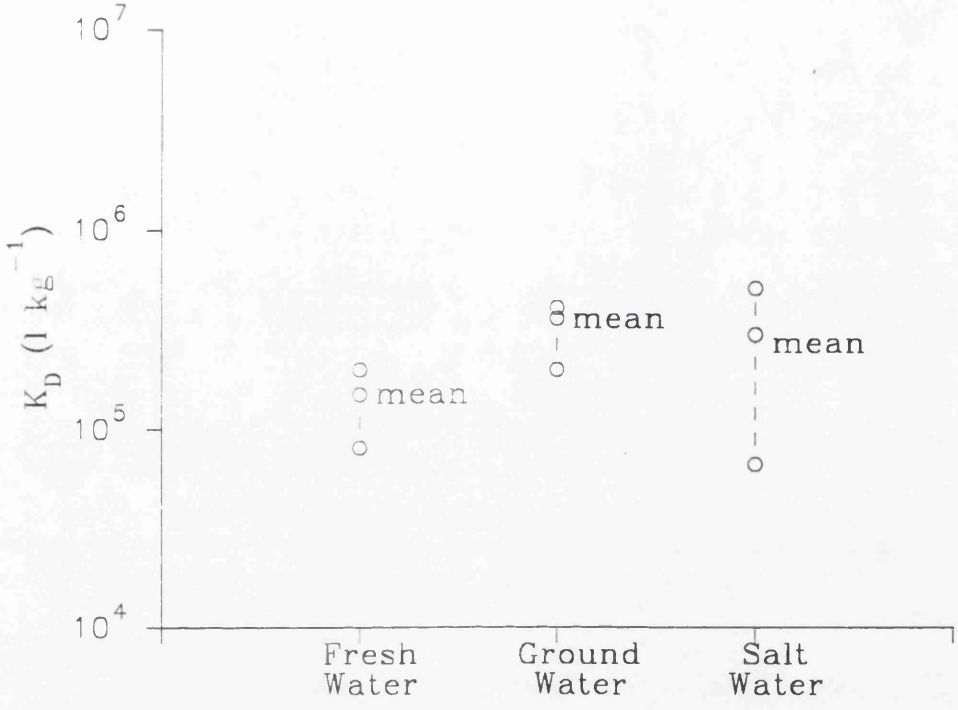

Fig 4.76 Range of K_D values (log scale) obtained from leaching 40–45 cm depth interval with various aqueous media.

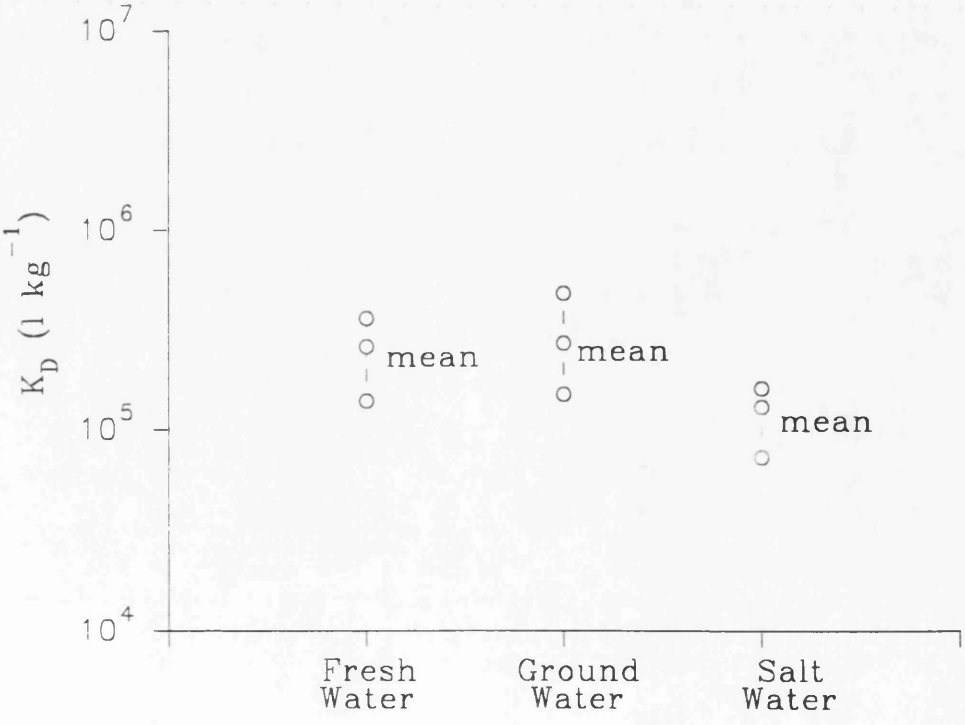

b. 40-45 cm

The results of the leaching of the 40-45 cm depth interval with seawater are listed in Table 3.36 and illustrated in Fig 4.74b. The results show an increasing K_D with increasing volume of water implying that initial desorption removes a portion of the more available ^{137}Cs and the more resistant ^{137}Cs is less readily removed. The range of K_D values is slightly lower than the corresponding values for the freshwater and ground water samples and also lower than the 0-5 cm interval. The total quantity of ^{137}Cs desorbed is 19% which is considerably greater than the quantities reported for the other leaches.

The range of K_D values produced from the flow desorption experiments are illustrated in Figs 4.75 and 4.76 for the 0-5 cm and 40-45 cm intervals respectively. They clearly show that for each depth interval, the range of K_D values obtained overlap. This indicates that the K_D values are very similar ($\sim 10^5$ l kg^{-1}) for each individual leaching media. In addition, the K_D values for the 40-45 cm depth intervals are generally lower than the corresponding 0-5 cm interval.

In order to investigate the potential impact that competing cations could have on the retention of ^{137}Cs, two desorption experiments were undertaken. Two sediment samples from the 0-5 cm interval were leached with 50 l of 10% KCl and 50 l of 10% NH_4Cl with the results being listed in Tables 3.37. The results reveal K_D values for ^{137}Cs of 5.1×10^4 l kg^{-1} in KCl and 2.2×10^5 l kg^{-1} in NH_4Cl. The KCl leach removed 4.9% of the total ^{137}Cs from the sample compared with only 1.2% for the NH_4Cl solution. The lower K_D value for KCl suggests some degree of ion exchange between the Cs^+ within the sediment and K^+ ions in solution. The results support previous observations of generally tightly bound ^{137}Cs with a proportion in a more labile or available phase which can be desorbed. The order of Cs^+ displacement contrasts with observations by Alberts *et al.*, (1983) who reported the order of cation displacement of ^{137}Cs from illite in freshwater sediment was $NH_4^+ > K^+ = Cs^+$. However, the authors do provide a rider that there is no universal order of selectivity for ion exchangers and the selectivity depends on the properties of both the cations and the exchanger surface. The ionic radius of K^+ and NH_4^+ are very similar with a crystalline radius of 1.33 Å and 1.43 Å for K^+ and NH_4^+ respectively and a hydrated radius of 2.5 Å for K^+ and 2.45 Å for NH_4^+

(Alberts *et al.*, 1983). Therefore, both cations exhibit similar size and charge and would be expected to displace Cs^+ from similar sites.

4.6.4 Batch Experiment

The batch experiment described in Section 3.7.1 was not a success. 1 kg of sediment was mixed for two minutes with 25 l of freshwater and left to settle for a period of one week. The water was then syphoned off and passed through the filtration system, however, the filter papers soon became blocked with fine particulate material. The experiment was repeated with an increased settling period of 30 days, but the filter papers again became blocked with fine particles. The length of time it took to pass 25 l of water through the filtration process, changing each filter paper as soon as it become blocked, was 25 days involving a total of 13 filter papers. During this period, the experiment was subject to changing conditions with an increasing concentration of sediment in a reducing volume of water, resulting in the finest particles being syphoned off and retained on the filter paper. This could have led to a potential loss of ^{137}Cs, associated with the finest particles, from the experiment. The KCFC cartridges used to extract the caesium from the water also become blocked after only about 10 litres.

The results from the initial 25 l are illustrated in Table 3.38 and produce lower K_D values ($\sim 10^4$ l kg^{-1}) than the flow desorption experiment. The variation may reflect a degree of equilibrium with the batch system not achieved in the flow desorption experiment, which permits increased removal of ^{137}Cs. The logistical problems with this experiment rendered it impractical. Despite increasing the period for settling to 60 days, the filter papers still became blocked with fine particles. Whether these particles were clays, colloids or micro organisms produced in the warm stagnant water of the opaque plastic container was not ascertained. These fundamental problems regarding filtration could not be overcome.

4.6.5 Conclusions

The K_D results obtained from these desorption experiments are higher than published K_D values for the Irish Sea and Clyde Sea area of 10^2-10^3 l kg^{-1}. Stanners

and Aston (1982) and McCartney *et al.*, (1993) observed K_D values for the Irish Sea of 10^2 l kg^{-1} and 10^3 l kg^{-1} respectively, while Baxter *et al.,* (1979) reported K_D values of 10^2 l kg^{-1} for the Clyde Sea area. These values were obtained from observations within the marine environment and do not relate to desorption of ^{137}Cs from saltmarsh environments.

In contrast, the adoption of a flow desorption experiment using contaminated sediment from the Solway floodplain permits an estimation of the desorption K_D for ^{137}Cs in these environments. The Sellafield derived radiocaesium within the consolidated merse would have had sufficient time to equilibrate with the sediment matrix and to diffuse into the interlaminar sites of the clay particles. Continuous leaching with aqueous media percolating through the samples would partially reflect environmental conditions within the merse and provide information on the desorption characteristics of ^{137}Cs in the merse samples.

In laboratory experiments, Stanners and Aston (1982) demonstrated a 30% loss of ^{137}Cs from Newbiggin intertidal sediment samples when in contact with seawater from the eastern Irish Sea. Samples were shaken in flasks for periods of up to 10 days before being separated using a centrifuge. The sediment was gamma counted and the loss of caesium from the sediment attributed to desorption. There was no reference to the ^{137}Cs content of the seawater from the Irish Sea and it is possible that there could have been some contribution of ^{137}Cs to the experiment from this source. Despite this, the K_D values obtained were 10^2 l kg^{-1}, indicating that the ^{137}Cs was relatively mobile and that the process of fixation within the sediment matrix was reversible. These observations by Baxter *et al.,* (1979) and Stanners and Aston (1982) were drawn from investigations of recently contaminated sediments from the surface layers of the marine sediments. More recent work by Hunt and Kershaw (1990) and McCartney *et al.,* (1993) have reported re-dissolution of up to 70% of ^{137}Cs from the marine sediments of the Irish Sea and it is reasonable to assume that the remaining ^{137}Cs is more tightly bound.

Sholkovitz *et al.,* (1983) devised deep tank experiments which exposed sediments from Buzzards Bay, USA to overlying seawater which produced K_D values for ^{137}Cs of 7×10^2 l kg^{-1}. These values are similar to the results reported by Santschi *et al.*,

(1983) of 1.4 x 10^2 l kg^{-1} for a series of microcosm experiments when ^{134}Cs tracer was added to sediments from Narragansett Bay. There are certain problems attached to the use of uptake experiments, primarily related to changes which may occur during the course of the experiment. A caesium tracer when initially added to sediment samples may be easily removed, however, through time, the Cs^+ may sorb onto clay particles within the sample which may then experience changes due to coating with organics which could prevent desorption. In addition, the tracer may have insufficient time to equilibrate within the system, preventing a realistic assessment of the desorption potential of the sediment.

These experiments by Stanners and Aston (1982), Sholkovitz *et al.,* (1983) and Santschi *et al.*, (1983) have indicated that ^{137}Cs is relatively mobile within the sediment matrix and that the K_D values derived from various locations, range between 10^2 and 10^3 l kg^{-1}. The process of ^{137}Cs sorption would therefore appear to be reversible on the basis of these studies. These results contrast markedly with the observations in the present work. The K_D values for ^{137}Cs derived from the large volume flow desorption experiment, which exposed contaminated sediment to short term contact with a leaching medium and was extended over a prolonged period of time, produced K_D values which are all consistently around 10^5. This implies that here the ^{137}Cs is less available than in other environments and that the nuclide is tightly held within the sediment. It has been well established that re-dissolution of ^{137}Cs has been occurring for a number of years (Hunt and Kershaw, 1990; and McCartney *et al.*, 1993). This implies that the more labile ^{137}Cs is removed prior to on-shore transfer, therefore, the ^{137}Cs deposited at Southwick Water would be primarily in the more resistant phases. These observations support the findings of the sequential extraction experiments (Table 3.26) where over 84% of the ^{137}Cs was found to be in the residual phase and between 12-15% in the more acid soluble fraction.

The variations between the present work and the earlier observations by Stanners and Aston (1982), Sholkovitz *et al.*, (1983) and Santschi *et al.*, (1983) can be explained by the site specific nature of the locations. Stanners and Aston (1982) investigated intertidal sediments at a time when the Sellafield discharges were relatively high and re-dissolution was not significant compared to the present. In

addition, Sholkovitz *et al.*, (1983) and Santschi *et al.*, (1983) investigated offshore sediments and not saltmarsh deposits as in the present study. These are essentially different systems which were investigated and variations in K_D values would be expected. Information on the mineralogy of the sediments investigated by these authors is not available but similarities with the present study would appear highly unlikely given that these sample sites were located in high energy environments.

The location of the present sampling site within the low energy environment of a saltmarsh provided samples which contain between 2% and 6% clay content (Table 3.23). These clays, were identified as chlorites and illites, and as such provide suitable sites for ^{137}Cs binding which may be relatively inaccessible to ion displacement by competing ions or by the laws of mass action.

4.7 NEUTRON ACTIVATION ANALYSIS OF SEDIMENT SAMPLES

The primary objective of this part of the study was to investigate the behaviour of stable caesium (^{133}Cs) in the saltmarsh sediments of Southwick merse since the presence of ^{133}Cs may influence the distribution of ^{137}Cs within this environment. The influence of ^{133}Cs was investigated by defining the total caesium concentration in the sediment and characterising the release of ^{133}Cs through freshwater leaching. The technique used for determination of ^{137}Cs was NAA, which also produced, as by-products, a considerable amount of additional geochemical data.

The results of the NAA of samples from sections SC1 (at the MHWM) and S3.10 (10 m inland from the MHWM) are listed in Tables 3.37 - 3.41. The results for ^{133}Cs in SC1 are illustrated in Fig 4.77a and exhibit an almost constant concentration profile with depth. The absence of any systematic variation suggests that the distribution of ^{133}Cs is not involved to any significant extent in geochemical cycling in this sediment. In order to investigate the release or desorption characteristics of ^{133}Cs from the sediment samples, a series of desorption experiments was undertaken. Approximately 100 g of contaminated sediment from SC1 (0-5 cm) was suspended in 1 l of freshwater and shaken for one minute. The suspension was left to settle out over variable periods of time. The aqueous phase was filtered, reduced in volume and the crystalline residue scraped into polythene

vials for irradiation. The results of this experiment are listed in Table 3.42 and the resultant K_D values for ^{133}Cs are presented in Table 3.43. These results indicate that desorption increases through time. Short term contact (8 days) produced limited desorption which increased when the period of contact between the aqueous and solid phases was extended with the trend in the results suggesting that the system was probably close to equilibrium after 64 days. The K_D values produced from this experiment are all around 10^6, indicating that ^{133}Cs is strongly retained within the sediment, probably by the clay particles, and is very difficult to remove. The decline in K_D values reported in Table 3.43 corresponds to the period that the sediment was in contact with the freshwater, and it is possible that the lower K_Ds could result from longer exposure but the trend suggests that the system was approaching equilibrium after 64 days. These K_D values are one order of magnitude higher than the flow desorption experiments discussed in Section 4.6 and together with the contrasting distribution of ^{137}Cs in SC1 (Fig 4.1a) suggest that the distribution and behaviour of stable caesium does not have a significant influence on radiocaesium in this system. It is also apparent that the radiocaesium in the saltmarsh sediment is less tightly bound to the particles than is the stable caesium. The concentration of ^{133}Cs in the intertidal sediment is slightly lower than in the saltmarsh sediment, consistent with observed variations in radiocaesium concentrations and probably being a consequence of the presence of finer sediment in the saltmarsh than in the intertidal zone.

The NAA experiment produced a large quantity of data which provide information on the geochemical behaviour of a range of elements within the saltmarsh sediments at Southwick merse. Fig 4.77 illustrates the concentration profiles of Fe, Br and Sm which can provide information on diagenetic recycling within section SC1 and also indicate the sediment source. The Fe profile (Fig 4.77b) shows an almost constant value with no variation at depth. If diagenetic recycling were occuring a profile exhibiting a pronounced decline with depth would be formed, reflecting the reduction of Fe^{3+} to Fe^{2+} at depth. This is clearly not the case for SC1 and indicates that the sediments at the MHWM are oxic. The Br profile (Fig 4.77c) exhibits more pronounced variation than either the ^{133}Cs or Fe profiles, however there is no systematic trend and the values do not indicate diagenetic recycling. The Sm profile (Fig 4.77d) shows constant values to a depth of 50-60

Fig 4.77 Concentration profiles of ^{133}Cs, Fe, Br and Sm from sediment samples from SC1.

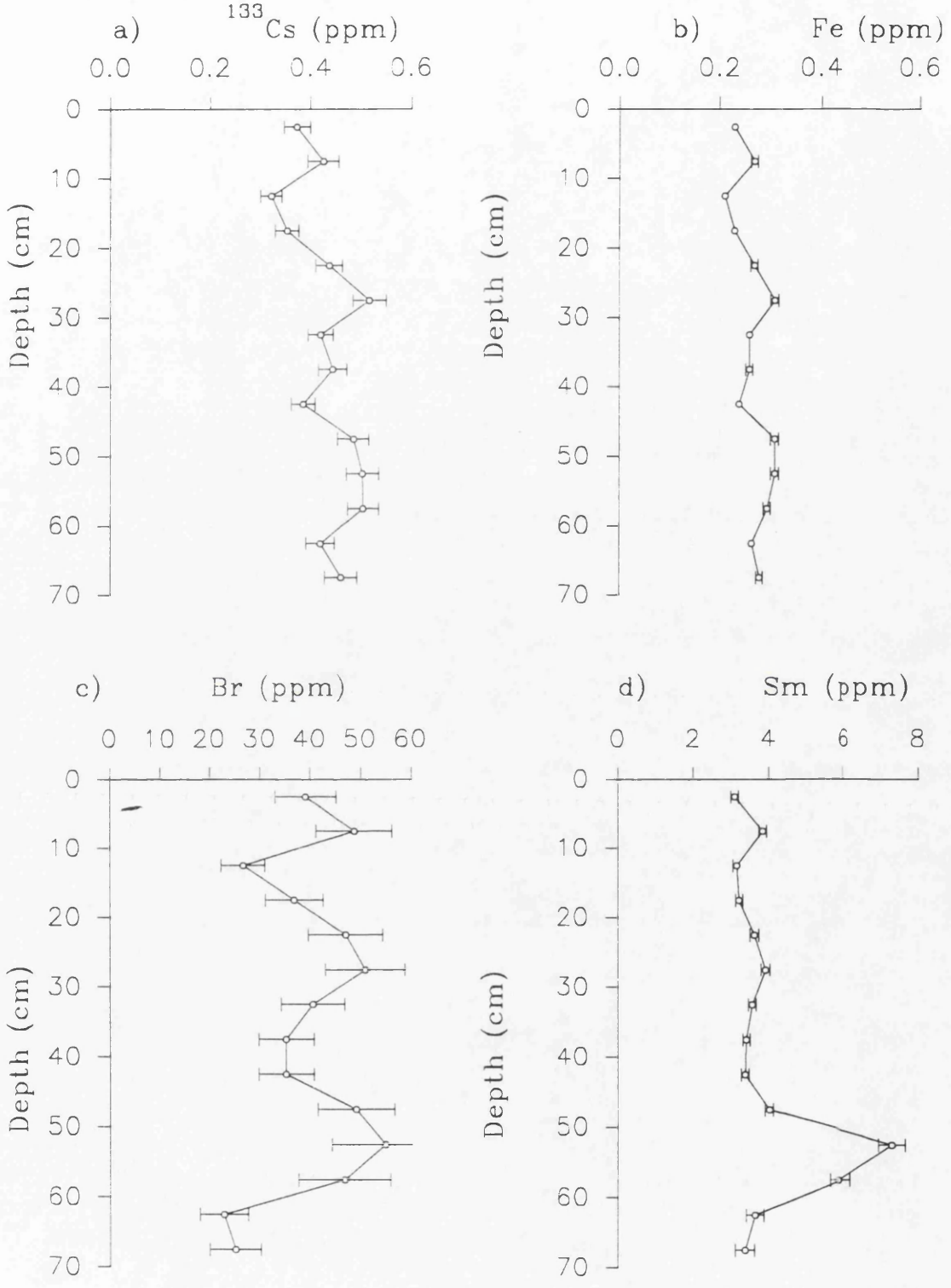

Fig 4.78 Concentration profiles of ^{133}Cs, Fe, Br and Sm from sediment samples from S3.10.

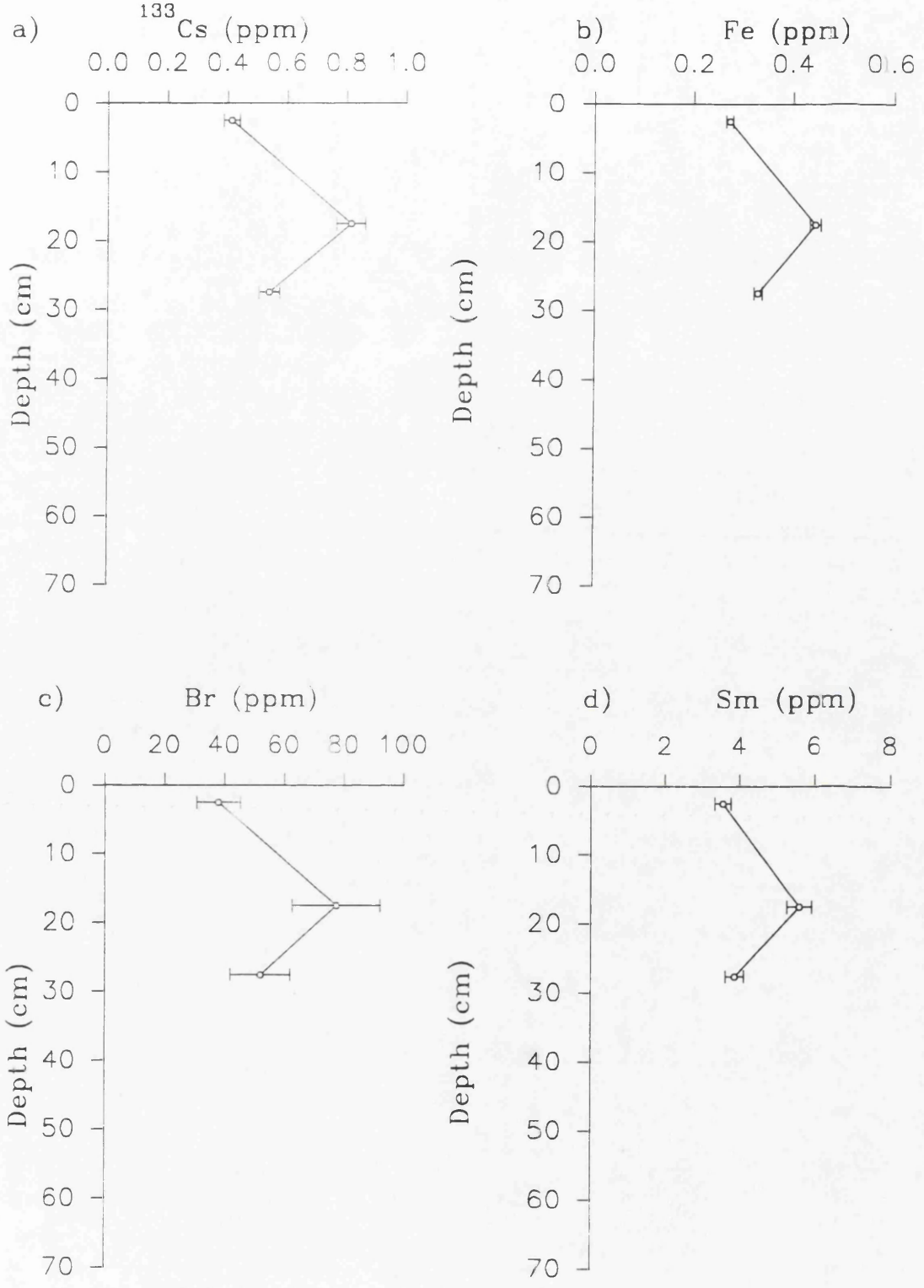

cm where a pronounced peak is observed, below this the values remain almost constant. This profile contrasts with the ^{137}Cs (Fig 4.1a) where the maximum concentration was observed at 37.5 cm. This variation may indicate a change in sediment at 50 - 60 cm depth.

All four profiles are generally very similar, with a uniform distribution and indicate that the sediment samples from SC1 are well mixed and do not exhibit any evidence of diagenetic recycling. The uniform distribution suggests that the source of the material is most likely to be particulate material from the Irish Sea sediments.

The concentration profiles from S3.10 (Fig 4.78), located 10 m inland from SC1 at the MHWM permits comparison of the geochemical conditions operating at each site. Only three depth intervals were analyzed from S3.10 and the profiles indicate increasing concentrations at a depth of 15-20 cm followed by a decline at 25-30 cm. All four profiles are similar suggesting that the variations may be the result of differences in sediment type with depth rather than diagenetic recycling. The concentrations of ^{133}Cs in the top 20 cm (Fig 4.78a) are higher than the corresponding values in SC1 and may reflect increased clay content at this inland site. The concentrations of Fe, Br and Sm are also correspondingly higher.

The results of the NAA of sedimentary material and the desorption experiment indicate that stable caesium is more tightly bound to the sediment matrix than ^{137}Cs and is not easily removed. The uniform distribution of ^{133}Cs in SC1 contrasts markedly with the corresponding profile for ^{137}Cs and indicates that distribution of radiocaesium is not significantly affected by the distribution of stable caesium.

CONCLUSIONS

Comparison of radionuclide concentration and activity ratio profiles with data for the Sellafield discharges indicates that the dominant supply mechanism of Sellafield waste to the study sites involves re-distribution of contaminated silt and that the sediment profiles preserve a record of the time integrated Sellafield discharge rather than the annual variations. A simple model capable of explaining the general shapes of the observed profiles and predicting future trends in radionuclide concentrations in the sediment has been constructed by examining and interpreting the behaviour of the ratio between the radionuclide concentrations and the Sellafield integrated discharge as a function of depth and therefore time with these cores.

The lateral distribution of radionuclides deposited within the floodplain has shown that deposition of contaminated material is influenced by the elevation, topography and vegetation cover of the merse environment. The highest concentrations have been recorded at some distance inland from the MHWM, reflecting the deposition of radionuclides associated with the finer clay particles in lower energy environments.

The total inventories of ^{137}Cs, ^{241}Am and $^{239+240}Pu$ due to deposition of Sellafield derived waste were considerably larger than inventories previously reported for the Solway floodplain. Inventories of up to 1,300,000 Bqm^{-2} of ^{137}Cs were reported which are two orders of magnitude greater than the highest recorded inventory attributable to Chernobyl fallout within this area.

The vertical distributions of radionuclides within the floodplain decline inland from the MHWM. The gradual decline in the depth of occurrence of the sub-surface maximum reflects a reduction in energy of the system on moving inland, conducive to deposition of entrained material. This is supported by the observation that the maximum radionuclide concentrations increase inland. An interesting observation involves comparison of radionuclide activity ratios within the vertical profiles with the corresponding Sellafield annual discharge and integrated activity values which indicates that up to 70% of the ^{137}Cs, theoretically associated with the sedimentary

material prior to deposition on site, has been lost through re-dissolution. This observation supports the findings of Hunt and Kershaw (1990) and McCartney *et al* (1993) who reported a loss of ^{137}Cs from the sediments of the Irish Sea.

The spatial distribution of radionuclides within the saltmarsh environments has implications for environmental monitoring programmes. A model of the spatial distribution of the radionuclides in saltmarsh sediments has been developed to permit sampling of the largest inventories which will enable more accurate assessment of potential human exposure hazards. This model has also permitted estimation of a general budget for the floodplain sediments of the Solway Firth. The budget determined by this method represents $>0.005\%$ of the ^{137}Cs integrated discharge from Sellafield.

This observation suggests that the dilute and disperse policy adopted by BNFL for dealing with the discharge of low level liquid radioactive effluent from Sellafield has been partially successful. Evidence from several authors (Hetherington, 1975; MAFF, 1977-1989; Hunt, 1985; BNFL, 1977-1989 and Kershaw *et al*, 1990) supports the observation that radionuclide concentrations in the surface sediments of coastal sites in the Irish Sea basin have declined in the last 10 years. This decline is partially due to the corresponding decline in the Sellafield discharges over the same period, but also reflects the effects of dilution of contaminated sediment. This current research identified the principal supply mechanism of radionuclides to the floodplain deposits as transport of contaminated sediment. This process results in dilution of contaminated particulate material with relatively clean sediment, resulting in a decline in surface sediment concentrations at depositional sites. This process will continue to operate for the foreseeable future and, with the decline in Sellafield discharges, will result in continued dilution producing lower surface concentrations but with an increase in radionuclide inventories.

The second component of the 'Dilute and Disperse' policy, namely dispersion has arguably been less successful. The radionuclides discharged from Sellafield have been predominantly confined to the Irish Sea basin. The actinides, ^{241}Am and $^{239+240}Pu$, are essentially confined to the area of fine sediment off the Cumbrian coast. These particle reactive radionuclides are transported by water movements

to the low energy environments of the Irish Sea basin, most notably the saltmarshes and estuaries of Lancashire, Cumbria and south west Scotland. According to Hunt and Kershaw (1990) less than 4% of $^{239+240}Pu$ has been transported out of the Irish Sea through the North Channel. The conservative behaviour of ^{137}Cs discharged from Sellafield has essentially conformed to the 'Dilute and Disperse' policy with less than 10% remaining within the sediments of the Irish Sea. Despite this, there are areas of the coastline which are highly contaminated with ^{137}Cs effluent from Sellafield.

As discussed in Chapter 4, the radionuclides are transported on-shore and become incorporated into the sediments of the floodplain. The geochemical behaviour of the radionuclides within these deposits indicates that ^{137}Cs is tightly bound to the sediment and is not easily removed. $^{239+240}Pu$ is associated with the organic and secondary Fe/Mn mineral phases within the sediment and despite an apparent change in speciation as a consequence of diagenetic degradation of organic matter, plutonium appears to be effectively immobile in the salt marsh sediments. The observation that ^{137}Cs is tightly bound to the sediment is supported by the flow desorption experiments which have produced K_D values of 10^5 l kg^{-1}. These values are higher than previously reported for the Irish Sea but are only applicable to this site. The geochemical associations and flow desorption experiment data combined with the observation of a systematic loss with time of ^{137}Cs from the material being deposited at the location of Core SC1, provide compelling evidence that the more available ^{137}Cs within the sediment has been removed and the residual material is very difficult to remove.

The NAA of the sediment samples has established that stable caesium is uniformly distributed throughout the profile of SC1 and does not have a detrimental impact on the up-take of ^{137}Cs.

REFERENCES

ADAS. The Analysis of Agricultural Materials, 2ndEdition. MAFF Reference Book 427, HMSO, pp226, 1981.

Alberts J. J. and Orlandini K. A. Laboratory and field studies of the relative mobility of $^{239+240}Pu$ and ^{241}Am from lake sediments under oxic and anoxic conditions. Geochim. et Cosmochim. Acta 45, 1931-1939, 1981.

Alberts J. J., Wahlgren M. A., Orlandini K. A. and Durbahn C. A. The distribution of $^{239+240}Pu$, ^{238}Pu, ^{241}Am and ^{137}Cs among chemically defined components of sediments, settling particulates and net plankton of Lake Michigan. J. Environ. Radioactivity, 9, 89-103, 1989.

Allen J. R. L. Modern period muddy sediments in the Severn Estuary (southwestern U.K.): A pollution based model for dating and correlation. Sed. Geol., 58, 1-21, 1988.

Allen J. R. L. Evolution of saltmarsh cliffs in muddy and sandy systems: A qualitative comparison of British west coast estuaries. Earth Sur. Proc. and Landforms., 14, 85-92, 1989.

Allen J. R. L. Saltmarsh accretion and sea level movement in the inner Severn Estuary, Southwest Britain: the archaelogical and historical contribution.
J. of Geol. Soc., 148, 485-494, 1991.

Assinder D. J. Behaviour of plutonium in the intertidal sediments of the eastern Irish Sea. Ecological Aspects of Radionuclide Release, British Ecological Society, Ed. P. J. Coughtrey, pp 189-197, 1983.

Assinder D. J., Hamilton-Taylor J., Kelly M., Mudge S. and Bradshaw K. Field and laboratory measurements of the rapid remobilization of plutonium from estuarine sediments. J. Radioanal. Nuc. Chem., Articles, 138, 2, 417-424, 1990.

Assinder D. J., Kelly M. and Aston S. R. Tidal variations in dissolved and particulate phase radionuclide activities in the Esk Estuary, England, and their distribution coefficients and particulate activity fractions. J. Environ. Radioactivity., 2, 1-22, 1985.

Aston S. R., Assinder D. A. and Kelly M. Plutonium in intertidal coastal and estuarine sediments in the northern Irish Sea. Est., Coastal Shelf Sci. 20 761-771, 1985.

Aston S. R., Assinder D. J., Stanners D. A. and Rae J. E. Plutonium occurrence and phase distribution in sediments of the Wyre Estuary, Northwest England. Marine Pollut. Bullet. 12, 9, 308-314, 1981e.

Aston S. R. and Duursma E. K. Concentration effects on ^{137}Cs, ^{65}Zu, ^{60}Co and ^{106}Ru sorption by marine sediments with geochemical implications. Netherlands Jour. of Sea Res., 6, 225-240, 1973.

Aston S. R. and Stanners D. A. The determination of estuarine sedimentation rates by $^{134}Cs/^{137}Cs$ and other artifical radionuclide profiles. Est. Coastal Shelf Sci., 9, 529-541, 1979.

Aston S. R. and Stanners D. A. Plutonium transport and deposition and immobility in Irish Sea intertidal sediments. Nature, 289, 581-582, 1981a.

Aston S. R. and Stanners D. A. Americium in intertidal sediments from the coastal environs of Windscale. Marine Pollut. Bullet., 12, 5, 149-153, 1981b.

Aston S. R. and Stanners D. A. Observation on the deposition, mobility anb chemical associations of plutonium in intertidal sediments. In Techniques for Identifying Transuranic Speciation in Aquatic Environments. I.A.E.A. pp209-217, 1981c.

Aston S. R. and Stanners D. A. Gamma emitting fission products in surface sediments of the Ravenglass Estuary. Mar. Poll., 13, 4, 135-138, 1982a.

Aston S. R. and Stanners D. A. Local variability in the distribution of Windscale fission products in estuarine sediments. Est. Coastal Shelf Sci., 14, 167-174, 1982b.

Aston S. R. and Stanners D. A. The transport and deposition of Americium in intertidal sediments of the Ravenglass Estuary and its relationship to plutonium. Environ. Pollut., Series B, 3, 1-9, 1982c.

Baker C. W. The determination of radiocaesium in sea and fresh waters. Ministry of Agriculture Fisheries and Food, Technical Reports Series, No.16, 1-8, 1975.

Baker C. W. Radiochemical techniques for determining some naturally occurring radionuclides in Marine Environmental Materials. Nucl. Instr. Meths. Phys. Res., 223, 218-223, 1984.

Baxter M. S., Cook G. T. and McDonald P. An assessment of artificial radionuclide transfer from Sellafield to South West Scotland. DOE Report No. DOE/RW/89/127, 1989.

Baxter M. S., McKinley I. G., MacKenzie A. B. and Jack W. Windscale radiocaesium in the Clyde sea area. Marine Pollut. Bullet., 10, 116-120, 1979.

Begg F. PhD Thesis University of Glasgow, 1992.

Belderson R. H. Holocene sedimentation in the western half of the Irish Sea. Marine Geology, 2, 147-163, 1964.

Belderson R. H. and Stride A. H. Tidal currents and sand wave profiles in the north eastern Irish Sea. Nature, 222, 74-75, 1969.

Ben-Shaban Y. A. PhD Thesis University of Glasgow, 1989.

BNFL. Nuclear Fuel Reprocessing Technology. British Nuclear Fuels Limited, Risley, UK. 3-9, 1985.

BNFL. Annual Report and Accounts, 1986-87. British Nuclear Fuels Limited, Risley, UK. pp60, 1986.

BNFL. Annual Reports on radioactive discharges and monitoring of the environment. British Nuclear Fuels Limited, Risley, UK, 1971-1990.

BNFL. Annual Report on radioactive discharges and monitoring of the environment. British Nuclear Fuels Limited, Risley, UK. 12-14, 1989.

BNFL. Annual Report on radioactive discharges and monitoring of the environment. British Nuclear Fuels Limited, Risley, UK. vol. 1, 1990.

Boni A. L. Rapid ion exchange analysis of radiocaesium in milk, urine, sea water and environmental samples. Anal. Chem., 38, 89-92, 1966.

Bradley P. E., Scott E. M., Baxter M. S. and Ellet D. J. Radiocaesium in local and regional coastal water modelling exercises. Radionuclides in the Study of Marine Processes. 61-71, Proc. International Symp., University of East Anglia, Norwich, 1991.

Brisbin L. Jr., Beyers R. J., Geiger R. A., Dopson R. W. and Gentry J. B. Patterns of radiocaesium in the sediments of a stream channel contaminated by production reactor effluents. Health Physics, 27, 19-27, 1974.

Bruland K. W., Koide, M. and Goldberg E. D. The Comparative Marine Geochemistries of Lead 210 and Radium 226. Jour. Geophys. Res., 79, 21, 1974.

Burd P. The saltmarsh survey of Great Britain: An Inventory of British Saltmarshes. Nature Conservancy Council 17. ISSN 0952-4738, 1989.

Burton P. J. Laboratory studies on the remobilisation of actinides from Ravenglass estuary sediment. AERE Harwell Report HL85/1318(c10), Pub. Sci. Tot. Environ. 52(1/2), 123-145, 1986.

Calmet D. and Guegueniat P. M. Behaviour of radionuclides released into coastal waters. IAEA Technical Document 329, Ed. Pentreath R. J., 1985.

Cambray R. S. Annual discharge of long lived radionuclides to the sea and to the atmosphere from Sellafield works, Cumbria 1957-1981, AERE M3269. Harwell, pp6, 1982.

Cambray R. S. and Eakins J. D. Studies in Environmental Radioactivity in Cumbria Part 1. Concentrations of Plutonium and Caesium-137 in Environmental samples from West Cumbria and a possible maritime Effect. AERE-R9807, Harwell, pp31, 1980.

Cambray R. S., Cawes P. A., Garland J. A., Gibson J. A. B., Johnson P., Lewis G. N. J., Newton D., Salmon L. and Wade B. O. Observations On Radioactivity From The Chernobyl Accident. Nuclear Energy, 26, 6, 77-101, 1987.

Camplin W. C., Mitchell N. T., Leonard D. R. P. and Jefferies D. F. Radioactivity in surface coastal waters of the British Isles: monitoring of fallout from the Chernoybl reactor accident. Aquatic Environment Monitoring Report No15, MAFF ISSN0142-2499, Lowestoft. pp32, 1986.

Canberra Industries. Spectran AT software. Canberra Industries, Inc., Meriden, USA, 1986.

Cawse P. A. Studies In Environmental Radioactivity In Cumbria, Part 4. Caesium-137 and Plutonium in soils of Cumbria and the Isle of Man. AERE-R9851. Harwell, pp39, 1980.

Cawse P. A. and Horrill A. D. A survey of caesium-137 and plutonium in British soils in 1977. AERE R 10155 Report, UKAEA, Harwell.

Chester R. and Aston S. R. The partitioning of trace metals and transuranics in sediments. Techniques for Identifying Transuranic Speciation in Aquatic Environments. IAEA Vienna 173-193, 1981.

Chester R., Murphy K. J. T., Towner J. and Thomas A. The partitioning of elements in crust dominated marine aerosols. Chem. Geol., 54, 1-15, 1986.

Clark M. J. and Smith F. B. Wet and dry deposition of Chernobyl releases. Nature, 332, 245-249, 1988.

Coleman N. T. and Le Roux F. H. Ion-exchange displacement of cesium from soil vermiculite. Soil Sci., 99, 4, 243-250, 1965.

Comans R. N. J., Holler M. and De Preter P. Sorption of Cs on illite: non equilibrium behaviour and reversibility. Geochim. Cosmochim. Acta, 55, 433-440, 1991.

Cook G. T., Baxter M. S., Duncan H. J., Toole J. and Malcolmson R. Geochemical association of plutonium in the Caithness environment. Nucl. Instr. Meth. Phys. Res., 223, 517-522, 1984a.

Cook G. T., Baxter M. S., Duncan H. J. and Malcolmson R. Geochemical associations of plutonium and γ emitting radionuclides in Caithness soils and marine particulates. J. Environ. Radioactivity, 1, 119-131, 1984b.

Coughtrey P. J., Jackson D., Jones C. H., Kane P. and Thorne M. C. Radionuclide distribution and transport in terrestial and aquatic ecosystems. Vol. 4, pp224-301, A. A. Balkema, Rotterdam, 1984.

Countryside Commission for Scotland. Scotlands Scenic Heritage. ISBN 0902226 42 S, 1987.

Covell D.F. Anal. Chem., 31, 1785, 1959.

Cronan D. S. Geochemistry of recent sediments from the central north eastern Irish Sea, Report no. 70/17, Inst. Geol. Sci. 20pp, 1970.

Cremers A., Elsen A., De Preter P. and Maes A. Quantitative analysis of radiocaesium retention in soils. Nature, 335, 1988.

Cronan D. S. Recent sedimentation in the central north eastern Irish Sea. Report No 69/8, Inst. Geol. Sci. pp10, 1969.

Davies K. S. Qualitative and quantitative aspects of ^{137}Cs fixation by soils and sediments in the Ravenglass Estuary, Cumbria. M.Sc. Imperial College, London, 1990.

Davison W. Spezzano P. and Hilton J. Remobilization of caesium from freshwater sediments. Jour. Environ. Radioactivity, 1993.

Day J. P. and Cross J. E. ^{241}Am from the decay of ^{241}Pu in the Irish Sea. Nature 292, 43-45, 1981.

Duursma E. K. Techniques and methods of interfacial transfer and transport processes in the sediment-water interlayer. Techniques for Identifying Transuranic Speciation in Aquatic Environments. IAEA Vienna, 219-227, 1981.

Dyer K. R. (Ed.). Review of oceanographic processes influncing radioactive waste dispersal in the Irish Sea. Inst. Ocean. Sci. Report No. 232, 64pp, 1986.

Eakins J. D., Pattenden N. J., Cambray R. S., Lally A. E. and Playford K. Radionuclide deposits in soil in the coastal region of Cumbria. In Studies of Environmental Radioactivity in Cumbria Part 2. AERE R9873. AERE, Harwell, UK., 1981.

Eakins J. D. and Lally A. E. The transfer of actinide bearing sediments from the Irish Sea by spray. Sci. Total Environ., 35, 23-32, 1984.

Eakins J. D., Morgan A., Baston G. M. N., Pratley F. A., Yarnold L. P. and Burton P. J. Studies in Environmental Radioactivity in Cumbria, Part 8. Plutonium and Americium in the Intertidal sands of North West England, DOE Report No. DOE/RW/87.071., 1987.

Eakins J. D., Morgan A., Baston G. M. N., Pratley F. W., Strange L. P. and Burton P. J. Measurements of α emitting plutonium and americium in the intertidal sands of west Cumbria, UK. J. Environ. Radioactivity, 11, 37-54, 1990.

Edgington D. N., Alberts J. J., Wahlgren M. A., Karttunen J. O. and Reeve C. A. Plutonium and Americium in Lake Michigan sediments. Transuranium Nuclides in the Environment. Proc. Int Symp. San Francisco, IAEA, 493-514, 1976.

Edgington D. N. and Nelson D. M. The chemical behaviour of long lived radionuclides in the marine environment. Proc. Int. Symp. on Behaviour of Long Lived Radionuclides in the Environment. La Spezia, Italy, Comm. Euro. Comm., Luxembourg EUR 19-69., 1984.

Edgington D. N. Characterization of transuranic elements at environmental levels. Techniques for Identifying Transuranic Speciation in Aquatic Environments. IAEA Vienna 3-25., 1981.

Eicke H. F. Distribution of transuranic isotopes in the surface waters of the North Sea and adjacent regions. In Techniques for Identifying Transuranic Speciation in Aquatic Environments. ST/PUB/613 IAEA Vienna, 1981.

Erten H. N. et al. Sorption/desorption of Cs on clay and soil fractions. Sci. Tot. Environ. 69, part A, 269-296, 1988.

Evans D. W., Alberts J. J. and Clark III R. A. Reversible ion exchange fixation of ^{137}Cs leading to mobilization from reservoir sediments. Geochim. Cosmochim. Acta, 47, 1041-1049, 1983.

Fahad A. A., Ali A. W. and Shihals R. M. Mobilization and fractionation of ^{137}Cs in calcareous soils. Jour. Radioanal. Nucl. Chem. Articles, 130, 1, 195-201, 1989.

Fleer A. P. and Bacon M. P. Determination of ^{210}Pb and ^{210}Po in seawater and marine particulate matter. Nucl. Instr. Meth. Phys. Res., 223, 243-249, 1984.

Francais C. W. and Brinkley F. S. Preferential adsorption of ^{137}Cs to micaceous minerals in contaminated freshwater sediment. Nature, 260, 1976.

Frey R. W. and Basan P. B. Coastal saltmarshes. Coastal Sedimentary Environments Ed. R. A. Davis Jr. 225-302, 1985.

Friedlander G., Kennedy J. W., Macias E. S. and Miller J. M. Nuclear and Radiochemistry, 3rd Edition. Publ. John Wiley and Sons, New York, 1981.

Garland J. A., McKay W. A., Cambray R. S. and Burton P. J. Man-made radionuclides in the environment of Dumfries and Galloway. Nucl. Energy, 28, 6 369-392, 1989.

Gillham R. W., Cherry G. A. and Lindsay L. E. Caesium distribution coefficients in unconsolidated geological materials. Health Physics, 39, 637-649, 1980.

Graham M. C., MacKenzie A. B., Allan R. L., Cook G. T., Scott R. D., Pulford I. D. and Livens F. R. IR spectroscopy in the investigation of radionuclide binding in saltmarsh sediment in SW Scotland. In: Proc. Int. Conf. Heavy Metals in the Environment, Toronto, 1993.

Greenwood N. N. and Earnshaw A. Chemistry of the Elements. Pergamon Press Ltd. Oxford, UK, 1984.

Hamilton E. I. Studies in labelled coastal and estuarine ecosystems : an overview. In Ecological Aspects of radionuclide Release, Ed. Coughtrey P.J., British Ecological Society 177-187, 1983c.

Hamilton E. I. The disposal of radioactive waste into the environment: the presence of hot particles containing Pu and Am in the source term. Minerlogical Magazine 49, 177-194, 1985.

Hamilton E. I. and Clarke K. R. The recent sedimentation history of the Esk Estuary, Cumbria, UK.: the application of Radiochronology. Sci. Total Environ. 35 325-386, 1984.

Hamilton-Taylor J., Kelly M., Mudge S. and Bradshaw K. Rapid remobilisation of plutonium from estuarine sediments. Jour. Environ. Radioactivity, 5, 409-423, 1987.

Hardy E. P., Krey P. W. and Volchok H. L. Global inventory and distribution of fallout plutonium. Nature 241, 444-445, 1973.

Hetherington J. A. The behaviour of plutonium nuclides in the Irish Sea. In Environmental Toxicity of Aquatic Radionuclides - models and mechanisms, Ed. Miller M. N. and Stannard J. N., Ann Arbor Michigan, 81-106, 1975.

Hetherington J. A. The uptake of plutonium nuclides by marine sediments. Marine. Sci. Commun. 4, 239-274, 1978.

Hetherington J. A., Jefferies D. F., Mitchell N. T., Pentreath R. J. and Woodhead D. S. Environmental and public health consequences of the controlled disposal of transuranic elements to the marine environment. Transuranic Nuclides In The Marine Environment. IAEA-SM-199/11, 139-154, 1976.

Horrill A.D. Concentrations and spatial distribution of radioactivity in an ungrazed saltmarsh. In: Ecological Aspects of radionuclide Release, British Ecological Society, Ed. Coughtrey P. J., 199-215, 1983.

Howarth M. J. Currents in the eastern Irish Sea. Oceano. Mar. Biol. Ann. Rev. 22 11-53, 1984.

Hunt G. J. Timescales for dilution and dispersion of transuranics in the Irish Sea near Sellafield. Sci. Total. Environ. 46, 261-278, 1985.

Hunt G. J. and Kershaw P. J. Remobilisation of artificial radionuclides from the sediment of the Irish Sea. Jour. Rad. Protection, 10, 2, 147-151, 1990.

IAEA. Sediment K_D's and concentration factors for radionuclides in the marine environment. IAEA Vienna, 1985.

ICRP-60. Recommendations of the International Commission on Radiological Protection. ICRP-60, ISSN 0146-6453. ICRP, 21, 1-3, 1990.

Iu K. L., Pulford I. D. and Duncan H. J. Influence of water logging and lime or organic matter additions on the distribution of trace metals in an acid soil, manganese and iron. Plant and Soil, 59, 317, 1981.

Jeandel C., Martin J. M. and Thomas A. J. Plutonium and other artificial radionuclides in the Seine Estuary and adjacent areas. Techniques for Identifying Transuranic Speciation in Aquatic Environments, IAEA Vienna, 89-101, 1981.

Jefferies D. F., Steele A. K. and Preston A. Further studies on the distribution of ^{137}Cs in British coastal waters-I. Irish Sea. Deep Sea Research, 29, 6a, 713-738., 1982.

Jefferies D. F. and Steele A. K. Observed and predicted concentrations of ^{137}Cs in seawater of the Irish Sea, 1970-1985. Jour. Environ. Radioactivity, 10, 173-189, 1989.

Jefferies D. F., Preston A. and Steele A. K. Distribution of Caesium-137 in British coastal waters. Mar. Poll. Bull. 4, 8, 118-121, 1973.

Johnson R. L. The transport mechanisms of clay and fine silt in the north Irish Sea. Mar. Geol. 52, M33-M41, 1983.

Jones D. G., Roberts P. D. and Miller J. M. The distribution of gamma emitting radionuclides in surface subtidal sediments near the Sellafield plant. Estuarine Coastal Shelf Sci. 27, 143-161, 1988.

Jones D. G., Miller J. M. and Roberts P. D. The distribution of ^{137}Cs in surface intertidal sediments from the Solway Firth. Mar. Poll. Bull. 15, 5, 187-194.

Joseph A. B., Gustafson P. F., Russell I. R., Schuert E. A., Volchok H. L. and Tamplin A. Sources of radioactivity and their characteristics. In Radioactivity in the Marine Environment, National Academy of Sciences, Washington. 6-41, 1971.

Katz J. J., Seaborg G. T. and Morss L. R. The Chemistry of the Actinide Elements. Vol. 1 and 2, 2nd Edition, Chapman and Hall, London, 1986.

Keeney-Kennicutt W. L. and Morse J. W. The redox chemistry of Pu (V) O^{+2} interaction with common mineral surfaces in dilute solutions and seawater. Geochim. Cosmochim Acta, 49, 2577-2588, 1985.

Kelly M., Emptage M., Mudge S., Bradshaw K. and Hamilton-Taylor J. The relationship between sediment and plutonium budgets in a small micro tidal estuary: Esk Estuary, Cumbria, UK. J. Environ. Radioactivity, 13, 55-74, 1991.

Kelly M., Mudge S., Hamilton Taylor J. and Bradshaw K. The Behaviour of Dissolved Pu in the Esk Estuary UK. In: Radionuclides: A Tool for Oceanography. Proc. Int. Symp. Cherbourg, France. Eds. J. C. Guary, P. Guegueniat and R. J. Pentreath. Publ. Elsevier Science Publishers Ltd, London, 321-330, 1987.

Kershaw P. J., Brealey J. H., Woodhead D. S. and Lovett M. B. Alpha emitting hot particles in Irish Sea sediments. Sci. Tot. Environ. 53, 1-2, 77-87, 1986.

Kershaw P. J., Pentreath R. J., Woodhead D. S. and Hunt G. J. A review of radioactivity in the Irish Sea. A report prepared for the Marine Pollution Monitoring Management Group. Aquat. Environ. Monit. Rep., MAFF, Lowestoft, 65pp.

Kershaw P. J., Swift D. J., Pentreath R. J. and Lovett M. B. Plutonium redistribution by biological activity in Irish Sea sediments. Nature, 306, 774-775., 1983.

Kershaw P. J., Swift D. J. and Denoon D. C. Evidence of recent sedimentation in the eastern Irish Sea. Mar. Geol. 85, 1-14, 1988.

Kershaw P. J., Woodhead D. S., Malcolm S. J., Allington D. J. and Lovett M. B. A sediment history of the Sellafield Discharges. J. Environ. Radioactivity, 12, 201-241, 1990.

Kershaw P. J. Radiocarbon dating of Irish Sea sediments. Estuarine Coastal Shelf Sci., 23, 295-303, 1986.

Keyser R. M. and Raudorf T. W. Germanium Radiation Detector Manufacturing: Process and Advances. EGandG Ortec, Oak Ridge, Tennessee.

Khan, M. Q. Studies on the measurement of extractable and minerlizable nitrogen in soil. PhD. thesis University of Glasgow, 1987.

Kheboian C. and Bauer C. F. Accuracy of sequential extraction procedures for metal speciation in model aquatic sediments. Anal. Chem. 59, 1417-1423, 1987.

Kressin I. K. Electrodeposition of Plutonium and Americium for High Resolution α spectrometry. Anal. Chem., 49, 6, 842-845, 1977.

Lederer C. M. and Shirley V. S. (Eds). Table of Isotopes. 7th Edition, John Wiley and Son, New York, 1978.

Li Y. H., Burkhardt L., Buckholtz M., O'Hara F. and Santschi P. H. Partition of radiotracers between suspended particles and seawater. Geochim. Cosmochim. Acta 48, 2011-2019, 1984.

Livens F. R. and Baxter M. S. Particle size and radionuclide levels in some West Cumbrian soils. Sci. Tot. Environ. 70, 1-17, 1988.

Livens F. R., Baxter M. S. and Allen S. E. Physio-chemical associations of plutonium in Cumbrian soils. In: Speciation of Fission and Activation Products in the Environment. Ed. Bulman R. A. and Cooper J. R., Elsevier, London pp143-150, 1985.

Livens F. R. and Baxter M. S. Chemical associations of artificial radionuclides in Cumbrian soils. J. Environ. Radioactivity, 7, 75-86, 1988.

Lovett M. B. and Nelson D. M. Determination of some oxidation states of plutonium in seawater and associated particulate matter. In: Proc. Symp. Techniques for identifying transuranic speciation in Aquatic Environments, Ispra, Italy. IAEA, 27-35, 1980.

MacKenzie A. B. A proposed approach to the study of radionuclide geochemistry in intertidal sediments. Techniques for Identifying Transuranic Speciation in Aquatic Environments, IAEA Vienna, 257-262, 1981.

MacKenzie A. B. and Scott R. D. Sellafield waste radionuclides in Irish Sea intertidal sediments. Environ. Chem. and Health, 15, 213, 173-183, 1993.

MacKenzie A. B. and Scott R. D. Some aspects of coastal marine disposal of low level liquid radioactive waste. The Nuclear Engineer, 25, 4, 110-122, 1984.

MacKenzie A. B., Scott R. D. and Williams T. M. Mechanisms for northwards dispersal of Sellafield waste. Nature 329, 42-45, 1987.

MacKenzie A. B. and Scott R. D. Radiocaesium and plutonium in intertidal sediments from southern Scotland. Nature, 299 613-616, 1982.

MacKenzie A. B. and Scott R. D. Separation of Bismuth-210 and Polonium-210 from aqueous solutions by spontaneous adsorption on copper foils. Analyst 104, 1151-1158, 1979.

MacKenzie A. B., Baxter M. S., McKinley I. G., Swan D. S. and Jack W. The determination of ^{134}Cs, ^{137}Cs, ^{210}Pb, ^{226}Ra and ^{228}Ra concentrations in nearshore marine sediments and seawater. J. Radioanal. Chem., 48, 29-47, 1979.

MAFF. Radioactivity in surface and coastal waters of the British Isles. Aquatic Monitoring Reports. Ministry of Agriculture Fisheries and Food, Lowestoft UK, 1971-1990.

Maher W. A. Evaluation of a sequential extraction scheme to study the association of trace elements in estuarine and oceanic sediments. Bull. Environ. Contam. Toxicol., 32, 339-344, 1984.

Malcolme-Lawes D. J. Introduction to Radiochemistry. The MacMillan Press Ltd, London. Publ: Unwin Brothers Ltd, Surrey.

Marshall J. R. The morphology of the upper Solway saltmarshes.
Scottish Geographical Magazine 78, 81-99, 1962.

Mathew E. and Pillai K. C. Study of chemical speciation of plutonium in seawater sediment system. Techniques for identifying Transuranic Speciation in Aquatic Environments, IAEA Vienna, 195-207, 1981.

McCarthy W. and Nicholls T. M. Mass-spestrometric analysis of Plutonium in soils near Sellafield. J. Environ. Radioactivity, 12, 1-12, 1990.

McCartney M., Kershaw P. J. and Allington D. J. The behaviour of ^{210}Pb and ^{226}Ra in the Eastern Irish Sea. J. Environ. Radioactivity 12, 243-265, 1990.

McCartney M., Kershaw P. J., Woodhead D. S. and Denoon D. C. Artifical radionuclides in the surface sediments of the Irish Sea, 1968-88. Sci. Total Environ. submitted, 1992.

McDonald P., Allan R. L., MacKenzie A. B., Cook G. T. and Pulford I. D. Radionuclides in the coastal region of south west Scotland: dispersion, distribution and geochemistry. Analyt. Proceedings, submitted, 1992.

McDonald P., Cook G. T., Baxter M. S. and Thompson J. C. Radionuclide transfer from Sellafield to south-west Scotland. J. Environ. Radioactivity, 12, 285-298, 1990.

McDonald P., Cook G. T., Baxter M. S. and Thompson J. C. The terrestial distribution of artifical radioactivity in south-west Scotland. Sci. Total Environ. 111 59-82, 1992.

McHugh J. O. and Hetherington J. A. Airborne radioactivity on the Scottish Solway coast. J. Environ. Radioactivity, 5, 333-342, 1987.

McKay W. A. and Baxter M. S. The partitioning of Sellafield derived radiocaesium in Scottish coastal sediments. J. Environ. Radioactivity, 2, 93-114, 1985.

McKay W. A. and Bonnett P. J. P., Barr H. M. and Howorth J. M. Radiological assessment of radioactivity in tide washed pastures in south west Scotland. Jour. Environ. Radioactivity, 21, 77-106, 1993.

McKay W. A. and Pattenden N. J. The transfer of radionuclides from sea to land via the air: a review. J. Environ. Radioactivity, 12, 49-77, 1990.

McKay W. A. and Walker M. I. Plutonium and americium behaviour in Cumbrian nearshore waters. Jour. Environ. Radioactivity, 12, 267-283, 1990.

McKinley I. PhD Thesis, University of Glasgow, 1979.

McKinley I. G. and Alexander W. R. Constraints on the applicability of insitu distribution coefficient values. J. Environ. Radioactivity, 15, 19-34, 1992.

McKinley I. G., Baxter M. S., Ellet D. J. and Jack W. Tracer applications of radiocaesium in the Sea of the Hebrides. Est. Coastal and Shelf Sci., 13, 69-82, 1981.

McKinley I. G., Baxter M. S. and Jack W. A simple model of radiocaesium transport from Windscale to the Clyde Sea area. Est. Coastal Shelf Sci., 13, 59-67, 1981.

McLaren R. G. and Crawford D. V. Studies on soil copper 1 . The fractionation of copper in soils. J. Soil Sci. 24, 172-181, 1973.

Miller J. M., Thomas B. W., Roberts P. D. and Creamer S. C. Measurement of marine radionuclide distribution using a towed sea-bed spectrometer. Mar. Poll. Bull. 13, 9, 315-319, 1982.

Mitchell J. M., Vives Batlle, Ryan T. P., Schell W. R., Sanchez-Cabeza J. A. and Vidal-Quadras A. Studies on the speciation of plutonium and americium in the western Irish Sea, Proc. Int. Symp., Radionuclides in the Study of Marine Processes. Kershaw P. J. and Woodhead D. S., 37-51, 1991.

Morris A. W., Mantoura R. F. C., Bale A. J. and Howland R. J. M. Very low salinity regions of estuaries: important sites for chemical and biological reactions. Nature, 274, 678-680, 1978.

Mudge S., Hamilton-Taylor J., Kelly M. and Bradshaw K. Laboratory studies of the chemical behaviour of plutonium associated with contaminated estuarine sediments. J. Environ. Radioactivity, 8, 217-237, 1988.

Murray C. N. and Avogadro A. Effect of long term release of plutonium and americium into an estuarine and coastal sea ecosystem. Techniques for Identifying Transuranic Speciation in Aquatic Environments IAEA Vienna, 103-116, 1981.

N.R.P.B. The risks of leukaemia and other cancers in Seascale from radiation exposure. N.R.P.B. R171., Didcot, UK, 1984.

N.C.C. The saltmarsh survey of Great Britain. Nature Conservancy Council 17 ISSN0952-4738, 1989.

Nelson D. M. and Lovett M. B. Oxidation state of plutonium in the Irish Sea. Nature, 276, 599-601, 1978.

Nelson D. M. and Lovett M. B. Measurements of the oxidation state and concentration of plutonium in interstitial waters of the Irish Sea. IAEA-SM-248/145, 105-118, 1981.

Nelson D. M., Orlandini K. A. and Penrose W. R. Oxidation states of Pu in carbonate-rich natural waters. Jour. Environ. Radioactivity, 9, 189-198, 1989.

Nisbet A. F., Salbu B. and Shaw S. Association of radionuclides with different molecular size fractions in soil solution implications for plant uptake. Jour. Environ. Radioactivity, 18, 71-84, 1993.

Ohnuki T. and Tanaka T. Migration of radionuclides controlled by several different migration mechanisms through a sandy soil layer. Health Physics, 56, 1, 47-53, 1989.

Oldfield F., Richardson N., Appleby P. G. and Yu L. ^{241}Am and ^{137}Cs activity in fine grained saltmarsh sediments from parts of the NE Irish Sea shoreline. Jour. Environ. Radioactivity, 19, 1-24, 1993.

Ordnance Survey. Landranger 84, 1:50000. Ordnance Survey, Southampton, 1987.

Ordnance Survey. Landranger 85, 1:50000. Ordnance Survey, Southampton, 1987.

Ordnance Survey. Landranger 83, 1:50000. Ordnance Survey, Southampton, 1987.

Ordnance Survey, 19. NX 45 NW, 1:10000. Ordnance Survey, Southampton.

Ordnance Survey, 19. NX 55 SE, 1:10000. Ordnance Survey, Southampton.

Ordnance Survey, 19. NX 45 SW, 1:10000. Ordnance Survey, Southampton.

Ordnance Survey, 19. NX 45 NE, 1:10000. Ordnance Survey, Southampton.

Ordnance Survey, 19. NX 85 SW, 1:10000. Ordnance Survey, Southampton.

Ordnance Survey, 19. NX 95 NW, 1:10000. Ordnance Survey, Southampton.

Ordnance Survey, 19. NX 85 NW, 1:10000. Ordnance Survey, Southampton.

Ordnance Survey, 19. NX 96 NE, 1:10000. Ordnance Survey, Southampton.

Orson R. A., Simpson R. L. and Good R. E. A mechanism for the accumulation and retention of heavy metals in tidal freshwater marshes of the Upper Delaware River estuary. Est. Coastal Shelf Sci. 34, 171-186, 1992.

Pantin H. M. Quaternary sediments of the northern Irish Sea. In: The Quaternary History of The Irish Sea, Ed. Kidson C. and Tooley M.J., Seel House Press, Liverpool, 27-54, 1977.

Pantin H. M. Quaternary sediments from the north-east Irish Sea: Isle of Man to Cumbria. Bull. Geol. Surv. Great Britain, 64, p43, 1978.

Parkinson J. A. and Horrill A. D. An Assessment of variation due to laboratory and field conditions in the measurement of radionuclides. Nucl. Instr Meths. Phys. Res., 223, 598-601, 1984.

Peirson D. H., Cambray R. S., Cawse P. A. Eakins J. D. and Pattenden N. J. Environmental radioactivity in Cumbria. Nature Articles 300, 27-31, 1982

Penrose W. R., Metta D. N., Hylko J. M. and Rinckel L. A. The reduction of Pu(V) by aquatic sediments. Jour. Environ. Radioactivity, 5, 169-184, 1987.

Pentreath R. J. Nuclear power man and the environment. The Wykeham Science Series. Taylor and Francais Ltd, London, 1980.

Pentreath R. J. Alpha emitting nuclides in the marine environment. Nucl Instr. Meth. Phys. Res. 223, 493-501, 1984.

Pentreath R. J., Harvey B. R. and Lovett M. B. Chemical speciation of transuranium nuclides discharged into the marine environment. In: Speciation of Fission and Activation Products in the Environment, Ed. Bulman R. A. and Cooper J. R., 312-325, Elsevier, London, 1986.

Pentreath R. J., Lovett M. B., Jefferies D. F., Woodhead D. S., Talbot J. W. and Mitchell N. T. Impact on public radiation exposure of transuranium nuclides discharged in liquid waste from fuel element reprocessing at Sellafield, UK. In: Radioactive Waste Management, 5, 315-329, IAEA, Vienna, 1984.

Pentreath R. J., Woodhead D. S., Kershaw P. J., Jefferies D. F. and Lovett M. B. The behaviour of plutonium and americium in the Irish Sea. Rapp. P.-v. Reun. Cons. int. Explor. Mer. 186, 60-69, 1986.

Perkins R. W. and Thomas C. W. Worldwide Fallout. In: Transuranium Elements in the Environment, Ed. Hanson W. C., Technical Information Centre/US DOE 53-82, 1980.

Prandle D. and Beechey J. The dispersion of ^{137}Cs from Sellafield and Chernobyl in the N.W. European Shelf Seas. Proc. Int. Symp., Radionuclides in the Study of Marine Processes, Ed. Kershaw P.J. and Woodhead D.S. 84-93, 1991.

Prout W. E., Russell E. R. and Groh H. J. Ion exchange absorption of caesium by potassium hexacyanocobalt II ferrate II. Jour. Inorg. Nuc. Chem., 26, 473-479, 1965.

Ramster J. W. and Hill H. W. Current system in the northern Irish Sea. Nature, 224, 59-61, 1969.

Ranwell D. S. Ecology of Saltmarshes and Sand Dunes. Chapman and Hall, London, 1972.

Rhodes D. W. The effect of pH on the uptake of radioactive isotope from solution by soil. Proceedings of the Soil Science Society of America, 21, 389-392, 1957.

Salomon J. C., Guegueniat P. and Breton M. Mathematical model of ^{210}Sb transport and dispersion in the Channel. In: Proc. Int. Symp., Radionuclides in the Study of Marine Processes. Ed. Kershaw P.J. and Woodhead D.S., 1991.

Santschi P. H. and Honeyman B. D. Radionuclides in Aquatic Environments. Radiat. Phys. Chem., 34, 2, 213-240, 1989.

Santschi P. H., Yuan Hui Li, Adler D. M., Amburer I., Bell J. and Nyffeler U. P. The relative mobility of natural (Th, Pb and Po) and fallout (Pu, Am, Cs) radionuclides in the coastal marine environment: results from model ecosystems (MERL) and Narragansett Bay. Geochim. Cosmochim. Acta, 47, 201-210, 1983.

Sawhney B. L. Selective sorption and fixation of cations by clay minerals: a review. Clay and Clay Minerals, 20, 93-100, 1972.

Schulz R. K. Soil chemistry of radionuclides. Health Phys. 11, 1317-1324, 1965.

Segal M. and Morris C. The legacy of Chernobyl. Chemistry in Britain, Oct. 904-908, 1991.

Selby M. J. Earth's Changing Surface: An Introduction To Geomorphology. Clarendon Press London, 185-187, 1985.

Sholkovitz E. R., Cochran K. J. and Carey A. E. Laboratory studies of the diagenesis and mobility of ^{239,240}Pu and ^{137}Cs in nearshore sediments. Geochim. Cosmochim. Acta, 47, 1369-1379, 1983.

Sills G. C. and Edge M. J. Sediment behaviour in the Irish Sea. DOE Report No.DOE/RW/079, 1989.

Smith T. J., Parker W. R. and Kirby R. Sedimentation studies relevant to low level radioactive effluent dispersal in the Irish Sea, Part 1. Radionuclides in Marine sediments. I.O.S. Report 110. Unpublished Manuscript, Godalming, UK, 1980.

Stanners D. A. and Aston S. R. An improved method of determining sedimentation rates by the use of artificial radionuclides. Est. Coastal Shelf Sci., 13, 101-106, 1981a.

Stanners D. A. and Aston S. R. ^{134}Cs:^{137}Cs and ^{106}Ru:^{137}Cs ratios in intertidal sediments from the Cumbrian and Lancashire coasts, England. Est. Coastal Shelf Sci. 13, 409-417, 1981b.

Stanners D. A. and Aston S. R. Desorption of ^{106}Ru, ^{134}Cs, ^{137}Cs, ^{144}Ce and ^{241}Am from intertidal sediment contaminated by nuclear fuel reprocessing effluents. Est. Coastal Shelf Sci. 14, 687-691, 1982.

Steers J. A. The Coastline of Scotland. Cambridge University Press, 112-119, 1973.

Strather J. W., Dionian J., Brown J., Fell T. P. and Muirhead C. R. The risks of leukaemia and other cancers in Seascale from radiation exposure. N.R.P.B. R171 Addendum pp158, 1986.

Tessier A., Campbell P. G. C. and Bisson M. Sequential extraction procedure for the speciation of particulate trace metals. Anal. Chem., 51, 7, 844-851, 1979.

Tivy J. and O'Hare G. Human Impact on the Ecosystem. Oliver and Boyd, Edinburgh, 1981.

Topping, P. G. and MacKenzie, A. B. A test for the use of neutron activation analysis for clay source characterization. Archaeometry, 30 92-101, 1988.

Van Straaten and Kuenen P. H. Tidal action as a cause of clay accumulation. Jour. Sed. Petrology, 28, 4, 406-413, 1958.

Wilkins B. T., Green N., Stewart S. P. and Major R. O. Factors affecting the association of radionuclides with soil phases. In: Speciation of Fission and Activation Products in the Environment. Eds. R. A. Bulman and J. R. Cooper. Elsevier Applied Science Publishers, 1986.

Williams S. J., Kirby R., Smith T. J. and Parker W. R. Sedimentation studies relevant to low level radioactive effluent dispersal in the Irish Sea. Part II Sea bed, morphology, sediments and shallow sub-bottom stratigraphy of the eastern Irish Sea. I.O.S. Report 120. Unpublished Manuscript, 1981.

Wilson M. J., Bain D. C. and Duthie D. M. L. The soil clays of Great Britain II, Scotland. Clay Minerals, 19, 709-735, 1984.

Woodhead D. S. Mixing processes in near shore sediments as inferred from the distribution of radionuclides discharged into the north east Irish Sea from BNFL Sellafield. In: Radionuclides A Tool for Oceanography, 331-340. Proc. Int. Symp., Cherbourg, France, Ed. Guegueniat P. and Pentreath R. J., 1988.